

Towards grounding nuclear physics in QCD

Christian Drischler^{a,b,c}, Wick Haxton^{b,c}, Kenneth McElvain^{b,c}, Emanuele Mereghetti^d, Amy Nicholson^e, Pavlos Vranas^{f,c}, André Walker-Loud^{c,b,f}

^a Facility for Rare Isotope Beams, Michigan State University, MI 48824, United States

^b Department of Physics, University of California, Berkeley, CA 94720, United States

^c Nuclear Science Division, Lawrence Berkeley National Laboratory, Berkeley, CA 94720, United States

^d Theoretical Division, Los Alamos National Laboratory, Los Alamos, NM 87545, United States

^e Department of Physics and Astronomy, University of North Carolina, Chapel Hill, NC 27516-3255, United States

^f Physical and Life Sciences, Lawrence Livermore National Laboratory, Livermore, CA 94550, United States

Abstract

Exascale computing could soon enable a predictive theory of nuclear structure and reactions rooted in the Standard Model, with quantifiable and systematically improvable uncertainties. Such a predictive theory will help exploit experiments that use nucleons and nuclei as laboratories for testing the Standard Model and its limitations. Examples include direct dark matter detection, neutrinoless double beta decay, and searches for permanent electric dipole moments of the neutron and atoms. It will also help connect QCD to the properties of cold neutron stars and hot supernova cores. We discuss how a quantitative bridge between QCD and the properties of nuclei and nuclear matter will require a synthesis of lattice QCD (especially as applied to two- and three-nucleon interactions), effective field theory, and ab initio methods for solving the nuclear many-body problem. While there are significant challenges that must be addressed in developing this triad of theoretical tools, the rapid advance of computing is accelerating progress. In particular, we focus this review on the anticipated advances from lattice QCD and how these advances will impact few-body effective theories of nuclear physics by providing critical input, such as constraints on unknown low-energy constants of the effective (field) theories. We also review particular challenges that must be overcome for the successful application of lattice QCD for low-energy nuclear physics. We describe progress in developing few-body effective (field) theories of nuclear physics, with an emphasis on HOBET, a non-relativistic effective theory of nuclear physics, which is less common in the literature. We use the examples of neutrinoless double beta decay and the nuclear-matter equation of state to illustrate how the coupling of lattice QCD to effective theory might impact our understanding of symmetries and exotic astrophysical environments.

Contents

1 Motivation	2
1.1 Fundamental Symmetry Tests and Experimentally difficult/inaccessible observables	6
2 Lattice QCD	9
2.1 Challenges for nuclear physics applications	12
2.2 Status and challenges for single nucleons	15
2.3 Status and challenges for two-nucleons	17
2.3.1 Two-nucleon controversy	19

2.3.2	Nuclear Structure and Reactions	29
3	Nuclear Effective (Field) Theories	30
3.1	Single Nucleon Effective Field Theory	33
3.2	Chiral Effective Field Theory	38
3.3	Nuclear Effective Theory: HOBET	46
3.3.1	The Bloch-Horowitz Equation	50
3.3.2	HOBET's Operator Expansion	52
3.3.3	Pionful HOBET's Power Counting for the NN System	54
3.3.4	Fitting HOBET Short-Range LECs	59
3.3.5	A-body HOBET	61
3.3.6	Effective Operators in HOBET	65
3.3.7	HOBET in a Box	66
3.3.8	HOBET Outlook	70
4	Neutrinoless Double Beta Decay	71
4.1	Light-Majorana neutrino exchange	72
4.2	Short-range NMEs	75
5	Nuclear-Matter Equation of State	77
6	Outlook	84

1. Motivation

A number of high-profile, high-impact nuclear and particle physics experiments are planned over the next decade that will test the limits of the enormously successful Standard Model (SM) of particle physics, probing for subtle violations of symmetries at low energies or new particles and interactions at the energy frontier. We are quite certain that the SM, with its many seemingly arbitrary parameters, is incomplete, and hope the discovery of new physics will provide the hints needed to deduce what lies beyond the SM. A more fundamental theory could allow us to address some of the most important open questions in physics:

- How did the Big Bang generate the matter-antimatter asymmetry, avoiding the fate of a universe filled only by radiation?
- What is dark matter, and does it interact with visible matter other than gravitationally?
- What is the origin of the neutrino mass, why are neutrinos so much lighter than other fermions, why are their mixing angles larger?
- Are neutrinos their own antiparticles, and is there a connection between neutrino properties and the universe's matter-antimatter asymmetry?
- What is dark energy, and why do dark matter and dark energy play roughly comparable roles in the evolution of our universe?

Some of the experiments designed to explore these questions are prioritized in the 2015 NSAC Long Range Plan for Nuclear Science [1] and the High Energy Physics P5 report [2]. They include large-scale, ultra-clean detectors to search for the elastic scattering of heavy dark matter (DM) particles off nuclei, employing targets such as Xe, Ar, Ge, and others [3–11], as well as new technologies sensitive to lighter particles, should DM particle masses not be associated with the weak scale [12–14]. They include neutrinoless double beta decay searches for lepton number violation and Majorana masses, with ton-scale experiments use of elements such as Xe, Ge and Te planned for deep underground sites at the Gran Sasso National Laboratory, SNOLAB, China Jinping Underground Laboratory and Kamioka Observatory [15–19, 19–29]. The search for new sources of CP violation among first-generation quarks are motivating new efforts to measure electric dipole moments (EDM) of the neutron and of atomic nuclei, including ^{199}Hg [30], ^{225}Ra [31], and potentially ^{229}Pa : the latter two are long-lived unstable isotopes where the effects of CP violation are expected to be greatly enhanced due to nuclear level degeneracies and collectivity. The Facility for Rare Isotope Beams (FRIB) at Michigan State University (MSU) will produce these isotopes at rates sufficient to allow high-statistics EDM measurements in traps. Construction is beginning on the Deep Underground Neutrino Experiment (DUNE), a multi-kiloton liquid Ar detector that will record neutrinos produced in Fermilab’s Long-Baseline Neutrino Facility (LBNF), as they arrive at the Sanford Underground Research Facility after traveling through 1300 kilometers of rock [32, 33]. Together with other long-baseline experiments such as J-PARC’s T2K, the results will determine the neutrino mass hierarchy and the value of one of three neutrino CP phases. Japan’s megaton-scale water Cherenkov detector Hyper-Kamiokande will be used in the J-PARC neutrino program, in searches for proton decay of unprecedented sensitivity, and as an observatory for astrophysical neutrinos from a variety of sources. FermiLab and J-PARC are also planning extraordinarily sensitive tests of flavor violation, probing $\mu \rightarrow e$ conversion in the nuclear field [34–36].

These are just a subset of the efforts to find new physics in the next decade. Common to almost all of these experiments is the use of complex nuclei as “laboratories” for probing beyond-the-Standard-Model (BSM) phenomena. This connects fundamental physics to one of the main subjects of this paper: developing effective (field) theories (EFT/ETs) of nuclear physics, rooted in the SM, that will make the nucleus into a more quantitative laboratory for BSM searches.

Other exciting laboratories can be found in astrophysics; for instance, core-collapse supernovae or binary neutron-star mergers produce matter at extremes of temperature, density, and isospin asymmetry. As these conditions are difficult to probe in terrestrial experiments [37] (see also Sec. 1.1), the emergence of multi-messenger astrophysics is placing new demands on theory to provide a more predictive nuclear-matter equation of state (EOS). Progress is needed if we are to answer long-standing questions such as *What is the origin of elements heavier than iron?* Multi-messenger astronomy encompasses electromagnetic, cosmic-ray, neutrino, and gravitational-wave (GW) detection. KAGRA and other next-generation gravitational wave observatories will improve the sensitivity and extend the frequency range of observations. In addition, more will be learned about the maximum mass and mass/radius relationship of neutron stars. The need for a quantitative nuclear-matter EOS grounded in first-principles QCD has never been greater. At very high densities, $n \gtrsim 60 n_0$, relative to nuclear saturation density $n_0 \sim 0.16 \text{ fm}^{-3}$ ($\rho_0 \sim 2.7 \times 10^{14} \text{ g cm}^{-3}$), perturbative QCD (pQCD) [38–42] has already been used to guide the construction of the EOS over the range of densities relevant for neutron stars [43, 44].

Chiral effective field theory (EFT) has become the standard approach for deriving nuclear (many-body) forces that respect the symmetries of low-energy QCD. A variety of many-body

frameworks have been employed in conjunction with chiral EFT to generate low-density EOSs valid up to $\sim (1 - 2) n_0$. Parameterizations of the EOS or the speed of sound have been used to extrapolate the low-density EOS systematically to intermediate densities relevant for neutron stars, $n \sim (2 - 10) n_0$, without making assumptions on the composition of nuclear matter at these densities (see, e.g., Ref. [45]). The aforementioned stellar observations provide important constraints on the extrapolated EOS; for instance, neutron-star radii are most sensitive to the EOS at $\sim 2 n_0$ [46]. To improve these extrapolations, constraints on the EOS at nuclear densities must be tightened; for instance, by reducing quantified truncation errors in the EFT expansion.

Furthermore, three-nucleon forces generally play an important role for nuclear phenomena such as driplines and saturation (see Ref. [47] for a review). Better constraints on the isospin $T = 3/2$ channel (e.g, three interacting neutrons) are particularly important for neutron-rich matter. Lattice QCD (LQCD) calculations of three-neutron interactions can thus help to pin down the EOS at nuclear densities (see Sec. 1.1). Alternatively, the functional renormalization group (FRG) [48] is a very promising non-perturbative method for computing the nuclear-matter EOS at intermediate densities directly from quark-gluon degrees of freedom [49]. Clustering of quarks into nucleons as well as the emergence of long-range correlations between nucleons make the QCD-based FRG approach increasingly difficult towards lower densities; especially, since the average inter-nucleon distance is still larger than 1 fm at $3 n_0$. We will discuss the details of such calculations in Sec. 5. For a review of nuclear-matter calculations using FRG methods applied to chiral Lagrangians we refer the reader to Ref. [50].

The fundamental theory of nuclear physics is QCD, a well-accepted cornerstone of the SM. However, the nucleons, which make up atomic nuclei, are themselves composite states of fundamental particles – massless gluons and nearly massless quarks. The deceptively simple equations of QCD describing the interactions between quarks and gluons give rise to the strongly-coupled, non-perturbative strong interactions. At low temperatures and densities, the quarks and gluons are confined into colorless, composite states of strongly interacting matter, the hadrons. For example, the nucleons are composite states with the quantum numbers of three quarks and a mass of ~ 1 GeV (see Ref. [51] for the most comprehensive breakdown of the nucleon mass from QCD). The emergence of nucleons, whose masses are 95% due to interactions, is a remarkable feature of QCD.

After confinement, there is a relatively small residual interaction binding protons and neutrons into atomic nuclei with a typical binding energy per nucleon of ~ 8 MeV. While this energy scale is two orders of magnitude smaller than the confinement scale, it is still very strong compared to the other known forces. In conjunction with the other two interactions of the SM, electromagnetism as well as the weak force, the entirety of the rich field of nuclear physics *emerges* from QCD: from the forces binding protons and neutrons into the nuclear landscape, to the fusion and fission reactions between nuclei, to the prospective interactions of nuclei with BSM physics, and to the unknown state of matter at the cores of neutron stars. *How does this emergence take place exactly? How is the clustering of quarks into nucleons and alpha particles realized? What are the mechanisms behind collective phenomena in nuclei as strongly correlated many-body systems? How does the extreme fine-tuning required to reproduce nuclear binding energies proceed?* – are big open questions in nuclear physics. To give answers joint efforts of LQCD along with EFT/ETs are required.

Exascale computing offers us the opportunity to develop a predictive theory of nuclear structure and reactions, rooted in the SM, with quantifiable theoretical uncertainties. This is the focus of this review, with an emphasis placed on the connections between QCD and EFT/ETs of nuclear physics.

The foundational layer of this theoretical framework is LQCD, a formulation of QCD in which spacetime is discretized and truncated while respecting gauge-invariance [52], leading to a finite-dimensional path integral, which may then be sampled numerically using Monte Carlo methods, see Sec. 2 for details. LQCD is the only non-perturbative regulator of QCD low-density regime in which all sources of systematic uncertainty can be quantified, controlled, and improved. Therefore, LQCD offers the promise of quantitatively understanding the emergence of nuclear physics from QCD and the SM. However, because LQCD is formulated in terms of quark and gluon degrees of freedom in Euclidean spacetime, our ability to determine properties of complex systems directly from QCD is very limited. This sets the stage for EFT/ETs constrained by LQCD.

In the exascale era, we can hope to compute the structure, spectrum, and reactions of nucleons and light nuclei directly from the SM. In order to connect to more complex systems and processes, we must couple the results from LQCD calculations to EFTs and effective theories (ETs) of nuclear physics. The concepts and rules behind EFTs and ET are very similar with the main difference that EFTs relate to quantum field theories and ETs to quantum mechanics. EFT/ETs form the basis of our modern understanding of nuclear physics and we will discuss them in some detail in Sec. 3. The most popular realizations of EFT/ETs are formulated in terms of nucleon (and pion and delta) degrees of freedom, whose interactions are described by a series of operators of increasing irrelevancy based on the symmetries of low-energy QCD and dictated by a power counting scheme. In principle, EFT/ETs provide a complete, model-independent description of the underlying physics over the range of energies for which they are valid. At each order in the EFT/ET expansion, the theory depends on a finite number of unknown couplings, called low-energy constants (LECs), that encode the effects of unresolved short-distance physics. Once these LECs are determined by experimental data of one set of observables, the theory can be used to make predictions for other observables. The advantage of the systematic expansion underlying EFT/ET approaches is their capability to provide theoretical uncertainties by estimating contributions from neglected higher orders (truncation errors). In addition, uncertainties in the (experimental or lattice) data constraining the LECs as well as approximations in the methods solving the nuclear many-body problem contribute to the overall uncertainty budget of any predicted observable.

In nuclear physics, the LECs are commonly extracted from two- and few-body observables by matching computed quantities to measured observables such as binding energies or charge radii. In order to root nuclear physics in QCD, it is desirable to determine these LECs by requiring that observables extracted from correlation functions computed in the EFT/ETs and from QCD agree, at a given resolution scale and at a given order in the EFT/ET expansion, much in the same way the coefficient of the four-fermion operators in Fermi's theory of weak interactions can be determined by matching to the full electro-weak SM, for example by matching the muon-decay amplitude in full SM and with the W and Z bosons integrated out, to determine Fermi's constant, G_F . The non-perturbative nature of QCD at low energies has so far prevented this quantitative matching, but the growth in computational power and algorithmic advances has brought us to the era in which it is beginning in earnest. In practice, the best determination of the LECs will happen through a combination of matching to LQCD calculations and also applying constraints from physical processes, where LQCD in particular can help pin down LECs that are very difficult to impossible to access from experimental measurements, such as few-neutron or hyperonic systems as well as the LECs that accompany quark-mass dependent operators.

In addition to determining the LECs, by varying the quark masses in LQCD calculations, we can map out the convergence pattern of the EFT/ETs and determine their range of validity. As

an example, we will discuss constraints on chiral perturbation theory in the nucleon sector from LQCD results in Sec. 3.1.

Another key aspect of nuclear EFT/ETs that necessitates LQCD input is the determination of matrix elements of BSM operators, for which there is no experimental information available. LQCD can be utilized to compute the hadronic and nuclear matrix elements of such operators, and thus make controlled predictions of the SM background and the possible BSM signal in fundamental symmetry tests of the SM.

In the next subsection, we describe in more detail the impact LQCD can have for fundamental-symmetry tests of the SM and for observables which are extremely difficult or inaccessible experimentally. We then provide a brief introduction to LQCD in Sec. 2, emphasizing particular challenges in applying LQCD to nuclear physics, reviewing the state of the field, and highlighting the most important challenges that must be overcome. In Sec. 3, we introduce EFT/ETs of nuclear physics, chiral EFT and Harmonic Oscillator Based Effective Theory (HOBET) and then discuss the particular input from LQCD to these EFT/ETs that will enable the most progress. In Secs. 4 and 5, we use neutrinoless double beta decay ($0\nu\beta\beta$) and the nuclear-matter EOS as specific examples to elaborate upon the connection between LQCD and EFT/ETs of nuclear physics. We then provide an outlook in Sec. 6

1.1. Fundamental Symmetry Tests and Experimentally difficult/inaccessible observables

Low-energy tests of fundamental symmetries, such as searches for the violation of CP, lepton number or baryon number, provide an important window on physics beyond the SM, as they are competitive and complementary to high-energy collider experiments, see for example Refs. [53, 54]. In order to interpret bounds and, in the future, signals in low-energy precision experiments, to disentangle different BSM models, and to quantitatively compare the reach of experiments at the intensity and energy frontiers, it is necessary to develop a smooth connection between physics at the microscopic level, often described in terms of quark- and gluon-level effective operators, and theoretical predictions obtained with hadronic and nuclear degrees of freedom. The last few years have witnessed a growing awareness in the community of the need to replace estimates from models of the strong interactions (e.g., large N_c techniques, QCD sum rules, naive dimensional analysis estimates) with controlled, first principle calculations of mesonic, one- and few-nucleons observables, which can be input for nuclear EFT/ETs.

LQCD calculations in the mesonic sector are already mature and provide precise input for SM and BSM contributions to, for example, meson weak decays [55], meson- antimeson oscillations [55], and CPV in kaon decays [56]. LQCD calculations of hadronic corrections to the muon anomalous magnetic moment are starting to compete with phenomenological extractions, and promise a roadmap towards controlled theoretical uncertainties, see the recent comprehensive theory review [57].

The nuclear calculations relevant for low-energy symmetry tests typically include the evaluation of the matrix element of a weak operator between strongly interacting states (nucleons or nuclei). The required LQCD input depends on the form of the weak operator. The simplest cases involve observables that are dominated by one-body operators. For example, dark matter-nucleus scattering cross sections and non-standard corrections to nuclear β decays are mediated by the coupling of weakly interacting particles to quark bilinears that, below the hadronization scale, translate in couplings to a single nucleon, possibly via pionic contributions [58–63]. In these cases, LQCD can provide nucleon charges and form factors. For the vector and axial currents, which are induced by SM interactions, the comparison between LQCD and experimental extractions of the form factors

translates into tests of possible BSM contributions, becoming more and more stringent as the accuracy of LQCD calculations increases [64]. LQCD calculations are even more important for currents that do not appear in the SM, or are not easily extracted from data. Notable examples are the nucleon scalar and tensor charges, the strange and charm content of the nucleon, and the nucleon axial form factor. We will discuss some of these calculations in Sec. 2. Two-body contributions to the vector, axial, scalar, pseudoscalar and tensor currents are expected to be subleading. These operators can be systematically constructed in chiral EFT [60–63] but often involve LECs, in particular those corresponding to BSM currents, that cannot be experimentally determined. The first LQCD evaluations of two-nucleon matrix elements have appeared [65, 66], allowing a cross-check of the size of two-body effects, and to determine unknown LECs, albeit for heavy pion masses and the caveats discussed in Sec. 2.3.1.

Baryon-number violating processes such as proton decay and neutron-antineutron oscillations are also dominated by matrix elements between one incoming and one outgoing hadron. In these cases, the processes are mediated by three- and six-quark operators, respectively, with the LQCD calculations under good control [67, 68].

Theoretical predictions of the EDM of the nucleon, light nuclei, and diamagnetic atoms involve more complicated matrix elements. While the nucleon EDM induced by the EDMs of the light quarks is related to the well determined nucleon tensor charges [55, 69–71], in the case of CP violation from the QCD $\bar{\theta}$ term and from purely hadronic dimension-six operators in the SM-EFT Lagrangian (e.g., the quark and gluon chromo-EDMs) one has to evaluate a four-point function, with the insertion of the CP-violating source and of the electromagnetic current on the nucleon. These calculations are very challenging, especially for the QCD $\bar{\theta}$ term, and only recently some promising results have started to appear [72–76]. The intricate mixing pattern of BSM operators [77–79] further complicates the extraction of the nucleon EDM, even as the application of gradient flow techniques to this field has allowed for significant progress [74, 75, 79]. The calculation of EDMs of light nuclei and of the Schiff operator, relevant for atomic EDMs, require in addition the estimate of time-reversal-violating (TV) non-derivative pion-nucleon couplings. As shown in Refs. [80–85], for all chiral-breaking TV operators these can be related to corrections to the meson and baryon spectrum, reducing the problem of TV pion-nucleon couplings to the evaluation of generalized pion and nucleon sigma terms, which should be tractable on the lattice [84].

Finally, predictions of $0\nu\beta\beta$ half-lives and hadronic parity-violating (PV) observables involve the evaluation of two-body matrix elements on hadronic/nuclear states. The form of the two-body operators can be derived using nuclear EFTs and will in general include long-range, pion-range and short-range contributions. In the case of light-Majorana neutrino exchange (the so called “standard mechanism”), the long-range piece of the $0\nu\beta\beta$ transition operator is determined in terms of the nucleon axial and vector form factors [86, 87], while non-standard long-range mechanisms involve the nucleon scalar, pseudoscalar and tensor form factors [88–90]. The nucleon-nucleon PV potential and corrections to the $0\nu\beta\beta$ transition operator from dimension-nine quark-level operators have pion-range contributions [91–93], demanding the evaluation of new pion-pion and pion-nucleon matrix elements [94, 95]. Finally, the PV potential and the $0\nu\beta\beta$ transition operators from standard and non-standard mechanisms also have short-range pieces, which can be determined from LQCD calculations of nucleon-nucleon scattering amplitudes. New insights using large N_c indicate the most important matrix element to be determined for understanding the observed strength of various PV amplitudes is the isospin-2 matrix element [96], which is the easiest one to tackle with LQCD [97].

This brief and incomplete survey of fundamental symmetries tests highlights how LQCD will play a more and more important role in connecting models of BSM physics to nuclear observables, a connection that is necessary for a quantitative understanding of the form of physics beyond the SM. Another important role for LQCD is to help constrain components of EFT/ETs that are extremely challenging or impossible to isolate experimentally, such as those relevant to neutron stars.

Neutron stars are the densest objects in the observable universe (besides black holes) [98–101] and unique laboratories for studying neutron-rich matter under extreme conditions. These conditions are difficult (if not impossible) to reproduce in laboratory experiments [37], even at rare isotope facilities such as RIBF (RIKEN) or FRIB (MSU) and FAIR (GSI). From the theory side, LQCD can pave the way for QCD-based calculations of the nuclear-matter EOS as well as finite nuclei [102, 103]. Solving the full many-body problem with $A \geq 4$ directly from LQCD with physical quark masses, nonetheless, cannot be expected in the foreseeable future despite exascale computing capabilities. Low-energy EFT/ETs of QCD, on the other hand, are powerful approaches to derive nuclear potentials and external currents as well as extrapolate lattice results to the physical regime. The unknown LECs encoding unresolved short-distance physics can be constrained by LQCD calculations of two- and few-nucleon systems. Applying many-body frameworks to these microscopic potentials combined with Renormalization Group (RG) methods [104, 105] is a promising joint approach towards truly *ab initio* nuclear-structure and -reaction studies across the nuclear chart.

Three-nucleon forces play an important role for nuclear phenomena, such as driplines along isotopic chains or nuclear saturation [47, 106]. The isospin $\mathcal{T} = 3/2$ components (e.g., three interacting neutrons), however, are only weakly constrained by experimental (few-body) data (see, e.g., Refs. [107–110]) but are crucial at the neutron-rich extremes. Particularly, constraints from LQCD calculations of few-neutron systems, which are difficult to access experimentally, may provide important insights that can lead to much improved predictions for key quantities of nuclear physics and astrophysics, such as the nuclear symmetry energy (especially beyond nuclear saturation density) [47, 111]. A preliminary LQCD calculation of the $\mathcal{T} = 3/2$ system was presented two years ago [112], but not yet with enough statistics to determine the interaction energy. We will discuss these points in more detail in Sec. 3.2.

The composition of neutron stars at the high densities near the inner core is an open question (see Refs. [98–101, 113, 114] for reviews). Degrees of freedom heavier than nucleons may be favored due to the occurring high chemical potentials, such as strange matter in the form of hyperons (Y). However, scattering with hyperons is experimentally very difficult to realize. The limited amount of data from hyperon-nucleon (YN), yet alone hyperon-hyperon (YY), scattering makes the development of hypernuclear potentials challenging. Dominant constraints, in fact, come from binding and excitation energies of hypernuclei. Such potentials have been derived from chiral EFT [115–123] and applied to hypernuclei as well as matter [124–133] (for studies with phenomenological potentials see also Refs. [134–141]). However, these chiral EFT derivations rely on a perturbative expansion about the $SU(3)$ chiral limit, and as we will discuss in Sec. 3.1, LQCD calculations have shown that $SU(3)$ baryon chiral perturbation theory is not a converging expansion, even at next-to-leading order. These chiral EFT potentials are therefore likely qualitative at best.

Obtaining more constraints on hypernuclear potentials is essential for solving the *hyperon puzzle* (see, e.g., Refs. [113, 142–145]): the presence of hyperons in neutron stars, although probable given the high central densities, causes a softening of the EOS that seems to be incompatible with

observations of $\sim 2 M_\odot$ neutron stars [146–149]. Lattice results for baryon systems with at least one strange quark, such as YN phase shifts, may help to overcome these experimental limitations directly from QCD [150, 151]. Such observables are computationally less expensive compared to pure nucleon systems as the reduced number of light quarks in the system leads to a milder signal-to-noise ratio in the LQCD calculations, see Sec. 2.1. This will shed light on many-body hypernuclear forces (i.e., YNN, YYN, etc.) and consequently the role of hyperons in neutron stars.

Very neutron rich nuclei are short-lived in the laboratory, but form the ground state of nuclear matter under the conditions that prevail in core collapse and in neutron star mergers, where neutron fluxes are so high that neutron capture is fast compared to beta decay. It is thought that many of the heavy nuclei we find on Earth are the children of the species synthesized in such neutron-rich astrophysical explosions, in the process of rapid neutron capture (or the *r*-process) [152–154]. One of the main purposes of RIBs such as RIKEN RIBF [155] and FRIB [156] is to create such nuclei in the laboratory, determining their masses and decays rates, and thereby allowing us to more quantitatively describe the *r*-process [157]. This in turn will make nucleosynthetic yields a more powerful test of the astrophysical environments that sustain the nucleosynthesis. The properties of such nuclei may help us test our understanding of nuclear interactions within neutron-rich material: very weakly bound nuclei found near the drip-line [158–161] tend to have extended neutron halos [162, 163]. Properties of those halos can be related to the pressure of a neutron gas at subnuclear densities, providing an additional constraint on the EOS.

2. Lattice QCD

LQCD is a non-perturbative regularization of QCD that is amenable to a numerical implementation. The QCD path integral is implemented on a discretized spacetime lattice with the quark fields defined on the sites and the gauge fields defined on the links between sites. The lattice spacing a serves as an ultraviolet (UV) regulator while the finite spatial and temporal extents serve as an infrared (IR) regulator. Even with such a truncated space, it is not possible to perform the path integral exactly with classical computers. By Wick rotating to Euclidean spacetime,

$$Z = \int [dU] e^{-S_G(U)} \int [d\bar{\psi} d\psi] e^{-S_\psi(U, \bar{\psi}, \psi)} \quad (1)$$

the path integral can be evaluated stochastically, provided the fermion action

$$S_\psi = a^4 \sum_x \bar{\psi}_x [\not{D}(U) + m] \psi_x ,$$

is real valued. In this case, $0 < e^{-S_\psi}$ and so this term can be treated as a Boltzmann weight. $S_G(U)$ is the gauge action which is also real valued. A Hybrid Monte Carlo (HMC) algorithm [164] is used to generate a stochastic sampling of gauge fields U with a probability according to these weights. If the fermion action were complex, such as with a finite chemical potential, the known HMC methods will not work, except for perturbatively small (phenomenologically uninteresting) values of the chemical potential. There is a substantial effort to explore methods of simulating at finite density, but that is beyond the scope of this article. For a nice review of finite density, see Ref. [165] and another promising new idea, the review in Ref. [166]. We also do not address processes involving real-time dynamics, focusing instead on observables that we expect to be accessible to lattice QCD in the exascale era.

The discretized Dirac operator couples fermions at neighboring sites. Therefore, a gauge link field

$$U_\mu(x) = e^{iaA_\mu(x)}, \quad (2)$$

is used which transforms under gauge rotations $\Omega(x)$ as $U_\mu(x) \rightarrow \Omega(x)U_\mu(x)\Omega^\dagger(x+\hat{\mu})$ with $\hat{\mu} = an_\mu$ a vector of length a in the μ direction. Then, $\bar{\psi}(x)\gamma_\mu U_\mu\psi(x+\hat{\mu})$ and similar operators that appear in S_ψ , are gauge invariant [52].

The simplest gauge action is given by a sum over the smallest “plaquettes” that tile the lattice,

$$S_G(U) = \beta \sum_n \sum_{\mu < \nu} \text{Re} \left[1 - \frac{1}{N_c} \text{Tr} U_{\mu\nu}(n) \right], \quad (3)$$

where \sum_n = sum over all sites and the plaquette is

$$\begin{aligned} U_{\mu\nu}(n) &= U_\mu(n)U_\nu(n+\hat{\mu})U_{-\mu}(n+\hat{\mu}+\hat{\nu})U_{-\nu}(n+\hat{\nu}) \\ &= U_\mu(n)U_\nu(n+\hat{\mu})U_\mu^\dagger(n+\hat{\nu})U_\nu^\dagger(n). \end{aligned} \quad (4)$$

Expanding the gauge links for small lattice spacing, the gauge action can be shown to be

$$S_G(U) = \frac{\beta}{2N_c} a^4 \sum_{n,\mu,\nu} \frac{1}{2} \text{Tr} [G_{\mu\nu}(n)G_{\mu\nu}(n)] + \mathcal{O}(a^6), \quad (5)$$

where $G_{\mu\nu}$ is the standard gluonic field strength tensor, which in the continuum is given by $G_{\mu\nu} = \partial_\mu A_\nu - \partial_\nu A_\mu - i[A_\mu, A_\nu]$. This defines the parameter

$$\beta = \frac{2N_c}{g_0^2}, \quad (6)$$

to match the lattice onto QCD in the continuum limit with the gauge coupling, g_0 .

The fermion fields are Grassmann variables, which are not simple to handle on computers. However, the QCD action is quadratic in the fermion fields, allowing for an analytic manipulation of the fermionic integral to a form suitable for computation. This involves the introduction of pseudo-fermions, which are bosonic degrees of freedom

$$\begin{aligned} Z_\psi &= \int [d\bar{\psi} d\psi] e^{-a^4 \bar{\psi}_x [\not{D}(U) + m]_{xy} \psi_y} \\ &= \text{Det}[\not{D}(U) + m] \\ &= \int [d\phi^\dagger d\phi] e^{-a^4 \phi_x^\dagger [\not{D}(U) + m]_{xy}^{-1} \phi_y}. \end{aligned} \quad (7)$$

In this expression, we have explicitly written the Dirac operator as a spacetime matrix, which happens to be very sparse. One of the most demanding aspects of LQCD is to solve the inverse Dirac operator for small quark masses, as the Dirac matrix becomes increasingly ill-conditioned with decreasing quark mass: the smallest eigenvalue is set by the light quark mass which is much smaller than a typical QCD scale. The full dimension of the Dirac matrix is $12V \times 12V$ where $12 = 3$ colors \times 4 spins and $V = N_L^3 \times N_T$ with N_L spatial sites and N_T temporal sites. A typical state-of-the-art computation has $N_L = L/a = 64$ and $N_T = T/a = 128$ resulting in a matrix of

size $\mathcal{O}(400 \text{ M} \times 400 \text{ M})$. Significant effort has gone into optimizing the solution of the inverse Dirac operator, as historically this step has represented 90% or more of the effort required for LQCD calculations (see for example [167]). The advent of GPU accelerated compute nodes has been a disruptive innovation for LQCD, as GPUs are particularly fast at performing matrix-vector and matrix-matrix multiplications, two key kernels for solving $[\mathcal{D}(U) + m]^{-1}$. This, for example, has led to the optimized QUDA library for performing key LQCD routines on NVIDIA GPUs [168, 169].

Once a set of gauge field configurations are generated using a given discretization of the QCD action, any number of observables may be computed on this set. A stochastic estimate of the observable is then given by

$$\langle \mathcal{O} \rangle = \frac{1}{N_{\text{cfg}}} \sum_{i=1}^{N_{\text{cfg}}} \mathcal{O}(U_i) + \mathcal{O}\left(N_{\text{cfg}}^{-1/2}\right), \quad (8)$$

where the stochastic error vanishes with the square-root of the number of configurations, N_{cfg} . This assumes each configuration is statistically independent, which is generally not the case in LQCD calculations as the configurations are generated from an ergodic Markov chain Monte Carlo; however, the auto-correlation effects are typically accounted for when results are presented. These autocorrelation effects are thought to only become problematic for very fine lattices, with $a \lesssim 0.05 \text{ fm}$, when the autocorrelation length becomes so large that $\mathcal{O}(1 \text{ M})$ configurations with standard algorithms are required to produce enough stochastically independent configurations to properly sample the path integral (see for example Ref. [170]). Typical calculations involve $\mathcal{O}(1000)$ nearly statistically independent configurations.

In order to recover QCD, there are three extrapolations/interpolations that must be carried out: the continuum limit, $a \rightarrow 0$, the infinite volume limit, $V \rightarrow \infty$, and the physical quark mass limit, $m_q \rightarrow m_q^{\text{phys}}$. Uncertainties from each of these are systematically improvable, enabling predictions of nuclear and hadronic processes with quantifiable uncertainties.

The Flavour Lattice Averaging Group (FLAG), which is the lattice community equivalent to the PDG, provides a set of criteria (Sec. II in Ref. [171]) which may be used as a rule of thumb for the minimum number and value ranges of lattice spacings, volumes, and quark masses necessary for controlling or quantifying the systematics associated with each parameter. For example, at least three values of each of the extrapolation parameters, a , L , and m_π , are generally preferred (although this can vary in certain scenarios). For the lattice spacings and pion (quark) masses, the lowest values should be below 0.1 fm and 200 MeV, respectively. All volumes are expected to be greater than 2 fm, and if fewer than 3 volumes are studied, a more stringent requirement, depending on the pion mass, is placed on the size of the volumes. A rule of thumb is to hold $m_\pi L \gtrsim 4$ [172, 173], which corresponds to $L \sim 5.8 \text{ fm}$ at physical pion mass. It should be noted that the numbers and ranges of parameters necessary for a given calculation depends strongly on the observable, target precision, method, analysis, etc., so these criteria are presented here merely as guidelines based on the collective experience of the community.

The use of many different discretized versions of QCD in LQCD computations is beneficial, and a particular choice is often referred to as a *lattice action*. For example, there are substantial challenges to include fermions which respect chiral symmetry in LQCD calculations [174]. This has led to the development of a number of different discretizations of the fermion action with varying degrees of complexity. The most commonly used ones are Wilson, Staggered, Domain Wall, Overlap and their variants. We refer the reader to the nice review in Ref. [175] for more details. Each lattice action defines a different UV theory which can be expanded as an effective

local action close to the continuum limit [176, 177]. For all lattice actions, at mass-dimension four the only operators are those of QCD, and so there is a universality of the continuum limit which should be observed if all calculations are performed sufficiently close to the continuum limit and a continuum extrapolation is performed.

Some of the simplest observables are derived from two-point correlation functions, in which creation and annihilation operators of fields (source and sink operators) are chosen with the quantum numbers of the system of interest and separated in Euclidean time t . The Euclidean time behavior of such correlation functions, $C(t)$, may be shown to behave as,

$$C(t) = \sum_n Z_n^{\text{snk}} Z_n^{\dagger \text{src}} e^{-E_n t} , \quad (9)$$

where the sum runs over the infinite tower of states having the quantum numbers of the operators, and $Z_n^{\text{src}}(Z_n^{\dagger \text{snk}})$ represents the overlap between the chosen source (sink) operator and the wavefunction of eigenstate n . In the large Euclidean time limit, the lowest energy state for quantum numbers specified by the interpolating fields dominates the correlation function, allowing for a precise determination of the ground state hadron spectrum, for example.

Matrix elements are traditionally computed using three point correlation functions in which the quark level operator of interest is inserted at a third Euclidean time between the source and sink, requiring a second time to be made large, which increases the numerical cost and the complexity of properly isolating the ground state matrix elements. Additional methods exist in which the effects of the operators are instead folded into modified quark propagators, which are then inserted into correlation function calculations [65, 178–184].

In practice, particularly for calculations involving nucleons as discussed in the following subsections, the limit of large Euclidean time can be difficult to reach due to computational limitations, particularly as the physical pion mass is lowered towards its physical value. Thus, while calculations at the physical pion mass are necessary to lend confidence in the ultimate results from LQCD predictions, calculations at heavier than physical pion masses can be used in conjunction to improve the precision of results interpolated to the physical pion mass point, provided the chiral extrapolation is well behaved.

2.1. Challenges for nuclear physics applications

While simple in concept, the application of LQCD to problems of interest in nuclear physics is hindered by a few well-known challenges beyond those discussed above. The first serious challenge one encounters is an exponentially bad signal-to-noise (S/N) problem that manifests from the stochastic evaluation of the path integral, Eq. (8). The variance of the correlation function of a nucleon is dominated at late times by a three-pion state. Therefore, in the long time limit, the S/N ratio decays exponentially as [185]

$$\mathcal{R}(t) \xrightarrow[t \rightarrow \infty]{} \sqrt{N_{\text{stoch}}} e^{-(M_N - \frac{3}{2}m_\pi)t} , \quad (10)$$

where M_N and m_π are the nucleon and pion masses and N_{stoch} is the number of stochastic samples. Overcoming this S/N problem at late times requires exponentially more statistics, while at early times, the signal is polluted by excited states. Furthermore, the correlation function at neighboring times is highly correlated, and so the late time behavior, as the noise grows, is susceptible to correlated fluctuations, making it non-trivial to robustly identify the ground state of the correlation

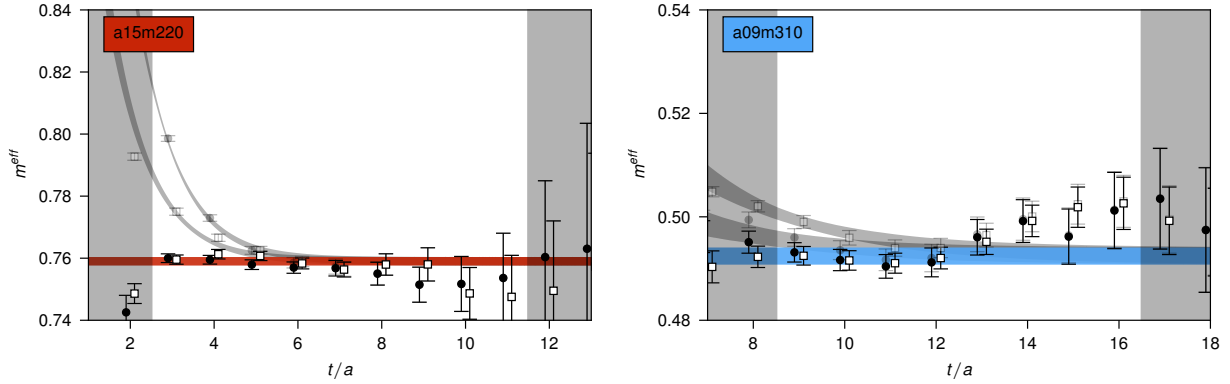


Figure 1: Effective mass plots of the nucleon from Ref. [64] which suffer from correlated, late time fluctuations, making it more challenging to identify the ground state. The top plot is from a calculation with $a \sim 0.15$ fm and $m_\pi \sim 220$ MeV while the bottom is for $a \sim 0.09$ fm and $m_\pi \sim 310$ MeV.

function. For example, Fig. 1 shows two sample effective mass plots from Ref. [64] of the nucleon mass which suffer from these correlated late time fluctuations.

These problems become exacerbated when computing the structure of the nucleon or multi-nucleon systems. For nucleon structure calculations, there are two challenges. First, there are two times which must be taken large as the current insertion must be far away from both the source and the sink time. Second, achieving high-momentum transfers is difficult since the ground state energy grows with momentum but the variance couples to zero-momentum states, increasing the energy gap in Eq. (10). To alleviate this issue, a modified quark smearing algorithm with a momentum profile centered about non-zero momentum has been shown to work well up to momentum transfers of the order $Q \sim 3$ GeV [186].

For multi-nucleon systems, the argument of the exponential of the S/N ratio scales as $A(M_N - \frac{3}{2}m_\pi)t$, where A is the number of nucleons. Fortunately, it has been observed that for early Euclidean times up to a little over $t = 1$ fm, the S/N is not degrading exponentially, but is roughly constant for up to a few baryons [187, 188]: a region in time which has been coined the “Golden Window” [189]. It was also observed that shortly after the Golden Window, the characteristic energy scale associated with the noise became worse than $(M_N - \frac{3}{2}m_\pi)$. Whether this is a real effect or just a signal of the grossly degraded signal (challenging the ability to reliably estimate the mean and variance of the correlation functions), this further emphasizes the need to determine the few-nucleon correlation functions early in Euclidean time before the S/N becomes overwhelming.

Beyond the S/N challenge, additional complications for multi-nucleon systems include:

- The nuclear physics of interest resides in the small energy difference $\Delta E = E_{AN} - A m_N \ll A m_N$. For the deuteron ($A = 2$), the interaction energy is a mere 0.1% of the total mass at the physical pion mass.
- Multi-nucleon systems exhibit complex excitations, creating a large density of states with splittings of order ΔE . Additionally, each relative momentum mode of the system corresponds to an additional excited state, and these energy gaps are also $O(\Delta E)$. Resolving these energy gaps without sophisticated operators requires that the correlation function be determined at a time given roughly by $t_{\Delta E} \sim 1/\Delta E$, which is well into the region where the noise has swamped the signal. For a volume of $L = 6.4$ fm at the physical pion mass, the first non-zero back-to-back

momentum mode (each nucleon moving with one unit of equal and opposite momentum) has an energy gap to the first elastic scattering state of $\Delta E \sim 40$ MeV leading to a time-scale of $t_{\Delta E} \sim 5$ fm. However, in existing calculations at heavy pion masses, the two-nucleon correlation function becomes swamped by the noise before 2 fm. The ability to resolve these energy gaps will become exponentially worse as the pion mass is reduced.

- There is a factorial growth in the number of quark-level Wick contractions required to construct multi-nucleon systems which scales as $N_u! \times N_d!$ where N_u and N_d are the number of *up* and *down* quarks required for the system of interest. While important algorithmic methods have been developed to dramatically reduce the number of required contractions by exploiting symmetries of the system of interest [190–193], these methods only work for unrealistically simple “wavefunctions” in which all the quarks originate from the same space-time point or are otherwise identical. For example, a proton p or neutron n requires two contractions. With the simplest contraction routines, pp , the triton pnn , and ^4He $ppnn$ require 48, 2880 and 518,400 contractions, respectively. These costs exceeds the cumulative sum of all other parts of the LQCD calculations.

The challenges facing LQCD computations of two or more baryons are greater than imagined even a few years ago. The first calculation of two-nucleons with dynamical sea-quarks was carried out in 2006 with a single lattice spacing and pion masses $m_\pi \sim \{350, 490, 590\}$ MeV [194]. Shortly after that, the first implementation of the HAL QCD potential was introduced with quenched LQCD calculations [195]. This was followed by several calculations including hyperon-nucleon interactions over a period of a few years, culminating in the first identification of a bound di-baryon system with LQCD [196, 197], the H-dibaryon [198].

Based upon the progress at the time, the first exascale Scientific Grand Challenge report for nuclear physics [199] (2009) estimated that sustained 10-Petaflop-years would yield an understanding of two-nucleon interactions at the physical pion mass. However, over the lifetime of the Titan Supercomputer (a 27 Petaflop peak computer operating from 2012–2017 at the Oak Ridge Leadership Computing Facility), there has only been a single calculation of NN interactions with a lighter pion mass $m_\pi \sim 300$ MeV [200], which is at the upper edge of the optimistic range where the two-nucleon EFT can be extrapolated to [201, 202]. In the follow up 2016 DOE Exascale Requirement Review for Nuclear Physics [203], it was estimated that in 2020, we would have complete calculations at the physical quark masses (and continuum and infinite volume limits) of two-nucleon and hyperon-nucleon interactions.

The present situation (in early 2021) is that it is still unclear whether or not two nucleons form a bound state with pion masses as heavy as $m_\pi \sim 800$ MeV, there has been no continuum scaling study of two-nucleon interactions and there are still no results with pion masses lighter than $m_\pi \sim 300$ MeV, though there are preliminary results (conference proceedings) with low statistics from HAL QCD using their alternative potential method. While the actual availability of near-exascale computing is behind the projected availability when the first 2009 exascale report was written, and perhaps a year behind when the 2016 report was prepared [1, 203] this alone does not explain the lag in LQCD results. This review describes some of the progress the field has made that has led us to recognize that LQCD treatments of systems of two or more nucleons are more challenging than originally anticipated. The importance of creating more accurate projections of results, and understanding how to maximize the scientific output per node hour, has become more acute as the cost of the supercomputers has become very non-trivial with the Sierra and Summit supercomputer costing a few hundred million US Dollars and Frontier, the Exascale computer to

be delivered to OLCF, costing a projected \$600M US dollars.¹ An excellent place to start is the two-nucleon bound state controversy at $m_\pi \sim 800$ MeV. While we can not offer a resolution, which will require extensive computations that do not currently exist, we can use this controversy to highlight the challenges of these LQCD computations. First, we begin with a brief review of single nucleon properties.

2.2. Status and challenges for single nucleons

As discussed above, there are in principle an infinite number of valid lattice actions, which are expected to give different results for a given lattice spacing; only in the continuum limit do we expect results from the different actions to reproduce QCD. Therefore, a lattice QCD calculation performed on a single lattice spacing should be interpreted as a model, at best a controlled approximation to QCD, whose systematic errors cannot be quantitatively measured. In this review, we bias our highlights to those computations which have a controlled extrapolation to the physical point in all three systematics (the physical pion mass, continuum and infinite volume limits).

In the last few years, we have witnessed the emergence of the first LQCD results of properties of single nucleons with controlled extrapolations to the continuum, infinite volume and physical pion mass limits, so we focus on such calculations in this section. A reproduction of the ground state spectrum of octet and decuplet baryons was first achieved in 2008 [204]. Seven years later, a reproduction of the neutron-proton mass splitting was achieved including dynamical QED effects with an accuracy of ~ 300 keV [205]. More recently, there have been determinations of the static charges of the nucleon [64, 70, 206–209] and the elastic form factors [210] which have included full continuum, infinite volume and physical pion mass extrapolations. In contrast, determinations of light and heavy meson properties have progressed to the point that they are routinely reviewed and averaged by FLAG [171]. The precision of these results rivals what can be achieved from experiment and phenomenology and the LQCD results play a central role in unitarity tests of the CKM Matrix. Signaling a paradigm shift, for the first time, properties of nucleons were included in the most recent FLAG review [55].

The most ubiquitous nucleon quantity appearing in weak interactions is the nucleon axial coupling (often referred to as the axial charge, or g_A). It was initially thought this would be a “gold-plated” quantity for benchmarking the success of LQCD applications to nucleon matrix elements, but it has proven to be a challenging quantity to determine, leading the field to estimate that a determination with a 2% uncertainty would be possible by 2020 with near-exascale computers (such as Summit at ORNL) [207, 211]. However, the use of an unconventional strategy [184] that included the use of early Euclidean time results, where the stochastic noise is exponentially smaller, allowed for a determination of g_A with 1% precision in 2018 utilizing Titan era supercomputers [64]. Whether one can fully control and quantify excited state contributions when including early Euclidean times has been cause for concern within the community and merits stringent checks on the results. Such checks are discussed extensively in Ref. [64]; a comprehensive discussion of excited state contamination in calculations of g_A will be a focus for a future review [212]. Here, we make two comments: first, a point that continues to be misunderstood in much of the literature is that the method utilized [65, 178–184] suppresses excited state contamination above and beyond the typical exponential suppression governed by the mass gap which is what enables the use of early

¹See for example [https://en.wikipedia.org/wiki/Summit_\(supercomputer\)](https://en.wikipedia.org/wiki/Summit_(supercomputer)) and the Frontier press release linked at the url <https://www.olcf.ornl.gov/frontier/>.

time results. The point has not been entirely lost however, as we have seen the use of early time results (as well as late) in other nucleon structure calculations [213–215] as originally advocated in Ref. [216] to the best of our knowledge.

Second, the tension between the results from CalLat and PNDME, which use many of the same HISQ configurations but different valence actions, arises from the continuum extrapolation with the results on the finest ensemble used by PNDME pulling their result to a lower value [70, 217]. It has been pointed out that the span of source-sink separation times used by PNDME is particularly small on the finest ensemble, just under 0.25 fm, which is also the most susceptible to statistical correlations in neighboring time slices [218]. Further, PNDME has uncovered a fitting systematic in the analysis of their correlation functions which was not previously incorporated, which is the inclusion of the nucleon-pion excited state. This state has not been systematically included in any calculations utilizing the standard fixed source-sink separation method, though it has been included in the analysis of the Feynman-Hellmann calculations [184]. However, its inclusion both by PNDME and the CalLat groups is sub-optimal as it is only included in the analysis of operators which are still local hadronically, meaning, they have not incorporated an explicit nucleon-pion source-sink creation/annihilation operator which can be used to diagonalize the correlation functions in terms of the eigenstates of the Hamiltonian.

What is most important for g_A , or any matrix element, is to demonstrate that the ground state matrix element is not sensitive to the various models of excited states used in the correlation function analysis [64]. Nevertheless, when the nucleon-pion state is explicitly included in the analysis of the PNDME results, they observe a significant increase in their value of g_A on ensembles with close to the physical pion mass [219]. When these larger values of g_A results are incorporated into the chiral extrapolation, the tension between the PNDME extrapolation and that of CalLat [64] is alleviated [220], though the specific formulation they use is in some contradiction with the χ PT inspired theory estimate [221].

Theoretical studies of quantities which may be precisely measured experimentally, such as g_A , can signal new physics when discrepancies are found. Calculations of quantities that have not yet been observed in nature, such as tensor and scalar isovector currents, may also be used to constrain potential BSM interactions. Lattice QCD results for these quantities have been performed by several groups, with global averages reported in Ref. [55]. See Ref. [53] for a nice review of how precision neutron beta-decay measurements constrains heavy BSM physics.

Isoscalar charges represent processes mediated via electromagnetic, weak neutral, or dark matter interactions. For example, the tensor isoscalar and isovector charges quantify contributions to the nucleon electric dipole moment from quark electric dipole moments, and are therefore relevant for probes of CP violation. Lattice calculations of these quantities present additional technical difficulties due to the presence of so-called “disconnected” diagrams, involving a quark loop at the operator insertion. These contributions require calculating propagators between all possible lattice points, and therefore scale with the lattice volume. In practice, they are often estimated stochastically or sometimes disregarded altogether.

There is currently significant tension between LQCD results and phenomenological determinations of one interesting quantity, the pion-nucleon sigma term $\sigma_{\pi N}$, the source of the primary uncertainty in estimating the spin-independent coupling of dark matter to nuclei. The LQCD results tend to favor smaller values of $\sigma_{\pi N} \sim 40$ MeV [215, 222–225] (see also the latest determination with the most complete continuum, infinite volume and physical quark mass extrapolations/interpolations [226]) while the best phenomenological determination is $\sigma_{\pi N} = 59.1 \pm$

3.5 MeV [227]. The phenomenological extraction makes very few assumptions and relies upon a dispersive understanding of pion-nucleon scattering, while the LQCD calculations provide a direct determination of the matrix elements. It has been proposed [228] that LQCD be used to directly determine the pion-nucleon scattering lengths such that they can be compared to those that are input to Ref. [227].

2.3. Status and challenges for two-nucleons

As discussed earlier in Sec. 2, LQCD calculations are necessarily performed in a finite Euclidean volume typically with periodic spatial boundary conditions. The finite volume means there are no asymptotic states and so direct access to scattering amplitudes, as one would perform experimentally, is not possible [229]. However, there is substantial literature on the ‘‘Lüscher method’’ [230, 231] to relate the finite volume spectrum to the infinite volume scattering amplitudes [232–239], including boosted systems [240–247], coupled channels [237, 246] and states of arbitrary spin [248]. There is also significant effort in extending the method to handle three-particle systems which is nearly complete [249–258] (see Sec. 3.3.7 for the construction of an effective theory in finite volume, which has also been performed in Refs. [150, 259–261]).

The Lüscher method provides a mapping between the finite-volume energy spectrum, in particular the shift in the energy levels from their non-interacting values, to the infinite volume scattering phase shifts. The underlying assumptions, which do not rely on perturbation theory or non-relativistic expansions, are:

1. The theory is unitary;
2. The range of the interaction is smaller than the spatial dimensions of the volume and the exponentially suppressed corrections, scaling as $e^{-m_\pi L}$, are negligibly small;
3. The total energy of the two-particle system is below the first inelastic threshold not taken into account;

In periodic volumes, the boundary conditions induce an unphysical mixing of various partial waves due to the reduced symmetry of the cubic volume. In practice, one must truncate the basis of partial waves considered, which is a controlled approximation for low-energy scattering. In the limiting case of a single channel in the most symmetric state (the A_1 cubic representation for a spin-0 system) where one truncates all but the S -wave interactions, one has the relation [232, 233]

$$p \cot \delta(p) = \frac{1}{\pi L} S \left(\left(\frac{pL}{2\pi} \right)^2 \right), \quad S(\eta) \equiv \lim_{\Lambda \rightarrow \infty} \sum_{\mathbf{j}}^{\Lambda} \frac{1}{|\mathbf{j}|^2 - \eta} - 4\pi\Lambda, \quad (11)$$

where p is the relative momentum of the two-particle system satisfying $E = 2\sqrt{m^2 + p^2}$ (for non-interacting systems, $\mathbf{p}_n = 2\pi\mathbf{n}/L$, but the interactions distort this relation), L is the size of the periodic box, and δ is the corresponding phase shift at that momentum. The sum is over all integer three-vectors such that $|\mathbf{j}| < \Lambda$. The function $S(\eta)$ has poles precisely at the non-interacting energies, showing consistency with the poles on the left hand side corresponding to $\delta \rightarrow 0$.

A significant challenge for these calculations is that the interaction energies are small compared to the total energy of the system and so the shift in the value of p from the non-interacting values $|\mathbf{p}_n|$ are small. Thus, one requires statistical precision at the multiple sigma level on the difference in the total energy from the non-interacting levels to ensure that the uncertainty in the scattering

phase shifts does not become grossly magnified by the proximity to these poles. Phase shifts for two-meson systems have been studied extensively due to their exponentially milder statistical noise compared to nucleons. For a nice review, see Ref. [262]. Systems containing a single baryon are considerably noisier than purely mesonic systems which has limited calculations to meson-baryon scattering to just a few [263–270].

Baryon-baryon calculations include NN [194, 200, 271–278], YN and YY [150, 189, 196, 197, 272, 277, 279–281] and light (hyper-)nuclei up to $A = 4$ [188, 200, 272, 273], in all cases with $m_\pi \gtrsim 300$ MeV. The two-nucleon calculations are of particular interest in the s -wave channels, where fine-tuning and the appearance of real or virtual bound states may be studied. The hyperon-nucleon calculations may be important for understanding the EOS in neutron stars and can be directly compared with hyper-nuclei being produced at J-PARC, the upcoming JLab, and FAIR experiments.

The challenges with these calculations have also inspired new approaches, beginning with the HAL QCD potential [195, 282–289] and, more recently, an idea to extract the infinite volume scattering amplitudes from finite volume spectral functions [290]. The HAL QCD potential method was inspired by a successful application of $I = 2 \pi\pi$ wavefunctions to determine the scattering phase shifts [291]. It has been used to study NN, YN, and YY interactions [197, 280, 292–294]. They have also studied the $\Lambda_c N$ interactions, parity odd interactions [295] and a first exploration of the three-nucleon potential [296]. Most recently, they have some first results at the physical pion mass in YN and YY channels [297–299] as well as a first look at the two-nucleon interactions at the physical pion mass [300].

Before discussing the controversy, we first provide a brief high-level summary of the HAL QCD potential method [195, 282–289]. Instead of directly relating the energy levels to the scattering amplitude via the Lüscher quantization condition, a coordinate space ratio correlation function is constructed

$$R(\mathbf{r}, t) = \frac{C_{NN}(\mathbf{r}, t)}{(C_N(t))^2}, \quad (12)$$

where the two particle correlation function is given by

$$C_{NN}(\mathbf{r}, t) = \sum_{\mathbf{x}} \langle N(\mathbf{x} + \mathbf{r}, t) N(\mathbf{x}, t) N^\dagger(0) N^\dagger(0) \rangle. \quad (13)$$

$N(\mathbf{x}, t)$ is an interpolating field with quantum numbers of the nucleon. The standard correlation functions used in the Lüscher method can be obtained from Eq. (13) by a Fourier transform over the relative coordinate. Alternatively, Eq. (12) can be used as a Nambu-Bethe-Salpeter wavefunction to extract scattering phase shifts [195, 291, 301]. A time-dependent version has also been developed [285]

$$\left[\frac{\partial_t^2}{4M} - \partial_t - H_0 \right] R(\mathbf{r}, t) = \int d^3 s U(\mathbf{r}, \mathbf{s}) R(\mathbf{s}, t), \quad (14)$$

where H_0 is the kinetic-energy operator. The strategy is to determine $U(\mathbf{r}, \mathbf{s})$, which then provides a complete description of the elastic NN scattering states below the particle production threshold. There are several required assumptions for this strategy to be valid, and if satisfied, it provides an alternative means of determining the infinite volume elastic scattering amplitudes.

First, one must assume that in the range of t used to determine $U(\mathbf{r}, \mathbf{s})$, the inelastic single-nucleon states appearing in the numerator and denominator of Eq. (12) exactly cancel and that

the two-nucleon inelastic states are numerically negligible within the numerical precision to which $R(\mathbf{r}, t)$ can be determined. Otherwise, $U(\mathbf{r}, \mathbf{s})$ is not energy independent, which invalidates the method [288]. Such an energy dependence should, in principle, manifest as a t dependence of the extracted potential U . In Ref. [289], HAL QCD constructs the potential for the $\Xi\Xi$ system at several values of t , and within their statistical precision, do not observe any t dependence. However, it should be noted that the same expectation, that systematic errors should manifest as time dependence in the extracted result, is true when extracting energy levels via the Lüscher method, thus, similar scrutiny may need to be applied.

Assuming these systematics are under control, the time-dependent method, Eq. (14) allows for the relaxation of the requirement of ground-state saturation of the correlation function as the same potential describes all of the elastic two-nucleon scattering states. In practice, the engineering of good single-nucleon operators has a long history, however, it is generally observed that contamination from inelastic states can persist into the typical time ranges used for two-nucleon calculations [302], unless multiple single-nucleon operators are combined [187, 189, 274, 278, 302]. Such engineered operators have not been utilized within the potential method.

A practical approximation that must be made to determine $U(\mathbf{r}, \mathbf{s})$ is that one must assume it can be well approximated by a local gradient expansion

$$U(\mathbf{r}, \mathbf{s}) = \left[V_C(r) + V_\sigma(r) \boldsymbol{\sigma}_1 \cdot \boldsymbol{\sigma}_2 + V_{LS}(r) \mathbf{L} \cdot \mathbf{S} + \dots + V_{N^2LO}(\mathbf{r}) \frac{\nabla^2}{\Lambda^2} + \dots \right] \delta^3(\mathbf{r} - \mathbf{s}), \quad (15)$$

where the potential has been decomposed into a central term, V_C , a spin-dependent term V_σ , spin-orbit coupling terms, V_{LS} , etc. The gradient expansion then continues with higher order terms appearing at NLO in ∇^2/Λ^2 (denoted as N^2LO). The suppression scale, Λ in this gradient expansion is not clearly defined, making the task of rigorously showing whether all neglected orders are small compared to the leading terms and whether the series converges at low orders, a difficult one.

If all of these systematic uncertainties are shown to be under control, the HAL QCD potential offers a nice alternative to the Lüscher method for determining two-nucleon (two-baryon) interactions at low-energies.

2.3.1. Two-nucleon controversy

An unresolved controversy in the literature is that results generated using the HAL QCD potential method do not agree, even qualitatively, with results generated from a more common method: even with heavy pion masses in the $SU(3)$ flavor limit ($m_\pi \sim 800$ MeV) [272, 276] as well as intermediate pion masses of $m_\pi \sim 450 - 510$ MeV [273, 275], where the S/N problem is exponentially less severe than at light pion masses, LQCD calculations using Lüscher's method have observed that the deuteron becomes more deeply bound and the di-neutron also becomes bound, while applications with the HAL QCD potential have concluded there are no bound states in either channel for similar pion masses [285, 303]. Complicating the issue, calculations coming from different groups utilize different sets of gauge configurations, so it is often not possible to isolate the issue to be due only to a given method, and not also from underlying discretization effects or other lattice systematics. The HALQCD group has performed comparisons between the two methods on a single set of configurations, focusing largely on the $\Xi\Xi$ system, and have pointed to operator dependence as being the leading source of discrepancy between the methods [304, 305].

In more detail, calculations which use compact, hexa-quark creation operators at the source in which all 6 quarks originate from the same spacetime point, observe deeply bound states (and

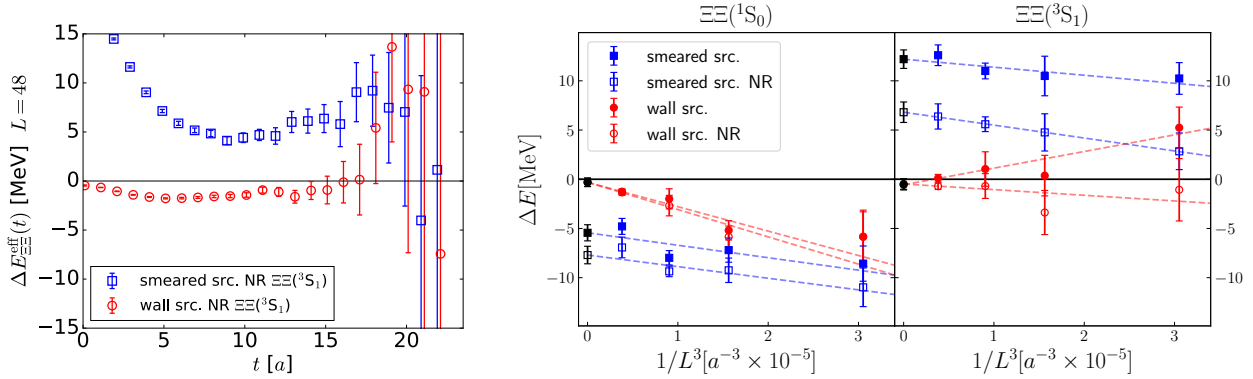


Figure 2: LEFT: Effective mass of the $\Xi\Xi(^3S_1)$ ratio correlation function with a non-relativistic (NR) Gaussian smeared source (top) and wall source (bottom) on the $L = 48$ volume [304]. RIGHT: Extrapolation of ground state energies in both channels on all four volumes comparing the Gaussian smeared and wall sources. The interaction energies were extracted from a late time-region where the single baryon effective mass is dominated by the ground state ($t \gtrsim 1$ fm). Note, for scattering states (vs bound states) the interaction energy must extrapolate to 0 in the infinite volume limit ($1/L^3 \rightarrow 0$). In this work, HALQCD determined that the smeared source exhibited evidence of a fake plateau at early times, and therefore the energies extracted using this source were unphysical. Yamazaki et al. [306, 307] responded to these findings with an order of magnitude increase in statistics, and concluded that the wall source agreed at late times with the early time plateau of the smeared source, contrary to the HALQCD conclusions. However, the study was performed on a different set of quenched configurations and so a direct comparison with the work of HAL QCD can not be performed. Further, the results from the smeared source in the $\Xi\Xi(^3S_1)$ channel simply can not be correct on the physical ground noted for the $L \rightarrow \infty$ limit above. See the text for more detail.

sometimes two) in the various two-baryon channels including the $nn(^1S_0)$ and deuteron (3S_1) [272, 273, 275]. In contrast, calculations which use spatially diffuse (displaced nucleons [276, 278, 302]) or momentum based [281] creation operators observe more shallow bound states or no bound states. The HAL QCD potential is generally constructed from a very diffuse wall-source creation operator for the quark fields and finds no bound states.

If the broader nuclear physics community is to have confidence in LQCD results of two-nucleon interactions, two-nucleon electroweak and BSM matrix elements and more, it is critical to resolve this discrepancy and robustly identify which techniques faithfully reproduce the strong interactions that emerge from QCD. We will review the state of the LQCD results and the current discrepancy.

It is tempting to brush off this controversy as arising from some unresolved systematic uncertainty with the HAL QCD method. However, HAL QCD has explored criticisms of their method, finding no obvious issues [289]. Further, they have highlighted deficiencies in the application of the standard method which require further scrutiny. The extreme cost of the numerical calculations is a significant contributor to the slow progress in resolving the discrepancy and identifying which of the results are correct, if any.

The controversy, and its resolution, essentially boil down to two questions:

1. In the application of Lüscher's method, have the true eigenstates of the system been resolved or are there unrealized systematic uncertainties that have led to the false identification of the spectrum?
2. Are all of the extra assumptions and systematic uncertainties in the HAL QCD method fully controlled?

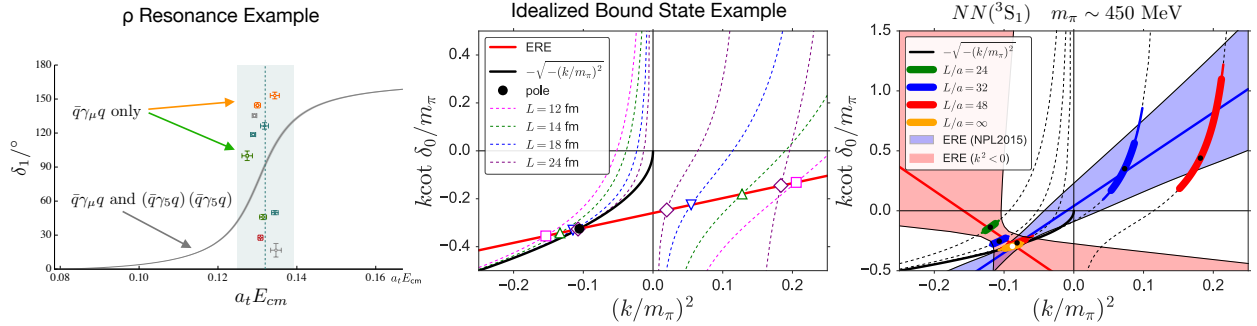


Figure 3: LEFT (figure adapted from Ref. [308]): The gray Breit-Wigner-like curve represents a determination of the phase shift near the ρ -resonance when both local ρ -like ($\bar{q}\gamma_\mu q$) and $\pi\pi$ - and KK -like ($(\bar{q}\gamma_5 q)(\bar{q}\gamma_5 q)$) operators are used to determine the spectrum. The scattered energy levels in the vertical light-blue band are determined from a set of operators that only include the local ones, which do not lie upon the phase shift curve as is required by the Lüscher quantization condition. MIDDLE (figure adapted from Ref. [309]): An idealized bound state example. The dashed lines are determined from the Lüscher quantization condition upon which all allowed values of $k \cot \delta$ and k^2 must lie for a particular volume. In this idealized example, one can see at low-momentum, the effective range expansion (ERE) extrapolates smoothly through the extracted values. RIGHT (figure adapted from Ref. [309]): HAL QCD analyzed the $k^2, k \cot \delta$ values from the calculations showing bound states. Plotted is an example from the NPLQCD calculation with $m_\pi \sim 450$ MeV [275]. In this case, they observed the ERE determined from the negative shifted energy levels is not consistent with that determined from the positively shifted levels.

At this time, the literature contains suggestive evidence, from both sides, but no conclusive proof. We begin with the first point.

HAL QCD speculates that in the application of Lüscher's method, the calculations suffer from the false identification of the ground state plateau due to contamination from excited two-nucleon elastic scattering states that are not properly resolved [304]. Central to their speculation are a few key points:

- A. With one exception [281] (which was not criticized), all LQCD calculations of two-baryon systems utilize only a single source in any given analysis, such that an operator basis diagonalization to more faithfully project onto the eigenstates of the system is not possible, and therefore, they rely upon the Euclidean time dependence to filter the excited states before the noise swamps the signal. Complicating the analysis, the correlation functions are not positive definite, so the excited states can contribute with opposite sign as the ground state;
- B. The lowest energy of the two-nucleon system depends upon the creation operator used (wall source versus Gaussian smeared source for the quarks, or spatially displaced two-nucleon operators versus local), leading to extracted energies which are multiple sigma apart. At face value, this observation may be troubling as the true ground state of the theory can not depend upon the the basis of creation/annihilation operators;
- C. Using the criteria advocated by NPLQCD (Refs. [277, 310] for example), which state that the ratio correlation function can be used provided the fitting window does not begin until the single nucleon correlator has been saturated by the ground state, leads to a scenario in the $\Xi\Xi(^3S_1)$ system with $m_\pi \sim 510$ MeV where the ground state energy, determined from a fit in the observed plateau region generated from Gaussian smeared sources, is a positively shifted scattering state which, when extrapolated to infinite volume, results in a finite interaction energy. This is not physically possible for a scattering state, as asymptotically the interaction

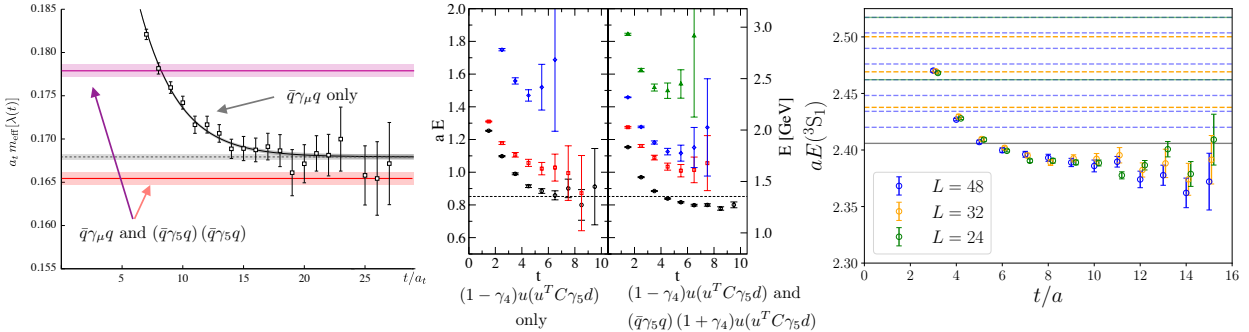


Figure 4: LEFT ($I = 1 \pi\pi$ scattering [315]): If only local $\rho = \bar{q}\gamma_\mu q$ operators are used, one obtains a very reasonable looking spectrum with no obvious by-eye or by-analysis indication the ground state is wrong. If one expands the basis of operators to include both the local ρ -like operator and also two-pion operators, $(\bar{q}\gamma_5 q)(\bar{q}\gamma_5 q)$, then one obtains a different spectrum with eigenvalues that are different by multiple sigma. MIDDLE (figure adapted from Ref. [264]): The same observation has been made in the negative parity nucleon channel when using only the local negative parity nucleon operator or when also using non-local πN operators. RIGHT (Effective mass of the $NN(^3S_1)$ system at $m_\pi \sim 800$ MeV generated from a hexa-quark source operator [310]): Superimposed on the effective mass plot are the threshold (solid gray line) and non-interacting two-nucleon energy levels (dashed lines) for the three volumes used.

energy scales as $\Delta E \propto L^{-3}$. When wall sources are used, the energies extrapolate to zero in both channels, which is consistent with physical scattering states. See Fig. 2 adapted from Ref. [304];

D. HAL QCD proposed “consistency checks” to perform on the extracted energy levels which can diagnose if they are consistent with expectations from the Lüscher quantization condition [309]. Such consistency checks are commonly used (but not by any name) in two-meson scattering calculations, see for example Ref. [308]. If a particular eigenenergy was poorly fit, or there were missing operators that led to a false plateau, when these energy levels are then passed through the Lüscher quantization with the appropriate effective range or K-matrix or similar parameterization, these energy levels typically “stick out like sore thumbs” [311], see Fig. 3. The analysis of HAL QCD found issues in nearly all calculations with deep bound states [200, 271–276, 312], though NPLQCD has refuted the observation [277, 310] for the $m_\pi \sim 800$ MeV data [274]. In a similar vein, low-energy theorems [313] were applied to the $m_\pi \sim 450$ MeV data [275] and it was found that the LQCD results are self-inconsistent [314]: the binding energies in the deuteron and di-neutron channels, when processed with the low-energy theorems, lead to scattering lengths and effective ranges that are incompatible with the effective range expansion phase shift analysis results from the same LQCD computation.

A key component of the HAL QCD criticism is that energy levels extracted, including the negatively shifted energy levels, are not the true spectrum, but are false plateaus arising from a pollution of the two-nucleon elastic scattering excited states. How plausible is this speculation?

One observation from the two-meson LQCD calculations that has been acknowledged for more than a decade is the need to use a large basis of interpolating operators that overlap with the complete set of states in the system of study in the energy range of interest, otherwise the resulting spectrum can be systematically biased without a clear indication of the problem from the correlation function analysis. For example, it has been clearly demonstrated that for $I = 1 \pi\pi$ scattering, a basis of operators that is purely local (“single-particle”), such as $\bar{q}(x)\gamma_\mu q(x)$, or purely non-

local, $\bar{q}(x)\gamma_5 q(x)\bar{q}(y)\gamma_5 q(y)$ (“two-particle”), both fail to individually produce the correct spectrum. Either set of operators on its own produces effective mass plateaus that appear like well defined energy levels, but in fact, they are linear combinations of the true eigenstates, which lie multiple sigma away [315]. If both sets of operators are used, a more complete spectrum is recovered, which we believe to be the correct spectrum, see Fig. 4. For example, the $\bar{q}\gamma_\mu q$ energy level determined in the left panel of Fig. 4 is like one of the energy levels appearing in the light-blue vertical band in the left panel of Fig. 3. The same kind of false-plateaus also appear in the negative parity πN scattering system when only local three-quark operators are used and not also the pion-nucleon-like operators [264]. This issue is discussed in more detail in the review article Ref. [262].

Without a large basis of operators that can be used to diagonalize the correlation function and project onto eigenstates of the system, the rough estimate for the length in time one needs to examine the correlation function is set by the inverse gap to the lowest lying excited state, $t \sim 1/\Delta_{10}$. At the physical pion mass, with $m_\pi L = 4$, the excited state of the single nucleon is expected to look roughly like a nucleon-pion system in a P -wave

$$\begin{aligned} E_1^{N\pi} &= \sqrt{m_N^2 + p^2} + \sqrt{m_\pi^2 + p^2} + \delta E_{\pi N}(p) \\ &\simeq m_N + \frac{p^2}{2m_N} + \sqrt{m_\pi^2 + p^2} + \delta E^{\pi N}(p) \\ &\simeq 1.03m_N + 1.9m_\pi + \delta E_{\pi N}(p), \text{ for } p \sim \frac{2\pi}{L} \end{aligned} \quad (16)$$

where the momentum p will be distorted from a quantized level due to the interactions and in the last line, we have approximated p by the lowest quantized mode. One observes the excited state gap can be relatively large, $\Delta_{10} \simeq 2m_\pi$, if the interaction energy is small compared to the pion mass. Contrast this with the excited state gap to the first two-nucleon scattering state

$$\begin{aligned} E_1^{NN} - 2m_N &\simeq \frac{p^2}{m_N} + \delta E^{NN}(p) \\ &\simeq \frac{(2\pi)^2}{m_N L^2} + \delta E^{NN}(p), \text{ for } p \sim \frac{2\pi}{L}, \end{aligned} \quad (17)$$

where again, we have approximated the momentum by the first quantized mode, in which case numerically, $\Delta_{10} \sim m_\pi/3$. Some in the literature advocate the need for having $m_\pi L \sim 8$ rather than 4 [196, 239, 271], which would lead to another factor of 4 suppression in the gaps between excited states. As the volume is increased, not only are the excited state gaps reduced but the number of low-lying excited states below the inelastic threshold increases: above, we only considered the first elastic scattering state. At the physical pion mass, for $m_\pi L = 4$, there are three states (including the ground state) below the inelastic pion-production threshold ($E = 2m_N + m_\pi$) while for $m_\pi L = 8$, there are 12 states below the inelastic threshold.

Responding to Ref. [304], Yamazaki et al. [306, 307] carried out a high statistics calculation with two orders of magnitude larger statistics, since, as they comment, the wall source results take the longest Euclidean time for the ground state to saturate the correlation function. They show a clear consistency between both the wall and smeared sources, and notably it is the wall source which becomes consistent at late times with the smeared source value that is reached at earlier times, provided enough statistics are used to resolve the correlation function at late time. Unfortunately, the results were not determined on the same set of correlation functions as in Ref. [304] and so a direct comparison can not be made.

NPLQCD responded [277, 310] by pointing out that the scattering states in their calculation have a large volume dependence, while the ground state energies (which are negatively shifted from threshold) are essentially volume independent, see Fig. 4. This is the expected finite volume behavior for physical bound states versus scattering states. While very compelling, these arguments are not proof of correctness. If the number of elastic states creating the fake plateau were fixed as the volume increased, then it would require a practically unbelievable conspiracy for the fake plateau to be volume independent. But, as we discussed above, as the volume is increased, both the gap to the excited elastic scattering states reduces and the number of states that appear in a fixed energy window, and therefore the number of states potentially contributing to a “false plateau”, grows significantly. In the $m_\pi \sim 800$ MeV NPLQCD results [272, 277, 310], with quoted masses in MeV of [272] $M_N = 1633.43(55)$ and $m_\pi = 806.93(22)$, the approximate gap to the first excited state, Δ_{10} and the number of excited states below the inelastic pion production threshold ($2M_N + m_\pi$) are given by

L	n_{states}	$\Delta_{10}[\text{MeV}]$	$1/\Delta_{10}[\text{fm}]$
24	12	76.5	2.58
32	21	43.4	4.56
48	47	19.3	10.2

The lowest lying non-interacting excited state levels are superimposed on the NPLQCD effective mass data in the right panel of Fig. 4, indicating a very dense set of low-lying elastic scattering excited states.

This observation is also not proof that the NPLQCD results are wrong. Rather, we are providing a plausibility explanation for how the effective masses in these systems can be misleading. Take a similar situation as an example, that of excited state contamination to single nucleon matrix elements. Using χ PT to provide a model of the excited states, Bär demonstrated that the excited state contamination results in an over-estimation of the axial, scalar and tensor charges for typical source-sink separation times utilized in the computations [316, 317]. This result utilized the first pion-nucleon excited state summed over the first few momentum modes allowed in the finite volume. In contrast, Hansen and Meyer demonstrated that if one uses a larger tower of excited states then the extracted matrix elements will be underestimated by a comparable amount [318]. Two different theoretical models of excited states, both rooted in the underlying physics, predict the opposite sign volume correction and the “truth” likely lies somewhere in between. These results are a demonstration that the change in the number of relevant excited states can have a dramatic impact on the inferred long-time value of the matrix element. As the volume is increased and more excited states become relevant, it is plausible that the systematic bias would be statistically volume independent.

Clearly, in order to determine the two-nucleon interactions, one must suppress the single nucleon inelastic states, such that a signal can be obtained early in Euclidean time before the noise overwhelms the correlation functions, but perhaps more important, it is imperative to have interpolating operators that highly suppress all but one of the allowed elastic scattering momentum modes either through a diagonalization of an operator basis or from very good operators. Otherwise, one would have to determine with sub-percent level precision the two-nucleon energy at late Euclidean time, but this is practically impossible given the exponentially degrading S/N for the two-nucleon system. What is required are more dedicated studies of these two-nucleon calculations with enough control over the overlap of the operators onto the states so that more definitive conclusions can be drawn.

There are two additional points of note. First, HAL QCD has demonstrated that, if instead of individually projecting the final state nucleons to definite momentum at the sink, one instead uses the spatial wavefunction determined from solving their potential, then the spectrum from the Lüscher analysis agrees with the spectrum obtained by their potential [305]. While this is interesting, it could also be a symptom of the unresolved systematic uncertainty associated with the creation/annihilation operators used that HAL QCD has belabored and in this case, you get out what you put in.

Second, related to this apparent source operator dependence of the spectrum (key point B., above), it has been known for some time that the local hexa-quark interpolating operator used as a source, in which all 6 quarks originate from the same spacetime location, is sub-optimal for coupling to the two-nucleon scattering states. One example of this is that it is observed that the overlap of such operators onto the excited states is comparable or larger than the overlap of the operator onto the ground state. Such sources also do not allow one to compute most of the higher partial waves, which in the NN systems all have large phase shifts. In order to address these issues, CalLat performed a calculation at $m_\pi \sim 800$ MeV (the same configurations with $L = 24, 32$ as NPLQCD [272]) in which the two nucleons were displaced from each other and arranged in such a way to try and maximize the overlap with the maximal number of low-lying representations of the cubic group (low-partial waves) [276]. They observed:

1. When the two-nucleons at the source were displaced, the overlap factor for the lowest energy state became dominant;
 - (a) The lowest energy state in the 3S_1 channel had a significantly smaller negative energy shift and was consistent with either a shallow bound state or a continuum scattering state;
 - (b) The lowest energy state in the 1S_0 channel was consistent with a scattering state and not a bound state;
2. When the source nucleons were created at the same space-time location as in the NPLQCD calculation [272], the lowest energy state is consistent with a deeply bound state in both channels.

CalLat speculated the deep bound state might have a large overlap with a compact hexa-quark operator but not with the diffuse non-local operator and conversely, the shallow-bound state has a large overlap with the non-local operator but not the hexa-quark operator. This speculation was motivated by the $\Delta t \simeq 1$ fm length of time in which there was a multi-sigma splitting between the energy levels associated with the different operators. HAL QCD pointed out that the phase shift analysis performed by CalLat [276] was flawed as it imposed an unphysical sign of the residue of the more deeply bound state (which may also lay outside the range of applicability of the effective range expansion). While the application of the effective range was flawed, this does not alter the conclusion about the possible existence of a second negatively shifted energy level. Without new results, more definitive conclusions can not be drawn.

Regarding potential issues with the HAL QCD method, the collaboration has been addressing some of the criticisms about the lack of quantitative control over the various systematics in the potential method. These are highlighted in a paper studying the systematics of a calculation of the potential and scattering parameters for the $\Xi\Xi$ system [289]. Away from the $SU(3)$ flavor-symmetric point, assuming the light quark masses are smaller than the strange quark mass, the $\Xi\Xi$ channels are stochastically less noisy than the two-nucleon channels, which should make it easier to study the

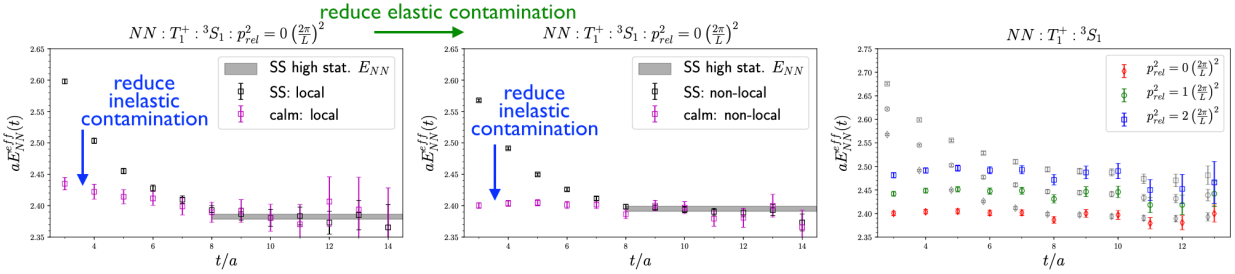


Figure 5: Studies of the effects of two-nucleon elastic excited state and inelastic single-nucleon excited state contamination and source operator dependence for two-nucleon correlators from Ref. [302]. In the two plots on the left, the gray data shows the time dependence of the two-nucleon correlators using only one optimized single-nucleon operator, while the purple data shows the time dependence of the two-nucleon correlators using instead a linear combination of single-nucleon operators produced from the Matrix Prony technique for diagonalizing operators [187–189]. Clear contamination from single-nucleon inelastic excited states is seen even at late times in the absence of diagonalization techniques for using multiple single-nucleon operators. Reduction of two-nucleon excited states can be seen when comparing the left (local two-nucleon operator) to the right (spatially displaced operator). The plot on the far right shows the clear separation of multiple two-nucleon excited states using the local (gray data) and spatially displaced (colored) operators projected onto different relative momenta. While the displaced operators give a far cleaner signal early in time, the local operator agrees with these energy levels at late times, showing that the energy levels also display operator independence.

systematic effects. The main systematics to be addressed stem from excited state contamination, finite volume, and the cutoff in the gradient expansion, Eq. (15). In their work, these points are each studied and no clear problems are noted, however, there is still room for additional debate as to whether these systematics have been fully controlled.

For the issue of excited states, as discussed above, the time-dependent potential method, Eq. (14) in principle offers the relaxed requirement of only needing to sufficiently suppress inelastic excited states with Euclidean time, as opposed to the Lüscher method requirement of single-state saturation. While this method certainly reduces worry about one's ability to correctly resolve the closely spaced two-nucleon elastic scattering states, in practice, while the community has been exploring the engineering of good single-nucleon operators for well over a decade, it has been difficult to sufficiently suppress single-nucleon inelastic excited states, even for Euclidean times exceeding ~ 1 fm, except through the linear combination of multiple operators [187–189]. It has been shown by the CalLat collaboration [276] that clean projections onto elastic scattering states might be made simply through the use of different geometric configurations of the two-nucleons at the source (to the extent at which we trust that these are the correct energy levels, see above), while linear algebra methods are necessary to reduce the much larger inelastic state contamination, even at late times [278, 302] (see Figs. 5).

HAL QCD is also investigating the application of their method to more challenging channels, such as $I = 1 \pi\pi$ with the ρ resonance. Their first application uncovered issues with at least the application of smeared sinks when trying to map out the phase shift in this resonant channel [319]. However, a follow up publication found that with heavy pion masses, for which the ρ meson is deeply bound, the potential method and traditional methods agree on the spectrum [320], albeit it with a large quoted systematic uncertainty. More recently, they also studied the S -wave kaon-nucleon interactions [321]. For the existing applications of the potential to two-baryon systems, the time at which the potential is determined is earlier than the time at which the effective mass of the single nucleon correlation function plateaus, and therefore, there is an implicit assumption that

in the ratio correlation function, Eq. (12), the single nucleon excited states in the numerator and denominator cancel to the point of being numerically negligible when determining the potential. So far, it has not been explicitly demonstrated that this cancellation is exact enough as when the potential is constructed with larger Euclidean times, the noise becomes sufficiently large that it is not possible to detect a difference. This does not rule out the possibility of undetected inelastic pollution of the more precisely determined potential from earlier times.

With the potential method, failure to fully suppress inelastic excited states could show up as source operator dependence, or time dependence of the potential. HAL QCD explores both of these in Ref. [289]. They find that the overall potential appears independent of time using their wall sources for the single-nucleons by plotting the full potential for several different times and noting no significant deviations. However, no attempt is made to extrapolate to infinite times, nor are data points which are clearly trending in one direction with time taken into account. Points nearby in Euclidean times are highly correlated, and error bars tend to grow with Euclidean time, such that an observable with slow Euclidean time dependence can be easily misinterpreted, much the same as when studying plateaus in the Lüscher method. Furthermore, both the sizes of the time deviations and error bars vary with the spatial distance measured in the potential. A full study of excited state contamination might look much like it does for the Lüscher method: plateaus are demonstrated for each data point, $V(r)$ over several time ranges with no clear trend in the data pointing to a slow Euclidean time dependence, and/or extrapolations to infinite Euclidean time are performed for each point.

A second demonstration of the lack of excited state contamination in Ref. [289] comes from comparing the use of two different source operators. It is noted that at earlier times the potential produced using the two sources do not agree, but that they begin to at later times. However, the error bars on the potential from the smeared source have grown significantly at this point, so it is difficult to draw strong conclusions.

A similar argument may be made about studies of finite volume effects. Here again, the potentials are overlaid and no significant difference is seen. While worries about correlated statistical fluctuations are absent when comparing different volumes, the same principle that was presented in the previous paragraph for a satisfactory study of excited state dependence may be applied to finite volume. In particular, a study of the volume dependence for different spatial separations in $V(r)$ is crucial, and this must be done for each physical system of interest. Unfortunately, the tail of the potential at large r , which may be crucial for correctly identifying finely-tuned bound states in nucleon-nucleon scattering and is most likely to be affected by finite volume effects, often has the largest statistical error bars. Therefore, establishing volume independence by simply comparing multiple volumes is difficult in this region. See Sec. 3.3.7 for a nice treatment of incorporating the periodic boundary conditions into a two-nucleon interaction framework. Such a construction could be adopted in the HAL QCD potential analysis.

Finally, HAL QCD has investigated the effects of the cutoff in the gradient expansion. In Ref. [289] they use differences in the potentials calculated using different source operators to calculate the potential to the next order beyond LO ($N^2\text{LO}$). From this they conclude that, at least for the wall source, the LO potential is unchanged. An important assumption made here is that deviations from using different sources are due only to differences stemming from the cut off in the gradient expansion, and not to residual contamination from inelastic excited states (i.e. the potentials calculated using two different sources should agree as long as the gradient expansion has converged). While suggestive, this does not satisfactorily demonstrate convergence. It would

be ideal to independently show control over the inelastic excited state contamination and cut off in the gradient expansion: even if one could demonstrate the correlation function was free of all inelastic excited state contamination at early time, there would still be systematic uncertainties arising from the truncation of the gradient expansion. Furthermore, particularly because the gradient expansion does not have a well-defined small expansion parameter, showing convergence of a series necessitates at least the explicit calculation of multiple orders, compared independently to each other.

A resolution of the controversy remains unfortunately murky. Both methods have been defended against the criticism presented about them, though not in a completely satisfactory way. Irrespective of any potential issues within the HAL QCD potential method, HAL QCD has uncovered issues with the standard Lüscher calculations that must be resolved, and which are very suggestive that there are larger systematic uncertainties in the calculations than are currently reported. It is clear that new ideas and methods are needed to resolve the discrepancy, and additionally, cooperation to coordinate a set of gauge configurations on which all methods are performed, such that the discrepancy can be isolated to the method and its application. Some examples of further reading on the issues can be found in Refs. [278, 322–327].

Many members of the community agree that a resolution of the issue will require more sophisticated interpolating operators that allow for the construction of a hermitian, positive definite set of correlation functions including operators for which the individual momentum projection is performed at both the source and sink [328, 329].²

Such methods have not been used for two-baryon systems, with one recent exception [281], due to the significant increase in numerical cost associated with the method. The benefit of the method is that it generates a positive definite matrix of correlation functions that can be diagonalized by solving a generalized eigenvalue problem [330], with each eigenstate given by a linear combination of interpolating operators. This is the common practice in the LQCD calculations of two-meson systems [308, 331–339] (and now a first look at the three meson system [340, 341]). The momentum projection at the source further provides an additional volume averaging as compared to the methods with spatially fixed nucleon sources, whether they are local or non-local, such that the increased cost of the computations may not be as high as otherwise one might presume. Such a basis will allow for a much more confident determination of the true spectrum from the LQCD calculations. Of course, with finite statistics, and a finite operator basis, one can never be 100% certain of the results, but it will be a significant step forward from the current methods. Furthermore, one will be able to quantitatively address how much the momentum project at the sink works to isolate a single elastic scattering state.

Such a computation of the H-dibaryon was performed with a basis of momentum-space to momentum-space operators, and also compared the results to those arising from a hexa-quark interpolating operator, at a pion mass of $m_\pi \sim 960$ MeV [281]. A bound state was observed in the H-dibaryon channel using the momentum space operators just as NPLQCD [272] and HAL QCD [197, 303] observe at this heavy pion mass, and the value of the binding energy is consistent

²A step in this direction was proposed by CalLat, inspired by the Matrix Prony analysis methods used to analyze high statistics NPLQCD results [187, 189]. Rather than perform the Matrix Prony rotation after producing the correlation functions, one could first find an optimal single-nucleon through Matrix Prony and insert that nucleon into the two-nucleon contraction routine [278, 302]. This showed great promise, particularly when the displaced nucleon source operator was used [276]. However, this only suppresses contamination from the inelastic single-nucleon excited state and does not address the issue of the closely packed elastic scattering states.

with that reported by HAL QCD and not with the deep bound state observed by NPLQCD with $B \sim 80$ MeV. It was observed that the hexa-quark creation operator on its own also gave rise to a bound state, was consistent with the shallow bound state result, but had so much more stochastic noise that conclusions are difficult to be drawn. While suggestive that the deep bound state may be fictitious, one can not draw a strong conclusion, as the hexa-quark must be included in the same basis as the momentum space operators in order to rule out a deep bound state coupling strongly to the local hexa-quark operator. Furthermore, the lattice ensembles were different, and in this calculation, the strange quark was quenched, so that a direct comparison cannot be made to existing calculations.³ In Ref. [343], it was shown in quenched and partially quenched LQCD calculations, the long-range part of the potential has an extra term (which vanishes in the QCD limit, $m_q^{\text{val}} \rightarrow m_q^{\text{sea}}$) that scales as $(m_q^{\text{sea}} - m_q^{\text{val.}})e^{-m_\pi r}$ rather than the well known Yukawa potential, $\frac{1}{r}e^{-m_\pi r}$.

In order for the broader nuclear physics community to have confidence in LQCD results of two-nucleon interactions, two-nucleon electroweak and BSM matrix elements and more, it is critical to resolve this discrepancy.

2.3.2. Nuclear Structure and Reactions

One of the main goals of this big endeavor is to be able to predict the structure and reactions of nuclei with a quantitative connection to the Standard Model. Such matrix elements are related to the search for dark matter, permanent electric dipole moments in light and heavy nuclei, the search for $0\nu\beta\beta$, hadronic parity violation and more. Such calculations are numerically more challenging than the two-body interactions and they require additional formalism first introduced by Lellouch and Lüscher [344] to relate the finite volume matrix elements to the infinite volume transition amplitudes, a topic which has gained considerable attention as of late [246, 345–353].

The main challenge as of now for computing even two-nucleon matrix elements is that first, one must have sufficient control over the two-nucleon interaction calculations, which as we have just discussed, have a number of issues that must be resolved. In order to relate the finite volume matrix elements to their infinite volume counterparts, one need not only know the phase shift at a given energy, but one must also know the derivative of the phase shift. For transitions near a resonance or generically, when the interaction is strong, these correction factors can be $O(1)$ [347–353] or larger and so even if all that is required is a 20% uncertainty on some matrix element, these finite volume effects must be understood and controlled.

Despite these challenges, it is important to push the boundaries, and in particular, the NPLQCD Collaboration has performed a number of proof-of-principle calculations extracting two-nucleon matrix elements from LQCD: magnetic moments [354]; $np \rightarrow d\gamma$ [355]; pp fusion [65]; the isotensor axial polarizability [356]; $2\nu\beta\beta$ matrix elements [357]; the isoscalar scalar, axial and tensor matrix elements [66]; and a first calculation of gluonic matrix elements [358]. CalLat has performed a preliminary computation of the $I = 2$ hadronic parity violating amplitude for the NN system, also with heavy pion masses [97]. In each of these cases, the calculations were performed with sufficiently heavy pion masses that NPLQCD has found the initial and final two-nucleon states to be deeply

³In LQCD, if a quark is quenched, this is equivalent to sending its mass to infinity such that the fermion determinant associated with this flavor becomes a trivial multiplicative constant. Such techniques were common more than a decade ago as the majority of the HMC cost is associated with computing the fermion determinants. Quenching introduces an uncontrolled systematic error, but with a possible rigorous connection in the large N_c limit in which the fermion loops decouple [342].

bound. In this limit, the finite volume formalism mentioned above is not needed, and so it is still not understood exactly how challenging the computations will be. However, it is encouraging to see such calculations being performed. Hopefully soon, they will exist with sufficiently light pion masses that a direct connection with nuclear Effective (Field) Theories can be made, as discussed in the next section.

A more complicated application one can envision is the nuclear response to an axial current, as is needed to understand the neutrino-nuclear cross sections for the DUNE experiment [32, 33]. This program is quite challenging as what is needed is an understanding of the cross section with a momentum transfer of $O(1\text{GeV})$. This is precisely the region where both perturbative QCD and Effective (Field) Theory are not applicable. Nevertheless, there are still computations from LQCD that can be instrumental in reducing the systematic uncertainty in the modeling of the nuclear response functions.

First, LQCD can be used to determine the nucleon axial form factor for which a handful of calculations exist at the physical pion mass [359, 359–362] and extrapolated to the continuum limit [360, 363]. There remain non-trivial subtleties in understanding the excited state contamination in these calculations, in particular, the nucleon-pion state [316, 317, 364, 365]. The lattice community is beginning to try and incorporate such corrections [219, 366] though only the most recent is in close agreement with the strategy motivated by chiral symmetry constraints [367]. The second step is to perform calculations of the $N \rightarrow N\pi$ transition form factors (which has been demonstrated with mesons [368, 369]) as well as control over the πN scattering states [268]. Next, LQCD calculations of two-nucleon form factors must be performed. While a full LQCD calculation of the Argon response function will likely never happen, the one-, two- and few-nucleon matrix element calculations can be used as benchmarks that the Monte Carlo event generators can be calibrated against for light nuclear systems, such that some of the model dependence can be removed in the estimate of the full nuclear response function. They can also be used to constrain few-body corrections used in the nuclear EFT calculations, such as Ref. [370].

This is a very ambitious program, but we should see exciting progress towards these goals in the exascale computing era.

3. Nuclear Effective (Field) Theories

The evaluation of properties of light nuclei directly from LQCD will be extremely challenging due to the fermion sign problem, the exponential growth in noise with increasing nucleon number (see Secs. 2.1–2.3). But there is an attractive alternative for creating a controlled theory of finite nuclei based on QCD – an EFT/ET formulated in terms of nucleons (and possibly pions and deltas), for which the onset of the S/N problem can be postponed, if not mitigated all together, based upon the particular many-body method used. This approach can be successful because nuclei are relatively dilute fermi systems – the probability of finding clusters of nucleons acting at one time through strong, short-range interactions declines rapidly with the number of nucleons in the cluster.

EFT/ETs are naturally organized in terms of short-range terms, capturing the unresolved UV physics, from the long-range pion exchange effects and medium range effects arising from multi-pion exchanges etc. The short-range physics can be added back in through an effective-operator expansion, with coefficients that can be fitted either to experimental data, or alternatively taken from LQCD, once LQCD calculations reach the necessary precision in the exascale era. Low-momentum observables can then be predicted with quantifiable errors, determined from the rate of convergence

of the operator expansion. This coupling of LQCD and EFT/ETs is important for rooting our understanding of nuclear physics in the SM but becomes acutely important for observables related to BSM searches for which there is no alternative means of assessing the unknown short-distance physics.

EFT/ETs are powerful theoretical tools to describe physical processes over a specified range of energy scales in terms of effective instead of the fundamental degrees of freedom. The procedure is to construct the most general Lagrangian consistent with the symmetries of the underlying theory and then compute all Feynman graphs which contribute to a given process. “The result will simply be the most general possible S -matrix consistent with analyticity, perturbative unitarity, cluster decomposition, and the assumed symmetry principles” [371]. The EFT will only be effective if certain conditions are met. First, one should choose the effective degrees of freedom that are relevant at the energy scale of interest since this may impact the rate of convergence of the EFT considerably:

“You may use any degrees of freedom you like to describe a physical system, but if you use the wrong ones, you’ll be sorry.” [372]

For example, the small excitation energy of the delta resonance leads to resonance saturation of pion-nucleon couplings in the delta-less (Δ) EFT for nucleons, which renders these LECs (somewhat) unnaturally large and thus affects the convergence. For nuclear-physics applications, one might expect a faster convergence of delta-full EFT, where the delta resonance is treated as an explicit degree of freedom in addition to nucleons and pions.

Second, there must be a well-defined perturbative expansion to organize the infinite set of operators and their resulting Feynman diagrams. The parameter or parameters controlling this perturbative expansion most often arise from ratios of IR and UV scales, which set the bounds of validity of the EFT. For example, in chiral perturbation theory (χ PT) [373], a low-energy EFT of QCD, the pion mass naturally emerges as an IR scale.

χ PT is formulated to respect the approximate chiral symmetry of the QCD Lagrangian for the light quark flavors. Considering the up and down quarks, and neglecting their masses, the QCD action has a global $SU(2)_L \otimes SU(2)_R$ chiral symmetry. While the small light quark masses explicitly break this symmetry, the dominant chiral symmetry breaking arises from the spontaneous breaking from the QCD vacuum down to the vector subgroup, which is also known as isospin symmetry for the two light flavors. This spontaneous chiral symmetry breaking leads to a large splitting of the degeneracy of the parity partner states, such as the nucleon and the negative parity nucleon. It also gives rise to the relatively light pions that emerge as pseudo-Nambu-Goldstone bosons. Their masses, $m_\pi^2 \propto m_l$, vanish as the average light quark mass, m_l , goes to zero (named the chiral limit).

The masses of all other hadrons composed of light quarks, such as the rho-meson or the nucleons, do not vanish in the chiral limit and are of $\mathcal{O}(1)$ GeV. This emergent scale of QCD is also observed to be approximately the UV scale associated with chiral symmetry breaking, which has been phenomenologically determined to be $\Lambda_\chi \sim 4\pi F_\pi$ ($F_\pi \sim 92$ MeV). For sufficiently small external pion momentum of order of the pion mass, χ PT gives rise to a perturbative EFT, where the small parameter controlling the expansion is given by

$$\epsilon_\pi^2 = \frac{m_\pi^2}{\Lambda_\chi^2}. \quad (18)$$

This results in a rapidly converging perturbative expansion. One can then define a power counting scheme and work to a fixed order in ϵ_π^2 , retaining all Feynman diagrams that contribute to a given

process up to the specified order, $n \geq 0$. The order one works to, i.e., leading order (LO), next-to-leading order (NLO) etc., is set by the desired precision of the result as the theoretical uncertainty arising from the neglected contributions is expected to scale roughly as $(\epsilon_\pi^2)^{n+1}$, assuming the asymptotic nature of the expansion has not set in and that there are no unnaturally large coefficients in the expansion.

The strange quark mass is sufficiently light that it can be advantageous to formulate a three-flavor variant of χ PT based on an approximate $SU(3)$ chiral symmetry incorporating kaons and the eta pseudo-scalar meson [374]. $SU(3)$ χ PT is less convergent than the $SU(2)$ variant as the kaon mass is significantly heavier than the pion mass and the number of virtual states propagating in loop diagrams grows with the number of flavors N_F .

While the form of EFT/ET operators are restricted by the underlying symmetries, their scale- as well as scheme-dependent coefficients, the LECs, must be determined either through comparisons with the fundamental theory or by constraining the predicted amplitudes to reproduce experimental data. A critical aspect of EFTs is that the LECs are process independent. Therefore, assuming a converging expansion, if the LECs are constrained by one set of observables, they can be used to predict other observables. This makes EFT/ETs powerful and predictive.

Many of the LECs accompany operators which explicitly depend upon the quark masses and so they cannot be reliably determined through a comparison with experimental results alone. This is precisely where the interplay between LQCD and EFT allows us to build a quantitative bridge between QCD and low-energy EFTs of nuclear physics as we are free to vary the quark masses in LQCD calculations. Practically, LQCD calculations get more expensive as the light quark mass is reduced towards the physical value, for the reasons discussed in Sec. 2. The common practice has therefore been to perform calculations with the strange quark fixed near its physical value and with the light quark masses approaching their physical value from above.⁴ In the process, the LECs of $SU(2)$ and $SU(3)$ χ PT have been determined, the results of which are a central part of the FLAG reviews [55, 171].

For simple quantities, LQCD has been reliably used to explore in detail the range of convergence of the various formulations of χ PT. This has been performed for $SU(2)$ χ PT, see for example Refs. [378–380] and the review in Ref. [381]. It has been determined that an NLO extrapolation of pion quantities works well up to $m_\pi^{\text{max}} \sim 350$ MeV, provided the minimum pion mass used is near the physical value. The $N^2\text{LO}$ contributions can raise the range of convergence a little, but a complete breakdown occurs beyond $m_\pi \sim 500$ MeV [381]. For $SU(3)$ χ PT, it has been observed that the expansion to $N^2\text{LO}$ is sufficient to interpolate quantities about the physical strange quark mass, but that for a reliable determination of the $SU(3)$ LECs, such as the decay constant, F_0 and condensates $\langle \bar{q}q \rangle$ in the $SU(3)$ chiral limit, one is restricted to values of the strange quark mass $m_s \lesssim 0.7 m_s^{\text{phys}}$ [382]. To achieve the desired theoretical precision, $SU(2)$ χ PT with external kaons has been developed [383–385].

The inclusion of matter fields in χ PT, such as nucleons, is the subject of the next section. After discussing what we have learned from LQCD about the convergence pattern of baryon χ PT

⁴Another approach has been to hold the sum of the up, down, and strange quark masses fixed at their physical value and to approach the physical masses by reducing the light quark masses while simultaneously increasing the strange quark mass [375, 376]. This approach is also utilized by the CLS Collaboration [377]. While this method has advantages related to renormalization of Wilson fermions and smooth extrapolations to the physical mass point, from the χ PT point of view, it forces the use of an extrapolation that depends upon the kaon mass as well as the pion mass.

(Sec. 3.2) we turn to the EFT of the two-nucleon sector and its extension to many-body nuclear physics. NN EFT and nuclear chiral EFT are often reviewed in the literature. We therefore in this article focus not on an extensive review, but rather try and highlight specific places where we anticipate NN/chiral EFT making contact with LQCD and specifically, how LQCD may help improve our understanding of the EFTs. We instead refer the reader to these selected reviews [386–389] as well as a very recent and more in depth discussion of the interplay between NN/chiral EFT and many body methods as well as connections to LQCD [390]. We then provide a more in depth introduction to Harmonic Oscillator Based Effective Theory (HOBET), a non-relativistic theory of nuclear interactions (Sec. 3.3). We discuss the power counting of HOBET and compare and contrast it with other well-known strategies for many-body nuclear physics calculations such as the no-core-shell-model (NCSM), Quantum Monte Carlo (QMC), self-consistent Greens functions and lattice EFT, which are extensively discussed in the literature. We refer the reader to Refs. [391], [392, 393], [394, 395] and [396, 397], respectively, as well as references therein for more in depth reviews of these methods.

3.1. Single Nucleon Effective Field Theory

In building an EFT of nuclear structure and reactions, it is critical to verify that the single-nucleon EFT upon which it is built is converging. While a determination of the NLO LECs of χ PT with LQCD is now a standard component of the FLAG reviews [171], the situation is different for baryons: the most recent FLAG review [55] is the first to include baryon quantities.

The first challenge in incorporating nucleons in an EFT is that their masses do not vanish in the chiral limit, which complicates the power counting and the renormalization of the LECs [398]. Multi-loop corrections can generate finite contributions to the S -matrix elements that scale with arbitrarily large powers of M_0/Λ_χ , where M_0 is $\lim_{m_\pi \rightarrow 0} M_N$.

To overcome this challenge, Jenkins and Manohar developed heavy-baryon χ PT (HB χ PT) [399], inspired by heavy-quark effective theory [400], where a non-perturbative expansion is formulated about the rest mass of the nucleon in the chiral limit. In this way, the power counting is restored, as the nucleon mass only appears in inverse powers in the chiral Lagrangian, as well as in radiative loop corrections. The original formulation utilized the three-flavor expansion about the $SU(3)$ chiral limit, incorporating the interactions of the pions, kaons, and eta with the hyperons. It also incorporated the decuplet resonances as explicit degrees of freedom, given that the mass gap between the octet and decuplet baryons is comparable to the pseudoscalar meson masses.

A substantive difference in the chiral expansion of matter fields from the pseudoscalar mesons is that the loop corrections for matter fields generate odd powers of the meson masses. For example, the first non-trivial correction to the nucleon mass from virtual pions is given by

$$\delta M_N^{(3)} = -\frac{3\pi g_A^2}{2} \frac{m_\pi^3}{(4\pi F_\pi)^2} = -\frac{3\pi g_A^2}{2} \epsilon_\pi^3 \Lambda_\chi, \quad (19)$$

which is non-analytic in the quark mass as $m_\pi^2 \propto m_l$. We also observe that the coefficient of this NLO correction to the nucleon mass is large, $3\pi g_A^2/2 \simeq 7.6$. This is a common feature of baryon χ PT such that the convergence is challenged, not only by a larger expansion parameter, ϵ_π , as compared to ϵ_π^2 for pions, but also the coefficients appearing in the expansion tend to be larger than $\mathcal{O}(1)$.

When considering non-static quantities, such as form factors with some characteristic soft momentum scale q , it is common to denote Q as a generic small expansion parameter representing

both, the pion mass and the soft momentum scale in this double expansion. The chiral expansion is then expressed in powers of

$$Q = \frac{q}{\Lambda_\chi} \sim \frac{m_\pi}{\Lambda_\chi}, \quad (20)$$

where typically, the soft momentum scale is counted as the same order as the pion mass. Working to $\mathcal{O}(n)$ implies determining all corrections which scale as Q^n with respect to the LO contribution ($n = 0$). The corrections at different orders do not necessarily map to the same order for different observables. For example, the LO correction to the nucleon mass scales as $m_\pi^2/\Lambda_\chi = \Lambda_\chi Q^2$, the NLO, Eq. (19), as $\Lambda_\chi Q^3$, the N²LO as $\Lambda_\chi Q^4$ etc. In the literature, it is common to encounter results described as order Q^n and/or NⁿLO.

The non-relativistic treatment of the nucleon in HB χ PT leads to a power series expansion of all operators in inverse powers of the nucleon mass in the chiral limit, M_0 , as well as the chiral symmetry breaking scale, Λ_χ . Each new operator in this expansion is accompanied by an unknown LEC that must be determined. Some of the LECs can be exactly determined by enforcing Lorentz invariance perturbatively, which goes under the name reparameterization invariance [401]: the coefficient of the NLO kinetic operator is exactly fixed by the LO kinetic operator

$$\mathcal{L}_\partial = \overline{N} i v \cdot D N - \overline{N} \frac{D_\perp^2}{2M_0} N, \quad (21)$$

where v_μ is the four-velocity of the nucleon, D_μ is the chiral covariant derivative, and $D_\perp^2 = D^2 - (v \cdot D)^2$ [399, 401]. In the rest frame of the nucleon $v_\mu^T = (1, 0, 0, 0)$. This reparameterization invariance also ensures that the propagator for the nucleon has the expected non-relativistic kinetic correction, when such terms need to be included:

$$S_N(p) = \frac{i}{v \cdot p - \frac{\mathbf{p}^2}{2M_0} + i\varepsilon}. \quad (22)$$

The original formulation of HB χ PT was constructed for both the octet and decuplet baryons, as an expansion about the $SU(3)$ chiral limit. LQCD calculations of the baryon spectrum [402, 403] and meson-baryon scattering lengths [263] have established that this $SU(3)$ chiral expansion does not converge for these observables at the physical value of the strange-quark mass for a range of light-quark masses spanning the physical value. Given the larger value of the kaon and eta masses, and an expansion parameter that scales linearly rather than quadratically in these masses, this may not be surprising. However, this theory has enjoyed much phenomenological success and so it is instructive to use LQCD results to understand when the patterns of $SU(3)$ flavor symmetry breaking are expected to yield more than a qualitative guide to physical phenomena.

One approach has been to formulate observables based upon the combined expansions of large N_c [404, 405] and $SU(3)$ flavor [406–409]. In the large N_c limit, there is an extra contracted spin-flavor symmetry which further constrains the LECs. The HB χ PT Lagrangian constructed to incorporate these constraints is given in Ref. [410]. In the large N_c limit, the spin-1/2 and spin-3/2 states become degenerate, leaving the decuplet as stable asymptotic states. Their explicit inclusion is also necessary to observe the predicted suppression of certain radiative corrections as well [411].

The combined $SU(3)$ -flavor and large- N_c expansions lead to a predicted scaling of linear combinations of octet and decuplet masses. These were compared to LQCD results over a range of pion masses from 300–800 MeV, with the strange-quark mass held fixed near its physical value [402] with good qualitative agreement with these predictions [412]. This was studied in more detail in

Ref. [413]. Another interesting feature to emerge was the observation of evidence for non-analytic light-quark mass dependence in the spectrum. A restriction to a subset of the mass relations led to a determination of the $SU(3)$ axial couplings consistent with phenomenological determinations, $D = 0.70(5)$ and $F = 0.47(3)$, and a convergence pattern that is not immediately problematic [414]. Such studies led to a renewed interest in performing LQCD calculations with varying numbers of colors [415–417], which is required for a more extensive study of such mass relations, the convergence of HB χ PT, and a quantitative understanding of the patterns of $SU(3)$ flavor and large N_c symmetry breaking in QCD.

A practical approach to understand properties of hyperons has been to formulate $SU(2)$ EFTs for these states with external strange quarks [232, 383, 418–420]. The convergence pattern for the baryons should improve as the strangeness is increased since the value of the axial couplings to these hyperons decreases, thus reducing the strength of the pion-cloud corrections to observables. Such an $SU(2)$ flavor formulation for hyperons was not favorable during the advent of HB χ PT since there was insufficient experimental data to reliably constrain the extra LECs, which result for each strangeness channel. In the era of precision results from LQCD with near-physical pion masses, we can now reliably constrain these EFTs and use them to make a number of predictions.

Shortly after HB χ PT was formulated, the chiral Lagrangian for nucleons and pions based upon the approximate $SU(2)$ chiral symmetry was constructed [421]. The delta-resonances were not explicitly included and later, it was argued that below the resonance threshold, the dominant effects of these states could be incorporated in certain LECs through resonance saturation [422]. We denote this theory $SU(2)$ HB χ PT(Δ). Subsequently, $SU(2)$ HB χ PT including explicit delta-resonances was formulated, which has come to be known as the small-scale expansion (SSE) [423, 424], in which the delta-nucleon mass splitting, $\Delta = M_\Delta - M_N \approx 2m_\pi$, is treated as a small scale with the same counting,

$$Q = \frac{q}{\Lambda_\chi} \sim \frac{m_\pi}{\Lambda_\chi} \sim \frac{\Delta}{\Lambda_\chi}. \quad (23)$$

There is a long list of literature discussing the impact of including or not including explicitly delta-resonances in the EFT without a clear consensus; especially, one interesting idea of counting $\delta = \frac{m_\pi}{\Delta} \sim \frac{\Delta}{\Lambda_\chi}$ in the power counting [425]. Certainly, when the energy scale of the external probe, such as in Compton scattering, approaches the resonance region, a static treatment of the cross sections with the effects of the delta only contained within LECs is bound to fail. On the other hand, if one does not utilize large N_c , the delta-resonances are not asymptotic states and so care must be taken to incorporate them in the EFT [426]. See Ref. [427] for a review of nucleon Compton scattering in EFT which touches on these issues.

Including the delta-resonances in HB χ PT is not the only challenge the theory faces. One issue is the determination of the scalar matrix element at non-zero momentum transfer, which is often referred to as the sigma term. In this process, a new kinematic small scale enters the problem, $1 - \frac{t}{4m_\pi^2}$ with the Mandelstam parameter $t = q^2$. Neglecting this small parameter leads to an unphysical kinematic singularity. To remedy the problem, one is required to re-sum the NLO kinetic corrections to the nucleon such that the leading recoil term is included and the propagator is given by Eq. (22).

Alternatively, an IR regularization was introduced for baryon χ PT. The full relativistic nucleon field and an infrared regulator are used to separate the long-range pion effects with non-analytic dependence upon the quark mass from the short-range contributions, which exhibit only a polynomial quark-mass dependence [428]. Issues with carrying out this IR regularization beyond one-loop

led to a generalization that works for multi-loop integrals and is called the extended-on-mass-shell regularization [429–431]. It has been observed, but not understood formally, that these new regularization schemes tend to lead to improved convergence patterns as compared to HB χ PT for pion masses heavier than the physical values, and also for $SU(3)$ HB χ PT [432, 433]. It has also been observed that the use of a finite-range regulator, in the form of a dipole regulator [434], also improves the convergence pattern of HB χ PT [435, 436].

Lattice QCD is the perfect tool to help quantify which of these many EFTs and/or regularization schemes is preferred by QCD near the physical value of the pion mass. Over the last few years, this process has begun and most recently, we now have constraints from LQCD with precise calculations at the physical pion mass. In one of the earliest comparisons of baryon χ PT with LQCD results at relatively light pion masses, an interesting phenomenon was observed: to a very good approximation, independent of the discretization method, the nucleon mass scales linearly with the pion mass⁵

$$M_N \simeq 800 \text{ MeV} + m_\pi, \quad (24)$$

correctly predicting the nucleon mass at the physical point, $M_N = 938 \pm 9$ MeV [402, 437]. New results showed the same tendency with pion masses as light as $m_\pi \sim 175$ MeV [438, 439].

We know that this linear pion mass dependence cannot persist to arbitrarily small pion masses. The leading prediction for the pion mass dependence of the nucleon mass is m_π^2 , since $m_\pi^2 \propto m_l$, in all known, well founded theoretical descriptions of the nucleon. This linear pion mass dependence has at least two significant implications, however. If this dependence holds between the physical pion mass and $m_\pi \sim 200$ MeV, the predicted value of the pion-nucleon sigma term is $\sigma_{\pi N} \simeq 67 \pm 5$ MeV [438], which is in sharp contrast with other LQCD determinations [215, 222–225] and consistent with the phenomenological determination that uses low-energy pion-nucleon scattering constraints [227]. There might be underestimated systematic uncertainties in the LQCD determination of the sigma term, or it might be demonstrated that this phenomenological *ruler* fit is not consistent with sufficiently precise computations of the nucleon mass.

The more problematic implication is that in order to reproduce such a linear pion-mass dependence, the contributions to the nucleon mass from different orders in the chiral expansion have to conspire in such a way that there is almost no curvature. This can only happen through a delicate cancellation, which also arises from the cancellation of large terms [402, 437]. This does not bode well for $SU(2)$ HB χ PT having a well-converging expansion.

We can use a recent determination of g_A over a range of pion masses $130 \text{ MeV} \lesssim m_\pi \lesssim 400 \text{ MeV}$ [64] to explore the convergence in more detail. For example, downloading the Jupyter Notebook provided with this work,⁶ one can run the `xpt_3` and `xpt-full_4` analyses by selecting them from the `switches["ansatz"] ["type"]` list. These two analyses use the complete $N^2\text{LO}$ [440] and $N^3\text{LO}$ [441] $SU(2)$ HB χ PT(Δ) extrapolation formulae. The $N^2\text{LO}$ expression is given by the first line of the following $N^3\text{LO}$ expression,

$$\begin{aligned} g_A = & g_0 + c_2 \epsilon_\pi^2 - \epsilon_\pi^2 (g_0 + 2g_0^3) \ln(\epsilon_\pi^2) + g_0 c_3 \epsilon_\pi^3 \\ & + \epsilon_\pi^4 \left[c_4 + \tilde{\gamma}_4 \ln(\epsilon_\pi^2) + \left(\frac{2}{3} g_0 + \frac{37}{12} g_0^3 + 4g_0^5 \right) \ln^2(\epsilon_\pi^2) \right]. \end{aligned} \quad (25)$$

⁵Pseudo-numerologists will be amused to note that all the octet baryon masses exhibited linear pion-mass dependence, at a fixed strange quark mass, with slopes consistent at 1-sigma with 2/3, 1/2 and 1/3 for the Λ , Σ and Ξ baryons respectively [402].

⁶Clone the CalLat github repository at https://github.com/callat-qcd/project_gA.

In Table 1, we list the order-by-order contributions from these two extrapolations at the physical pion mass. As with the nucleon mass, the coefficient of the NLO \ln term is also large $g_0 + 2g_0^3 \simeq 5$. At face value, these results are indicative of a failing perturbative expansion. In the $N^2\text{LO}$ analysis, while the NLO contribution is significantly smaller than the LO contribution, the $N^2\text{LO}$ contribution has opposite sign and is twice as large as the NLO contribution. Adding a higher order contribution makes the convergence pattern worse. The NLO contribution becomes an order of magnitude larger, the $N^2\text{LO}$ contribution stays roughly the same, but the $N^3\text{LO}$ term is opposite in sign from NLO and almost as large. The $N^3\text{LO}$ analysis is a zero-degree-of-freedom fit, however, so definite conclusions can not be drawn, but if these results hold, it signals a breakdown of $SU(2)$ $\text{HB}\chi\text{PT}(\Delta)$, even at the physical pion mass.

The yet-to-be published results generated with those of Ref. [64] can also be used to explore the convergence pattern of the nucleon mass and explore the linear pion mass dependence, which we show in Fig. 6. We observe that these LQCD results are consistent with both the $N^2\text{LO}$ $SU(2)$ $\text{HB}\chi\text{PT}$ without delta extrapolation as well as the linear (in m_π) extrapolation. In this case, the slope is allowed to vary as a function of the discretization scale

$$M_N = M_0 + \alpha_1 m_\pi + \beta_1 m_\pi a^2, \quad (26)$$

where a is the lattice spacing. As before [402, 437], it is observed that over a large range of pion masses, the $\text{HB}\chi\text{PT}$ fit conspires to produce this very linear dependence observed in the LQCD results. In order to place better constraints on the range of convergence of $SU(2)$ $\text{HB}\chi\text{PT}(\Delta)$, a combined analysis of M_N and g_A is currently being performed, as the LECs of the two observables become coupled at NLO and beyond.

An exception to this poor convergence pattern is the QCD (vs QED) corrections to $M_n - M_p$. In this quantity, the NLO contributions cancel, leaving [442, 443]

$$\begin{aligned} \delta M_N = \delta & \left\{ \alpha_N \left[1 - \epsilon_\pi^2 \frac{6g_A^2 + 1}{2} \ln(\epsilon_\pi^2) \right] \right. \\ & \left. + \beta_N \epsilon_\pi^2 \right\}, \end{aligned} \quad (27)$$

where $2\delta \equiv m_d - m_u$. The coefficient of the $N^2\text{LO}$ \ln term is $\frac{1}{2}(6g_A^2 + 1) \simeq 5.3$. A LQCD calculation found strong evidence in support of this predicted non-analytic quark mass dependence as well as a converging expansion [444].

If $SU(2)$ $\text{HB}\chi\text{PT}(\Delta)$ does not converge, it is still possible that $SU(2)$ $\text{HB}\chi\text{PT}(\Delta)$ will be a converging EFT at low orders. For g_A , there is a partial cancellation between virtual corrections involving nucleon and delta loops, a consequence of the large N_c limit [406, 407]. However, for the nucleon mass, the virtual nucleon and delta corrections add with the same sign and are of a comparable magnitude. It is essential to have a set of LQCD results which determine the nucleon and delta spectrum as well as the matrix elements and transition matrix elements, such that a quantitative comparison with both Δ -full and Δ -less $\text{HB}\chi\text{PT}$ can be performed. Such results will be possible with exascale computing.

Table 1: Order-by-order contribution to g_A at the physical pion mass resulting from $N^2\text{LO}$ and $N^3\text{LO}$ $SU(2)$ $\text{HB}\chi\text{PT}$ extrapolation of the results in Ref. [64] without explicit delta degrees of freedom.

$N^n\text{LO}$	LO	NLO	$N^2\text{LO}$	$N^3\text{LO}$
$N^2\text{LO}$	1.237(34)	-0.026(30)	0.062(14)	—
$N^3\text{LO}$	1.296(76)	-0.19(12)	0.045(63)	0.117(66)

3.2. Chiral Effective Field Theory

Going beyond the single-nucleon sector, EFTs are the key ingredients for connecting LQCD results to *ab initio* nuclear structure and reaction studies across the nuclear chart. Rather than aiming for direct applications of LQCD to these nuclei [102, 103], the basic strategy is to constrain EFT/ETs from LQCD calculations in the two- and few-body sector and to use the derived potentials and external currents combined with *ab initio* many-body frameworks to solve the nuclear many-body problem. In this section, we give a brief overview of chiral EFT in Weinberg power counting and of RG-invariant chiral EFT, before discussing HOBET, an effective theory directly constructed in the harmonic oscillator basis [445–447], in the next Section.

Chiral EFT [387–389, 448–450] was pioneered by Steven Weinberg in the early 1990s [451–453]. Weinberg observed that, for systems with more than one nucleon, the power counting rules of χ PT cannot be applied directly to scattering amplitudes, because of the infrared enhancement of diagrams whose intermediate states consist purely of propagating, almost on-shell, nucleons. These (“reducible”) diagrams are enhanced by small energy denominators, scaling as p^2/M_N rather than p , and need to be resummed at all orders. The nonperturbative nature of nuclear scattering amplitudes manifests itself in the existence of bound states, i.e., the nuclei, which cannot be obtained in perturbation theory. On the other hand, (“irreducible”) diagrams whose intermediate states contain interacting nucleons and pions are not enhanced and follow the usual χ PT power counting. Weinberg realized that the S -matrix for scattering processes involving A nucleons is obtained by patching together irreducible diagrams with intermediate states consisting of A free-nucleon propagators; or, equivalently, by solving the Schrödinger equation for A nucleons with a potential V that is defined by the sum of irreducible diagrams. Chiral EFT, the EFT that extends χ PT to the $A \geq 2$ sector, provides a perturbative expansion of the nuclear potential and external currents in powers

$$Q = \frac{p}{\Lambda_b} \sim \frac{m_\pi}{\Lambda_b}. \quad (28)$$

Just as with the single-nucleon, Eq. (20), this is a double expansion in soft momentum and the pion mass, which are typically treated as the same order, as implied by this equation. If p is substantially different from m_π , in principle, one should work to different orders in p/Λ_b and m_π/Λ_b to have a fixed relative theoretical uncertainty. In practice, this is not very practical but



Figure 6: Extrapolation analysis of M_N versus the pion mass. The nucleon mass results are those determined in the published analysis of g_A [64], and the two-point correlation functions used are available with that publication. However, there has not yet been a dedicated publication of the nucleon mass results themselves, but one is in preparation by CalLat with updated statistics and new ensembles. The black dashed line is the fit from Refs. [402, 437] in 2008. The curved magenta band is the result of an N^2 LO $SU(2)$ HB χ PT(Δ). The gray band is the continuum-extrapolated result arising from a linear-in- m_π analysis using Eq. (26). The solid red, green, and blue lines are the central values from this analysis plotted at the three lattice spacings used in Ref. [64]. The black star is the physical value of the nucleon mass, which is not used in any fit.

purely of propagating, almost on-shell, nucleons. These (“reducible”) diagrams are enhanced by small energy denominators, scaling as p^2/M_N rather than p , and need to be resummed at all orders. The nonperturbative nature of nuclear scattering amplitudes manifests itself in the existence of bound states, i.e., the nuclei, which cannot be obtained in perturbation theory. On the other hand, (“irreducible”) diagrams whose intermediate states contain interacting nucleons and pions are not enhanced and follow the usual χ PT power counting. Weinberg realized that the S -matrix for scattering processes involving A nucleons is obtained by patching together irreducible diagrams with intermediate states consisting of A free-nucleon propagators; or, equivalently, by solving the Schrödinger equation for A nucleons with a potential V that is defined by the sum of irreducible diagrams. Chiral EFT, the EFT that extends χ PT to the $A \geq 2$ sector, provides a perturbative expansion of the nuclear potential and external currents in powers

$$Q = \frac{p}{\Lambda_b} \sim \frac{m_\pi}{\Lambda_b}. \quad (28)$$

Just as with the single-nucleon, Eq. (20), this is a double expansion in soft momentum and the pion mass, which are typically treated as the same order, as implied by this equation. If p is substantially different from m_π , in principle, one should work to different orders in p/Λ_b and m_π/Λ_b to have a fixed relative theoretical uncertainty. In practice, this is not very practical but

it is understood, for small momenta, the truncation uncertainty will be dominated by the m_π expansion while at large momenta, the derivative truncation uncertainty will dominate [454]. A more sophisticated treatment of the truncation error, with a smooth momentum interpolation, has been constructed in a Bayesian framework [455].

Unfortunately, unlike the single-nucleon case, the breakdown scale Λ_b , which is largely phenomenologically motivated from so-called Lepage plots [456], is found to be lower than Λ_χ and even lower than $m_\rho \approx 770$ MeV; typically, $\Lambda_b \sim 500$ MeV, so Q is usually larger than in the single-nucleon case,

$$Q \sim \frac{m_\pi}{\Lambda_b} \approx \frac{140 \text{ MeV}}{500 \text{ MeV}} \approx \frac{1}{3}. \quad (29)$$

When considering processes in which all momenta $p \ll m_\pi$, pionless EFT [386, 457–461] is a powerful approach. In pionless EFT, pions are treated as heavy degrees of freedom and strong interactions are represented by contact two-, three- and higher-body operators, supplemented by long-range electromagnetic interactions. The double expansion in Eq. (28) reduces to a single expansion in p/Λ_b , with breakdown scale $\Lambda_b \sim m_\pi$, which becomes increasingly accurate when lowering p^2 . The power counting of pionless EFT is built around the fine tunings observed in the 1S_0 and 3S_1 channels. In the NN sector, the theory contains two S -wave LECs at LO that can be determined in terms of the S -wave scattering lengths, or of the deuteron binding energy and the position of the 1S_0 virtual state in the complex plane. At $\mathcal{O}(Q)$, there appear two two-derivative interactions, which are fit to the 1S_0 and 3S_1 effective ranges. All remaining interactions, including, e.g., contact interactions in the P -waves, arise at $\mathcal{O}(Q^2)$ or higher. In the three-body sector, the integral equations for the nd scattering amplitude in the doublet channel computed with only short-range two-body forces do not have a unique solution in the limit of infinite regulator cutoffs [459, 462, 463]. This demands the inclusion of a single LO three-nucleon (3N) force [459, 462, 463], which can be fit, e.g., to the triton binding energy or the nd scattering length. A two-derivative 3N force appears at $\mathcal{O}(Q^2)$ [464]. No four-nucleon (4N) force is needed at LO [465]. Pionless EFT has been shown to converge very well in the NN [460, 461] and 3N sector [466, 467], while recently studies of nuclei as heavy as ${}^{16}\text{O}$ and ${}^{40}\text{Ca}$ have been performed [468, 469]. The determination of how far in A and to which class of nuclei and observables the reach of pionless EFT extends is an open subject of investigation. In addition to purely QCD processes, pionless EFT has been used to calculate electromagnetic form factors [470, 471], weak processes such as $np \rightarrow d\gamma$, proton-proton fusion, tritium β decays and di-neutron two-neutrino double beta decay [357, 472–474], and low-energy parity-violating NN scattering [475–477]. These calculations usually involve new NN LECs, which can be fitted to data, or to LQCD simulations [65, 355, 478].

Chiral interactions up to $N^4\text{LO}$ are shown in Fig. 7. The potential receives long- and intermediate-range contributions from one- and multiple-pion exchanges, respectively, and short-range contributions from physics at scales beyond Λ_b . While the importance of the long- and intermediate range components follows from the power counting of χ PT in the one-nucleon sector, a crucial assumption of Refs. [451–453] is that also the size of short-range interactions is determined by naive dimensional analysis (NDA) [451, 452, 480]. This assumption defines the organization scheme of chiral EFT operators that is commonly named Weinberg power counting (WPC). In WPC, the nuclear potential at LO consists of a two-nucleon component V_{NN} , given by the long-range 1π -exchange potential and by two S -wave chiral-invariant contact interactions, C_S and C_T . Soon after Weinberg’s seminal papers, the derivation of V_{NN} was extended to $N^2\text{LO}$, where 7 contact operators (up to P -waves) as well as the 2π exchange potential enter the expansion [481–484]. This $N^2\text{LO}$ potential

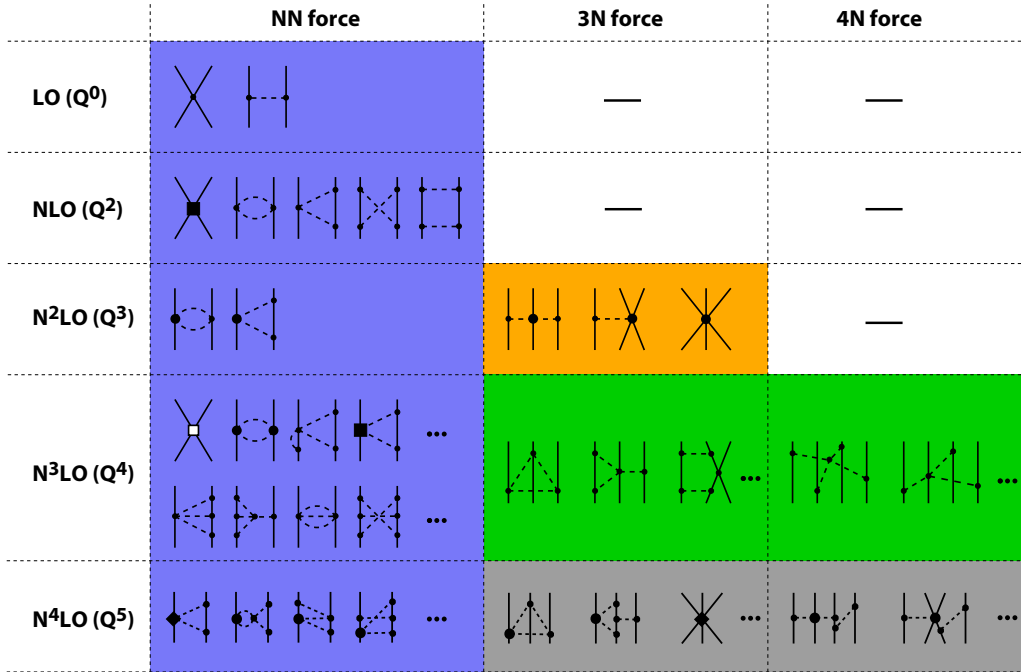


Figure 7: Hierarchy of chiral nuclear forces up to N^4LO in WPC. Nucleons (pions) are depicted by solid (dashes) lines. Blue-, orange-, and green-shaded diagrams are available for many-body calculations, whereas the gray-shaded interactions are under development (3N forces) or have not been worked out yet (4N forces). The figure has been modified from Ref. [479], see also Refs. [388, 448].

yields a good description of NN scattering data. With the inclusion of $\mathcal{O}(Q^4)$ [388, 485, 486] and $\mathcal{O}(Q^5)$ corrections [454, 487, 488], chiral EFT potentials are now able to fit scattering data up to laboratory energy $E_{\text{lab}} \sim 300$ MeV with a $\chi^2/\text{datum} \sim 1$ [388, 485, 487, 488], comparable to high-quality phenomenological potentials such as Argonne v_{18} [388] (see Refs. [387–389, 449] for detailed reviews). This impressive success, coupled with the theoretically appealing connection to QCD, has generated great interest in the nuclear structure community, and chiral potentials and currents are increasingly being used in *ab initio* calculations of nuclear properties, weak transitions, and BSM nuclear matrix elements.

The unknown LECs in chiral and pionless EFT can, in principle, be determined directly from QCD, but are usually fit to experimental data due to the challenging nonperturbative nature of low-energy QCD. There is, however, a subtle distinction as pointed out in Ref. [468]: when fitting to LQCD data, the predictions of the resulting EFT are consequences of QCD itself, whereas when matching to experiment, consequences of any underlying theory having the same (low-energy) symmetries as QCD. The first LQCD calculations of light nuclei have been performed a few years ago with pion masses of $m_\pi \sim 800$ MeV [272, 274], 510 MeV [273] and 300 MeV [200]. Pionless EFT has been matched to the results at $m_\pi \sim 800$ MeV [468, 469, 489, 490] and 510 MeV [490] and used to compute lattice nuclei including ^{16}O [468, 469] and even ^{40}Ca [469].

This matching was performed by taking the binding energies computed from LQCD as input to the pionless EFT. For NN interactions, the Lüscher method can be used to convert the finite

volume energy levels to infinite volume phase shifts, which can be used to constrain parameters of the EFT directly, or through an effective range expansion, see for example Ref. [274].

Alternatively, for non-relativistic systems, one can construct the EFT/ET in a finite volume. If done properly, this will include all the unphysical partial-wave mixing that occurs in a periodic volume with cubic instead of the full $\mathcal{O}(3)$ symmetry of the infinite volume. These effects become significantly more important for boosted systems where the center-of-mass momentum is not zero and the partial-wave mixing is enhanced. Instead of processing the results through the Lüscher method, or the equivalent for three or more nucleons, one directly matches the energy levels in the finite volume by tuning the volume of the EFT/ET to match that of the LQCD calculation. See Sec. 3.3.7 for more details. For two-baryon systems, this direct matching will likely involve an equivalent amount of effort as applying the Lüscher method, but when LQCD calculations of three or more baryons become common, particularly those which include scattering states as well as the bound nuclei, it will likely be simpler to match the EFT/ET calculations to LQCD results of the energy spectrum and directly determine the LECs, rather than process them through the multi-body Lüscher formalism that is being developed [251–253, 257].

A first step in this direction explored the two-neutron system, using auxiliary-field diffusion Monte Carlo [392, 393, 491], in an S -wave at zero total momentum in finite volumes of various sizes [492]. The volumes were sufficiently large that the partial-wave mixing was irrelevant at the precision computed, but also, out of reach for present and projected near future LQCD calculations, except for the smallest one (see Ref. [493] for how this will work for three- and four-neutron systems). The determination of LECs in the nuclear EFT/ETs will become particularly exciting as LQCD computations progress and can be used to compute properties of systems in which experimental data is controversial, limited or unavailable, such as few-neutron systems, see, e.g., Ref. [494], and few-baryon systems with one or two hyperons.

One particular scheme that could be imagined is a direct matching between LQCD calculations of few-nucleon systems (the spectrum and reactions to external probes) and the lattice regularized nuclear EFT (NLEFT) we mentioned earlier [396, 397]. NLEFT [495, 496] is the formulation of chiral EFT with a lattice UV regulator. As such, it is natural to simulate on a finite lattice and one could imagine constructing the lattices to match the volumes in size and boundary conditions directly to the LQCD calculations. On its own, NLEFT has been successfully utilized to describe properties of light and medium nuclei, beginning with constraints in the two- and three- nucleon sectors to constrain the experimental phase shifts and binding energies. One of the first significant successes was the description of the Hoyle state [497], one of the more famous fine-tunings in nuclear physics critical to stellar nuclear fusion [498] which is related to the clustering of α particles [499]. These methods were also utilized to describe alpha clustering in ^{16}O [500], showing the predictive reach of NLEFT. Then, BSM currents constrained with LQCD in two- and three- nucleon systems could be propagated into calculations of nuclei using this scheme.

To gain confidence in a theory of nuclear structure and reactions based on this coupling between LQCD and EFT/ET, it is important that the theoretical uncertainties in the EFT/ET expansion are well understood and under control. The size of the expansion parameter in Eq. (29) is such that the perturbative expansion will converge, albeit slowly, provided the LECs are natural and one can work at low-enough orders. As is common in χ PT and baryon χ PT, the theoretical truncation error can be estimated from the first order not included in the analysis [454, 501]. Such theoretical error estimates were applied to few-body calculations [502–507] and nuclear-matter calculations [508, 509]. More recently, Bayesian methods have been developed for parameter [510,

[511] and truncation-error estimation [455, 512, 513].⁷ Bayesian inference of breakdown scales, model checking and selection give important insights into the efficacy of EFT expansions. A comprehensive recipe for Bayesian uncertainty quantification in nuclear physics has been worked out by the BUQEYE collaboration [514]. The connection with NLEFT also would provide a natural means to assess the convergence pattern and associated theory uncertainty since it is formulated in chiral EFT, and thus also prescribes a specific quark mass dependence, which could hopefully be used to match to LQCD computations at heavier than physical quark masses before those at the physical quark mass are available.

Chiral interactions, moreover, require an UV regularization scheme (that cuts off high momenta) associated with a cutoff scale Λ_{UV} [454]. Although the regulator choice should be arbitrary, due to the renormalization issues discussed below, in practice the actual functional form can have important consequences at a given order in the chiral expansion due to induced regulator artifacts [515]. This freedom has recently led to the development of various new families of chiral NN potentials with conceptually different regulators schemes: nonlocal [109, 487, 516–518], local [519, 520], and semilocal regularization in, both, coordinate [454, 501] and momentum space [488]. An overview of these NN potentials including a comprehensive Weinberg eigenvalue analysis can be found in Ref. [521]. Recently, the first study of selected properties of light nuclei up to $A = 16$ based on semilocal coordinate-space regularized NN and 3N forces at $N^2\text{LO}$ was presented by the LENPIC collaboration [507].⁸ There is evidence for the convergence of chiral EFT for NN scattering observables at the physical pion mass, for the moderate values of the ultraviolet cutoff (Λ_{UV}) typically used in nuclear calculations ($\Lambda_{\text{UV}} \sim 400 - 600$ MeV) [455, 501]

An important point to take into account when discussing theoretical uncertainties is the consistency of the EFT itself, and in particular whether the LECs included at each order are sufficient to guarantee that observables are insensitive to unphysical regulators introduced in intermediate steps of the calculation. Weinberg’s original papers did not address the subtle issue of renormalizability of scattering amplitudes. The singular nature of the LO NN potential, arising either from the contact interactions, which parameterize the “hard-core” of the nuclear force, or from the $1/r^3$ behavior of the tensor component of the 1π exchange potential, requires the aforementioned UV regulator in the solution of the Schrödinger equation. If the theory is correctly renormalized, observables should depend on inverse powers of Λ_{UV} , so that by taking $\Lambda_{\text{UV}} \gtrsim \Lambda_b$ one can ensure that the theoretical error is dominated by missing orders in the chiral EFT expansions, rather than by regulator artifacts. Kaplan, Savage, and Wise first pointed out that the requirement of nonperturbative renormalizability, essential for a consistent EFT, leads to conflicts with the NDA expectations of the scaling of contact interactions, which are based on perturbative arguments [480]. In Ref. [522], they realized that the interference between contact interactions and pion-exchange leads to logarithmic divergences proportional to $m_\pi^2 \log \Lambda_{\text{UV}}$ in the LO scattering amplitude for two nucleons in the 1S_0 channel. This divergence can be absorbed by a counterterm proportional to the quark mass, which, however, only appears at NLO in WPC. Renormalization requires the promotion of this counterterm to LO; or, alternatively, the demotion of the pion-exchange to subleading order [523, 524]. As we will discuss, this problem appears in essentially the same form for all long-range potentials with $\sim 1/\mathbf{q}^2$ behavior (at large $|\mathbf{q}|$), acting in the 1S_0 channel, e.g., photon exchange,

⁷The BUQEYE collaboration provides the well-documented Python package `gsum`, which allows analyzing the convergence pattern of EFT observables using Bayesian methods. See <https://buqeye.github.io> for more details.

⁸See also <http://www.lenpic.org>.

relevant for charge-independence breaking in NN scattering, or light-Majorana-neutrino exchange, important for $0\nu\beta\beta$. In all these cases, the renormalization of scattering amplitudes requires the long-range potential to be complemented with a short-range contact interaction, enhanced by two powers of $1/Q$ with respect to NDA [461, 525–527].

In the case of the strong interaction, the issue pointed out in Ref. [522] led Kaplan, Savage, and Wise [523, 524] to propose a different power counting scheme, in which pions are perturbative (KSW). Such a scheme works well in the 1S_0 channel, where the N²LO calculation of Ref. [528] satisfactorily reproduces phase shifts. However, the KSW power counting dramatically fails to converge in the $^3S_1 - ^3D_1$ and 3P_0 channels [528, 529], where pion-exchange plays a more important role. For the S -waves, an expansion around the chiral limit was proposed [530] in which the difference between the 1π exchange contribution at non-zero quark masses and in the chiral limit occurs at the same order as the $\mathcal{O}(m_\pi^2)$ counterterms. This expansion coincides with KSW in the 1S_0 channel, and with WPC in the $^3S_1 - ^3D_1$ channel, capturing the most desirable features of both schemes.

The iteration of the 1π exchange potential, however, leads to a second problem, highlighted by Nogga, Timmermans, and van Kolck in Ref. [531] (see also Ref. [532]). The authors found that in each attractive triplet wave where the 1π exchange is iterated, the r^{-3} singularity leads to divergences that require a contact interaction for renormalization. With the exception of the $^3S_1 - ^3D_1$ channel, these contact interactions only appear at higher orders in WPC. Their promotion would, of course, destroy the predictive power of the theory, since an infinite number of LECs would need to be fitted already at LO. Fortunately, in most higher partial waves the pion exchange is a small effect that can be treated in perturbation theory [531]. There are strong indications that 1π exchange is perturbative in the $^3P_2 - ^3F_2$ coupled channel, in the D -waves, and in all partial waves with $l > 3$ [528, 529, 533, 534]. This would imply that a local counterterm needs to be promoted to LO only in the 3P_0 wave. The need for a LO contact interaction in the 3P_0 channel also emerges in Lorentz-invariant formulations of chiral EFT [535, 536].

This work forms the basis of a renormalizable version of chiral EFT (i.e., RG-invariant chiral EFT) aimed at curing the shortcomings of WPC and KSW discussed above, which is an active field of research. The issue of how to incorporate subleading corrections has been discussed in Refs. [537–539], which included $\mathcal{O}(Q^2)$ corrections, while studies of the 3N sector have been carried out in Refs. [531, 540], and processes involving external weak currents have been studied in Ref. [541]. We stress that the consistency checks of the power counting of chiral operators that are provided by renormalization studies are particularly important for observables sensitive to BSM physics. In these cases, the ambiguities in the power counting cannot be resolved by including high-enough orders and fitting to data, but, to retain predictive power, it is necessary to identify all the needed operator structures at a given order. See Sec. 4.1 for an explicit example.

While providing a theoretically robust framework, RG-invariant chiral EFT has not achieved the same level of success as WPC. The main challenge for extending RG-invariant chiral EFT to higher orders and to systems with more nucleons is that subleading potentials become increasingly more singular than r^{-3} . While this is not an issue when the higher-order potentials are treated in perturbation theory [537–539], it might destroy renormalizability when the entire potential is iterated at all orders [537], as customarily done in WPC and in standard nuclear-structure calculations. On the other hand, a perturbative approach complicates the interface with *ab initio* many-body methods, to which the chiral potential in WPC can be applied straightforwardly. The success of WPC [388, 485, 487, 488], raises the possibility that WPC with cutoff variation in a small

window $Q < \Lambda_{\text{UV}} \lesssim \Lambda_b$, with the inclusion of sufficiently high orders, and with the appropriate choice of regulators might be equivalent to RG-invariant chiral EFT, an issue that is not fully settled [389]. We now return to the description of chiral EFT in WPC, its successes, and the role that LQCD can play in improving its predictive power.

Coming back to Fig. 7, we see that, in addition to organizing interactions in the NN sector, one success of chiral EFT, both in WPC and in its RG-invariant version, is that many-body forces appear naturally but are suppressed, i.e., $V_{\text{NN}} \gg V_{3N} \gg V_{4N} \dots$, so the total Hamiltonian up to N⁴LO reads

$$H(\Lambda; \lambda) = T + V_{\text{NN}}(\Lambda; \lambda) + V_{3N}(\Lambda; \lambda) + V_{4N}(\Lambda; \lambda), \quad (30)$$

where Λ (λ) is a momentum cutoff scale (resolution scale). The first nonvanishing 3N forces appear at N²LO (orange-shaded). The long-range 2π exchange is governed by the LECs $c_{1,3,4}$, consistent with the NN forces at this order. Different determinations of these LECs from πN or NN data show significant deviations but agree within the uncertainties (see Table I in Ref. [449]). Only a few years ago, Hoferichter *et al.* have significantly improved this through a low-energy analysis of πN scattering in the framework of Roy-Steiner equations [542, 543], with remarkably precise constraints on the πN LECs. The unnaturally large values for $c_{3,4}$ are due to resonance saturation [544–546] since Δ -resonances, are not explicitly included in the EFT. Including Δ -resonances, in general, is found to improve the rate of convergence of chiral EFT, so progress is made in deriving delta-full EFT to high orders [546–548].

The 3N LECs, c_D and c_E , emerge from the 1π -exchange-contact and the pure 3N contact interaction, respectively, which are usually fit to the ^3H binding energy combined with, e.g., the charge radius of ^4He [549], the ^3H β -decay half-life [550], or the nd scattering cross section [507, 551]. Also constraints from the empirical saturation point of nuclear matter have been studied recently [509]. There are no additional contact interactions from N²LO NN forces. At N³LO, subleading 3N interactions as well as first 4N forces (green-shaded) contribute without introducing unknown parameters. They depend, however, on the LO LECs $C_{S,T}$. Furthermore, 12 contact interactions⁹ (up to D -waves), contribute to the 2π exchange, and the leading 3π exchange are present. The derivation of the N⁴LO 3N interactions is work in progress [552–554], whereas the N⁴LO 4N forces have not been worked out yet (gray-shaded), making N³LO the highest order for consistent calculations including all many-body contributions up to this order.

In addition, significant progress in developing new optimization methods for nuclear interactions [109, 516, 517, 555], investigating Δ -full chiral potentials [556–558], studying the chiral convergence order-by-order up to N⁴LO [454, 487, 501, 518], even partly up to N⁵LO [559], and applying Similarity Renormalization Group (SRG) [560] techniques to systematically soften nuclear potentials for improving the convergence of many-body calculations [104, 549, 561, 562] along with advances in *ab initio* frameworks [563] has led nuclear physics to an era of precision [479].

The quantitative study of the weak sector of the SM and of nuclear observables sensitive to BSM physics requires the construction of external currents and symmetry-violating potentials. The strength of the chiral EFT approach is that currents and BSM potentials can be constructed consistently with the nuclear interactions, allowing for systematic and controlled calculations of weak and BSM processes. The electromagnetic currents and the SM vector and axial currents have been derived at N³LO [62, 63, 564, 565], resulting in precise calculations of magnetic moments and weak transitions in light nuclei [566, 567]. In particular, Ref. [567] showed that the “quenching”

⁹Three out of 15 LECs could be eliminated in recent chiral NN potentials using unitary transformations [488].

of g_A , required for shell-model calculations to reproduce the observed Gamow-Teller strengths in light nuclei, can be explained by the inclusion of enough correlations in the few-body wavefunctions and of two-body weak currents. Ref. [568] found a similar solution to the g_A quenching problem in medium-mass nuclei, by combining chiral EFT potentials and currents with many-body methods such as coupled-clusters and in-medium SRG (IM-SRG). Chiral EFT currents for DM-nucleus scattering have been considered at NLO [61], and have been used for calculations in light [569, 570] as well as heavy systems [571, 572]. At higher orders, the currents depend on new LECs, which cannot be extracted from data. LQCD calculations of, for example, scalar and tensor currents in light nuclei [66] will allow the determination of such LECs, an important task for precision calculations.

The NN chiral PV potential [92, 573, 574] and TV potential [575–579] have also been calculated at NLO, extending and completing phenomenological derivations [91, 580, 581]. Already at LO these potentials contain unknown LECs, whose first principle determination is crucial for testing the SM and for connecting nuclear EDMs with microscopic sources of CP violation. We conclude this section by summarizing the impact that LQCD calculations in the NN and 3N sector can have:

- LQCD will enable a study of the dependence of nuclear observables on fundamental QCD parameters, in particular the light quark masses. This study will directly address the issue raised in Ref. [522]. If the LECs accompanying the short-distance NN operators are found to have significant pion mass dependence, this is indicative that the short distance quark mass dependent operator should be promoted to LO to have a consistently renormalized theory. If the quark mass dependence is mild, this is indicative that the perturbative pion treatment is more appropriate [523, 524]. Resolving this question will enable an understanding of fine tunings observed in nuclear physics, such as the large scattering length and large effective range in the 1S_0 channel or the small binding energy of the deuteron, and guide us towards the establishment of a power counting which incorporates these fine tunings;
- Calculations of pion-nucleon and pion-nucleus scattering, of the ^3H GT matrix element, and of three-nucleon scattering will allow a first principle determination of low-energy constants such as $c_{1,3,4}$, c_D and c_E that enter chiral 3N forces at N^2LO , validating existing extractions or shedding light on how the theory may need to be improved. Related, c_1 is the LEC that gives the dominant contribution to the pion-nucleon sigma term ($\sigma_{\pi N}$) relevant to direct dark matter detection in which the phenomenological determination of $\sigma_{\pi N}$ [227] is in significant tension with the LQCD determination [215, 222–225]. A direct determination from LQCD may clear up this discrepancy or shed light on further issues. Finally, LQCD can provide a window on three-neutron interactions, which are not well determined experimentally;
- LQCD will provide a first principle determination of the YN and YNN interactions that are challenging to determine due to the limited experimental data. The limited constraints on our understanding of these hyper-nuclear interactions means we do not know if there are similar fine tunings or other issues present in these interactions that must be understood to form a converging EFT. For example, there is an indication from LQCD that the $n\Sigma^-$ interaction in the 3S_1 channel is strongly repulsive [150], although the conclusions rely on an expansion about the $SU(3)$ chiral limit. There also exist several calculations of YN interactions using the HAL QCD potential method including results at the physical pion mass [299]. Significant progress in understanding YN and YNN interactions will come from the comparison of the $SU(2)$ chiral EFT [232] with forthcoming LQCD results extrapolated to the physical pion mass point;

- For applications to searches of BSM physics, LQCD can determine LECs in the two-nucleon sector, which, in the case of BSM currents, cannot be extracted from data. Examples that we already mentioned are the short-range components of the two-body scalar and tensor charges, relevant for DM searches or searches of non-standard contributions to β decays, the short-range component of the neutrino potential for $0\nu\beta\beta$, and the parity-violating as well as parity- and time-reversal violating NN interactions. These calculations are necessary for the interpretation of low-energy probes of BSM physics. In addition, as we will further discuss in Sec. 4, they will allow to check the power counting of the EFT, and to quantitatively assess the impact of the renormalization issues discussed earlier.

3.3. Nuclear Effective Theory: HOBET

Harmonic Oscillator Based Effective Theory (HOBET) [445–447, 582–585] is an ET designed for traditional nuclear physics and its well-developed machinery – specifically, large-scale diagonalizations of Hamiltonians in an explicitly anti-symmetric Slater determinant basis over single particle harmonic oscillator (HO) states. HOBET was built to allow one to proceed from QCD to the nuclear scale in a single step, so that the effective interaction one constructs is precisely that needed for many-body calculations, with no cutoffs entering other than those that define the nuclear space. HOBET avoids the construction of a high-momentum NN interaction entirely.

HOBET starts with the Bloch-Horowitz equation, which is a formally exact expression for the effective interaction in a potential theory. The ET expansion is constructed from the well-known Talmi integrals [586], generalized for a nonlocal interaction, systematically removing r^n -weighted Gaussian moments of the interaction (with the known long range pion contribution removed). More formally, this expansion is systematic in the lowering operators of the harmonic oscillator, and is complete in any finite HO space. HOBET truncates this short-range expansion at a designated order. The pionful version represents all higher-order Gaussian moments – Talmi integrals lacking an LEC – by the pion contribution. The ET expansion has the attractive feature that the pion plays no role at short range, removing the difficulties that arise in EFTs that treat the tensor interaction as a $1/r^3$ potential between point nucleons, requiring care near $r = 0$.

HOBET preserves all symmetries of the original non-relativistic theory, including Galilean invariance. HOBET results are independent of the length scale defined by the oscillator parameter b and the quanta cutoff Λ defining the maximum energy of Slater determinants in the included space P . The rate of convergence does depend on the choice of these parameters, and is typically optimized by selecting b near $\sim 1/m_\pi \sim R$, where R is the nuclear radius. The theory is highly convergent for values of b in this natural range. This convergence has been explored in potential models and shown numerically to correspond to powers of bm_ρ where m_ρ represents the inverse range of the omitted short-range physics – as would be expected from the Talmi integrals themselves.

The HOBET expansion can be shown to correspond quite closely to those of conventional chiral EFTs, though with differences that arise because the included space is defined in terms of the total quanta in a multi-nucleon Slater determinant, while the chiral EFT cutoff is typically given by the momentum of individual nucleons. Chiral EFTs typically yield soft interactions appropriate for a momentum scale ~ 500 MeV, so that additional transformations are needed to derive an interaction appropriate for the still softer Hilbert spaces used in HO-based nuclear calculations. HOBET is a non-relativistic ET, as described in Sec. 3, that takes one directly from QCD to the Hilbert space most commonly used in non-relativistic many-body calculations, using phase shifts or a finite volume spectrum derived from NN LQCD calculations to fix the LECs in the ET expansion.

Unlike the EFT approaches previously discussed, which involve an operator expansion around $\mathbf{q} = 0$, HOBET’s expansion is around an intermediate scale defined by the HO oscillator parameter b , mimicking the balance nature strikes between kinetic energy minimization via delocalization, and potential energy minimization by grouping nucleons together, near the peak of the midscale nuclear attraction. The coordinate space/momentun space conjugacy of the HO captures this physics well. The HO has another property that is crucial, the ability to exactly preserve (Galilean) translational invariance. But with these properties comes a wrinkle that makes the ET quite interesting: a discrete HO basis excludes both UV and IR contributions. This requires one to organize the effective interaction to isolate short-range terms from longer range ones associated with the kinetic energy operator. This separation allows one to incorporate chiral symmetry into HOBET quite simply, through pionic interactions that act exclusively at relatively long range. This comes about because HOBET’s effective interaction can be expressed in terms of a single, complete operator expansion: the low-order operators associated with UV physics are governed by LECs that can be determined from scattering observables, while high-order IR operators are governed by the pion. Low-momentum observables can then be predicted with quantifiable errors, determined from the rate of convergence of the operator expansions.

HO basis functions are the unique discrete basis that preserves translational invariance, a crucial requirement in ET: a properly chosen included space (P -space) can be exactly factorized into relative and center-of-mass wave functions. The P -space plays another essential role: as we discuss below, finite HO bases require correction in the UV (omitted short-range interactions) and in the IR (as the harmonic oscillator is too confining). By using larger P -spaces, one can further separate the omitted UV and IR physics scales, improving the convergence. When HOBET is executed, it generates results that are simply related to the full solutions, namely exact eigenvalues and exact restrictions of the true wave functions to P . The theory is analytically continuous in energy, and specifically produces the continuum solutions for $E > 0$. This has the important property that the theory’s parameters – LECs that determine the strength of short-range operators – can be precisely related to phase shifts and other scattering parameters, which depend sensitively on E near threshold.

HOBET provides Galilean-invariant solutions of the Schrödinger equation and thus is an ET, in contrast to an EFT, which generates relativistically covariant solutions in quantum field theory. (This distinction between EFT/ETs is not universal, with others describing both as EFTs.) But whether the formulation is Galilean and quantum mechanical, or covariant and field theoretic, both follow the same rules. Both are formulated in a subset of a complete basis: chiral EFT interactions employ a momentum regulator with a scale Λ_{UV} , while HOBET employs a discrete Slater determinant basis spanning P with a total energy cutoff Λ_{SM} , as well as a length scale b , the harmonic oscillator size parameter. Both employ controlled expansions in effective operators that respect the underlying symmetries of the full theory (such as translational invariance/covariance, parity, time reversal, Hermiticity): the operator expansion produces an effective interaction that systematically corrects for the omission of degrees of freedom excluded by the chosen cutoffs. Properly converged solutions should be independent of the cutoffs employed – though cutoffs appropriately chosen for a given application can speed the rate of convergence, and thus the efficiency of the ET/EFT. Convergence is achieved below some momentum or energy scale, related to the cutoffs and to the order to which the expansion is carried out.

HOBET respects all of the rules of modern, systematic ET/EFTs, while also making use of the technology and intuition that has been accumulated through years of model-based approaches to nuclear structure and effective interactions.

Early attempts to produce an effective interaction recognized the critical role of repeated short-range scattering through the nucleon-nucleon hard core, which led to summation of the two-nucleon ladders to produce the bare two-nucleon reaction matrix G_0 [587]. Attempts were made to expand the effective interaction perturbatively in G_0 through generation of intermediate particle-hole excitations [588]. In the early 1970s, Barrett and Kirson [589], working in a shell model (SM¹⁰) basis, evaluated the effective interaction for ^{18}F , finding large third-order contributions to G that largely canceled against second-order contributions. The failure to converge was consistent with arguments made by Shucan and Weidenmüller [590, 591] that identified intruder states – states primarily residing outside of P , but with eigenvalues lying in the spectrum of PHP – as a generic source of non-perturbative behavior. The strong mixing of such states with nearby states in P is clearly problematic.

Such early perturbative efforts to derive a softened effective interaction appropriate to a low-momentum P -space, starting from a full-space NN hard core interaction, have been replaced by more modern non-perturbative techniques. One of these is the use of unitary transforms to reduce the strength of the coupling between P - and the excluded- or Q -space. The SRG approach employs a continuous sequence of unitary transforms, indexed by a continuous flow parameter s [560, 592–594], see also Ref. [595]. When the approach is used with the common choice of T , as the generator in a momentum basis, it suppresses off diagonal matrix elements, softening the interaction, and reducing that source of non-perturbative behavior, but if the transformation is pushed too far, the induced three- and higher-body contributions become dominant. Importantly, it does not address the role of T in the HO basis where it strongly connects P and Q . The IM-SRG extension of this idea operates directly on the A -body Hamiltonian expressed relative to a Slater determinant reference state to drive towards a block-diagonal form [596].

Another method in frequent use is the no-core shell model (NCSM). In this approach an improved interaction is constructed with multiple cutoffs, observables are computed for each cutoff, and extrapolated to no cutoff. If the improved interaction were an ET according to our definition, then extrapolation would not be needed, as results must be independent of the choice of cutoff. Various methods are used to produce the improved interaction including embedding a momentum-based EFT, pionless or chiral for example, in the HO basis, with the LECs fitted to phase shifts [469, 597, 598]. Such an embedding is a great improvement over simply taking matrix elements of the interaction in the truncated basis and exhibits much more rapid convergence as the cutoff is raised. However, the computational cost rises extremely rapidly with the cutoff, and the results obtained are not fully independent of the choice of P , e.g., varying with the choice of oscillator parameter b .

From an ET perspective, the treatment of the NN interaction in the approaches above is somewhat unnatural. The underlying UV theory is QCD, and the resulting ET we want to determine is formulated in P . The most straightforward approach would be a direct step from QCD to P , with available experimental (or, in the near future, LQCD) input used in P to fix the LECs of the operator expansion. Instead, the available experimental information – including detailed high-

¹⁰Throughout this section we use the abbreviation SM for shell model as opposed to Standard Model in the other sections.

momentum information that is not really needed in P – is encoded in a rather ill-behaved hard-core NN potential, only to be decoded later in a difficult renormalization step.

HOBET, in contrast, is an ET formulation designed to allow such a direct, one-step transition from QCD to P

1. It employs the same cutoffs – Λ_{SM} and b – that SM practitioners use, thereby avoiding the issue that arises in chiral interactions, which employ a momentum basis that is not orthogonal to the SM basis (which limits the scale Λ to which the potential can be softened in momentum space, through techniques like $V_{\text{low } k}$ [599–603]).
2. HOBET is explicitly continuous in energy, and thus treats bound states and continuum states on an equal footing. This is important for multiple reasons. First, it allows one to use scattering data directly, seamlessly connecting phase shifts to bound-state properties: much of the relevant information in phase shifts and mixing angles is connected with their rapid evolution with E near threshold: in the 1S_0 channel, the NN system is unbound by less than 100 keV. HOBET allows one to take a measured phase shift $\delta(E)$ in a region of rapid variation and relate it precisely to HOBET’s LECs. Second, HOBET’s energy dependence allows one to employ a finite HO basis – necessary for practical diagonalizations in P – while at the same time generating an infinite number of solutions, including continuum solutions that vary continuously with E . Third, it yields solutions that are simply related to the exact solutions, namely the exact eigenvalues and the exact projections of eigenfunctions onto the chosen HO basis. As projection does not preserve norms, this requires nonorthogonal solutions, which are a natural consequence of HOBET’s energy dependence.
3. HOBET manifests these attractive properties of energy-dependent ETs, at a very modest cost in additional complexity. Specifically, due to a clever reorganization of the underlying Bloch-Horowitz equation, HOBET’s LECs are energy independent.
4. HOBET builds on wisdom gained in the field over decades from model-based approaches like the SM. It does not implant a contact-gradient expansion appropriate to a plane-wave chiral EFTs onto a SM-like HO basis, as others have done [597, 604, 605], but instead employs an operator expansion built from HO raising and lowering operators. This connects HOBET’s LECs to familiar SM quantities, the Talmi integrals and their nonlocal generalization. The operator basis is complete.
5. The LECs for low-order operators, which encode the effects of missing UV physics on P , are fitted to experiment (e.g., phase shifts and mixing angles). One knows a priori that this UV expansion will be rapidly convergent, because Talmi integral expansions in nuclear physics are quite efficient.
6. The remaining LECs are determined by chiral symmetry, implemented as an operator expansion that begins in the IR and progresses to smaller $\langle r \rangle$, where it joins up with the UV expansion. HOBET’s implementation of chiral symmetry is simpler than that of Fig. 7. Chiral potentials separate out the entire contribution of the pion, idealizing it as an exchange between point nucleons. This introduces a singular r^{-3} tensor interaction that requires regularization, with attendant difficulties in renormalization as described in Sec. 3.1. In contrast, in HOBET all short-range physics is treated as unknown, pionic or otherwise, and absorbed into the UV LECs. Chiral symmetry is used to fix the values of LECs beyond those determined in the short-range

expansion. These IR LECs are all computable functions of experimentally known parameters, f_π and m_π . The dimensionless parameters controlling the convergence of the UV and IR expansions depend on b , which then can be adjusted to optimize the joining of the two expansions.

While HOBET developments have been reported in a series of technical papers [445–447, 582–585] and in Ref. [606], here we present an overview focused on the broad issues summarized above.

3.3.1. The Bloch-Horowitz Equation

In HOBET one constructs a Galilean-invariant effective interaction in a HO basis directly from observables. The theory’s cutoffs, Λ_{SM} and b , are defined at the nuclear scale, where multi-nucleon calculations can be done. The observables can be traditional experimental ones such as binding energies and phase shifts, but can also be the energy spectrum of two or three nucleons in a finite volume, computed in LQCD. Results, if fully converged, will be independent of the cutoff choices made.

$P(\Lambda_{\text{SM}}, b)$ typically consists of all Slater determinants up to an energy $\Lambda_{\text{SM}}\hbar\omega$, measured relative to the lowest energy configuration. This exploits the exact separability of such spaces, guaranteeing that the effective interaction is translationally invariant. The parameters describing P , namely Λ_{SM} and the oscillator parameter length scale b , are the theory’s cutoffs. Here $b^2 = \hbar/(M\omega)$ with M the nucleon mass and ω the oscillator angular frequency. Dimensionless energies are given in units of $\hbar\omega$, while the dimensionless two-nucleon Jacobi coordinate is $\mathbf{r} = (\mathbf{r}_1 - \mathbf{r}_2)/(\sqrt{2}b)$. We employ nodal quantum numbers $n = 1, 2, \dots$. Various details can be found in Appendix A of Ref. [606].

HOBET’s starting Hamiltonian is $H = T + V$, where T is the relative kinetic energy and V the potential, with Schrödinger equation full-space solutions

$$H |\psi_i\rangle = E_i |\psi_i\rangle . \quad (31)$$

Defining $Q = 1 - P$, with $(P + Q) = 1$, the solution of the effective interactions problem is given by the Bloch-Horowitz (BH) equation

$$\begin{aligned} PH^{\text{eff}}(E_i)P|\Psi_i\rangle &= E_i P|\Psi_i\rangle , \\ H^{\text{eff}}(E_i) &= H + H G_{QH}(E_i) QH , \\ G_{QH}(E_i) &\equiv \frac{1}{E_i - QH} . \end{aligned} \quad (32)$$

The equation must be solved self-consistently, as $H^{\text{eff}}(E_i)$ depends on the eigenvalue to be found: in practice solutions quickly converge on simple fixed-point iteration, typically in 5 – 6 cycles. As noted above, all non-zero $P|\psi_i\rangle$ are eigenstates of $H^{\text{eff}}(E)$. In particular, projections of continuum states can be generated continuously with E , apart from isolated eigenvalues where $P|\psi_i\rangle$ vanishes.

Solutions corresponding to projections imply an attractive evolution of eigenfunctions with increases in the energy cutoff Λ_{SM} : the eigenfunctions change through the addition of new components corresponding to the added shells, with previous components staying fixed. Correspondingly, one can define a growing norm for the wave function that reflects the new components added with increasing Λ_{SM} , reaching unity as $\Lambda_{\text{SM}} \rightarrow \infty$. Similarly, orthonormality of the eigensolutions is restored in this limit.

Equation (32) involves a potential that spans P and Q . The rewriting of this equation in a form more suggestive of an ET came about from a study of the full Green’s function in perturbation

theory,

$$\frac{1}{E-QH} = \frac{1}{E-H_0} + \frac{1}{E-H_0} Q(V - V_0) \frac{1}{E-H_0} + \dots, \quad (33)$$

where $H_0 = T + V_0$ is the HO Hamiltonian. Note that T and V_0 in the HO are hopping operators, connecting nearest neighbor HO shells of the same parity, but not distant shells. When this expansion was employed in H^{eff} , certain effective interaction matrix elements in P continued to oscillate even after hundreds of orders of perturbation theory. These matrix elements involved HO “edge states,” configurations in the last included shell in P , that are coupled to Q by T [582], indicative of convergence difficulties in the IR. This led to the Haxton-Luu reorganization of the BH equation in which IR and UV components are separated through a summation of QT to all orders,

$$H^{\text{eff}} = PEG_{TQ} \left[T - T \frac{Q}{E} T + V + VG_{QH} QV \right] EG_{QT} P, \\ G_{TQ} \equiv \frac{1}{E - TQ}, \quad G_{QT} \equiv \frac{1}{E - QT}. \quad (34)$$

This reorganization isolates almost all of energy dependence of the BH equation in the kinetic energy Green’s functions, which can be re-expressed in terms of the known free Green’s function G_T ,

$$EG_{QT} P = G_T \{ PG_T P \}^{-1}, \quad G_T \equiv \frac{1}{E - T}, \quad (35)$$

at the modest numerical cost of a matrix inversion in P .

As T is a hopping operator, the action of the Green’s function on the spatial components of basis states comprising P – for the NN case this would be $EG_{QT}|n\ell m_\ell\rangle$ – has no effect on components that do not reside in the last included shell. However, its action on an edge state modifies the wave function as in Fig. 8: at small r the shape remains that of the HO, while at larger r , on the left, with $E < 0$ the wave function takes on the shape of a bound state with an exponentially decaying wave function. At larger r , on the right, with $E > 0$ the wave function takes on the shape of a scattering wave. For $E < 0$ the extended tail becomes increasingly pronounced as $|E| \rightarrow 0$. The net effect is to alter matrix elements of short-range operators by a normalization, while building into H^{eff} long-range strong-interaction corrections (dominated by the pion) that would otherwise be missing, as we will describe in more detail later. One should not misconstrue EG_{QT} as creating a “tail” on the wave function. This operator is part of an exact rewriting of the BH H^{eff} that operates within a compact, translationally invariant HO space defined by P .

The first two terms within the bracket in Eq. (34) correct the kinetic energy to all orders. The remaining two terms provide the starting point for formulating the effective theory. They can be divided as follows

$$V + VG_{QH} QV \equiv V^{IR} + V^{UV} + VG_{QH} QV, \\ V^{IR} \rightarrow V_\pi^{IR}, \quad V^{UV} + VG_{QH} QV \rightarrow V_\delta. \quad (36)$$

Here V_δ represents the systematic operator expansion described in the next section, which accounts for all of the short-range physics residing in Q , that in a potential theory would be generated by the repeated scattering of QV . It also accounts for any short-range physics associated with V operating in P . This leaves the long range contributions of V in P , denoted V^{IR} , defined as physics beyond the range of our operator expansion. Thus V^{IR} depends on the order of the UV

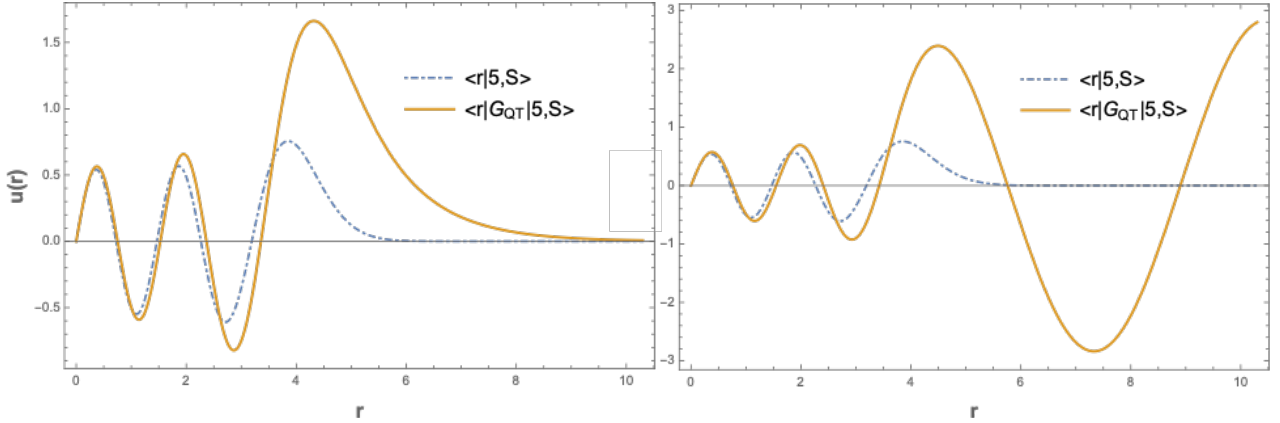


Figure 8: Transform of the fifth and highest S -channel state in P with $E = -1/2(1/2)$ on the left (right) (in $\hbar\omega$ units). The transformed state has been scaled to match the amplitude of the original basis function near the origin (dot-dashed lines). The exponential decay of a bound state and oscillations of a scattering state are reflected in the edge-state behavior.

expansion. Under the (testable) assumption that the pion dominates the long-range physics in P , we equate V^{IR} to V_π^{IR} .

With these replacements, pionful HOBET becomes a true effective theory: no reference to phenomenological potentials remains. The resulting H^{eff} is depicted in Fig. 9. Chiral symmetry and the kinetic energy operator govern the IR physics. The LECs for HOBET’s operator expansion are obtained by matching observables (UV) or computed from a chiral operator expansion (IR), as described below. Consequently HOBET is an effective theory in which QCD is reduced to the nuclear scale in one step.

3.3.2. HOBET’s Operator Expansion

While in principle one has freedom in defining an ET’s short-range expansion, in practice it is important to pay attention to the underlying physics to find the most suitable and efficient expansion. In chiral EFT the natural operator choice is a contact-gradient expansion, employing $\delta(\mathbf{r})$ and scalars built from ∇ : the expansion is around $\mathbf{q} = 0$ and operators built from ∇ select out powers of \mathbf{q} . HOBET is built on the HO, where excitations are created by raising operators acting on the zero mode. Coordinate and momentum space representations of the HO are conjugate, with the coordinate structure governed by the dimensionless parameter r_{12}/b , and the momentum-space structure by qb . The momentum expansion is about an intermediate scale determined by

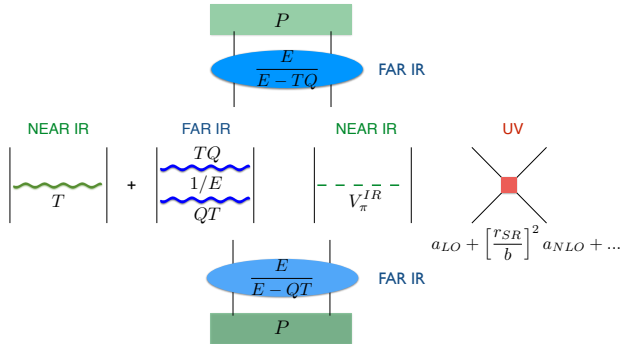


Figure 9: HOBET’s pionful effective interaction, appropriate to a HO where translational invariance requires P to be defined in terms of total quanta (in contrast to chiral interactions employing a momentum regulator). (Color: blue, green, red indicate far-IR, near-IR, and UV corrections.)

the inverse nuclear size. The natural operator basis is that built from the HO raising and lowering operators which act on the nodal quantum number, usually designated with n and beginning with $n=1$, as well as the angular momentum, usually designated with ℓ . This choice produces a correspondence between the progression of low-energy modes and the tower of short-range effective operators. There is a linear mapping between the LECs and the effective interaction matrix elements between the different HO states, e.g. the $n' = 1 \leftrightarrow n = 1$ matrix element is uniquely determined by the LO LEC (see the lower-left matrix element depicted in Fig. 10b). It also leads to a seamless division between the UV operators associated with V_δ and the IR operators associated with V_π^{IR} , greatly simplifying HOBET's UV and IR expansions, as described below.

This form of HOBET operators was first used in Ref. [447]. Here we follow Ref. [585], where a more conventional normalization was adopted.

We introduce the HO creation operators $(a_x^\dagger, a_y^\dagger, a_z^\dagger) \equiv a_i^\dagger$ and their conjugates

$$a_i^\dagger \equiv \frac{1}{\sqrt{2}} \left(-\frac{\partial}{\partial r_i} + r_i \right), \quad a_i \equiv \frac{1}{\sqrt{2}} \left(\frac{\partial}{\partial r_i} + r_i \right),$$

which satisfy the usual commutation relations. Here $\mathbf{r} = (\mathbf{r}_1 - \mathbf{r}_2)/\sqrt{2}b$ is the dimensionless Jacobi coordinate. Defining projections with good angular momentum, $a_M^\dagger = \hat{\mathbf{e}}_M \cdot \mathbf{a}^\dagger$ and $\tilde{a}_M = (-1)^M a_{-M}$, where $\hat{\mathbf{e}}_M$ is the spherical unit vector, we can form the scalar HO nodal raising/lowering operators $\hat{A}^\dagger \equiv \mathbf{a}^\dagger \odot \mathbf{a}^\dagger$, $\hat{A} \equiv \tilde{\mathbf{a}} \odot \tilde{\mathbf{a}}$

$$\hat{A} |n\ell m\rangle = -2 \sqrt{(n-1)(n+\ell-1/2)} |n-1\ell m\rangle,$$

where $|n\ell m\rangle$ is a normalized HO state. Using

$$\begin{aligned} \delta(\mathbf{r}) &= \sum_{n'n} d_{n'n} |n'00\rangle \langle n00| \\ d_{n'n} &\equiv \frac{2}{\pi^2} \left[\frac{\Gamma(n'+\frac{1}{2})\Gamma(n+\frac{1}{2})}{(n'-1)!(n-1)!} \right]^{1/2}, \end{aligned} \tag{37}$$

HOBET's short-range expansion can be carried out [447]. We obtain for the 1S_0 channel at N³LO

$$\begin{aligned} V_\delta^S &= \sum_{n'n} d_{n'n} \left[a_{LO}^S |n'0\rangle \langle n0| \right. \\ &\quad + a_{NLO}^S \left(\hat{A}^\dagger |n'0\rangle \langle n0| + |n'0\rangle \langle n0| \hat{A} \right) \\ &\quad + a_{NNLO}^{S,22} \hat{A}^\dagger |n'0\rangle \langle n0| \hat{A} \\ &\quad + a_{NNLO}^{S,40} \left(\hat{A}^{\dagger 2} |n'0\rangle \langle n0| + |n'0\rangle \langle n0| \hat{A}^2 \right) \\ &\quad + a_{N^3LO}^{S,42} \left(\hat{A}^{\dagger 2} |n'0\rangle \langle n0| \hat{A} + \hat{A}^\dagger |n'0\rangle \langle n0| \hat{A}^2 \right) \\ &\quad \left. + a_{N^3LO}^{S,60} \left(\hat{A}^{\dagger 3} |n'0\rangle \langle n0| + |n'0\rangle \langle n0| \hat{A}^3 \right) \right]. \end{aligned} \tag{38}$$

where the LECs a_{LO}, a_{NLO}, \dots carry units of energy. The HO matrix elements are

$$\langle n'(\ell' = 0 S)JM | V_\delta^S | n(\ell = 0 S)JM \rangle = d_{n'n} \left[a_{LO}^S - 2c_{n'n}^S a_{NLO}^S \right]$$

$$+ 4c_{n'n}^{S,22} a_{NNLO}^{S,22} + 4c_{n'n}^{S,40} a_{NNLO}^{S,40} - 8c_{n'n}^{S,42} a_{N3LO}^{S,42} - 8c_{n'n}^{S,60} a_{N3LO}^{S,60} \Big], \quad (39)$$

with the coefficients

$$\begin{aligned} c_{n'n}^S &= (n'-1) + (n-1), \\ c_{n'n}^{S,22} &= (n'-1)(n-1), \\ c_{n'n}^{S,40} &= (n'-1)(n'-2) + (n-1)(n-2), \\ c_{n'n}^{S,42} &= (n'-1)(n'-2)(n-1) + (n'-1)(n-1)(n-2), \\ c_{n'n}^{S,60} &= (n'-1)(n'-2)(n'-3) + (n-1)(n-2)(n-3). \end{aligned} \quad (40)$$

In tensor channels the angular momentum raising and lowering operators are needed, formed from the aligned coupling of the spherical creation and annihilation operators

$$\begin{aligned} \langle n\ell || [\mathbf{a}^\dagger \otimes \cdots \otimes \mathbf{a}^\dagger]_\ell || n0 \rangle &= (-1)^\ell \langle n0 || [\tilde{\mathbf{a}} \otimes \cdots \otimes \tilde{\mathbf{a}}]_\ell || n\ell \rangle \\ &= 2^{\ell/2} \sqrt{\frac{l!}{(2\ell-1)!!} \frac{\Gamma[n+\ell+\frac{1}{2}]}{\Gamma[n+\frac{1}{2}]}} \end{aligned} \quad (41)$$

where $|| \dots ||$ denotes a reduced matrix element. The needed operator expansion can then be constructed, e.g.,

$$V_\delta^{\text{SD}} = \sum_{n'n} d_{n'n} \left[a_{NLO}^{\text{SD}} \{ [\mathbf{a}^\dagger \otimes \mathbf{a}^\dagger]_2 |n'0\rangle \langle n0| + |n'0\rangle \langle n0| [\tilde{\mathbf{a}} \otimes \tilde{\mathbf{a}}]_2 \} \odot [\boldsymbol{\sigma}_1 \otimes \boldsymbol{\sigma}_2]_2 + \dots \right]. \quad (42)$$

Full results through N³LO for all contributing channels can be found in Ref. [447].

Equation (39) shows that HOBET's ladder operator expansion generates a characteristic dependence on nodal quantum numbers n, n' : a_{LO}^S is the only LEC contributing to the HO 1s-1s ($n = n' = 1$) matrix element, a_{NLO}^S is the only additional LEC contributing to the 1s-2s matrix element, etc. Consequently if one starts with an NN potential – the two-step process described previously for either a hard potential like Argonne v_{18} or a softer one like $V_{\text{low } k}$ – the LECs can be fixed in a scheme-independent way, once one computes individual matrix elements of the effective interaction. If a_{LO}^S is determined from the 1s-1s matrix element in a LO calculation, that value will not change at NLO, and so on. The s -wave LECs are determined by expanding the HO wave functions as a Gaussians times a finite polynomial in r^2 , then equating terms

$$\begin{aligned} &\int r'^2 dr' r^2 dr r'^2 p' e^{-r'^2/2} V_{\text{sr}}(r', r) r^{2p} e^{-r^2/2} \\ &\equiv \int r'^2 dr' r^2 dr r'^2 p' e^{-r'^2/2} V_\delta^S r^{2p} e^{-r^2/2}, \end{aligned} \quad (43)$$

where $p' = n' - 1$, $p = n - 1$, and $V_{\text{sr}} \equiv V^{UV} + VG_{QH}QV$: the LECs are determined by this nonlocal generalization of Talmi integrals [586].

3.3.3. Pionful HOBET's Power Counting for the NN System

HOBET can be summarized as follows:

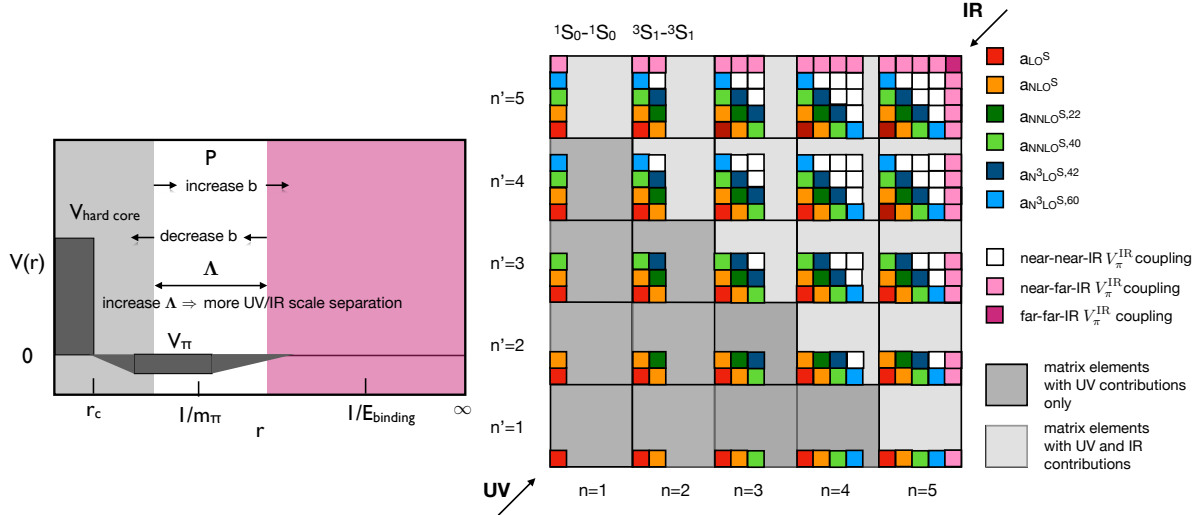


Figure 10: a) A schematic of HOBET’s Hilbert space decomposition into UV (shaded), P (white), and IR (pink) components. Λ_{SM} controls the separation of the UV-IR spaces, while b can be used to reposition P relative to the underlying NN potential. b) HOBET’s N^3LO $1S_0-1S_0/3S_1-3S_1$ operator structure for $\Lambda_{SM} = 8$. The large squares label HO matrix elements; the small ones indicate contributing operators/LECs. LECs determined in the UV expansion correct the short-range contributions to matrix elements. The IR expansion begins with the edge state-edge state LEC indicated in darker pink, moving toward the UV (lower orders) – which may require elaboration of the chiral expansion, to capture the needed physics. The chiral expansion generates all other LECs. Large squares with darker gray background indicate matrix elements entirely determined by the UV expansion at N^3LO ; those in light gray require in addition IR corrections.

1. HOBET’s effective interaction within P is completely defined by the set of LECs accompanying the ladder operators of Sec. 3.3.2. This includes a specific linear combination of operators/LECs associated with IR corrections in Q that are introduced through the edge states, and thus depend sensitively on E .
2. HOBET’s short-range or UV expansion fixes the lowest order LECs. This expansion quickly accounts for essentially all of the UV physics missing from P , encoding this information in a small set of LECs for the low-order operators, which are then determined by matching experiment (or LQCD).
3. The IR has a complementary expansion that exploits our knowledge of the long-distance nuclear problem. HOBET’s far-IR behavior is governed by the kinetic energy operator and by the binding energy E , which HOBET makes explicit. HOBET’s near-IR behavior is governed by chiral symmetry. All non-UV LECs are computable functions of E , f_π , and m_π .
4. HOBET’s IR treatment requires a chiral operator expansion analogous to that of Fig. 7. HOBET’s use of a single set of operators guarantees seamless matching of the UV and IR expansions. The IR chiral expansion needs to be accurate only beyond the range of the UV expansion.
5. Both expansions are controlled by dimensionless parameters that depend on b . Thus b can be tuned to optimize the intermediate point at which the two expansions meet.

Panel a) of Fig. 10 illustrates the connection between HOBET’s UV/IR operator structure to its cutoffs Λ_{SM} and b . For typical choices of b very strong “hard core” interactions – often modeled

in terms vector meson exchange, Pauli repulsion, etc. – as well as short-range contributions of pion exchange (including the sigma meson) are not resolved in P . HOBET treats all such short-range physics equivalently, determining its effects on the effective interaction in P in a few LECs for the lowest order operators in the expansion, fitting these to experimental observables. This contrasts with chiral EFT, where an attractive and singular potential associated with pion exchange is treated explicitly and must be regulated, with its short-range contributions separated out from other short-range physics (even though the point-pion potential has little relevance to the physical potential at short range). We would argue that HOBET’s agnostic treatment of short-range physics is more appealing in an ET. The diagram also shows that for a typical choice of b near the nuclear radius, $m_\pi b \sim 1$, so that over pion ranges, the bulk of interactions are absorbed into P . What remains is a distant tail of the pion that extends into the IR, which is treated in HOBET through edge-state matrix elements of V_π^{IR} .

The choice of Λ_{SM} and b influence how much and what type of physics is missing from P . HOBET’s answers are technically independent of b and Λ_{SM} – though a poor choice of these parameters can slow convergence, making it impractical to obtain a precise answer. Λ_{SM} determines the separation of the scales of UV and IR physics: Increasing Λ_{SM} decreases, for example, the amount of UV physics omitted from P , thus decreasing the complexity of the effective operator expansion. By adjusting b to smaller values one re-centers the peak resolution of P to smaller values of $\langle r \rangle$, pulling more short-range into P , where it will be iterated to all orders in solving the Schrödinger equation, and consequently putting more stress on the near-IR chiral expansion we describe below. An adjustment to larger values does the opposite. Thus in HOBET b can be tuned to optimize the meeting point between the short-range expansion and the chiral expansion for long-distance physics. The fact that “optimal” values for b are $\sim 1/m_\pi \sim R_N$ where R_N is the nuclear radius is not surprising because Nature does a similar optimization: nuclear radii reflect a balance between kinetic energy (minimized by complete delocalization) and potential energy (the midrange attraction influenced by the pion).

Figure 11 includes a local Gaussian potential representative of the UV physics not already captured in P , that must be taken into account through the effective operator expansion. It has the form

$$V_{UV}(r) = V_0 e^{-r_{12}^2/r_{sr}^2}, V_0 \sim -1.5 \text{ GeV}, \\ r_{sr} \sim 0.39 \text{ fm}.$$

This potential reproduces reasonably well the pattern of 1S_0 LECs derived in a detailed HOBET calculation that used the Argonne v_{18} potential [447]. (The parameters used in that work, $b = 1.7$ fm and $\Lambda_{SM} = 8$, are also employed in examples we show here.) This comparison of this potential to the Talmi integrands demonstrates the essentials of the UV convergence. The Talmi integrands peak, in our dimensionless radial units, at \sqrt{p} , $p = 0, 1, 2, \dots$ – so the peaks move apart more rapidly at small p . The UV potential (its absolute value is plotted) overlaps significantly with the Talmi integrals for $p = 0, 1$ (LO, NLO), a bit with $p = 3$ (N^2LO), and negligibly with $p = 4$ (N^3LO). With the representative Gaussian UV potential a dimensionless parameter $r_{sr}^2/(r_{sr}^2 + 2b^2)$ governs the convergence: the LECs drop off by this factor, from order to order. One has made an appropriate choice of b : the UV physics has been well captured, and there are enough contributing Talmi integrals to provide adequate resolution of its detailed structure.

If one moves b to small values, or if the short-range expansion were terminated at LO or NLO, there would be UV physics not adequately corrected in P by the short-range expansion. By

HOBET's rules, all physics outside the range of the UV expansion would be treated in the chiral expansion. This would stress that expansion – at short ranges multi-pion corrections dominate – and not be adequate, as non-pionic contributions would be missed. If one moves b to large values, resolution is lost unnecessarily, and the short-range expansion would now penetrate to larger radii where we know the interaction, due to chiral symmetry, wasting effort.

Figure 11 also shows the absolute value of the Yukawa-like 1S_0 potential from tree-level one-pion exchange (orange dashed line). It is apparent that a great deal of this interaction is absorbed into the first few Talmi integrals (more correctly, into HOBET's first few effective operators through the values assigned to their LECs). The pion is a contributor to V_{UV} in Eq. (36) that, together with $VG_{QT}QV$, is represented by the short-range expansion. Yet tree-level pion contributions to higher Talmi integrals decline slowly, leaving Talmi integrals for which, in our N^3LO example, we will have no fitted LECs: the dimensionless parameter governing this convergence is $\alpha \equiv \sqrt{2}bm_\pi \sim 1.68$ (see Fig. 12b). There are in fact an infinite number of contributing Talmi integrals, because in the edge states, V_π^{IR} is sandwiched between the Green's functions EG_{QT} . One thus sees that the IR corrections that must be added to P , to correct from strong interactions occurring at long distances, are controlled by E : this physics is a major advantage of an energy-dependent theory, as one has access to the parameter that determines the specific linear combination of states in Q that must be summed to give the needed IR correction. For bound states, as $|E| \rightarrow 0$, the IR strong interaction contribution are enhanced by the EG_{QT} propagator.

HOBET's IR or chiral expansion is not an LEC expansion, because the LECs for a technically infinite set of operators beyond N^3LO are completely determined by E , f_π , and m_π . It is instead a pion operator expansion, similar to (but we will argue simpler than) the corresponding operator expansion in chiral EFT of Fig. 7.

Just as the UV expansion starts at the UV corner of P – the $n' = 1 \leftrightarrow n = 1$ (so $p' = p = 0$ in Eq. (43)) matrix element is determined by a_{LO} – and then continues to larger $\langle r \rangle$, moving upward along the diagonal, it is helpful to view the IR chiral expansion in a complementary way, as a series that starts in the opposite IR corner of P – the $n' = 5 \rightarrow n = 5$ matrix element, determining the remaining LECs in a similar, step-wise fashion. Figure 10 guides our discussion: it graphically depicts an N^3LO 1S_0 calculation for $\Lambda_{SM} = 8$. The large boxes represent the needed P -space HO matrix elements. Within each box the small red, orange, green, and blue boxes represent the LO, NLO, NNLO, and N^3LO LECs determined in the short-range operator expansion. The pink (edge states – involving both interactions in P and corrections for long-range strong interactions in Q) and white boxes (interactions in P) represent the HO ladder operators beyond N^3LO , that we have argued (with b properly chosen) are determined by V_π^{IR} . The purpose of this discussion is to

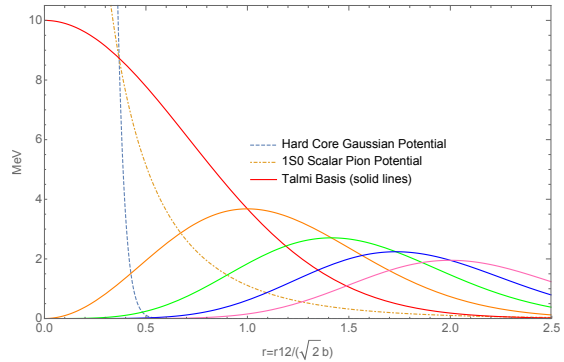


Figure 11: Talmi basis functions $e^{-r^2} r^{2(p'+p)}$ with $p'+p = (n'-1)+(n-1)$ ranging from 0 to 4 (corresponding to (LO, ..., N^4LO) and scaled with $10/p!$ for viewing. The peak of each curve is located at $r = \sqrt{p}$. Here $r = r_{12}/(\sqrt{2}b)$ is the dimension Jacobi coordinate. Superimposed on these are a Gaussian short-range 1S_0 NN potential characteristic the of UV physics that lies outside of the P -space, as described in the text, as well as the one-pion exchange potential contribution to the 1S_0 channel.

must be added to P , to correct from strong interactions occurring at long distances, are controlled by E : this physics is a major advantage of an energy-dependent theory, as one has access to the parameter that determines the specific linear combination of states in Q that must be summed to give the needed IR correction. For bound states, as $|E| \rightarrow 0$, the IR strong interaction contribution are enhanced by the EG_{QT} propagator.

HOBET's IR or chiral expansion is not an LEC expansion, because the LECs for a technically infinite set of operators beyond N^3LO are completely determined by E , f_π , and m_π . It is instead a pion operator expansion, similar to (but we will argue simpler than) the corresponding operator expansion in chiral EFT of Fig. 7.

Just as the UV expansion starts at the UV corner of P – the $n' = 1 \leftrightarrow n = 1$ (so $p' = p = 0$ in Eq. (43)) matrix element is determined by a_{LO} – and then continues to larger $\langle r \rangle$, moving upward along the diagonal, it is helpful to view the IR chiral expansion in a complementary way, as a series that starts in the opposite IR corner of P – the $n' = 5 \rightarrow n = 5$ matrix element, determining the remaining LECs in a similar, step-wise fashion. Figure 10 guides our discussion: it graphically depicts an N^3LO 1S_0 calculation for $\Lambda_{SM} = 8$. The large boxes represent the needed P -space HO matrix elements. Within each box the small red, orange, green, and blue boxes represent the LO, NLO, NNLO, and N^3LO LECs determined in the short-range operator expansion. The pink (edge states – involving both interactions in P and corrections for long-range strong interactions in Q) and white boxes (interactions in P) represent the HO ladder operators beyond N^3LO , that we have argued (with b properly chosen) are determined by V_π^{IR} . The purpose of this discussion is to

determine the operator form of V_π^{IR} , specifically what steps we must take to evolve that operator as we move from the most IR contribution to P – the upper right corner of Fig. 10 – downward along the diagonal, and eventually joining our UV ladder operator expansion. The starting point is the edge-edge state contribution indicated in dark pink in the figure, which contributes to the P -space $n' = 5 \leftrightarrow n = 5$ matrix element. Because this is an edge state, it involves an infinite series of Talmi integrals for which $p' + p \geq 8$, starting with $p' = p = 4$. This would be an N^8LO contribution in our UV operator terminology, very long ranged. For $p = 8$ the Talmi integrand peaks at $r = \sqrt{8}$ or $r_{12} = 4b \sim 6.8$ fm $\sim 4.8/m_\pi$. It is abundantly apparent that V_π^{IR} at N^3LO is very well approximated by one-pion exchange.

Moving inward, the next step will be the $p' = 4 \leftrightarrow p = 3$, $p' = 3 \leftrightarrow p = 4$ contributions – or N^7LO . This operator contributes to transitions involving one edge state (light pink in Fig. 10), being the shortest range component. This is the leading order chiral (longest range) contribution to the $n' = 5 \leftrightarrow n = 4$, $n' = 4 \leftrightarrow n = 5$ P -space matrix element, and an additional contribution to the $n' = 5 \leftrightarrow n = 5$ HO matrix element. For $p = 7$ the Talmi integrand peaks at $r_{12} = \sqrt{14}b \sim 6.4$ fm: large $\sqrt{p' + p}$ values correspond to contributions peaked at long distance.

One would continue this process through N^4LO . At each step one corrects P -space HO oscillator matrix elements further down the diagonal of Fig. 10 for the first time, and adds new corrections to matrix element above the diagonal. At N^4LO one joins onto the UV operator expansion, correcting for the first time the set of matrix elements immediately above the gray background area of Fig. 10 (matrix elements entirely determined by the N^3LO UV expansion).

The key question to ask is whether or not one-pion exchange (iterated to all orders in the Schrödinger equation, in combination with HOBET's short-range and kinetic energy operators) is an adequate description of HOBET's V_π^{IR} , or whether instead we need a more complicated treatment resembling the NN expansion of Fig. 7. A full and careful discussion of HOBET's chiral power counting, including the treatment of tensor contribution in triplet NN channels, will appear elsewhere [607]. HOBET has an intrinsically simple power counting, which we will elaborate on. First, the theory requires self-consistent solutions, which guarantees there is a fitted LEC in every channel. Thus, for example, the s-wave one-pion-exchange contact interaction that contributes to the 1S_0 channel is trivially absorbed into the fitted a_{LO} . More generally, while one could insist on treating pion exchange at all length scales as a point-nucleon exchange, it makes no sense to do so, because all short-range LECs are fitted to observables. All one would accomplish is to alter the numerical values of LECs, while leaving the physics unchanged. Finally, pion operator expansions are simpler in HOBET because P and Q are defined in terms of the total energy of a Slater determinant, a many-nucleon condition. This contrasts with the momentum cut in chiral EFTs, which allow one nucleon to scatter into Q (represented by a contact operator) while interacting with a second in P . For NN interactions in HOBET, either both nucleons are in P or both are in Q .

A simple channel to elucidate the counting is the ${}^3S_1 - {}^3S_1$, which is isoscalar and has no tensor contribution. In isoscalar channels one can reasonably approximate two-pion-exchange contributions by an isoscalar sigma exchange. We do so here, treating the sigma as elementary, because this approximation will allow us to isolate the dimensionless parameters governing the competition between one- and two-pion exchange. In the $T = 0$ channel the two-pion exchange is relativistically enhanced over one-pion exchange, allowing us to evaluate this enhancement against the suppression that accompanies HOBET's treatment of the pion as exclusively a long-range contribution, V_π^{IR} .

The potentials are

$$\begin{aligned} V_\pi(\mathbf{r}) &= \left(\frac{g_A}{\sqrt{2}f_\pi} \right)^2 \frac{m_\pi^3}{12\pi} \left[\frac{e^{-\alpha r}}{\alpha r} \sigma_1 \cdot \sigma_2 + \text{tensor} + \text{contact} \right] \tau_1 \cdot \tau_2 \\ V_{2\pi}(\mathbf{r}) &= -\frac{g_s^2}{4\pi} m_\sigma \frac{e^{-\alpha_\sigma r}}{\alpha_\sigma r} (\tau_1 \cdot \tau_2)^2, \end{aligned} \quad (44)$$

where the tensor contribution cannot contribute to the 3S_1 channel while the contact term cannot contribute to V_π^{IR} as the LO operator must be part of the UV expansion. Here $\alpha = \sqrt{2b}m_\pi$ and $\alpha_\sigma = \sqrt{2b}m_\sigma$, and the various constants are assigned values $g_A = 1.276$, $f_\pi = 130.4$ MeV, $m_\pi = 138.03$ MeV, $g_s^2 = 1.45$, and $m_\sigma = 650$ MeV.

The general formula for the LECs is

$$\begin{aligned} a_{\ell+p'+p}^{\ell,2p'+\ell,2p+\ell} &= \frac{(2\ell+1)!!}{2^\ell \ell!} \langle p'(\ell S)J; T | V(\mathbf{r}) | p(\ell S)J; T \rangle \\ R_{p\ell} &\equiv \frac{\pi}{p! \Gamma[\ell + p + \frac{3}{2}]} r^\ell e^{-r^2/2} \left(\frac{r^2}{2} \right)^p \end{aligned} \quad (45)$$

The superscripts of a give the angular momentum channel, and the number of derivatives applied to the left and right by the operator, and the subscript gives the operator order, yielding for example the correspondence $a_3^{0,4,2} = a_{N^3LO}^{S,42}$, as used in Eq. (38) for example. The relevant values of the operator order here are those beyond the order of the UV expansion. Using the monomial radial wave functions the matrix elements can be evaluated analytically for V_π and $V_{2\pi}$, yielding expressions involving error functions, governed by the dimensionless parameters α and α_σ . This formula determines the LECs corresponding to the white and pink boxes in Fig. 10, panel b).

With one underlying set of operators and two expansions that approach each other from the UV and IR sides. one has the opportunity to assess errors by studying the matching. This provides an empirical test of the adequacy of the chiral operator structure employed. For example, the standard HOBET calculations of Ref. [585] were done in N³LO, a choice that yields about a keV error in the binding energy of the deuteron. At the outset the simplest IR operator structure – just V_π^{IR} – was assumed, then this assumption was tested. An ideal testing ground is the 1F_3 partial wave, which has one contributing N³LO operator. The LEC was determined from the fit (see below) to phase shift data. That value was then matched to the value predicted by V_π^{IR} , with f_π treated as an adjustable variable: the standard value of f_π was obtained to within a few percent. This gave great confidence that the IR expansion – which describes N⁴LO LECs and higher – would be reliable at tree-level. This result is consistent with the conclusions drawn from Fig. 12.

The Lepage plot of Fig. 13 shows that HOBET is a rapidly convergent, predictive ET. HOBET was executed order by order using phase shifts taken from the Argonne v_{18} potential, then all of the matrix elements not used in the fit were predicted and compared to results computed directly from the potential. The scheme-independent procedure is described in Ref. [447]. The figure shows the fractional errors as a function of nodal quantum numbers, $n' + n$, of the matrix element. The lines show the trends. The rapid steepening of the lines with order demonstrate the kind of systemic improvement characteristic of a well-behaved ET.

3.3.4. Fitting HOBET Short-Range LECs

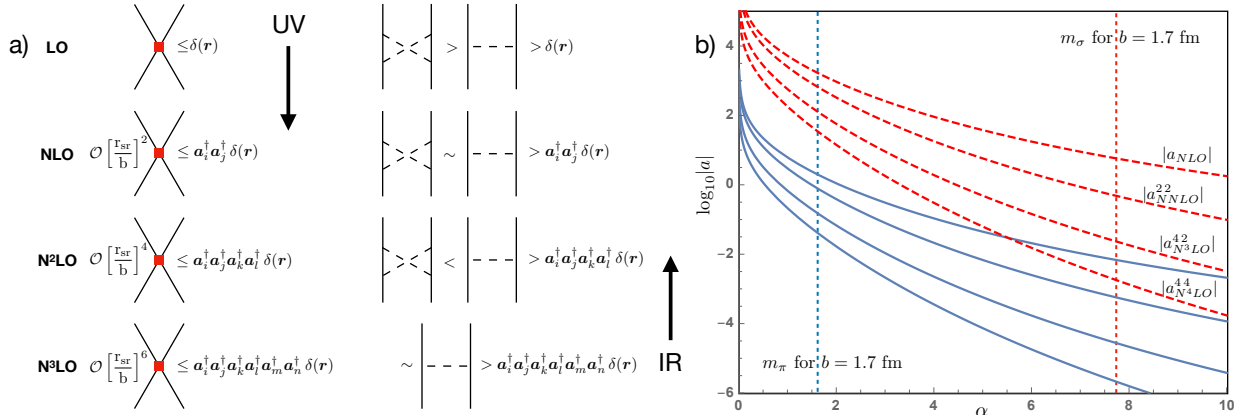


Figure 12: a) HOBET’s ${}^3S_1 - {}^3S_1$ effective interaction. The UV expansion (first column) proceeds from the top down, from the UV toward larger r , with convergence controlled by the dimensionless parameter r_{sr}^2/b^2 , discussed in the text. Various scalar operators are formed by combining the indicated ladder operators. The IR expansion (second column) proceeds from the bottom up, from the IR (where OPEP is sufficient) to smaller r , where more complicated operators might be needed in the chiral expansion. Each row thus indicates the theory for a given UV order. b) If one approximates the isoscalar contribution of $V_{2\pi}^{IR}$ as σ exchange, the IR LECs for both V_π^{IR} and $V_{2\pi}^{IR}$ can be evaluated analytically: they depend on the dimensionless parameter $\alpha = \sqrt{2}mb$, where m is the exchanged mass. UV calculations at LO, ..., N^3LO require the IR expansion to provide LECs of orders $\geq NLO, \dots, N^4LO$. The leading LECs are plotted for V_π (blue solid) and $V_{2\pi}$ (red dashed). The vertical dashed lines indicate the values for α and α_σ when $b=1.7$. While relativity suppresses the V_π contribution, the Yukawa falloff suppresses $V_{2\pi}$, with effects larger at higher order. One finds that $V_{2\pi}^{IR}$ is only a 5% correction in a N^3LO calculation, for the lowest order IR operator. In contrast, it is dominant at LO.

The Green’s function in $VG_{QH}QV$ results in a small residual energy dependence of the term being expanded. However, the expansion Eq. (38) contains lowering operators that are closely related to gradient operators and are therefore sensitive to the energy of the wave function. It was demonstrated in Ref. [585] that the small residual energy dependence can be absorbed by the highest order operators in a fit, leaving the LECs constant, making the fitting and evaluation of $H^{\text{eff}}(E)$ much simpler.

The energy independent LECs of the expansion in Eq. (38) can be fit to observables such as phase shifts in a straightforward way. Given a set of phase shift samples $\{E_i, \delta_i\}$ and LECs we can construct an approximate effective Hamiltonian

$$H^{\text{eff}}(E_i, \delta_i, \text{LECs}) P |\psi'_i\rangle = \epsilon_i P |\psi'_i\rangle, \quad (46)$$

where the eigenvectors and eigenvalues differ from E_i and $P |\psi_i\rangle$ due to the LEC values and order cutoff on the expansion. We minimize a cost function of the difference in eigenvalues while taking

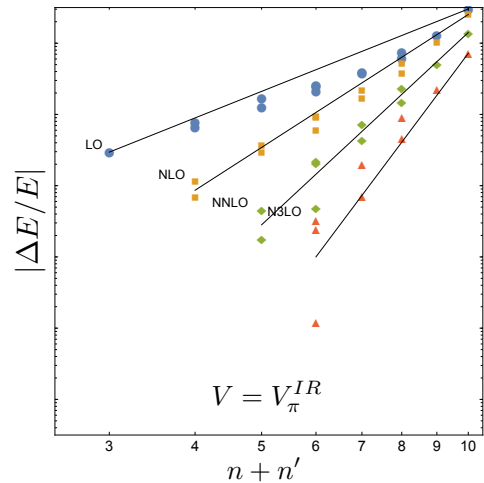


Figure 13: The Lepage plot of S -wave matrix elements of H^{eff} computed in HOBET in the deuteron (${}^3S_1 - {}^3D_1$) channel at the deuteron binding energy, starting from Argonne v_{18} phase shifts. The fractional error in H^{eff} – calculated by comparing the results to exact Argonne v_{18} H^{eff} matrix elements – is plotted vs. the sum of the nodal quantum numbers. All points plotted are predictions unconstrained by the fit.

into account the impact of omitted LEC orders.

$$\chi_{\text{order } N}^2 = \sum_{i \in \{\text{sample}\}} \frac{(\epsilon_i^N - E_i)^2}{\sigma_{N+1}(i)^2}, \quad (47)$$

where $\{\text{sample}\}$ represents the set of energy points used.

The variance σ_i^2 is an estimate of the contributions of omitted higher-order LECs not included in the fit.

$$\sigma_{N+1}^2(i) \sim \kappa_{N+1}^2 \sum_{\{a_j^{N+1}\}} \left(\frac{\partial \epsilon_i^{N+1}}{\partial a_j^{N+1}} \Big|_{a_j^{N+1}=0} \right)^2. \quad (48)$$

Here ϵ_i^{N+1} is the eigenvalue at one order beyond that being employed in the fit, κ the scale of the LECs of the next order, and $\{a_j^{N+1}\}$ is the set of LECs that contribute in that order. At low energies, high order contributions are suppressed. The theory variance automatically deemphasizes the samples where the as yet unknown values of higher-order LECs make large shifts in the H^{eff} eigenvalue. Using the variance in the fit function replaces the need to trim the sample set to the appropriate energy range for the fit's order.

Using cutoffs of $\Lambda_{\text{SM}} = 8$ and $b = 1.7$ fm, a one-pion-exchange potential (OPEP) for V_{IR} , and 40 phase shifts samples derived from the Argonne v_{18} potential [608] evenly spaced in k from 1 to 80 MeV in various channels, LECs up to N³LO were fit. From a small number of LECs parameterizing the small basis H^{eff} in each channel phase shifts are regenerated and compared to the original phase shifts in Fig. 14.

This convergence answers a persistent effective interactions problem first clearly analyzed in the early 1970s [589, 609, 610]. The exemplar used was of two nucleons outside an ^{16}O core. Various perturbative expansions of the effective interaction in a P -space were tried without success. The convergence problem was traced to a spectrum overlap between PHP and QHQ , preventing convergence of perturbative expansions. In HOBET all states of H overlapping P are included, avoiding the spectrum overlap problem. Energy dependence enables HOBET to carry much more information about the spectrum of H in a small P -space.

Early LQCD calculations of NN phase shifts with non-physical pion masses of 800 [274, 276] and 450 MeV [275] demonstrated the feasibility of computing phase shifts directly from QCD. Recent advances in supercomputers and techniques will soon give us access to physical pion mass results. Thus in the relatively near future, the HOBET program can be executed with such input. Section 3.3.7 describes how to adapt HOBET to use LQCD input in a more elegant way.

3.3.5. *A*-body HOBET

While the HOBET discussions here have focused on the two-body system – the operators, power counting, and LEC fitting – the goal of HOBET is to build a systematic effective theory of nuclei in which two and higher-body input data from experiment or LQCD can be propagated into more complicated *A*-body systems, to produce results with quantifiable uncertainties. The soundness of this approach is predicated on many years of shell model phenomenology, where a similar approach based on fitted potentials has been successful. While a full discussion of this topic is beyond the scope of this paper, we will describe how to embed the two-body effective interaction in an *A*-body system. This exercise establishes some interesting connections between HOBET and old concepts, such as the healing distance.

The discussion parallels that for the two-body interaction: we motivated results by using potential theory, but in the end sever all connections to a potential, creating a true ET. We assume an A -body Hamiltonian that is a sum of two-body terms

$$\hat{H} = \sum_{i < j}^A \left(\frac{2}{A} \hat{T}_{ij} + \hat{V}_{ij} \right) \equiv \sum_{i < j}^A \hat{H}_{ij}. \quad (49)$$

Here we employ “hats” on operators to stress that they are operators acting over the full Hilbert space. The factor of $2/A$ is needed to correctly produce the A -body relative kinetic energy from the two-body kinetic energy. We will in fact take $A=3$, to simplify the notation, as this is sufficient to illustrate the procedure for general A . The two- and three-body P -spaces P_{12} and P_{123} are defined by the conditions

$$\begin{aligned} P_{12} : \dot{\Lambda}_1 &\leq \Lambda_{SM}, \\ P_{123} : \dot{\Lambda}_1 + \dot{\Lambda}_2 &\leq \Lambda_{SM}, \end{aligned} \quad (50)$$

where $\dot{\Lambda}_1$ and $\dot{\Lambda}_2$ correspond to the dimensionless Jacobi coordinates $(\mathbf{r}_1 - \mathbf{r}_2)/\sqrt{2}b$ and $(2\mathbf{r}_3 - \mathbf{r}_1 - \mathbf{r}_2)/\sqrt{6}b$, respectively. In the following development we will use Λ_i without the dot to denote an operator measuring the spectator quanta to the pair not involving particle i .

The solution to the three-body effective interaction problem is given by the BH equation

$$P_{123}^{\Lambda_{SM}} \hat{H}_{123}^{\text{eff } \Lambda_{SM}} P_{123}^{\Lambda_{SM}} = P_{123}^{\Lambda_{SM}} \hat{H} \frac{E}{E - Q_{123}^{\Lambda_{SM}} \hat{H}} P_{123}^{\Lambda_{SM}}. \quad (51)$$

which for a two-body \hat{H} becomes

$$\hat{H}_{123}^{\text{eff } \Lambda_{SM}} = \left[\hat{H}_{12} + \hat{H}_{13} + \hat{H}_{23} \right] \frac{E}{E - Q_{123}^{\Lambda_{SM}} \hat{H}}. \quad (52)$$

One can expand this as a series in two-body scattering. Starting with representative entry \hat{H}_{12} from the brackets above

$$\begin{aligned} P_{123}^{\Lambda_{SM}} \hat{H}_{12} \frac{E}{E - Q_{123}^{\Lambda_{SM}} \hat{H}} P_{123}^{\Lambda_{SM}} &= P_{123}^{\Lambda_{SM}} \left[\hat{H}_{12} \frac{E}{E - Q_{12}^{\Lambda_{SM} - \Lambda_3} \hat{H}_{12}} \right. \\ &+ \hat{H}_{12} \frac{E}{E - Q_{12}^{\Lambda_{SM} - \Lambda_3} \hat{H}_{12}} Q_{123}^{\Lambda_{SM}} \frac{\hat{H}_{23}}{E} \frac{E}{E - Q_{23}^{\Lambda_{SM} - \Lambda_1} \hat{H}_{23}} \\ &\left. + \hat{H}_{12} \frac{E}{E - Q_{12}^{\Lambda_{SM} - \Lambda_3} \hat{H}_{12}} Q_{123}^{\Lambda_{SM}} \frac{\hat{H}_{13}}{E} \frac{E}{E - Q_{13}^{\Lambda_{SM} - \Lambda_2} \hat{H}_{13}} \right] + \dots \Big] P_{123}^{\Lambda_{SM}}. \quad (53) \end{aligned}$$

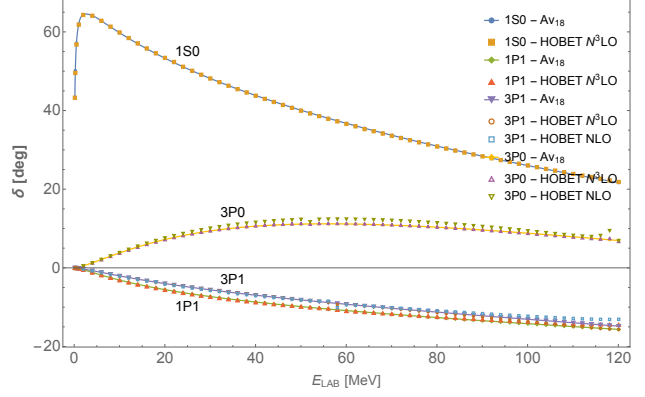


Figure 14: Phase shifts regenerated from LECs fit to data from 1 to 80 MeV and compared to the original phase shifts from Argonne v_{18} . In the 1S_0 channel the low energy behavior down to 50 keV associated with a resonance at ~ 74 keV is reproduced from data above 1 MeV. In the 3P_0 and 3P_1 channels even NLO results based on a single LEC reproduce phase shifts quite well.

We emphasize that multiple re-scattering terms always involve at least 3 particles. We will insert unity, e.g., $P_{12} + Q_{12} \equiv 1$, in the series above. For example, projector $P_{123}^{\Lambda_{SM}}$ can be written as

$$P_{123}^{\Lambda_{SM}} = P_{123}^{\Lambda_{SM}}(Q_{12}^{\Lambda_{SM}} + P_{12}^{\Lambda_{SM}}) = P_{12}^{\Lambda_{SM} - \Lambda_3}, \quad (54)$$

If Λ_3 exceeds Λ_{SM} then the superscript becomes negative, yielding an empty P_{12} , and limiting the three-body total quanta to Λ_{SM} . For the projector appearing in the multiple re-scattering terms

$$\begin{aligned} Q_{123}^{\Lambda_{SM}} &= (Q_{12}^{\Lambda_{SM}} + P_{12}^{\Lambda_{SM}})Q_{123}^{\Lambda_{SM}}(Q_{23}^{\Lambda_{SM}} + P_{23}^{\Lambda_{SM}}) \\ &\xrightarrow[\text{retain}]{} P_{12}^{\Lambda_{SM}}Q_{123}^{\Lambda_{SM}}P_{23}^{\Lambda_{SM}} \\ &\equiv Q_{123}^{\Lambda_{SM}}[\Lambda_3, \Lambda_1]. \end{aligned} \quad (55)$$

Dropping the two-body Q projectors will discard some three-body physics that we will later argue is both small and can be absorbed in the fitting of a three-body interaction. Here $Q_{123}^{\Lambda_{SM}}[\Lambda_3, \Lambda_1]$ a matrix whose basis can be practically limited to quanta of $\sim (A - 1)\Lambda_{SM}$, and whose nonzero elements in Q_{123} are

$$|\alpha'_{12}, \beta'_3\rangle\langle\alpha_{23}, \beta_1|, \quad (56)$$

where α represents the quantum numbers of the first Jacobi coordinate, and β the second Jacobi coordinate. The β_i subscript corresponds to the subscript of Λ_i which measures the spectator quanta of the state. While the Jacobi coordinates used in the ket and bra states differ in the ordering of the underlying single particle coordinates, they can be easily transformed into each other. The quanta associated with the two Jacobi coordinates are constrained by.

$$\Lambda_{SM} \geq \Lambda_{12} > \Lambda_{SM} - \Lambda_3, \quad \Lambda_{SM} \geq \Lambda_{23} > \Lambda_{SM} - \Lambda_1.$$

After such replacements, the retained linked two-body amplitudes that involve intermediate summations over an infinite Q_{123} can be replaced exactly by effective operators of feasible dimension, the needed matrix elements of which can be determined from our existing ET treatment of the two-body problem. The retained part of Eq. (53) reduces to “soft” operators

$$\begin{aligned} \hat{H}_{12} \frac{E}{E - Q_{123}^{\Lambda_{SM}} \hat{H}} \xrightarrow[\text{retain}]{} & \left[\hat{H}_{12}^{\text{eff } \Lambda_{SM} - \Lambda_3} + \left(\hat{H}_{12}^{\text{eff } \Lambda_{SM} - \Lambda_3} \frac{Q_{123}^{\Lambda_{SM}}[\Lambda_3, \Lambda_1]}{E} \hat{H}_{23}^{\text{eff } \Lambda_{SM} - \Lambda_1} \right. \right. \\ & \left. \left. + \hat{H}_{12}^{\text{eff } \Lambda_{SM} - \Lambda_3} \frac{Q_{123}^{\Lambda_{SM}}[\Lambda_3, \Lambda_2]}{E} \hat{H}_{13}^{\text{eff } \Lambda_{SM} - \Lambda_2} \right) + \dots \right] \end{aligned} \quad (57)$$

Note that the needed matrices can all be obtained from the two-body interaction $\hat{H}_{12}^{\text{eff } \Lambda_{SM}}$ via

$$\hat{H}_{12}^{\text{eff } \Lambda_{SM} - \Lambda_3} = \frac{E}{E - \hat{H}_{12}^{\text{eff } \Lambda_{SM}} Q_{SM_{123}}^{\Lambda}[\Lambda_3, \Lambda_3]} \hat{H}_{12}^{\text{eff } \Lambda_{SM}} \quad (58)$$

It should be apparent that the above steps identify every term in the three-body BH equation that can be determined from the two-body effective interaction: every term discarded includes at least one two-body scattering in Q_{123} that cannot be obtained from $\hat{H}_{12}^{\text{eff}}$. Consequently if we are executing HOBET as an ET, e.g., obtaining its two-body LECs for a cutoff Λ_{SM} from phase shifts, we do not have access to that information. Conversely, discarded terms involve consecutive

scatterings of distinct nucleon pairs, separated by high-energy states. These terms are then three-body for our choice of Λ_{SM} and expected to be dominantly short-range. HOBET distinguishes these UV unconstrained three-body terms from other three-body terms that can be computed from the two-body LECs and our IR operators, T and V_π^{IR} .

To build the next level of HOBET one would replace the UV three-body terms by an expansion as was done in the two-body case.

$$H_{123}^{eff} = P_{123}^{\Lambda_{SM}} \frac{E}{E - T_{123}Q_{123}^{SM}} \left[T_{123} - T_{123} \frac{Q_{123}^{SM}}{E} T_{123} + V_{123}^{IR} + V_{\delta,123} \right] \frac{E}{E - Q_{123}^{SM} T_{123}} P_{123}^{\Lambda_{SM}} \quad (59)$$

Equation (57) encodes our knowledge of induced three-body physics and determines V_{123}^{IR} . The residual plus the fundamental three-body interaction would then be fit by the expansion $V_{\delta,123}$, whose LECs would be determined from observables such as the $A = 3$ binding energy. Once this is done, no connection to a potential would remain: HOBET becomes a true ET at the three-body level, with experimental input encoded entirely in the LECs.

By faithfully following HOBET's principles, a connection has been made to an important concept in nuclear physics, the healing distance [611, 612]. Practitioners in the 1950s were greatly puzzled by the success of mean field descriptions of the nucleus, given the violence of the short-range scattering. This was resolved by recognizing that a nucleon pair within a nucleus undergoing repeated GeV hard-core scattering is limited to a natural distance/time scale given by the uncertainty principle of $c\Delta t \sim \text{fm}$. Thus pair wave functions quickly “heal” to their mean-field forms. One can envision integrating out the short-range scattering, to define the mean-field A -body result.

This is effectively the picture that describes the terms retained above - the terms HOBET was designed to cleanly isolate. Each two-body term embeds hard-core pair scattering between IR operators $E/E - QT$ which connect the short range scattering to the long-range physics of P_{12} : by replacing the hard-core scattering by effective operators, we remove the UV two-nucleon physics, while retaining the IR physics (the BH restriction of the true wave function to P). In pionful HOBET the IR contributions of V_π^{IR} are also included. The first term in Eq. (57) has a spectator dependence that has been previously noted as necessary in any calculation employing more than one oscillator shell [613]. When this term is used in the Schrödinger equation, the scattering within P by H_{ij}^{eff} is iterated to all orders. The remain terms involving scattering on multiple nucleon pairs in Q_{123} are three-body, but not short-range, as the associated two-nucleon short-range physics has been integrated [out](#), and the scattering begins and ends in P_{12} . That is, our careful separation of IR and UV effects have allowed us to divide the three-body physics into two components: the first corresponds to isolated two-nucleon short-range scattering that “heals” back to P_{12} and thus is IR from a three-body perspective, while the second has three nucleons interaction at short range, and is UV.

In actual calculations the interactions have been summed to all orders, which is more conveniently done using an antisymmetrized basis. (We avoided this choice above in favor of one that brings out the physics associated with spectator nucleons more clearly.) In principle, repeated applications of H_{ij}^{eff} can generate high quanta states. For example, one can see how the second Jacobi oscillator could reach Λ_{SM} quanta and then an application of H_{12}^{eff} could raise the first oscillator to Λ_{SM} quanta. An anti-symmetric state with $2\Lambda_{SM}$ quanta will have unbalanced components that will allow higher quanta states to be reached, but the amplitudes for those unbalanced components will be progressively smaller. In practice, we have seen saturation of results at a few quanta over $2\Lambda_{SM}$, reflecting the replacement the hard core with a much softer effective operator.

The calculation uses the fact that in an anti-symmetric basis with basis members x and y ,

$$\left\langle x \left| \sum_{i < j=2}^A \hat{O}_{ij} \right| y \right\rangle = c \left\langle x \left| \hat{O}_{12} \right| y \right\rangle, \quad c = A(A-1)/2.$$

Using this fact, the complete result can be obtained with a small rewrite of Eq. (51) at the cost of matrix inversion in the enlarged space. Following Eq. (55) we substitute H_{12}^{eff} for \hat{H}_{12} and evaluate in an anti-symmetrized basis carrying more than $(A-1)\Lambda_{SM}$ quanta for intermediate results.

$$P_{123}^{\Lambda_{SM}} \hat{H}_{123}^{\text{eff}} P_{123}^{\Lambda_{SM}} \xrightarrow{\text{retain}} P_{123}^{\Lambda_{SM}} c P_{12} \hat{H}_{12}^{\text{eff}} P_{12} \frac{E}{E - Q_{123}^{\Lambda_{SM}} c P_{12} \hat{H}_{12}^{\text{eff}} P_{12}} P_{123}^{\Lambda_{SM}}. \quad (60)$$

One can then evaluate the residual – the terms omitted by the replacement in Eq. (55) – by subtracting the retained terms from a numerically evaluated exact solution. As described above, we associate the residual with the three-body UV physics that would be absorbed by three-body contact operators and their LECs. We have done this evaluation for a variety of choices of b and Λ_{SM} in the 8 to 12 range. The three-body residual UV contribution to the binding energy is quite small, about 200 keV and decreasing with increasing Λ_{SM} [614], and significantly smaller than the known three-body shift of the triton. This is the first step in verifying the basic premise of HOBET: that if one carefully separates UV and IR physics, removing the effects of T and V_{π}^{IR} , one will find rapid convergence in the number of nucleons interacting at one time through the strong interaction at short distance. That is, nuclei are dilute Fermi systems. The large three-body terms are the ones easily calculated – because they are soft from a three-body perspective involving propagation in P_{12} between successive scatterings.

The procedures described here are now being applied to a series of light nuclei [614]. If these results substantiate what has been found for $A = 3$ – that almost all of the relevant three-body physics arises from two-body hard interactions sandwiched between IR physics governed by T and V_{π}^{IR} – then accurate predictions for light nuclei can be based on high-quality NN lattice results.

3.3.6. Effective Operators in HOBET

The BH equation also gives a prescription for operator evaluation. Given a short-range operator O ,

$$O_{ji}^{\text{eff},\Lambda}(E) = P \frac{E_j}{E_j - HQ} O \frac{E_i}{E_i - QH} P.$$

In the above, i and j label eigenstates of the Hamiltonian, or of the effective Hamiltonian. As discussed before, the Green's functions used above with appropriate boundary conditions reconstruct the full wave function from the projections of eigenstates. For bound states this boundary condition is simply that the wave function exponentially decays outside the range of the interaction.

While the above statement is formally correct, when using HOBET with LQCD input, the full Hamiltonian is not available. Instead, we would like to express the operator in a parallel way to the HOBET effective interaction, containing a lowering operator expansion with each operator paired with an LEC:

$$\begin{aligned} O_{ji}^{\text{eff}} &= P \frac{E_j}{E_j - HQ} O \frac{E_i}{E_i - QH} P, \\ &= P \frac{E_j}{E_j - TQ} \left[O + VQ \frac{E_j}{E_j - HQ} O + O \frac{E_i}{E_i - QH} QV \right] \end{aligned}$$

$$\begin{aligned}
& + VQ \frac{E_j}{E_j - HQ} O \frac{E_i}{E_i - QH} QV \Big] \frac{E_i}{E_i - QT} P, \\
& \rightarrow P \frac{E_j}{E_j - TQ} [O + O_\delta] \frac{E_i}{E_i - QT} P.
\end{aligned}$$

The last step depends on the operator O being short range so that the last three terms are capped on each end by a short-range operator, either O or V . The sum of the three terms is then short range and can be replaced by the same form of effective theory expansion as before. The expansion can then be fit to observables in the same way as H^{eff} . With H and O in hand, the matrix elements for O^{eff} can be calculated directly for different eigenstates i and j . Then the LECs can be fit in a scheme-independent way, showing a small energy dependence. The energy dependence is small because most of the energy dependence has been captured in the Green's function for G_{QT} . As was also the case with H^{eff} this residual energy dependence can be absorbed into the highest order LECs when fitting to observables across a range of energies, yielding an effective operator based on energy independent LECs.

Since the operator may not respect the same symmetries, channels omitted in H^{eff} such as O_δ^{SP} which violate parity may have to be included in the expansion. When the two-body effective operator is applied in an A -body context, the two-body P space is reduced by the quanta of the spectators in much the same way as the effective interaction becomes spectator dependent.

The next section, Sec. 3.3.7, will show how the effective interaction LECs can be fit directly to the two-nucleon spectrum in a finite volume, as can be produced from LQCD. The effective operator now has the same expansion form and we expect that much the same process can be used to fit the operator LECs to two nucleon operators evaluated in a finite volume. An important example where this can be applied is the $\Delta I = 2$ hadronic parity violating matrix element in proton-proton scattering.

3.3.7. HOBET in a Box

A way to make a deeper and more direct connection between LQCD and the HOBET effective interaction is to fit the LECs directly to finite volume observables such as the spectrum of two nucleons. A few key properties of HOBET make this possible. First, the only place that boundary conditions appear in HOBET is the Green's functions for G_{QT} . As long as the cut off HO basis and V_δ are shorter range than the volume, then the boundary conditions have been segregated into the Green's function, with the result that V_δ and the LECs controlling the expansion are independent of the volume, finite or infinite. Instead of using the Lüscher method to convert the finite volume LQCD spectrum to infinite volume phase shifts at the energies specified by the quantization condition, one can tune one set of HOBET LECs across one or more volumes of the same physical sizes as are used in the LQCD computations, until the FV spectrum is reproduced. These LECs can then be used to predict the infinite volume physics, be it bound state energies or the scattering phase shifts. Note, this also alleviates the need to perform an effective range expansion fit, or some other parameterization of the phase shift results, which can be problematic if there are deeply bound states.

Second, a 3D harmonic oscillator can be described equivalently in either spherical or Cartesian form. Spherical-Cartesian brackets give a unitary transformation between sets of states with the same number of quanta. In a finite volume or box, the effective theory is much easier to write in Cartesian form, where we can write the expansion for V_δ in terms of 1D HO lowering operators a_x, a_y, a_z , acting in the \hat{x}, \hat{y} , and \hat{z} directions with their own LECs. Example operators with

Cartesian LEC names can be found in Table 2. The LEC names begin with c to indicate that they are Cartesian LECs. The letter d simply separates the digit triples. To construct the name for an operator the left and right hand digit triples first encode the number of lowering operators to each side in the \hat{x} , \hat{y} , and \hat{z} directions. The triples are swapped and the digits for \hat{x} , \hat{y} , and \hat{z} ordered (in the same way in both triples) so as to make the resulting 6 digit number as large as possible. This gives all operators that are equivalent under cubic rotations or reflection the same LEC.

It is harder to express rotational invariance in the Cartesian form so we do not bother, generating a larger set of operators and associated LECs. While this expansion is written in terms of its own set of LECs it must describe the same V_δ . Using spherical-Cartesian brackets the matrix elements on non-edge states of P of the Cartesian form can be transformed to the spherical basis where the two expansions must be equal at the same order. $V_\delta^{\text{cart}} = V_\delta^{\text{sph}}$. This equality establishes a linear relation between the spherical LECs and the Cartesian LECs, which can now be replaced by linear combinations of the spherical LECs:

$$\begin{aligned} \text{c000d000} &= a_{\text{LO}}^{1S0}, \\ \text{c200d000} &= a_{\text{NLO}}^{1S0}, \\ \text{c200d200} &= a_{\text{NNLO22}}^{1S0} + (2/3)a_{\text{NNLO}}^{1D2}, \\ \text{c200d020} &= a_{\text{NNLO22}}^{1S0} - (1/3)a_{\text{NNLO}}^{1D2}, \\ \text{c110d110} &= 2a_{\text{NNLO}}^{1D2}. \end{aligned}$$

A nice side effect of the substitution is the automatic imposition of rotational invariance on the Cartesian V_δ . In the above equation you can see that the last three Cartesian LECs are functions of just two of the spherical LECs.

The periodic boundary conditions are enforced by working in a basis that respects them. The periodic box has side lengths L_i (coordinates from $-L_i/2$ to $+L_i/2$, and $i = 1 \dots 3$ for direction). A complete basis of states in the periodic box is a set of sine and cosine waves in each dimension such that $\phi(-L/2) = \phi(L/2)$. For calculation purposes we impose a cutoff N on the size of the basis, which is enlarged until results converge. We use normalized odd and even real wave functions.

$$\begin{aligned} \phi_{i,s,m}(x) &= \sqrt{2/L_i} \sin(\alpha_{i,m} x), & n &= 1, \dots, N/2 \\ \phi_{i,c,0}(x) &= \sqrt{2/L_i} (1/\sqrt{2}), & n &= 0, \\ \phi_{i,c,m}(x) &= \sqrt{2/L_i} \cos(\alpha_{i,m} x), & n &= 1, \dots, N/2, \end{aligned} \tag{61}$$

with $\alpha_{i,m} = 2\pi |m| / L_i$. Letting m range from $-N/2$ to $N/2$, the negative indices indicate the sine members and positive indices to indicate the cosine members of the basis. We can then write the basis of 3D solutions as

$$\phi_{\mathbf{m}}(x, y, z) = \phi_{m_x}(x) \phi_{m_y}(y) \phi_{m_z}(z). \tag{62}$$

Table 2: LECs and Cartesian operators

LEC	operators
c000d000	$\delta(r)$
c100d100	$(a_x^\dagger \delta(r) a_x + a_y^\dagger \delta(r) a_y + a_z^\dagger \delta(r) a_z)$
c100d010	$(a_x^\dagger \delta(r) a_y + a_x^\dagger \delta(r) a_z + a_y^\dagger \delta(r) a_z) + \text{h.c.}$
c200d000	$(a_x^{\dagger 2} + a_y^{\dagger 2} + a_z^{\dagger 2}) \delta(r) + \text{h.c.}$
c110d000	$(a_x^\dagger a_y^\dagger + a_x^\dagger a_z^\dagger + a_y^\dagger a_z^\dagger) \delta(r) + \text{h.c.}$
c200d200	$(a_x^{\dagger 2} \delta(r) a_x^2 + a_y^{\dagger 2} \delta(r) a_y^2 + a_z^{\dagger 2} \delta(r) a_z^2)$

Overlaps between these momentum states and HO states, specified with label n can be analytically calculated (see Chapter 9 in Ref. [606]):

$$\chi_{\mathbf{n},\mathbf{m}} = \langle \mathbf{n} | \mathbf{m} \rangle . \quad (63)$$

The kinetic energy operator depends on the possibly different side lengths L_i . For example, if the LQCD calculation involves a boosted system along an axis, with non-zero total momentum, this can be handled in part by reducing the box size in HOBET by the Lorentz contraction factor of the boost.

$$\hat{T}\phi_{\mathbf{m}}(x, y, z) = 2\pi^2 \left(\sum_i \frac{m_i^2}{L_i^2} \right) \phi_{\mathbf{m}} = \lambda_{\mathbf{m}} \phi_{\mathbf{m}}(x, y, z) . \quad (64)$$

The Green's functions in Eq. (34) can be computed by expansion over the periodic momentum basis.

$$EG_{QT}P = EG_T \{PEG_T P\}^{-1}P . \quad (65)$$

Using a bilinear eigenfunction expansion we can write the Green's function G_T as

$$EG_T(E; \mathbf{r}, \mathbf{r}') = \sum_{\mathbf{m}} \frac{E}{E - \lambda_{\mathbf{m}} + i\varepsilon} \phi_{\mathbf{m}}(\mathbf{r}') \phi_{\mathbf{m}}(\mathbf{r}) .$$

Applying this expansion to an HO state involves integrating over \mathbf{r}' and yields a sum over momentum states.

$$EG_T |\mathbf{n}\rangle = \sum_{\mathbf{m}} \frac{E}{E - \lambda_{\mathbf{m}} + i\varepsilon} \chi_{\mathbf{m},\mathbf{n}} |\mathbf{m}\rangle . \quad (66)$$

Inserting this into matrix elements for $\{PEG_T P\}$ yields

$$\langle \mathbf{n}' | EG_T | \mathbf{n} \rangle = \sum_{\mathbf{m}} \frac{E}{E - \lambda_{\mathbf{m}} + i\varepsilon} \chi_{\mathbf{n}',\mathbf{m}} \chi_{\mathbf{n},\mathbf{m}} , \quad (67)$$

which is a key component in the evaluation of the effective kinetic energy. See Section 5.2 in Ref. [606] for a derivation of the final expression below.

$$\begin{aligned} T_{\mathbf{n}',\mathbf{n}}^{\text{eff}} &= \left\langle \mathbf{n}' \left| EG_{TQ} \left[T + T \frac{Q}{E} T \right] EG_{QT} \right| \mathbf{n} \right\rangle , \\ &= E \left(\delta_{\mathbf{n}',\mathbf{n}} - \langle \mathbf{n}' | EG_T | \mathbf{n} \rangle^{-1} \right) . \end{aligned}$$

Other pieces of Eq. (34) can also be evaluated via the same process. The most expensive calculation is obtaining the matrix elements of V^{LR} , which involves a double sum over the momentum basis.

As before, LECs are fit using Eq. (47). Some care must be taken to ensure that when fitting a channel such as 1S_0 that the finite volume states used are from cubic representations overlapping the angular momentum of the channel.

Since a sufficient data set from LQCD is not yet available we generate a set of eigenstates of a known potential V_{test} in a finite volume. Then the method can be tested by first fitting the LECs of the finite volume H^{eff} to reproduce the eigenvalues. Then the LECs are used to construct infinite volume $H^{\text{eff}}(E_j)$ for a set of energies $\{E_j\}$, solving for phase shifts that result in energy self consistency. Given that the finite volume spectrum was generated from a known potential, the

phase shifts can then be compared to phase shifts derived directly from V_{test} . A sample V_{test} is given below and shown in Fig. 15. This potential has a long range OPEP behavior:

$$V_{\text{test}}^{\text{LR}}(r) = -130 \frac{\exp(-m_\pi r)}{m_\pi(r + 0.75 \text{ fm})} \text{ MeV}, \quad (68)$$

$$V_{\text{test}}(r) = V_{\text{test}}^{\text{LR}}(r) + 179.4 \exp(-4m_\pi r) \text{ MeV}. \quad (69)$$

A $\Lambda = 500$, $b = 1.7$ fm calculation in infinite volume yields a bound state at -4.0518 MeV, which we expect the HOBET interaction to predict. The spectrum in an $m_\pi L = 10$ box with $L = 14.3$ fm and $m_\pi = 138.039$ MeV was determined on lattices with sizes 350^3 , 400^3 , and 450^3 , enabling a continuum extrapolation of the energies of states shown in Table 3. For the fit at N³LO in the S -channel we choose the six states overlapping $L = 0$, yielding the LECs in Table 4. An error estimate from the truncation of the expansion can be made for HOBET results by exploring the natural range of the next order or in this case N⁴LO LECs using Eq. (48). Based on these LECs, a self consistent infinite volume bound state energy of -4.066 MeV was found by fixed point iteration, which should be compared to the -4.052 MeV value found in a large basis, yielding a difference similar in size to the omitted next order LECs.

Phase shifts have been generated directly from the potential, from the HOBET ET, and from a first order and second order Lüscher's method calculation based on Equation 8 of Ref. [235]. The Lüscher's formula results are used to fit an effective range expansion, including terms up to k^6 , to the phase shifts for five positive energies, which are in turn used to generate the phase shifts in Table 5. Column V should be considered the reference value. The second order Lüscher results depend on the accurate calculation of δ_4 directly from V_{test} . In normal practice the second order Lüscher formula only establishes a relationship between $\delta_0(E)$ and $\delta_4(E)$, so one would combine it with a multi-channel generalization of the effective range expansion, fit to all the data, to tease out the two values at each energy. In addition, the next order formula represents a cutoff on the angular momenta considered. In the HOBET formulation, no such cutoff is imposed. A last source of error for the Lüscher formula is that the tail of the potential does overlap the edge of the box, violating slightly the requirement for a region of free propagation where free propagating waves in Cartesian and spherical bases can be matched. HOBET does not have this requirement and images of V^{LR} from neighboring periodic iterations are included.

Table 4: S -channel LECs from fit to six states in $L = 14.3$ fm box. The LECs (given in MeV) show the expected order by order magnitude reduction.

LEC	a_{LO}^S	a_{NLO}^S	$a_{\text{NNLO}}^{40,S}$	$a_{\text{NNLO}}^{22,S}$	$a_{\text{N3LO}}^{60,S}$	$a_{\text{N3LO}}^{42,S}$
Value	70.0274	10.2596	1.94882	3.12887	0.13716	0.10177

In actual practice, there are other sources of error such as finite volume effects on particle masses that are exponentially suppressed in L and which are common to both the HOBET and Lüscher approaches, but the relative impact of these error sources and the previous ones have not been evaluated (the leading exponential corrections to the Lüscher relation have been derived for the isospin-2 $\pi\pi$ scattering length [615] and for the NN phase shifts [616], but they have not been compared in detail to LQCD calculations.) A study of these effects would be of interest. Fitting the HOBET LECs directly to the states found in an LQCD volume yields an accurate effective interaction which can be used for more than simply generating phase shifts. The interaction is also suitable for A -body calculations leading to projected wave functions that can be used for operator evaluation.

HOBET effective operators have a similar expansion that can also be related to a Cartesian finite volume form. This means that the operator LECs can be fit to finite volume LQCD results and the resulting infinite volume operator with the same LECs can then be used in a shell model context.

One exciting prospect is the fitting of a three-body effective interaction following the model of Eq. (38) that can be formulated in terms of lowering operators for two Jacobi coordinate oscillators. Fitting such an interaction in a finite volume would give a straightforward path to infinite volume three- and higher-body observables, a problem yet to be solved in the Lüscher formalism.

3.3.8. HOBET Outlook

HOBET's effective interaction corresponds to a single, complete set of operators whose LECs can be fit on the UV side to experiment, and determined on the IR side by chiral symmetry. These two expansions meet seamlessly at intermediate scales. HOBET's philosophy that all short-range physics should be treated as unknown and absorbed into the LECs of low-order operators, significantly simplifies HOBET's treatment of the pion, which is used only for long-distance corrections associated with high-order operators. The pionic physics simplifies as the order of the UV expansion increases, with the pion treatable at tree-level at and beyond N^3LO .

Table 3: The positive parity spectrum of $H = T + V_{\text{test}}$ in a periodic volume with $L = 14.3$ fm including the overlap with angular momentum states.

Rep	MeV	L=0	L=2	L=4	L=6
A_1^+	-4.4428	0.5	0	0.866	0
A_1^+	2.0314	0.155	0	0.988	0
E^+	7.5995	0	0.424	0.361	0.830
E^+	15.2980	0	0.474	0.393	0.788
A_1^+	21.6167	0.326	0	0.265	0.908
E^+	23.2423	0	0.468	0.597	0.651
A_1^+	29.4041	0.521	0	0.853	0.023
E^+	30.9457	0	0.567	0.428	0.704
A_1^+	35.2449	0.655	0	0.189	0.732
E^+	38.4043	0	0.882	0.176	0.437
A_1^+	45.1402	0.526	0	0.576	0.625

Table 4: Phase shifts in degrees from the potential V_{test} , HOBET, and Lüscher's method from a $L = 14.3$ fm periodic volume.

E [MeV]	From V_{test}	From HOBET	Leading Lüscher	Next Order Lüscher
1	142.023	141.931	142.498	142.269
2	128.972	128.860	129.515	129.166
4	113.602	113.464	114.159	113.552
8	96.919	96.752	97.552	96.330
10	91.473	91.296	92.212	90.651
15	81.672	81.480	82.849	80.398
20	74.876	74.691	76.670	73.303

HOBET forms a direct bridge from QCD to nuclear structure and observables. The effective interaction can be directly fit to the finite volume spectrum of nucleons calculated in LQCD. The LECs are independent of the volume, finite or otherwise, so the interaction matched to LQCD in several finite volumes can be immediately used in infinite volume.

The fact that the effective wave functions are simply projections of the full wave functions gives a straightforward implementation of effective operators. These effective operators also have a volume independent short-range expansion like the effective interaction and can also be fit to LQCD finite volume observables.

The resulting two-body effective interaction can be expanded into an A -body effective Hamiltonian where we expect rapid convergence in the number of interacting nucleons. Work is underway constructing a HOBET-enabled shell model implementation. NN scattering spectra from LQCD calculations are eagerly awaited to enable light nuclei calculations firmly anchored in QCD.

4. Neutrinoless Double Beta Decay

The search for lepton-number-violating (LNV) neutrinoless double-beta decay ($0\nu\beta\beta$), in which two neutrons are converted into protons with the emission of two electrons and no neutrinos, was originally suggested by Racah [617] and Furry [618] as a way to test Majorana’s proposal that the neutrino, thanks to its lack of electric charge, may be its own antiparticle. However, this process has not been observed to this day. In addition to being a second-order weak process, its rate is proportional to an effective absolute mass scale for the neutrinos. Current observational and experimental bounds indicate that the masses of active neutrinos have to be smaller than $0.1 - 1.0$ eV [619, 620], leading to another large suppression of this decay mode compared to typical nuclear decay energies of a few MeV and momenta of the order of ~ 100 MeV.

Despite these overwhelming challenges, an enormous world-wide effort to detect $0\nu\beta\beta$ is underway [15–19, 19–29], with the goal of answering fundamental questions on the nature of massive neutrinos that cannot be addressed by oscillation experiments alone. This experimental program has led to the precise measurement of the lepton-number-conserving two-neutrino double beta ($2\nu\beta\beta$) half-lives of various isotopes [621–629]. Ranging between 10^{19} and 10^{21} years, these are the rarest nuclear processes ever observed. In addition, the current generation of experiments has placed limits on the $0\nu\beta\beta$ half-lives at the level of $10^{25} - 10^{26}$ years [17, 19, 21, 22, 25–29]. The observation of $0\nu\beta\beta$ will determine that neutrinos are Majorana particles [630], and give insight on the absolute scale of neutrino masses and on the high-energy dynamics responsible for their generation. In addition, $0\nu\beta\beta$ will shed light on one of the most important open problems in contemporary physics, the origin of the matter-antimatter asymmetry. The observation of lepton number violation in $0\nu\beta\beta$ would provide support for “leptogenesis” scenarios [631], in which the lepton asymmetry induced by LNV and CP-violating decays of very heavy right-handed neutrinos is converted into a baryon asymmetry by nonperturbative SM processes. A recent discussion of the implications of $0\nu\beta\beta$ experiments on leptogenesis is given in Ref. [632].

Experimentalists utilize special nuclei for which double-beta decay is the only energetically allowed decay mode, e.g., ^{76}Ge , ^{130}Te , or ^{136}Xe . In the U.S., a next-generation ton-scale experiment is currently planned as one of the flagship enterprises outlined in the 2015 Long Range Plan for Nuclear Science [1]. Several different technologies, materials, and designs are being tested at WIPP and Sanford Laboratory, as well as at other laboratories around the world with large U.S. involvement. The European $0\nu\beta\beta$ effort is similarly denoted in the Astroparticle Physics European Consortium report [633]. Theoretical input is key not only for the planning stages behind these

next-generation experiments, but also for understanding different potential mechanisms behind the decay and the interplay with neutrino oscillation experiments, and for constraining models of BSM physics.

Figure 16 shows the effective $0\nu\beta\beta$ mass parameter $m_{\beta\beta}$ as a function of the lightest neutrino for the two possible neutrino mass hierarchies, inverted and normal (where the pair of neutrinos with the smallest mass splitting are the heaviest and lightest, respectively). The green bands denote the bounds from existing $0\nu\beta\beta$ experiments. The next generation of experiment aims at probing $|m_{\beta\beta}| \gtrsim 0.015$ eV, thus covering the full parameter space of the inverted mass hierarchy. However, Fig. 16 was obtained assuming that $0\nu\beta\beta$ is dominated by the exchange of light Majorana neutrinos, a minimal scenario realized in only a fraction of BSM models. In addition, the calculations of the nuclear matrix elements, even though performed with state-of-the-art many-body methods, are still affected by unquantified but necessarily large theoretical uncertainties, which affect our ability to extract microscopic LNV parameters, and thus falsify models of neutrino mass generation. In the next two Subsections we discuss the role LQCD and nuclear EFTs can play towards the reduction of these theoretical uncertainties, in both standard and non-standard $0\nu\beta\beta$ scenarios.

4.1. Light-Majorana neutrino exchange

The most studied scenario for $0\nu\beta\beta$ is the so called “standard mechanism”, in which LNV is mediated by the Majorana masses of three left-handed neutrinos. In the SM, a renormalizable Majorana mass term is forbidden by the $SU(2)_L \times U(1)_Y$ gauge symmetry of the theory. It is however possible to introduce a dimension-five gauge-invariant operator [645], suppressed by one power of the high-energy scale Λ , which, after electroweak symmetry breaking, gives rise to neutrino masses and mixings. To explain neutrino masses in the $0.1 - 1$ eV range, the scale associated with the operator has to be very high, $\Lambda \sim 10^{14}$ GeV. In the next section we will discuss additional scenarios, in which the effective LNV scale is lower, and higher-dimensional operators become competitive. In the standard mechanism there is a direct relation between the parameters constrained in oscillation experiments and those responsible for $0\nu\beta\beta$. Indeed, $0\nu\beta\beta$ rates are proportional to $m_{\beta\beta} = \sum U_{ei}^2 m_i$, where m_i are the masses of the neutrino eigenstates, and U_{ei} elements of the Pontecorvo-Maki-Nakagawa-Sakata (PMNS) mixing matrix [646, 647]. This relation is illustrated by the blue and orange bands in Fig. 16. The extraction of $m_{\beta\beta}$, and

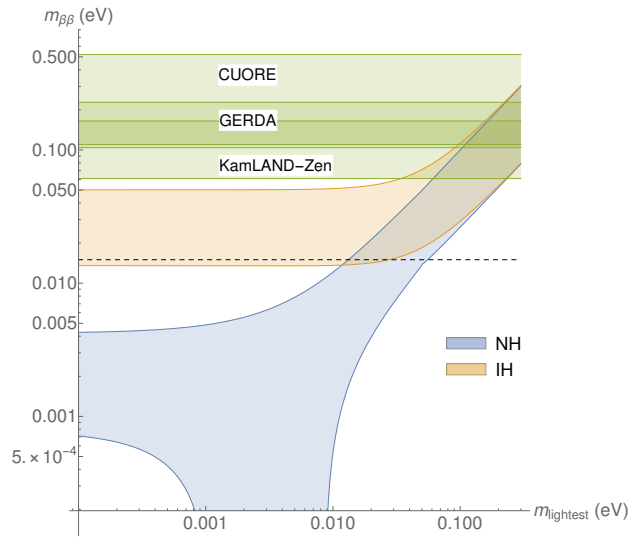


Figure 16: Effective neutrino Majorana mass $m_{\beta\beta}$ as a function of the lightest neutrino mass. The blue and orange regions are the predictions based on the neutrino oscillation parameters reported in Ref. [619] in the normal hierarchy (NH) and inverted hierarchy (IH). The bands include 3σ uncertainties on the oscillation parameters, and are obtained by marginalizing over the Majorana phases. The horizontal green bands show the current 90% confidence level upper limits on $m_{\beta\beta}$ from the KamLAND-Zen ^{136}Xe experiment [17], the GERDA ^{76}Ge experiment [29] and the CUORE ^{130}Te experiment [25]. $m_{\beta\beta}$ was extracted using the nuclear matrix elements in Refs. [634–644]. The dashed black line is a projection of the sensitivity of the next generation of $0\nu\beta\beta$ experiments [1].

thus of an absolute neutrino mass scale, from experiment requires precise calculations of the $0\nu\beta\beta$ half-lives, which in turn are proportional to the matrix elements of the nuclear $0\nu\beta\beta$ transition operator. The nuclei of interest are medium and heavy open-shell nuclei with complex nuclear structure, challenging to describe with nuclear theory. As a consequence, the nuclear matrix elements (NMEs) are affected by large theoretical uncertainties, giving rise to variations of up to a factor of ~ 2 depending on the many-body method employed (see Ref. [648] for a recent review and Ref. [649] that also provides a synopsis of current and future experiments).

The calculation of $0\nu\beta\beta$ NMEs with controlled theoretical uncertainties is one of the main goals of the nuclear physics community and is supported by a DOE Topical Collaboration¹¹. A large thrust in this effort has been towards improving existing methods, by, for example, extending the configuration space and constructing consistent operators for shell-model calculations, or adding correlations to quasiparticle random phase approximation, interacting boson model, and energy density functional calculations. These efforts are reviewed in detail in Ref. [648]. In addition, the goal of obtaining a direct connection between $0\nu\beta\beta$ rates and microscopic LNV parameters has spurred a new focus on *ab initio* calculations, in which the NMEs are computed taking chiral Hamiltonians fit to two- and few-nucleon data as a starting point for many-body methods such as coupled-clusters (CC) and IM-SRG [650]. As in the case of β decays discussed earlier, in the *ab initio* framework it is important to have a derivation of the transition operator V_ν that is consistent with the nuclear interaction. At LO, V_ν is a two-body operator, with a well known long-range component, represented by the exchange of a light Majorana neutrino between nucleons (see for example Ref. [86]). The neutrino interacts with the nucleons via the vector and axial form factors, and modern derivations of V_ν include the contributions of the induced pseudoscalar and weak magnetic form factors [87]. In the 1S_0 channel, the most relevant for $0\nu\beta\beta$, V_ν has a long-range Coulombic component given, at LO, by

$$V_{\nu L}^{^1S_0} = \frac{\tau^{(a)+}\tau^{(b)+}}{\vec{q}^2} \left(1 + 2g_A^2 + \frac{g_A^2 m_\pi^2}{(\vec{q}^2 + m_\pi^2)^2} \right), \quad (70)$$

where G_F^2 and $m_{\beta\beta}$ have been factored out [651].

At higher orders, in addition to the form factors, one has to consider two-body weak currents, which induce three-body corrections to V_ν [652, 653]. The three-body $0\nu\beta\beta$ operator involves the LECs $c_{1,3,4,6}$ and c_D , which also enter the chiral EFT three-body force, and whose determination was discussed in Sec. 3.2. Ref. [526] furthermore pointed out that in chiral EFT there arise non-factorizable corrections, that is genuine two-hadron contributions that are not captured by multiplying single-hadron weak form factors. These operators are induced by high-energy neutrinos, with $|\mathbf{q}| \gtrsim \Lambda_b$, which are not resolved in the EFT. They come with three unknown LECs, $g_\nu^{\pi\pi}$, $g_\nu^{\pi^N}$, and g_ν^{NN} , which can be determined by computing LNV scattering amplitudes, such as $\pi^- \rightarrow \pi^+ e^- e^-$ or $nn \rightarrow ppe^- e^-$ with LQCD. Results for the amplitude $\pi^- \rightarrow \pi^+ e^- e^-$ and thus for $g_\nu^{\pi\pi}$ have been recently obtained by two lattice groups [654–656].

In WPC $g_\nu^{\pi\pi}$, $g_\nu^{\pi^N}$ and g_ν^{NN} contribute at NLO, so their values are important for precision calculations but they would not significantly shift the NMEs. However, as previously discussed, WPC fails for Coulomb-like potentials in the 1S_0 channel, leading to the enhancement of short-range effects. The problem can be identified by studying the $nn \rightarrow ppe^- e^-$ scattering amplitude

¹¹See the website of the DBD Collaboration:
<https://a51.lbl.gov/~0nubb/webhome/>.

[527, 651]. At first order in the very weak perturbation $V_{\nu L}^{1S_0}$, the scattering amplitude is given by

$$\mathcal{A}_\nu = - \int d^3 \mathbf{r} \psi_{\mathbf{p}'}^{-*}(\mathbf{r}) V_{\nu L}^{1S_0}(\mathbf{r}) \psi_{\mathbf{p}}^+(\mathbf{r}), \quad (71)$$

where $\psi_{\mathbf{p}}^\pm(\mathbf{r})$ are scattering wavefunctions for two neutrons or two protons in the 1S_0 channel, obtained with the chiral EFT potential, which, at LO, consists of a contact interaction C that must be regulated (Sec. 3.2) and a Yukawa one-pion-exchange potential. In Fig. 17 we show results obtained with a local Gaussian regulator, with width R_S , but similar results are obtained in dimensional regularization or with a non-local momentum cutoff [527, 651]. For each value of R_S , $C(R_S)$ is fit to the 1S_0 np scattering length. Once C and the wavefunctions are determined, it is straightforward to evaluate Eq. (71). Since $|\mathcal{A}_\nu|^2$ is an observable (though in practice unmeasurable), the matrix element should not sensitively depend on the cut-off. However, as shown in Fig. 17, \mathcal{A}_ν diverges logarithmically as R_S is removed. To absorb the logarithmic divergence in the LO scattering amplitude it is sufficient to promote the counterterm g_ν^{NN} from NLO to LO, as shown by the purple dots in Fig. 17. A well defined observable requires V_ν to have a short-range component appearing at the same order as the usual Coulombic long-range piece [527, 651],

$$V_\nu^{1S_0} = \tau^{(a)+} \tau^{(b)+} \left\{ \frac{1}{\mathbf{q}^2} \left(1 + 2g_A^2 + \frac{g_A^2 m_\pi^2}{(\mathbf{q}^2 + m_\pi^2)^2} \right) - 2g_\nu^{\text{NN}} \right\}. \quad (72)$$

While the analysis was performed on scattering states, the same problem affects transitions between bounds states, as long as the nuclei are described in chiral EFT. The situation for the $0\nu\beta\beta$ operator mirrors what is observed in the study of charge-independence breaking (CIB) in nucleon-nucleon scattering. The charge-dependence of the nuclear force is manifest in the difference between the scattering lengths for pp , np and nn in the 1S_0 channel. In WPC, the CIB potential has a long-range component, mediated by photon exchange, and a pion-range component, induced by the electromagnetic pion mass splitting, which, as $V_{\nu L}$, behave as $1/\mathbf{q}^2$ at large $|\mathbf{q}|$. Both in pionless EFT [461, 525] and in chiral EFT [651], the Coulombic nature of the CIB potential induces logarithmic divergences and, in order to obtain regulator-independent phase-shifts and to reproduce the observed scattering lengths, it is necessary to introduce a CIB short-range interaction at LO in the EM coupling e^2 , enhanced by two orders with respect to WPC. We stress that the importance of short-range CIB effects is not peculiar to chiral EFT, but appears also in high-quality phenomenological potentials such as Argonne v_{18} and CD-Bonn [608, 657].

While the analysis of the renormalization of LNV scattering amplitudes and the analogy between CIB and LNV, which can be made formal by using the approximate chiral and isospin invariance of the QCD Lagrangian [527, 651], provide strong indication of the need of a LO short-range component of V_ν , they are not sufficient to determine the finite piece of g_ν^{NN} and thus its numerical impact on $0\nu\beta\beta$ NMEs. This is a perfect opportunity to highlight the symbiotic relationship between LQCD and EFT. This $0\nu\beta\beta$ $nn \rightarrow pp$ amplitude can be computed with LQCD in the exascale era and analyzed with EFT which will both determine the strength of the short range contribution, and thus the overall strength of the NMEs, as well as establish which power counting scheme describes the physics. It will also be interesting to match the LQCD calculations to HOBET, with an extension of the finite volume formulation (Sec. 3.3.7) that includes matrix elements of external currents, and see if such a short range operator is relevant in this ET.

Such calculations are computationally and theoretically challenging due to the need for the insertion of two vector and axial current operators, leading to a so-called four-point function

calculation. Computationally, this requires the calculation of propagators from all points on the lattice and ending on all points (all-to-all propagators), to ensure proper momentum projection at all times. These volume by volume computational operations become daunting when coupled with the nucleon signal-to-noise problem discussed in Sec 2. In Refs. [356, 357] an LQCD calculation was performed for $2\nu\beta\beta$, in which the effects of background axial fields were folded into modified propagators. This method avoids the calculation of expensive all-to-all propagators, but currently does not have a clear extension to $0\nu\beta\beta$. Interestingly, this calculation found that the effects of two-nucleon contact operators were enhanced in these processes relative to expectations from power-counting. While this calculation was performed with $m_\pi \sim 800$ MeV, it highlights the need for full, non-perturbative LQCD input for reliable double beta decay predictions. The formalism required to relate these four-point calculations to the infinite volume amplitudes of interest is more complex and has not been completely developed yet. Work along the lines of Refs. [349, 352] will provide this connection. Two promising LQCD calculations [654–656] have addressed some of these computational and theoretical issues in the much simpler $\pi^- \rightarrow \pi^+ e^- e^-$ process for $0\nu\beta\beta$, paving the way for future calculations of the full $nn \rightarrow ppe^- e^-$ process.

4.2. Short-range NMEs

The standard mechanism, while minimal, is by no means the only possible scenario for $0\nu\beta\beta$. In well-motivated models of BSM physics, the dimension-five Weinberg operator

$$\mathcal{L}^{(5)} = \frac{\mathcal{C}^{(5)}}{\Lambda} \left(\tilde{\varphi}^\dagger L \right)^T C \left(\tilde{\varphi}^\dagger L \right), \quad (73)$$

which generates a neutrino Majorana mass when the Higgs field φ gets its vacuum expectation value, is suppressed by additional small couplings, such that the exchange of new heavy particles are important. For example, left-right symmetric extensions of the SM lead naturally to the well-known seesaw mechanism, a favored explanation for the relative lightness of the neutrinos compared to all other SM particles [658, 659]. In these models, heavy right-handed neutrinos can also drive $0\nu\beta\beta$, and may even be dominant depending on the values of the masses and mixing parameters. While naively one

might expect heavy particle exchange to be suppressed by the large mass in the heavy propagator, light neutrino exchange is proportional to the tiny light neutrino mass, and is therefore also heavily suppressed. In a simple seesaw scenario, both the heavy neutrino propagator and the light neutrino mass scale roughly as $1/M_h$, where M_h is the mass of the heavy partner neutrino; which mechanism dominates depends upon the details of a particular model.

In addition to left-right symmetric models, there is an array of proposed new physics models containing heavy beyond the SM particles that may also drive these short-range processes. As

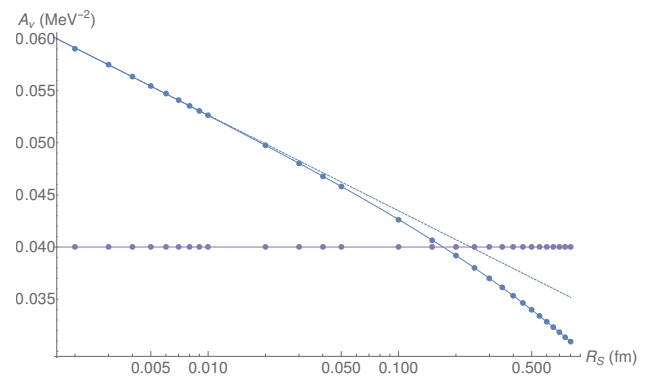


Figure 17: Absolute value of the $nn \rightarrow ppe^- e^-$ scattering amplitude A_ν , defined in Eq. (71), as a function of a Gaussian cut-off R_S . The amplitude is evaluated at the kinematic point $|\mathbf{p}| = 1$ MeV, $|\mathbf{p}'| = 38$ MeV, where \mathbf{p} and \mathbf{p}' are the relative momenta of the nn and pp pair, and the electrons are emitted at zero momentum. The blue points denote the matrix elements of the long-range operator $V_{\nu L}$, which, for small R_S , are well described by $A_\nu = a + b \log R_S$ (denoted by the dashed blue line). The purple points include the short-range counterterm g_ν^{NN} , which makes A_ν regulator independent.

an example, the decay may involve the exchange of heavy charged leptonic superpartners in R-parity violating supersymmetric extensions of the SM [660–662]. R-parity is imperative for the stability of the lightest superpartner, which is a dark matter candidate. Therefore, if theorists can relate experimental bounds to these supersymmetric models, we may be able to constrain potential R-parity violating parameters [93], even if $0\nu\beta\beta$ is never observed experimentally.

Mechanisms in which LNV arises at scales $\Lambda \gg v$ can be captured by higher dimensional operators in the SM-EFT. LNV operators have odd dimension [663], and they have been studied in several papers (see for example Refs. [93, 664–667]). In particular, Ref. [666] identified all the dimension-seven SM-EFT operators. The full list of dimension-nine $SU(2)_L \times U(1)_Y$ -invariant operators is still unknown, but Ref. [667] constructed the complete set of operators with four-quark and two-leptons, clarifying several issues in the literature. To calculate $0\nu\beta\beta$ rates, the LNV operators at the EW scale are matched onto $SU(3) \times U(1)_{\text{em}}$ -invariant operators at the QCD scale [89, 90], and then onto LNV interactions between pions, nucleons, electrons and neutrinos [88–90, 93, 668, 669]. Earlier derivations of the $0\nu\beta\beta$ transition operators [88, 668] relied on unwarranted assumptions, such as factorization of four-nucleon matrix elements, which lead to large, uncontrolled errors in the $0\nu\beta\beta$ half-lives. More modern constructions [90, 93] take into account the constraints from the symmetries of QCD, but still they require non-perturbative input from LQCD to determine the couplings in the $0\nu\beta\beta$ transition operators, and thus to model-independently connect various models and experimental detection rates. Lattice QCD can thus make an immediate and quantitative impact on the study on non-standard $0\nu\beta\beta$ scenarios.

The lowest-order chiral Lagrangian induced by SM-EFT LNV operators up to dimension-9 is given in Ref. [90], which built upon the seminal paper [93]. After integrating out heavy SM degrees of freedom, one finds two kinds of corrections. First, there are LNV charged-current interactions between quark bilinears, electrons and neutrinos. These induce long-range contributions to the transition operator, parameterized by the nucleon axial, vector, scalar, pseudoscalar and tensor form factors. As discussed in Sec. 2, these form factors can and have been calculated in LQCD, with good accuracy. The one exception is the recoil-order tensor form factor g'_T , which, playing a small role for non-standard β decay searches, has not yet been computed. As for the standard mechanism, a consistent power counting requires the transition operators induced by most non-standard charged-currents to have a short-range component as well [90], to be determined via a dedicated LQCD calculation. Only in the case of pseudoscalar charged-current the LO $0\nu\beta\beta$ transition operator is purely long-range.

The second kind of correction is represented by local dimension-nine LNV four-quark two-electron operators. The operators have been tabulated in Refs. [93, 667], and include “scalar” and “vector” operators, depending on the Lorentz transformation properties of the electron bilinear. Focusing on the scalar operators, one has

$$\begin{aligned} \mathcal{O}_{1+}^{++} &= (\bar{q}_L \tau^+ \gamma^\mu q_L) [\bar{q}_R \tau^+ \gamma_\mu q_R] , \\ \mathcal{O}'_{1+}^{++} &= (\bar{q}_L \tau^+ \gamma^\mu q_L) [\bar{q}_R \tau^+ \gamma_\mu q_R] , \\ \mathcal{O}_{2+}^{++} &= (\bar{q}_R \tau^+ q_L) [\bar{q}_R \tau^+ q_L] + (\bar{q}_L \tau^+ q_R) [\bar{q}_L \tau^+ q_R] , \\ \mathcal{O}'_{2+}^{++} &= (\bar{q}_R \tau^+ q_L) [\bar{q}_R \tau^+ q_L] + (\bar{q}_L \tau^+ q_R) [\bar{q}_L \tau^+ q_R] , \\ \mathcal{O}_{3+}^{++} &= (\bar{q}_L \tau^+ \gamma^\mu q_L) [\bar{q}_L \tau^+ \gamma_\mu q_L] + q_L \rightarrow q_R , \end{aligned} \quad (74)$$

where (\dots) and $[\dots]$ denote color contractions and the \mathcal{O}_{i+}^{++} and \mathcal{O}'_{i+}^{++} mix under renormalization. The contributions of these operators to two nucleon $0\nu\beta\beta$ have been categorized according to

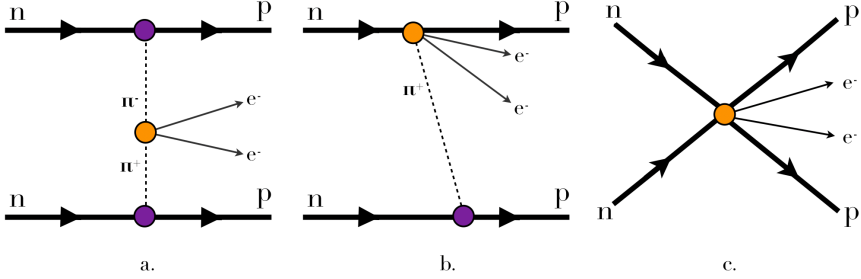


Figure 18: Diagrams contributing to two-nucleon $0\nu\beta\beta$ at (a) LO, (b) NLO, and (c) NNLO (from left to right), according to chiral EFT [93]. Yellow dots represent an insertion of any of the 4-quark operators from Eq. (74). Purple dots indicate pion-nucleon couplings. Note that the NLO diagram will not contribute at this order to the $0^+ \rightarrow 0^+$ nuclear transitions studied by experiment; they will, however, contribute at NNLO with a single derivative at the vertex.

chiral EFT (see Fig. 18), where the LO contributions occur via light pion exchange, and the N^2LO contributions include both a pion-nucleon contact operator, and a two-nucleon contact operator.

A complete calculation of the LO (in Weinberg power-counting) contribution from these operators, at the physical point with all systematics controlled has been presented in Ref. [95]. The lattice QCD calculation determined the matrix elements for the operators within a single pion state undergoing a $\pi^- \rightarrow \pi^+$ transition, which are then inserted into a modified pion potential for the two-nucleon system. The results from Ref. [95] confirm that the pion matrix elements of the operators \mathcal{O}_{1+}^{++} , \mathcal{O}'_{1+}^{++} , \mathcal{O}_{2+}^{++} , \mathcal{O}'_{2+}^{++} are of $\mathcal{O}(F_\pi^2 \Lambda_\chi^2)$, while \mathcal{O}_{3+}^{++} induces much smaller contributions, $\sim \mathcal{O}(F_\pi^2 m_\pi^2)$, in agreement with expectations from NDA and vacuum saturation. While the relative sizes of the matrix elements are also similar to the vacuum saturation predictions, the LQCD matrix elements are typically smaller, roughly by a factor of 0.3 or 0.4, indicating the importance of QCD dynamics. These results [95] enable a demonstration that the ‘‘factorization’’ assumption used in some of the literature, where matrix elements of the operators Eq. (74) between two neutrons and two protons are reduced to products of nucleon currents, does not accurately describe the hadronization and can lead to severe underestimates of the transition operator [90].

This pion exchange contribution Ref. [95] is LO in WPC. As noted in the previous subsection, such light-particle exchange effects can become enhanced and also require a short range operator to properly renormalize the amplitude (Fig. 18(c)), an effect that may also be important with pion-exchange [90]. Furthermore, in some models, such as left-right symmetric models with no mixing between left- and right-handed W bosons, the single pion LO contribution vanishes exactly and only higher-order contributions are present. Therefore, it is also important to perform the full LQCD calculation of the $nn \rightarrow ppe^-e^-$ amplitude in order quantify the importance of the various contributions appearing in Fig. 18 and understand which power counting is more correct. Such calculations will be possible in the exascale era.

5. Nuclear-Matter Equation of State

In this section, we review recent advances in nuclear-matter calculations based on chiral interactions and highlight potential connections to LQCD. We focus the discussion on the status of 3N forces as well as how such important contributions can be included in state-of-the-art calculations up to N^3LO (and beyond). These developments have gained importance because of the dawning

of multi-messenger astronomy. This new era began with the first direct detection of gravitational waves by the LIGO-Virgo collaboration in 2016 [670]. One year later followed the first multi-messenger observation of the binary neutron-star merger GW170817 [671–673]. Multi-messenger astronomy sheds light on long-standing problems, such as the synthesis of heavy elements in the universe through the r-process [152].

Neutron-rich matter plays a central role in this setting, covering physics over an extreme range of densities [47, 491, 674]. Constraining the EOS simultaneously from terrestrial experiments (e.g., at RIBF, FRIB, and FAIR at GSI), observations, and theory is therefore an active field of research. Advances on the theory side are of particular interest given novel observational constraints, such as precise radius measurements from the Neutron Star Interior Composition Explorer (NICER) [675, 676], or the planned Large Observatory for X-ray Timing (LOFT) [677, 678] and Enhanced X-ray Timing and Polarimetry (eXTP) missions [679]. LQCD calculations of two- and few-nucleon systems can bridge chiral EFT and QCD to provide truly QCD-based predictions for the EOS in the foreseeable future. In particular, matching chiral LECs to lattice data for which experimental data is either limited or unavailable (see Sec. 1.1) will help guide extrapolations of the EOS towards the high densities relevant for neutron stars. Reducing theoretical uncertainties in the low-density regime has important consequences for astrophysical applications. For instance, the neutron-star radii are most sensitive to the EOS at about twice saturation density [46].

Homogeneous nuclear matter is an ideal environment for testing nuclear forces derived in EFTs in medium. Additionally, it provides tight constraints of the EOS at nuclear densities and the structure of neutron stars [98, 113, 674]. Neutron and (isospin-)symmetric matter have been studied with chiral NN and 3N interactions in numerous many-body frameworks: coupled-cluster theory [109, 516, 680, 681], quantum Monte Carlo methods [503, 519, 520, 682, 683], self-consistent Green’s function method [684–690], and many-body perturbation theory (MBPT) [509, 549, 687, 691–698] (see, e.g., Ref. [47] for a review). On the other hand, only a few direct (and more involved) calculations of isospin-asymmetric matter are available [696, 698, 699]. This section focuses on recent advances in MBPT. Neutron matter is well-suited for deriving tight constraints on the neutron-rich EOS as well as testing different power counting schemes since all many-body forces up to N³LO are completely determined by the NN forces. The N²LO 3N forces associated with the 3N LECs $c_{D,E}$ vanish due to the coupling of pions to spin and the Pauli principle, respectively [700]. In addition, the term proportional to c_4 in the 3N two-pion exchange does not contribute.

The energy per nucleon $E/A(n, \beta)$ at zero temperature is a function of the total density $n = n_n + n_p$ and isospin-asymmetry $\beta = (n_n - n_p)/n$. Here, n_n (n_p) denotes the neutron (proton) density. Asymmetric matter can reasonably well be interpolated between symmetric ($\beta = 0$) and neutron matter ($\beta = 1$) using the quadratic expansion in β [696, 698, 699],

$$\frac{E}{A}(\beta, n) \approx \frac{E}{A}(\beta = 0, n) + \beta^2 E_{\text{sym}}(n), \quad (75)$$

or similar parametrizations, such as the one inspired by energy-density functionals in Ref. [701]. A typical proton fraction in (β -equilibrated) neutron-star matter is $x = n_p/n \sim 5\%$, corresponding to $\beta = 1 - 2x \sim 0.9$. Omitted higher-order corrections [702], such as the quartic term $\propto \beta^4$, give rise to non-analyticities [698, 703].

The nuclear symmetry energy in the expansion (75),

$$E_{\text{sym}}(n) \approx \frac{E}{A}(\beta = 1, n) - \frac{E}{A}(\beta = 0, n), \quad (76)$$

corresponds to the energy required to convert symmetric matter into neutron matter. It is a key quantity for the EOS and the structure of neutron stars [98, 704]. For instance, its slope at saturation density,

$$L = 3 n_0 \frac{dE_{\text{sym}}}{dn} \Big|_{n=n_0}, \quad (77)$$

is correlated with the neutron-star radius [46] and with properties of heavy nuclei measurable in laboratory experiments, such as the electric-dipole polarizability or the neutron-skin thickness of ^{208}Pb [705–707]. The Lead (Pb) Radius EXperiment (PREX) measured a remarkably large neutron-skin thickness of ^{208}Pb , $R_{\text{skin}} = 0.33_{-0.18}^{+0.16} \text{ fm}$ [708], but the uncertainties are too large to draw a definite conclusion. If the more accurate PREX-II confirms PREX’s central value, the EOS at nuclear densities is expected to be stiff, whereas the relatively small radius constraints from GW170817 suggest a soft EOS at about twice saturation density. This transition from a stiff to a soft EOS could indicate a phase transition (e.g., to exotic matter) inside neutron stars [709]. As pointed out in Sec. 1.1, future LQCD data can provide the constraints necessary to improve EFT interactions for strange matter in order to address (and eventually solve), e.g., the the long-standing *hyperon puzzle*.

Predictions of $E_{\text{sym}}(n_0) - L$ based on the neutron-matter calculations by Hebeler *et al.* [700, 701, 710] using MBPT with chiral NN and 3N interactions, and by Gandolfi *et al.* [682] using QMC methods with NN and 3N Hamiltonians adjusted to a range of symmetry energies are in remarkable agreement with empirical constraints (see Ref. [46, 701, 710] for details). In fact, theory provides the most precise determinations; especially, for the relatively uncertain L parameter.

Constraining the symmetry energy further from both, theory and experiment is an important task [111, 711]. The doubly magic ^{48}Ca is, to this end, of particular interest since it can be studied in *ab initio* calculations and experiments [563, 712, 713] such as the upcoming Calcium Radius Experiment (CREX) [714]. On the theory side, this requires, in particular, an improved treatment of 3N forces in many-body calculations [696] and reliable fit values for the two 3N LECs up to N³LO [509, 715].

Many-body frameworks for computing the EOS are generally formulated for NN interactions. Implementing 3N (and higher-body) forces directly in these frameworks is therefore not straightforward. Normal ordering with respect to a given reference state has become the standard approach for including dominant 3N contributions as density-dependent effective two-body potentials in many-body calculations of finite nuclei and nuclear matter (see Refs. [47, 104] for details). In infinite matter, the Hartree-Fock reference state is a natural choice.

Applying Wick’s theorem decomposes a general 3N Hamiltonian *exactly* into its normal-ordered zero-, one-, and two-body contributions and an irreducible (residual) three-body term [104]. Contributions from the latter can be assumed relatively small and are thus typically neglected (see also Refs. [716–718]); besides, it would require implementing 3N forces explicitly in many-body frameworks. At second order, this approximation has been assessed later by direct calculations for a set of chiral 3N interactions [509] up to N³LO.

Normal-ordering for 3N forces sums one particle over the (occupied) states in the Fermi sphere [700, 719],

$$\overline{V}_{3\text{N}} = \text{Tr}_{\sigma_3} \text{Tr}_{\tau_3} \int \frac{d\mathbf{k}_3}{(2\pi)^3} n_{\mathbf{k}_3}^{\tau_3} \mathcal{A}_{123} V_{3\text{N}}, \quad (78)$$

which involves the initial antisymmetrized 3N interaction $\mathcal{A}_{123} V_{3\text{N}}$, sums over spin and isospin quantum numbers σ_3 and τ_3 , respectively, and an integration over all momentum states weighted

by the neutron or proton distribution function $n_{\mathbf{k}}^{\tau_3}$; e.g., the Fermi-Dirac distribution function at zero temperature, $n_{\mathbf{k}}^{\tau_3} = \theta(k_F^{\tau_3} - |\mathbf{k}|)$, with the Fermi momentum $k_F^{\tau_3}$ being related to the proton and neutron density of the system, respectively.

The effective two-body potential (78) depends on the total momentum \mathbf{P} of the two remaining particles, in contrast to Galilean-invariant NN potentials. This additional momentum-dependence makes it conceptually and computationally difficult to combine effective potentials with genuine NN potentials in many-body calculations.

To elude these difficulties (and to make the derivation actually tractable), Refs. [700, 719] evaluated the effective two-body potential (78) semi-analytically by fixing $\mathbf{P} = 0$, an approximation that was assessed by comparing 3N Hartree-Fock energies. This approximation makes combining the effective potential \bar{V}_{3N} with a genuine NN potential straightforward, $V_{NN+3N} = V_{NN} + \xi \bar{V}_{3N}$. The combinatorial normal-ordering factor ξ depends on the specific calculation of interest, and can be derived using Wick's theorem as discussed, e.g., in Refs. [508, 696, 700]. The derivations of the effective two-body potential in Refs. [700, 719] are based on the operator definition of the N²LO 3N in neutron and symmetric matter. This approach ties the derivation to a specific isospin asymmetry and 3N interaction term. Changing one of them requires a rederivation of the effective potential, which is very tedious, especially, in view of the operator-rich N³LO 3N forces (see also Refs. [720–722]).

A generalized normal-ordering framework for asymmetric matter and arbitrary partial-wave decomposed 3N forces has been introduced along with an improved \mathbf{P} angle-averaging approximation in Ref. [696]. A comparison of 3N Hartree-Fock energies demonstrated that the new approximation is generally more stable beyond $n = 0.13 \text{ fm}^{-3}$; however, reasonable overall agreement was found up to about saturation density. Due to the development of an efficient method for the partial-wave decomposition of chiral 3N forces [723], normal-ordered 3N interactions can now be included in all partial-wave based infinite-matter calculations up N³LO without any additional efforts. In neutron matter, first applications to the EOS [687] and BCS pairing gaps [508] followed soon after. This paves the way for infinite-matter studies at consecutive orders in the chiral expansion as well as consistently-evolved many-body forces [561, 724] with controlled approximations. Such order-by-order calculations are mandatory for truncation-error analyses of the chiral expansion.

MBPT applied to soft(ened) potentials is a computational efficient framework, capable of estimating the many-body uncertainties through order-by-order comparisons. Despite these advantages, MBPT for infinite matter at zero temperature had only been applied up to third order in the many-body expansion, including the involved particle-hole diagram [694, 697, 725]; at finite temperatures, yet only at second order [693, 695, 726]. Improving the treatment of 3N forces beyond the Hartree-Fock approximation [687, 692] and the rapidly increasing number of diagrams [727, 728] towards higher orders, especially the ones with particle-hole excitations, were among the serious challenges.

The novel Monte Carlo framework for MBPT developed in Ref. [509] has overcome these challenges efficiently using automatic code generation based on the analytic expressions of chiral interactions and many-body diagrams directly in a single-particle basis. Lepage's adaptive Monte Carlo algorithm VEGAS [729] allows for the accurate computation of multi-dimensional momentum integrals. In a first application [509], NN (normal-ordered 3N) interactions up to fourth (third) order in MBPT were considered in addition to the residual 3N term at second order, which had only been evaluated for contact interactions [730]. These residual 3N contributions turned out to be

small relative to overall uncertainties from the chiral EFT expansion, as expected. Whether or not that turns out to be the case at third order will be interesting to see.

In a second application, the Monte Carlo framework was used to compute the complete fourth-order term in the Fermi-momentum (or $k_F a_s$) expansion of the ground-state energy of a dilute Fermi gas for the first time [731]. At this order, logarithmic divergences need to be renormalized, which gives rise to a non-analytic term. Comparisons against quantum Monte-Carlo results showed that the Fermi-momentum expansion converges well for spin one-half fermions in the region $|k_F a_s| \lesssim 0.5$. In addition, the range for the Bertsch parameter obtained from two Padé approximants, $\xi_{\text{Padé}} = 0.33 - 0.54$, was found to be consistent with the value extracted from experiments with cold atomic gases, $\xi \approx 0.376$, as well as the extrapolated value for the normal (i.e., non-superfluid) Bertsch parameter, $\xi_n \approx 0.45$ [732]. Resummation techniques (such as Padé approximants) greatly benefit from these high-order calculations. Future applications to the nuclear-matter EOS are therefore promising in order to extract “converged” results in calculations of slow many-body convergence.

Thanks to the automated generator of many-body diagrams recently developed by Arthuis *et al.* [728], the Monte Carlo framework can be applied to push MBPT for infinite matter to (arbitrary) high orders. Preliminary proof-of-principle calculations at fifth (and even sixth) order based on chiral NN potentials have already demonstrated the efficacy of the approach. The Monte Carlo framework has achieved a high level of parallelization and performance optimization by taking advantage of GPU acceleration. These advances set the stage for future applications to the nuclear-matter EOS at finite temperatures and arbitrary proton fractions. They moreover enable order-by-order studies of the chiral as well as the many-body convergence up to high orders for Bayesian uncertainty quantification [455, 513]. Work along these lines [733, 734] is currently in progress (see also Ref. [735]).

The advances in many-body methods have revealed major challenges with chiral interactions: none of the presently available interactions is capable of describing both, experimental ground-state energies and charge radii of nuclei, over a wide range of the nuclear chart [109, 715]. Most chiral NN and 3N interactions that were constrained in the two- and few-body sector are able to predict light nuclei in agreement with experiment; however, theoretical uncertainties increase with mass number (see, e.g., Ref. [517]), and significant discrepancies have been observed in heavy nuclei [517, 736, 737]. A simultaneous reproduction of experimental ground-state energies and charge radii has yet to be achieved. *Ab initio* calculations of medium-mass and heavy nuclei empirically indicate that realistic saturation properties of symmetric matter are important [109, 549, 558, 563, 738, 739]. Optimizing the chiral potential “NNLOsat” with respect to heavier nuclei [109] improves, as expected, the agreement with medium-mass nuclei as well as the empirical saturation point [563, 740–742]. Scattering phase shifts, on the other hand, can only be reproduced up to relatively low energies.

In a first attempt to fit nuclear interactions directly to the empirical saturation point, Ref. [509] studied saturation properties of chiral NN and 3N interactions up to N³LO as a function of c_D , which was related to c_E by matching the ³H binding energy. Sets of Hamiltonians with reasonable saturation properties, close to the empirical point but typically slightly underbound, could be identified for all considered NN interactions; specifically, the potentials by Entem *et al.* [487] with momentum cutoffs $\Lambda = 420, 450$, and 500 MeV.

Subsequent IM-SRG [596, 743] calculations of selected closed-shell nuclei up to ⁶⁸Ni with these potentials found that ground-state energies and charge radii have a significantly weaker dependence on c_D as compared to nuclear-matter calculations [715]. Furthermore, charge radii did not follow

the trend expected from the corresponding saturation densities. The Δ -full N²LO potential of Ref. [558], on the other hand, leads to better agreement with these observables, which might indicate similar issues with $SU(2)\text{HB}\chi\text{PT}(\Delta)$ as discussed in Sec. 3.1. This clearly shows that a quantitative understanding of the empirical correlation between nuclear saturation and properties of medium-mass to heavy nuclei needs further investigation.

The remarkable (phenomenological) success of the NN and 3N interactions fit by Hebeler *et al.*, foremost the softest potential labeled “1.8/2.0”, in reproducing ground-state energies of closed-shell nuclei from ^4He to ^{100}Sn may provide useful hints in this direction, even though their charge radii also tend to be too small [739, 742]. These SRG-evolved N³LO NN potentials combined with bare N²LO 3N forces exhibit reasonable saturation properties (see the Coester band in Ref. [509]), but were only fit to two- and few-body observables. Quantifying theoretical uncertainties in calculations with these potentials is, however, very difficult since NN and 3N forces are treated at different orders (and not consistently evolved). The use of such inconsistent potentials has been greatly reduced, though, in favor of full N²LO calculations, while N³LO 3N potentials are being actively developed (e.g., by the LENPIC collaboration).

Figure 19 shows the state-of-the-art MBPT calculations of Ref. [509] in neutron matter (top row) and symmetric nuclear matter (bottom row). The 3N forces were fit to the triton as well as the empirical saturation point (gray box). For each momentum cutoff, $\Lambda = 450$ and 500 MeV, three Hamiltonians with different c_D/c_E values were considered (see legend). These six Hamiltonians collapse to two lines (corresponding to the two momentum cutoffs) in neutron matter because the shorter-range leading 3N interactions do not contribute, as already discussed. The 4N Hartree-Fock energies are small compared to the overall uncertainties, only $\approx -(150 - 200)$ keV for the two cutoffs and isospin asymmetries, and thus were not included in Fig. 19. The annotated values represent the predictions for the symmetry energy and the L parameter at saturation density. Both are predicted with remarkable accuracy.

In contrast to N³LO, the results for the energy per particle of symmetric matter are clearly separated for the two momentum cutoffs at N²LO, indicating a reduced cutoff dependence at N³LO. The uncertainty bands estimate the chiral convergence following the EKM approach introduced in Ref. [454], with $Q = p/\Lambda_b$, breakdown scale $\Lambda_b = 500$ MeV, and average Fermi momentum $p = \sqrt{3/5} k_F$. Although the bands overlap and get smaller from N²LO to N³LO, as expected, the uncertainties remain relatively large with several

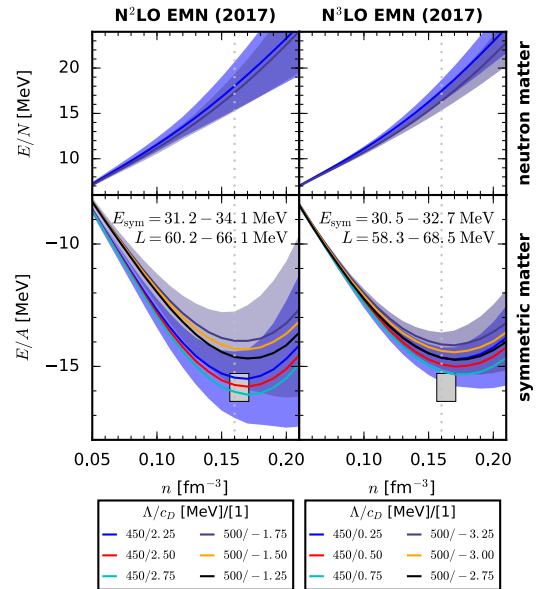


Figure 19: Energy per particle in neutron matter (top row) and symmetric nuclear matter (bottom row) based on consistent chiral NN and 3N at N²LO (first column) and N³LO (second column) that were fit to the empirical saturation region (taken from Ref. [509]). The fitted Hamiltonians are labeled by Λ/c_D in the legend. The blue ($\Lambda = 500$ MeV) and gray ($\Lambda = 450$ MeV) bands estimate the theoretical uncertainty following Ref. [454]. The gray box denotes the empirical saturation point as obtained from a set of energy-density functionals.

MeV at saturation density. The dominant uncertainty in these calculations comes from the chiral convergence. A few years back, the uncertainties in the neutron-matter EOS were dominated by c_i variation in the 3N forces (see Fig. 10 in Ref. [47]). This has considerably changed with the precise Roy-Steiner equation analysis performed by Hoferichter *et al.* Comparing these values to LQCD extractions will be possible in the exascale computing era.

Determining LECs robustly from two- and few-body data is important for model checking and selection of chiral EFT derived within different power countings. Nuclear matter allows for this validation to be performed in medium, with important consequences for nuclear-structure applications. Future LQCD results will provide here guidance as well as insights into the weakly-constrained isospin $\mathcal{T} = 3/2$ components of the 3N forces [112], which are crucial for the neutron-rich matter EOS (as discussed in Sec. 1.1).

Astrophysical applications of the nuclear-matter EOS necessitate a wide range of densities that is usually beyond the reach of nuclear EFTs; for instance, typical central densities of neutron stars exceed nuclear saturation density many times. The nuclear-matter EOS thus might undergo phase transitions (e.g., to exotic matter). Up to which densities chiral EFT converges is *a priori* unknown and should be manifested in the uncertainty bands for the observables. Bayesian methods are powerful in inferring EFT truncation errors and breakdown scales from data.

Piece-wise polytropic expansions [744] and speed-of-sound parametrizations of the EOS [745], guided by causality and observational constraints, have been studied extensively to construct the high-density EOS without making assumptions on the composition of matter. The speed of sound is not necessarily continuous when using polytropic expansions. The precise mass measurements of two neutron stars with $\sim 2 M_\odot$ [146–148] provide strong constraints for the extrapolations since all realistic EOS have to be compatible with these lower maximum-mass limits (see Fig. 11 in Ref. [701]). Recently, Cromartie *et al.* raised the lower maximum-mass limit by measuring a neutron star with $2.17^{+0.11}_{-0.10} M_\odot$ [149]. The uncertainties, however, are still relatively large compared to the other measurements. On the other hand, precisely measuring neutron-star radii is much more challenging, e.g., due to the small number of suitable neutron stars [113]. Other observational constraints come from, e.g., gravitational-wave detections (tidal deformabilities) [671–673] or neutron-star radius measurements. GW170817 has been used to constrain the radius of a $1.4 M_\odot$ neutron star to be $\lesssim 14$ km [673, 746–748](see also Refs. [749, 750]). The most stringent constraints on neutron-star

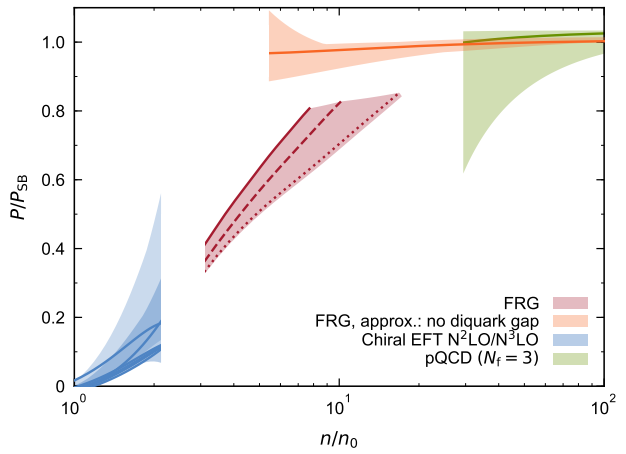


Figure 20: Pressure P of symmetric nuclear matter divided by the pressure of the free quark gas P_{SB} as a function of the normalized density n/n_0 as obtained from chiral EFT (blue bands), FRG (red band), including results from an approximation without accounting for a diquark gap (orange band), and pQCD (green band). The blue bands correspond to the results shown in Fig. 19. This figure was taken from Ref. [49].

On the other hand, precisely measuring neutron-star radii is much more challenging, e.g., due to the small number of suitable neutron stars [113]. Other observational constraints come from, e.g., gravitational-wave detections (tidal deformabilities) [671–673] or neutron-star radius measurements. GW170817 has been used to constrain the radius of a $1.4 M_\odot$ neutron star to be $\lesssim 14$ km [673, 746–748](see also Refs. [749, 750]). The most stringent constraints on neutron-star

radii were recently determined, $R_{1.4 M_\odot} = 11.0^{+0.9}_{-0.6}$ [751]. A comprehensive Bayesian analysis of the EOS exploring the impact of future direct radius measurements can be found in Ref. [45].

The Tolman-Oppenheimer-Volkoff (TOV) equations [752, 753], two coupled differential equations, connect the mass-radius (M - R) relation of nonrotating neutron stars to the EOS bidirectionally. That means, the M - R relation can be calculated given an EOS, and vice versa, the EOS mapped given simultaneous M - R measurements of neutron stars. Such M - R constraints have been inferred (e.g., in Ref. [754]), while NASA’s NICER mission has recently provided its first joint M - R measurement of the millisecond pulsar PSR J0030+0451 [755–758]. More data is to be expected in the near future. This will tighten the uncertainties of the high-density extrapolations considerably. Observations, however, provide only indirect constraints on the EOS in contrast to microscopic calculations.

Leonhardt *et al.* [49] used two complimentary microscopic approaches to study the zero-temperature EOS of symmetric nuclear matter over a wide range of densities as shown in Fig. 20: at $n \leq 2 n_0$, based on the Monte Carlo framework applied to a set of modern chiral NN and 3N interactions (blue bands), while at $n \geq 3 n_0$, directly based on QCD using the FRG (red band), which matches the high-density limit of pQCD (green band).

Specifically, Fig. 20 shows the pressure P divided by the pressure of the free quark gas P_{SB} as a function of density in units of nuclear saturation density, n/n_0 . The blue uncertainty band estimates the EFT truncation error using order-by-order calculations with consistent NN and 3N up to $N^3\text{LO}$. Although the two approaches break down individually at $n \sim (2 - 3) n_0$, the results in the different regimes indicate a promising consistency that seems to allow smooth interpolations for the construction of the EOS over a wide range of densities.

A similar comparison in neutron-rich matter is essential for astrophysical applications. That requires an extension of the FRG framework in Ref. [49] to matter with arbitrary proton fractions. On the other hand, the temperature dependence of the EOS can be studied once the Monte Carlo framework has been extended to finite temperatures. Work along these lines is in progress.

This is an exciting era for nuclear physics and nuclear astrophysics. Once chiral EFT has been connected to LQCD, the outlined approach combining EFT and FRG calculations will enable truly QCD-based (i.e., *ab initio*) predictions of the nuclear-matter EOS with reduced theoretical uncertainties, from the low to the high densities inside neutron stars. This will enable the construction of the EOS as a function of density, isospin-asymmetry and temperature that can be used in large-scale astrophysical simulations, aiming at understanding the process of nucleosynthesis in the universe.

6. Outlook

The exascale computing era will be particularly exciting for the field of nuclear physics and nuclear astrophysics. The disruptive growth in computational power (see Ref. [759] as a lattice QCD example) will allow us to construct a predictive theory of nuclear structure and reactions, rooted in the Standard Model of particle physics and organized in a *tower of effective (field) theories*, built on distinct degrees of freedom, and matched in the regions of overlap. In turn, this will enable us to make robust predictions of nuclear processes with fully quantifiable theoretical uncertainties, which can be confronted with upcoming experimental measurements aimed at searching for BSM physics with unprecedented sensitivity, as well as understanding the behavior of nuclear matter under extreme conditions within the era of multi-messenger astronomy.

High-performance computing has already enabled us to reach milestones, some that were hard to foresee just a few years ago, such as high-precision lattice QCD calculations of single nucleon observables at the physical point, with progress made toward developing systematic control over multi-nucleon scattering and reactions, and the first *ab initio* calculations of medium-mass nuclei based on chiral NN and 3N interactions. For example, as shown in Figure 1 of Refs. [563, 713], the recent rapid growth of the reach in mass number A of *ab initio* nuclear-structure calculations has been fueled by algorithmic advances and high-performance computing. This makes it necessary to revisit and improve uncertainties in the input Hamiltonians derived from (chiral) EFT. As lattice QCD progresses to deliver two- and three-nucleon observables, we will see an earnest connection between QCD and EFT/ETs such that a truly *ab initio* understanding of nuclear physics will become a reality in the foreseeable future.

Acknowledgements

We are grateful to our collaborators for many stimulating discussions over the years. We especially thank R. Briceño, V. Cirigliano, R.J. Furnstahl, B. Hörz, R. Machleidt, J. Menéndez, and W. Weise for their very insightful comments on this article. C.D. acknowledges support by the Alexander von Humboldt Foundation through a Feodor-Lynen Fellowship. E.M. acknowledges support from the LDRD program of Los Alamos National Laboratory. This work is supported in part by the US Department of Energy, the Office of Science, the Office of Nuclear Physics, and SciDAC under awards DE-SC00046548, DE-AC52-06NA25396 and DE-AC0205CH11231, under DOE LLNL Contract No. DE-AC52-07NA27344 and under National Science Foundation Award 1630782.

References

- [1] A. e. a. Aprahamian, Reaching for the horizon: The 2015 long range plan for nuclear science (2015). <https://inspirehep.net/literature/1398831>.
- [2] S. Ritz, et al., Building for Discovery: Strategic Plan for U.S. Particle Physics in the Global Context, https://science.energy.gov/~/media/hep/hepap/pdf/May-2014/FINAL_P5_Report_053014.pdf, 2014.
- [3] B. J. Mount, et al., LUX-ZEPLIN (LZ) Technical Design Report (2017). [arXiv:1703.09144](https://arxiv.org/abs/1703.09144).
- [4] D. Akerib, et al. (LUX-ZEPLIN), Projected WIMP sensitivity of the LUX-ZEPLIN dark matter experiment, Phys. Rev. D 101 (2020) 052002. doi:[10.1103/PhysRevD.101.052002](https://doi.org/10.1103/PhysRevD.101.052002). [arXiv:1802.06039](https://arxiv.org/abs/1802.06039).
- [5] E. Aprile, et al. (XENON), Dark Matter Search Results from a One Ton-Year Exposure of XENON1T, Phys. Rev. Lett. 121 (2018) 111302. doi:[10.1103/PhysRevLett.121.111302](https://doi.org/10.1103/PhysRevLett.121.111302). [arXiv:1805.12562](https://arxiv.org/abs/1805.12562).
- [6] X. Cui, et al. (PandaX-II), Dark Matter Results From 54-Ton-Day Exposure of PandaX-II Experiment, Phys. Rev. Lett. 119 (2017) 181302. doi:[10.1103/PhysRevLett.119.181302](https://doi.org/10.1103/PhysRevLett.119.181302). [arXiv:1708.06917](https://arxiv.org/abs/1708.06917).
- [7] J. Liu, X. Chen, X. Ji, Current status of direct dark matter detection experiments, Nature Phys. 13 (2017) 212–216. doi:[10.1038/nphys4039](https://doi.org/10.1038/nphys4039). [arXiv:1709.00688](https://arxiv.org/abs/1709.00688).
- [8] R. Ajaj, et al. (DEAP), Search for dark matter with a 231-day exposure of liquid argon using DEAP-3600 at SNOLAB, Phys. Rev. D100 (2019) 022004. doi:[10.1103/PhysRevD.100.022004](https://doi.org/10.1103/PhysRevD.100.022004). [arXiv:1902.04048](https://arxiv.org/abs/1902.04048).
- [9] P. Agnes, et al. (DarkSide), DarkSide-50 532-day Dark Matter Search with Low-Radioactivity Argon, Phys. Rev. D98 (2018) 102006. doi:[10.1103/PhysRevD.98.102006](https://doi.org/10.1103/PhysRevD.98.102006). [arXiv:1802.07198](https://arxiv.org/abs/1802.07198).
- [10] R. Agnese, et al. (SuperCDMS), First Dark Matter Constraints from a SuperCDMS Single-Charge Sensitive Detector, Phys. Rev. Lett. 121 (2018) 051301. doi:[10.1103/PhysRevLett.122.069901](https://doi.org/10.1103/PhysRevLett.122.069901), [10.1103/PhysRevLett.121.051301](https://doi.org/10.1103/PhysRevLett.121.051301). [arXiv:1804.10697](https://arxiv.org/abs/1804.10697), [erratum: Phys. Rev. Lett.122,no.6,069901(2019)].
- [11] L. Baudis, The Search for Dark Matter (2018). doi:[10.1017/S1062798717000783](https://doi.org/10.1017/S1062798717000783). [arXiv:1801.08128](https://arxiv.org/abs/1801.08128).
- [12] N. Du, et al. (ADMX), A Search for Invisible Axion Dark Matter with the Axion Dark Matter Experiment, Phys. Rev. Lett. 120 (2018) 151301. doi:[10.1103/PhysRevLett.120.151301](https://doi.org/10.1103/PhysRevLett.120.151301). [arXiv:1804.05750](https://arxiv.org/abs/1804.05750).

- [13] M. Battaglieri, et al., US Cosmic Visions: New Ideas in Dark Matter 2017: Community Report, in: U.S. Cosmic Visions: New Ideas in Dark Matter College Park, MD, USA, March 23-25, 2017, 2017. URL: <http://lss.fnal.gov/archive/2017/conf/fermilab-conf-17-282-ae-ppd-t.pdf>. [arXiv:1707.04591](https://arxiv.org/abs/1707.04591).
- [14] P. W. Graham, D. E. Kaplan, J. Mardon, S. Rajendran, W. A. Terrano, L. Trahms, T. Wilkason, Spin Precession Experiments for Light Axionic Dark Matter, Phys. Rev. D97 (2018) 055006. doi:[10.1103/PhysRevD.97.055006](https://doi.org/10.1103/PhysRevD.97.055006). [arXiv:1709.07852](https://arxiv.org/abs/1709.07852).
- [15] J. B. Albert, et al. (nEXO), Sensitivity and Discovery Potential of nEXO to Neutrinoless Double Beta Decay, Phys. Rev. C97 (2018) 065503. doi:[10.1103/PhysRevC.97.065503](https://doi.org/10.1103/PhysRevC.97.065503). [arXiv:1710.05075](https://arxiv.org/abs/1710.05075).
- [16] J. Martín-Albo, et al. (NEXT), Sensitivity of NEXT-100 to Neutrinoless Double Beta Decay, JHEP 05 (2016) 159. doi:[10.1007/JHEP05\(2016\)159](https://doi.org/10.1007/JHEP05(2016)159). [arXiv:1511.09246](https://arxiv.org/abs/1511.09246).
- [17] A. Gando, et al. (KamLAND-Zen), Search for Majorana Neutrinos near the Inverted Mass Hierarchy Region with KamLAND-Zen, Phys. Rev. Lett. 117 (2016) 082503. doi:[10.1103/PhysRevLett.117.109903](https://doi.org/10.1103/PhysRevLett.117.109903), [10.1103/PhysRevLett.117.082503](https://doi.org/10.1103/PhysRevLett.117.082503). [arXiv:1605.02889](https://arxiv.org/abs/1605.02889), [Addendum: Phys. Rev. Lett. 117, no. 10, 109903 (2016)].
- [18] J. Shirai (KamLAND-Zen), Results and future plans for the KamLAND-Zen experiment, J. Phys. Conf. Ser. 888 (2017) 012031. doi:[10.1088/1742-6596/888/1/012031](https://doi.org/10.1088/1742-6596/888/1/012031).
- [19] C. E. Aalseth, et al. (Majorana), Search for Neutrinoless Double- β Decay in ^{76}Ge with the Majorana Demonstrator, Phys. Rev. Lett. 120 (2018) 132502. doi:[10.1103/PhysRevLett.120.132502](https://doi.org/10.1103/PhysRevLett.120.132502). [arXiv:1710.11608](https://arxiv.org/abs/1710.11608).
- [20] N. Abgrall, et al. (LEGEND), The Large Enriched Germanium Experiment for Neutrinoless Double Beta Decay (LEGEND), AIP Conf. Proc. 1894 (2017) 020027. doi:[10.1063/1.5007652](https://doi.org/10.1063/1.5007652). [arXiv:1709.01980](https://arxiv.org/abs/1709.01980).
- [21] M. Agostini, et al. (GERDA), Results on Neutrinoless Double- β Decay of ^{76}Ge from Phase I of the GERDA Experiment, Phys. Rev. Lett. 111 (2013) 122503. doi:[10.1103/PhysRevLett.111.122503](https://doi.org/10.1103/PhysRevLett.111.122503). [arXiv:1307.4720](https://arxiv.org/abs/1307.4720).
- [22] J. B. Albert, et al. (EXO-200), Search for Majorana neutrinos with the first two years of EXO-200 data, Nature 510 (2014) 229–234. doi:[10.1038/nature13432](https://doi.org/10.1038/nature13432). [arXiv:1402.6956](https://arxiv.org/abs/1402.6956).
- [23] K. Alfonso, et al. (CUORE), Search for Neutrinoless Double-Beta Decay of ^{130}Te with CUORE-0, Phys. Rev. Lett. 115 (2015) 102502. doi:[10.1103/PhysRevLett.115.102502](https://doi.org/10.1103/PhysRevLett.115.102502). [arXiv:1504.02454](https://arxiv.org/abs/1504.02454).
- [24] S. Andringa, et al. (SNO+), Current Status and Future Prospects of the SNO+ Experiment, Adv. High Energy Phys. 2016 (2016) 6194250. doi:[10.1155/2016/6194250](https://doi.org/10.1155/2016/6194250). [arXiv:1508.05759](https://arxiv.org/abs/1508.05759).
- [25] C. Alduino, et al. (CUORE), First Results from CUORE: A Search for Lepton Number Violation via $0\nu\beta\beta$ Decay of ^{130}Te , Phys. Rev. Lett. 120 (2018) 132501. doi:[10.1103/PhysRevLett.120.132501](https://doi.org/10.1103/PhysRevLett.120.132501). [arXiv:1710.07988](https://arxiv.org/abs/1710.07988).
- [26] M. Agostini, M. Allardt, A. M. Bakalyarov, M. Balata, I. Barabanov, L. Baudis, C. Bauer, E. Bellotti, S. Belegurov, S. T. Belyaev, et al., Background-free search for neutrinoless double- β decay of ^{76}Ge with GERDA, Nature 544 (2017) 47. doi:[10.1038/nature21717](https://doi.org/10.1038/nature21717). [arXiv:1703.00570](https://arxiv.org/abs/1703.00570).
- [27] J. B. Albert, et al. (EXO), Search for Neutrinoless Double-Beta Decay with the Upgraded EXO-200 Detector, Phys. Rev. Lett. 120 (2018) 072701. doi:[10.1103/PhysRevLett.120.072701](https://doi.org/10.1103/PhysRevLett.120.072701). [arXiv:1707.08707](https://arxiv.org/abs/1707.08707).
- [28] O. Azzolini, et al. (CUPID-0), First Result on the Neutrinoless Double- β Decay of ^{82}Se with CUPID-0, Phys. Rev. Lett. 120 (2018) 232502. doi:[10.1103/PhysRevLett.120.232502](https://doi.org/10.1103/PhysRevLett.120.232502). [arXiv:1802.07791](https://arxiv.org/abs/1802.07791).
- [29] M. Agostini, et al. (GERDA), Improved Limit on Neutrinoless Double- β Decay of ^{76}Ge from GERDA Phase II, Phys. Rev. Lett. 120 (2018) 132503. doi:[10.1103/PhysRevLett.120.132503](https://doi.org/10.1103/PhysRevLett.120.132503). [arXiv:1803.11100](https://arxiv.org/abs/1803.11100).
- [30] B. Graner, Y. Chen, E. G. Lindahl, B. R. Heckel, Reduced Limit on the Permanent Electric Dipole Moment of $\text{Hg}199$, Phys. Rev. Lett. 116 (2016) 161601. doi:[10.1103/PhysRevLett.116.161601](https://doi.org/10.1103/PhysRevLett.116.161601). [arXiv:1601.04339](https://arxiv.org/abs/1601.04339), [Erratum: Phys. Rev. Lett. 119, no. 11, 119901 (2017)].
- [31] M. Bishof, et al., Improved limit on the ^{225}Ra electric dipole moment, Phys. Rev. C94 (2016) 025501. doi:[10.1103/PhysRevC.94.025501](https://doi.org/10.1103/PhysRevC.94.025501). [arXiv:1606.04931](https://arxiv.org/abs/1606.04931).
- [32] R. Acciarri, et al. (DUNE), Long-Baseline Neutrino Facility (LBNF) and Deep Underground Neutrino Experiment (DUNE) (2015). [arXiv:1512.06148](https://arxiv.org/abs/1512.06148).
- [33] R. Acciarri, et al. (DUNE), Long-Baseline Neutrino Facility (LBNF) and Deep Underground Neutrino Experiment (DUNE) (2016). [arXiv:1601.05471](https://arxiv.org/abs/1601.05471).
- [34] Y. Kuno (COMET), A search for muon-to-electron conversion at J-PARC: The COMET experiment, PTEP 2013 (2013) 022C01. doi:[10.1093/ptep/pts089](https://doi.org/10.1093/ptep/pts089).
- [35] L. Bartoszek, et al. (Mu2e), Mu2e Technical Design Report (2014). doi:[10.2172/1172555](https://doi.org/10.2172/1172555). [arXiv:1501.05241](https://arxiv.org/abs/1501.05241).
- [36] A. Baldini, et al., A submission to the 2020 update of the European Strategy for Particle Physics on behalf of the COMET, MEG, Mu2e and Mu3e collaborations (2018). [arXiv:1812.06540](https://arxiv.org/abs/1812.06540).
- [37] P. Danielewicz, R. Lacey, W. G. Lynch, Determination of the equation of state of dense matter, Science 298 (2002) 1592–1596. doi:[10.1126/science.1078070](https://doi.org/10.1126/science.1078070). [arXiv:nucl-th/0208016](https://arxiv.org/abs/nucl-th/0208016).
- [38] B. A. Freedman, L. D. McLerran, Fermions and Gauge Vector Mesons at Finite Temperature and Density. 1. Formal Techniques, Phys. Rev. D16 (1977) 1130. doi:[10.1103/PhysRevD.16.1130](https://doi.org/10.1103/PhysRevD.16.1130).

- [39] B. A. Freedman, L. D. McLerran, Fermions and Gauge Vector Mesons at Finite Temperature and Density. 3. The Ground State Energy of a Relativistic Quark Gas, *Phys. Rev. D* 16 (1977) 1169. doi:[10.1103/PhysRevD.16.1169](https://doi.org/10.1103/PhysRevD.16.1169).
- [40] V. Baluni, Nonabelian Gauge Theories of Fermi Systems: Chromotheory of Highly Condensed Matter, *Phys. Rev. D* 17 (1978) 2092. doi:[10.1103/PhysRevD.17.2092](https://doi.org/10.1103/PhysRevD.17.2092).
- [41] A. Kurkela, P. Romatschke, A. Vuorinen, Cold Quark Matter, *Phys. Rev. D* 81 (2010) 105021. doi:[10.1103/PhysRevD.81.105021](https://doi.org/10.1103/PhysRevD.81.105021). [arXiv:0912.1856](https://arxiv.org/abs/0912.1856).
- [42] E. S. Fraga, A. Kurkela, A. Vuorinen, Interacting quark matter equation of state for compact stars, *Astrophys. J.* 781 (2014) L25. doi:[10.1088/2041-8205/781/2/L25](https://doi.org/10.1088/2041-8205/781/2/L25). [arXiv:1311.5154](https://arxiv.org/abs/1311.5154).
- [43] E. S. Fraga, A. Kurkela, A. Vuorinen, Neutron star structure from QCD, *Eur. Phys. J. A* 52 (2016) 49. doi:[10.1140/epja/i2016-16049-6](https://doi.org/10.1140/epja/i2016-16049-6). [arXiv:1508.05019](https://arxiv.org/abs/1508.05019).
- [44] E. Annala, T. Gorda, A. Kurkela, A. Vuorinen, Gravitational-wave constraints on the neutron-star-matter Equation of State, *Phys. Rev. Lett.* 120 (2018) 172703. doi:[10.1103/PhysRevLett.120.172703](https://doi.org/10.1103/PhysRevLett.120.172703). [arXiv:1711.02644](https://arxiv.org/abs/1711.02644).
- [45] S. K. Greif, G. Raaijmakers, K. Hebeler, A. Schwenk, A. L. Watts, Equation of state sensitivities when inferring neutron star and dense matter properties, *Mon. Not. Roy. Astron. Soc.* 485 (2019) 5363–5376. doi:[10.1093/mnras/stz654](https://doi.org/10.1093/mnras/stz654). [arXiv:1812.08188](https://arxiv.org/abs/1812.08188).
- [46] J. M. Lattimer, Y. Lim, Constraining the Symmetry Parameters of the Nuclear Interaction, *Astrophys. J.* 771 (2013) 51. doi:[10.1088/0004-637X/771/1/51](https://doi.org/10.1088/0004-637X/771/1/51). [arXiv:1203.4286](https://arxiv.org/abs/1203.4286).
- [47] K. Hebeler, J. D. Holt, J. Menendez, A. Schwenk, Nuclear forces and their impact on neutron-rich nuclei and neutron-rich matter, *Ann. Rev. Nucl. Part. Sci.* 65 (2015) 457–484. doi:[10.1146/annurev-nucl-102313-025446](https://doi.org/10.1146/annurev-nucl-102313-025446). [arXiv:1508.06893](https://arxiv.org/abs/1508.06893).
- [48] C. Wetterich, Exact evolution equation for the effective potential, *Phys. Lett. B* 301 (1993) 90–94. doi:[10.1016/0370-2693\(93\)90726-X](https://doi.org/10.1016/0370-2693(93)90726-X). [arXiv:1710.05815](https://arxiv.org/abs/1710.05815).
- [49] M. Leonhardt, M. Pospiech, B. Schallmo, J. Braun, C. Drischler, K. Hebeler, A. Schwenk, Symmetric nuclear matter from the strong interaction, *Phys. Rev. Lett.* 125 (2020) 142502. doi:[10.1103/PhysRevLett.125.142502](https://doi.org/10.1103/PhysRevLett.125.142502). [arXiv:1907.05814](https://arxiv.org/abs/1907.05814).
- [50] M. Drews, W. Weise, Functional renormalization group studies of nuclear and neutron matter, *Prog. Part. Nucl. Phys.* 93 (2017) 69. doi:[10.1016/j.ppnp.2016.10.002](https://doi.org/10.1016/j.ppnp.2016.10.002). [arXiv:1610.07568](https://arxiv.org/abs/1610.07568).
- [51] Y.-B. Yang, J. Liang, Y.-J. Bi, Y. Chen, T. Draper, K.-F. Liu, Z. Liu, Proton Mass Decomposition from the QCD Energy Momentum Tensor, *Phys. Rev. Lett.* 121 (2018) 212001. doi:[10.1103/PhysRevLett.121.212001](https://doi.org/10.1103/PhysRevLett.121.212001). [arXiv:1808.08677](https://arxiv.org/abs/1808.08677).
- [52] K. G. Wilson, Confinement of Quarks, *Phys. Rev. D* 10 (1974) 2445–2459. doi:[10.1103/PhysRevD.10.2445](https://doi.org/10.1103/PhysRevD.10.2445), [,319(1974)].
- [53] T. Bhattacharya, V. Cirigliano, S. D. Cohen, A. Filipuzzi, M. Gonzalez-Alonso, M. L. Graesser, R. Gupta, H.-W. Lin, Probing Novel Scalar and Tensor Interactions from (Ultra)Cold Neutrons to the LHC, *Phys. Rev. D* 85 (2012) 054512. doi:[10.1103/PhysRevD.85.054512](https://doi.org/10.1103/PhysRevD.85.054512). [arXiv:1110.6448](https://arxiv.org/abs/1110.6448).
- [54] J. Engel, M. J. Ramsey-Musolf, U. van Kolck, Electric Dipole Moments of Nucleons, Nuclei, and Atoms: The Standard Model and Beyond, *Prog. Part. Nucl. Phys.* 71 (2013) 21–74. doi:[10.1016/j.ppnp.2013.03.003](https://doi.org/10.1016/j.ppnp.2013.03.003). [arXiv:1303.2371](https://arxiv.org/abs/1303.2371).
- [55] S. Aoki, et al. (Flavour Lattice Averaging Group), FLAG Review 2019, *Eur. Phys. J. C* 80 (2020) 113. doi:[10.1140/epjc/s10052-019-7354-7](https://doi.org/10.1140/epjc/s10052-019-7354-7). [arXiv:1902.08191](https://arxiv.org/abs/1902.08191).
- [56] R. Abbott, et al. (RBC, UKQCD), Direct CP violation and the $\Delta I = 1/2$ rule in $K \rightarrow \pi\pi$ decay from the standard model, *Phys. Rev. D* 102 (2020) 054509. doi:[10.1103/PhysRevD.102.054509](https://doi.org/10.1103/PhysRevD.102.054509). [arXiv:2004.09440](https://arxiv.org/abs/2004.09440).
- [57] T. Aoyama, et al., The anomalous magnetic moment of the muon in the Standard Model, *Phys. Rept.* 887 (2020) 1–166. doi:[10.1016/j.physrep.2020.07.006](https://doi.org/10.1016/j.physrep.2020.07.006). [arXiv:2006.04822](https://arxiv.org/abs/2006.04822).
- [58] J. Goodman, M. Ibe, A. Rajaraman, W. Shepherd, T. M. P. Tait, H.-B. Yu, Constraints on Dark Matter from Colliders, *Phys. Rev. D* 82 (2010) 116010. doi:[10.1103/PhysRevD.82.116010](https://doi.org/10.1103/PhysRevD.82.116010). [arXiv:1008.1783](https://arxiv.org/abs/1008.1783).
- [59] V. Cirigliano, S. Gardner, B. Holstein, Beta Decays and Non-Standard Interactions in the LHC Era, *Prog. Part. Nucl. Phys.* 71 (2013) 93–118. doi:[10.1016/j.ppnp.2013.03.005](https://doi.org/10.1016/j.ppnp.2013.03.005). [arXiv:1303.6953](https://arxiv.org/abs/1303.6953).
- [60] V. Cirigliano, M. L. Graesser, G. Ovanesyan, I. M. Shoemaker, Shining LUX on Isospin-Violating Dark Matter Beyond Leading Order, *Phys. Lett. B* 739 (2014) 293–301. doi:[10.1016/j.physletb.2014.10.058](https://doi.org/10.1016/j.physletb.2014.10.058). [arXiv:1311.5886](https://arxiv.org/abs/1311.5886).
- [61] M. Hoferichter, P. Klos, A. Schwenk, Chiral power counting of one- and two-body currents in direct detection of dark matter, *Phys. Lett. B* 746 (2015) 410–416. doi:[10.1016/j.physletb.2015.05.041](https://doi.org/10.1016/j.physletb.2015.05.041). [arXiv:1503.04811](https://arxiv.org/abs/1503.04811).

- [62] A. Baroni, L. Girlanda, S. Pastore, R. Schiavilla, M. Viviani, Nuclear Axial Currents in Chiral Effective Field Theory, Phys. Rev. C93 (2016) 015501. doi:[10.1103/PhysRevC.93.049902](https://doi.org/10.1103/PhysRevC.93.049902), [10.1103/PhysRevC.93.015501](https://doi.org/10.1103/PhysRevC.93.015501), [10.1103/PhysRevC.95.059901](https://doi.org/10.1103/PhysRevC.95.059901). arXiv:[1509.07039](https://arxiv.org/abs/1509.07039), [Erratum: Phys. Rev.C95,no.5,059901(2017)].
- [63] H. Krebs, E. Epelbaum, U. G. Meißner, Nuclear axial current operators to fourth order in chiral effective field theory, Annals Phys. 378 (2017) 317–395. doi:[10.1016/j.aop.2017.01.021](https://doi.org/10.1016/j.aop.2017.01.021). arXiv:[1610.03569](https://arxiv.org/abs/1610.03569).
- [64] C. C. Chang, et al., A per-cent-level determination of the nucleon axial coupling from quantum chromodynamics, Nature 558 (2018) 91–94. doi:[10.1038/s41586-018-0161-8](https://doi.org/10.1038/s41586-018-0161-8). arXiv:[1805.12130](https://arxiv.org/abs/1805.12130).
- [65] M. J. Savage, P. E. Shanahan, B. C. Tiburzi, M. L. Wagman, F. Winter, S. R. Beane, E. Chang, Z. Davoudi, W. Detmold, K. Orginos, Proton-Proton Fusion and Tritium β Decay from Lattice Quantum Chromodynamics, Phys. Rev. Lett. 119 (2017) 062002. doi:[10.1103/PhysRevLett.119.062002](https://doi.org/10.1103/PhysRevLett.119.062002). arXiv:[1610.04545](https://arxiv.org/abs/1610.04545).
- [66] E. Chang, Z. Davoudi, W. Detmold, A. S. Gambhir, K. Orginos, M. J. Savage, P. E. Shanahan, M. L. Wagman, F. Winter (NPLQCD), Scalar, Axial, and Tensor Interactions of Light Nuclei from Lattice QCD, Phys. Rev. Lett. 120 (2018) 152002. doi:[10.1103/PhysRevLett.120.152002](https://doi.org/10.1103/PhysRevLett.120.152002). arXiv:[1712.03221](https://arxiv.org/abs/1712.03221).
- [67] Y. Aoki, T. Izubuchi, E. Shintani, A. Soni, Improved lattice computation of proton decay matrix elements, Phys. Rev. D96 (2017) 014506. doi:[10.1103/PhysRevD.96.014506](https://doi.org/10.1103/PhysRevD.96.014506). arXiv:[1705.01338](https://arxiv.org/abs/1705.01338).
- [68] E. Rinaldi, S. Syritsyn, M. L. Wagman, M. I. Buchoff, C. Schroeder, J. Wasem, Neutron-antineutron oscillations from lattice QCD, Phys. Rev. Lett. 122 (2019) 162001. doi:[10.1103/PhysRevLett.122.162001](https://doi.org/10.1103/PhysRevLett.122.162001). arXiv:[1809.00246](https://arxiv.org/abs/1809.00246).
- [69] N. Yamanaka, S. Hashimoto, T. Kaneko, H. Ohki (JLQCD), Nucleon charges with dynamical overlap fermions, Phys. Rev. D98 (2018) 054516. doi:[10.1103/PhysRevD.98.054516](https://doi.org/10.1103/PhysRevD.98.054516). arXiv:[1805.10507](https://arxiv.org/abs/1805.10507).
- [70] R. Gupta, Y.-C. Jang, B. Yoon, H.-W. Lin, V. Cirigliano, T. Bhattacharya, Isovector Charges of the Nucleon from 2+1+1-flavor Lattice QCD, Phys. Rev. D98 (2018) 034503. doi:[10.1103/PhysRevD.98.034503](https://doi.org/10.1103/PhysRevD.98.034503). arXiv:[1806.09006](https://arxiv.org/abs/1806.09006).
- [71] K. Ott nad, T. Harris, H. Meyer, G. von Hippel, J. Wilhelm, H. Wittig, Nucleon charges and quark momentum fraction with $N_f = 2 + 1$ Wilson fermions, PoS LATTICE2018 (2018) 129. doi:[10.22323/1.334.0129](https://doi.org/10.22323/1.334.0129). arXiv:[1809.10638](https://arxiv.org/abs/1809.10638).
- [72] M. Abramczyk, S. Aoki, T. Blum, T. Izubuchi, H. Ohki, S. Syritsyn, Lattice calculation of electric dipole moments and form factors of the nucleon, Phys. Rev. D96 (2017) 014501. doi:[10.1103/PhysRevD.96.014501](https://doi.org/10.1103/PhysRevD.96.014501). arXiv:[1701.07792](https://arxiv.org/abs/1701.07792).
- [73] T. Bhattacharya, B. Yoon, R. Gupta, V. Cirigliano, Neutron Electric Dipole Moment from Beyond the Standard Model, 2018. arXiv:[1812.06233](https://arxiv.org/abs/1812.06233).
- [74] J. Kim, J. Dragos, A. Shindler, T. Luu, J. de Vries, Towards a determination of the nucleon EDM from the quark chromo-EDM operator with the gradient flow, PoS LATTICE2018 (2019) 260. doi:[10.22323/1.334.0260](https://doi.org/10.22323/1.334.0260). arXiv:[1810.10301](https://arxiv.org/abs/1810.10301).
- [75] J. Dragos, T. Luu, A. Shindler, J. de Vries, A. Yousif, Confirming the Existence of the strong CP Problem in Lattice QCD with the Gradient Flow, Phys. Rev. C 103 (2021) 015202. doi:[10.1103/PhysRevC.103.015202](https://doi.org/10.1103/PhysRevC.103.015202). arXiv:[1902.03254](https://arxiv.org/abs/1902.03254).
- [76] S. Syritsyn, T. Izubuchi, H. Ohki, Calculation of Nucleon Electric Dipole Moments Induced by Quark Chromo-Electric Dipole Moments and the QCD θ -term, PoS Confinement2018 (2019) 194. doi:[10.22323/1.336.0194](https://doi.org/10.22323/1.336.0194). arXiv:[1901.05455](https://arxiv.org/abs/1901.05455).
- [77] T. Bhattacharya, V. Cirigliano, R. Gupta, E. Mereghetti, B. Yoon, Dimension-5 CP-odd operators: QCD mixing and renormalization, Phys. Rev. D92 (2015) 114026. doi:[10.1103/PhysRevD.92.114026](https://doi.org/10.1103/PhysRevD.92.114026). arXiv:[1502.07325](https://arxiv.org/abs/1502.07325).
- [78] M. Constantinou, M. Costa, R. Frezzotti, V. Lubicz, G. Martinelli, D. Meloni, H. Panagopoulos, S. Simula, Renormalization of the chromomagnetic operator on the lattice, Phys. Rev. D92 (2015) 034505. doi:[10.1103/PhysRevD.92.034505](https://doi.org/10.1103/PhysRevD.92.034505). arXiv:[1506.00361](https://arxiv.org/abs/1506.00361).
- [79] M. Rizik, C. Monahan, A. Shindler, Renormalization of CP-Violating Pure Gauge Operators in Perturbative QCD Using the Gradient Flow, PoS LATTICE2018 (2018) 215. doi:[10.22323/1.334.0215](https://doi.org/10.22323/1.334.0215). arXiv:[1810.05637](https://arxiv.org/abs/1810.05637).
- [80] R. J. Crewther, P. Di Vecchia, G. Veneziano, E. Witten, Chiral Estimate of the Electric Dipole Moment of the Neutron in Quantum Chromodynamics, Phys. Lett. 88B (1979) 123. doi:[10.1016/0370-2693\(80\)91025-4](https://doi.org/10.1016/0370-2693(80)91025-4), [10.1016/0370-2693\(79\)90128-X](https://doi.org/10.1016/0370-2693(79)90128-X), [Erratum: Phys. Lett. 91B, 487 (1980)].
- [81] E. Mereghetti, W. H. Hockings, U. van Kolck, The Effective Chiral Lagrangian From the Theta Term, Annals Phys. 325 (2010) 2363–2409. doi:[10.1016/j.aop.2010.03.005](https://doi.org/10.1016/j.aop.2010.03.005). arXiv:[1002.2391](https://arxiv.org/abs/1002.2391).
- [82] J. de Vries, E. Mereghetti, A. Walker-Loud, Baryon mass splittings and strong CP violation in SU(3) Chiral Perturbation Theory, Phys. Rev. C92 (2015) 045201. doi:[10.1103/PhysRevC.92.045201](https://doi.org/10.1103/PhysRevC.92.045201). arXiv:[1506.06247](https://arxiv.org/abs/1506.06247).

- [83] C.-Y. Seng, M. Ramsey-Musolf, Parity-violating and time-reversal-violating pion-nucleon couplings: Higher order chiral matching relations, Phys. Rev. C96 (2017) 065204. doi:[10.1103/PhysRevC.96.065204](https://doi.org/10.1103/PhysRevC.96.065204). [arXiv:1611.08063](https://arxiv.org/abs/1611.08063).
- [84] J. de Vries, E. Mereghetti, C.-Y. Seng, A. Walker-Loud, Lattice QCD spectroscopy for hadronic CP violation, Phys. Lett. B766 (2017) 254–262. doi:[10.1016/j.physletb.2017.01.017](https://doi.org/10.1016/j.physletb.2017.01.017). [arXiv:1612.01567](https://arxiv.org/abs/1612.01567).
- [85] V. Cirigliano, W. Dekens, J. de Vries, E. Mereghetti, An ϵ' improvement from right-handed currents, Phys. Lett. B767 (2017) 1–9. doi:[10.1016/j.physletb.2017.01.037](https://doi.org/10.1016/j.physletb.2017.01.037). [arXiv:1612.03914](https://arxiv.org/abs/1612.03914).
- [86] W. C. Haxton, G. J. Stephenson, Double beta Decay, Prog. Part. Nucl. Phys. 12 (1984) 409–479. doi:[10.1016/0146-6410\(84\)90006-1](https://doi.org/10.1016/0146-6410(84)90006-1).
- [87] F. Simkovic, G. Pantelis, J. D. Vergados, A. Faessler, Additional nucleon current contributions to neutrinoless double beta decay, Phys. Rev. C60 (1999) 055502. doi:[10.1103/PhysRevC.60.055502](https://doi.org/10.1103/PhysRevC.60.055502). [arXiv:hep-ph/9905509](https://arxiv.org/abs/hep-ph/9905509).
- [88] H. Pas, M. Hirsch, H. V. Klapdor-Kleingrothaus, S. G. Kovalenko, Towards a superformula for neutrinoless double beta decay, Phys. Lett. B453 (1999) 194–198. doi:[10.1016/S0370-2693\(99\)00330-5](https://doi.org/10.1016/S0370-2693(99)00330-5), [,393(1999)].
- [89] V. Cirigliano, W. Dekens, J. de Vries, M. L. Graesser, E. Mereghetti, Neutrinoless double beta decay in chiral effective field theory: lepton number violation at dimension seven, JHEP 12 (2017) 082. doi:[10.1007/JHEP12\(2017\)082](https://doi.org/10.1007/JHEP12(2017)082). [arXiv:1708.09390](https://arxiv.org/abs/1708.09390).
- [90] V. Cirigliano, W. Dekens, J. de Vries, M. L. Graesser, E. Mereghetti, A neutrinoless double beta decay master formula from effective field theory, JHEP 12 (2018) 097. doi:[10.1007/JHEP12\(2018\)097](https://doi.org/10.1007/JHEP12(2018)097). [arXiv:1806.02780](https://arxiv.org/abs/1806.02780).
- [91] B. Desplanques, J. F. Donoghue, B. R. Holstein, Unified Treatment of the Parity Violating Nuclear Force, Annals Phys. 124 (1980) 449. doi:[10.1016/0003-4916\(80\)90217-1](https://doi.org/10.1016/0003-4916(80)90217-1).
- [92] S.-L. Zhu, C. M. Maekawa, B. R. Holstein, M. J. Ramsey-Musolf, U. van Kolck, Nuclear parity-violation in effective field theory, Nucl. Phys. A748 (2005) 435–498. doi:[10.1016/j.nuclphysa.2004.10.032](https://doi.org/10.1016/j.nuclphysa.2004.10.032). [arXiv:nucl-th/0407087](https://arxiv.org/abs/nucl-th/0407087).
- [93] G. Prezeau, M. Ramsey-Musolf, P. Vogel, Neutrinoless double beta decay and effective field theory, Phys. Rev. D68 (2003) 034016. doi:[10.1103/PhysRevD.68.034016](https://doi.org/10.1103/PhysRevD.68.034016). [arXiv:hep-ph/0303205](https://arxiv.org/abs/hep-ph/0303205).
- [94] J. Wasem, Lattice QCD Calculation of Nuclear Parity Violation, Phys. Rev. C85 (2012) 022501. doi:[10.1103/PhysRevC.85.022501](https://doi.org/10.1103/PhysRevC.85.022501). [arXiv:1108.1151](https://arxiv.org/abs/1108.1151).
- [95] A. Nicholson, et al., Heavy physics contributions to neutrinoless double beta decay from QCD, Phys. Rev. Lett. 121 (2018) 172501. doi:[10.1103/PhysRevLett.121.172501](https://doi.org/10.1103/PhysRevLett.121.172501). [arXiv:1805.02634](https://arxiv.org/abs/1805.02634).
- [96] S. Gardner, W. C. Haxton, B. R. Holstein, A New Paradigm for Hadronic Parity Nonconservation and its Experimental Implications, Ann. Rev. Nucl. Part. Sci. 67 (2017) 69–95. doi:[10.1146/annurev-nucl-041917-033231](https://doi.org/10.1146/annurev-nucl-041917-033231). [arXiv:1704.02617](https://arxiv.org/abs/1704.02617).
- [97] T. Kurth, E. Berkowitz, E. Rinaldi, P. Vranas, A. Nicholson, M. Strother, A. Walker-Loud, E. Rinaldi, Nuclear Parity Violation from Lattice QCD, PoS LATTICE2015 (2016) 329. doi:[10.22323/1.251.0329](https://doi.org/10.22323/1.251.0329). [arXiv:1511.02260](https://arxiv.org/abs/1511.02260).
- [98] J. M. Lattimer, The nuclear equation of state and neutron star masses, Ann. Rev. Nucl. Part. Sci. 62 (2012) 485–515. doi:[10.1146/annurev-nucl-102711-095018](https://doi.org/10.1146/annurev-nucl-102711-095018). [arXiv:1305.3510](https://arxiv.org/abs/1305.3510).
- [99] J. M. Lattimer, Neutron stars are gold mines, Int. J. Mod. Phys. E26 (2017) 1740014. doi:[10.1142/S0218301317400146](https://doi.org/10.1142/S0218301317400146).
- [100] J. M. Lattimer, M. Prakash, The physics of neutron stars, Science 304 (2004) 536–542. doi:[10.1126/science.1090720](https://doi.org/10.1126/science.1090720). [arXiv:astro-ph/0405262](https://arxiv.org/abs/astro-ph/0405262).
- [101] F. Özel, P. Freire, Masses, Radii, and the Equation of State of Neutron Stars, Ann. Rev. Astron. Astrophys. 54 (2016) 401–440. doi:[10.1146/annurev-astro-081915-023322](https://doi.org/10.1146/annurev-astro-081915-023322). [arXiv:1603.02698](https://arxiv.org/abs/1603.02698).
- [102] R. A. Briceño, Z. Davoudi, T. C. Luu, Nuclear Reactions from Lattice QCD, J. Phys. G42 (2015) 023101. doi:[10.1088/0954-3899/42/2/023101](https://doi.org/10.1088/0954-3899/42/2/023101). [arXiv:1406.5673](https://arxiv.org/abs/1406.5673).
- [103] C. McIlroy, C. Barbieri, T. Inoue, T. Doi, T. Hatsuda, Doubly magic nuclei from lattice QCD forces at $M_{PS} = 469 \text{ MeV}/c^2$, Phys. Rev. C97 (2018) 021303. doi:[10.1103/PhysRevC.97.021303](https://doi.org/10.1103/PhysRevC.97.021303). [arXiv:1701.02607](https://arxiv.org/abs/1701.02607).
- [104] S. K. Bogner, R. J. Furnstahl, A. Schwenk, From low-momentum interactions to nuclear structure, Prog. Part. Nucl. Phys. 65 (2010) 94–147. doi:[10.1016/j.ppnp.2010.03.001](https://doi.org/10.1016/j.ppnp.2010.03.001). [arXiv:0912.3688](https://arxiv.org/abs/0912.3688).
- [105] R. J. Furnstahl, The Renormalization Group in Nuclear Physics, Nucl. Phys. Proc. Suppl. 228 (2012) 139–175. doi:[10.1016/j.nuclphysbps.2012.06.005](https://doi.org/10.1016/j.nuclphysbps.2012.06.005). [arXiv:1203.1779](https://arxiv.org/abs/1203.1779).
- [106] F. Wienholtz, et al., Masses of exotic calcium isotopes pin down nuclear forces, Nature 498 (2013) 346–349. doi:[10.1038/nature12226](https://doi.org/10.1038/nature12226).
- [107] R. Lazauskas, Elastic proton scattering on tritium below the n - He-3 threshold, Phys. Rev. C79 (2009) 054007. doi:[10.1103/PhysRevC.79.054007](https://doi.org/10.1103/PhysRevC.79.054007). [arXiv:0903.4750](https://arxiv.org/abs/0903.4750).

- [108] M. Viviani, A. Deltuva, R. Lazauskas, J. Carbonell, A. C. Fonseca, A. Kievsky, L. E. Marcucci, S. Rosati, Benchmark calculation of n-³H and p-³He scattering, Phys. Rev. C84 (2011) 054010. doi:[10.1103/PhysRevC.84.054010](https://doi.org/10.1103/PhysRevC.84.054010). arXiv:[1109.3625](https://arxiv.org/abs/1109.3625).
- [109] A. Ekström, G. R. Jansen, K. A. Wendt, G. Hagen, T. Papenbrock, B. D. Carlsson, C. Forssén, M. Hjorth-Jensen, P. Navrátil, W. Nazarewicz, Accurate nuclear radii and binding energies from a chiral interaction, Phys. Rev. C91 (2015) 051301. doi:[10.1103/PhysRevC.91.051301](https://doi.org/10.1103/PhysRevC.91.051301). arXiv:[1502.04682](https://arxiv.org/abs/1502.04682).
- [110] H. Witala, J. Golak, R. Skibiński, K. Topolnicki, E. Epelbaum, K. Hebeler, H. Kamada, H. Krebs, U. G. Meißner, A. Nogga, Role of the total isospin 3/2 component in three-nucleon reactions, Few Body Syst. 57 (2016) 1213–1225. doi:[10.1007/s00601-016-1156-3](https://doi.org/10.1007/s00601-016-1156-3). arXiv:[1605.02011](https://arxiv.org/abs/1605.02011).
- [111] M. B. Tsang, et al., Constraints on the symmetry energy and neutron skins from experiments and theory, Phys. Rev. C86 (2012) 015803. doi:[10.1103/PhysRevC.86.015803](https://doi.org/10.1103/PhysRevC.86.015803). arXiv:[1204.0466](https://arxiv.org/abs/1204.0466).
- [112] J.-L. Wynen, E. Berkowitz, T. Luu, A. Shindler, J. Bulava, Three neutrons from Lattice QCD, PoS LAT-TICE2018 (2018) 092. doi:[10.22323/1.334.0092](https://doi.org/10.22323/1.334.0092). arXiv:[1810.12747](https://arxiv.org/abs/1810.12747).
- [113] A. L. Watts, et al., Colloquium : Measuring the neutron star equation of state using x-ray timing, Rev. Mod. Phys. 88 (2016) 021001. doi:[10.1103/RevModPhys.88.021001](https://doi.org/10.1103/RevModPhys.88.021001). arXiv:[1602.01081](https://arxiv.org/abs/1602.01081).
- [114] M. G. Alford, A. Schmitt, K. Rajagopal, T. Schäfer, Color superconductivity in dense quark matter, Rev. Mod. Phys. 80 (2008) 1455–1515. doi:[10.1103/RevModPhys.80.1455](https://doi.org/10.1103/RevModPhys.80.1455). arXiv:[0709.4635](https://arxiv.org/abs/0709.4635).
- [115] H. Polinder, J. Haidenbauer, U.-G. Meißner, Hyperon-nucleon interactions: A Chiral effective field theory approach, Nucl. Phys. A779 (2006) 244–266. doi:[10.1016/j.nuclphysa.2006.09.006](https://doi.org/10.1016/j.nuclphysa.2006.09.006). arXiv:[nucl-th/0605050](https://arxiv.org/abs/nucl-th/0605050).
- [116] H. Polinder, J. Haidenbauer, U. G. Meißner, Strangeness $S = -2$ baryon-baryon interactions using chiral effective field theory, Phys. Lett. B653 (2007) 29–37. doi:[10.1016/j.physletb.2007.07.045](https://doi.org/10.1016/j.physletb.2007.07.045). arXiv:[0705.3753](https://arxiv.org/abs/0705.3753).
- [117] H. Polinder, Hyperon-nucleon interactions in effective field theory, in: Proceedings, 9th International Conference on Hypernuclear and Strange Particle Physics (HYP 2006): Mainz, Germany, October 10-14, 2006, 2007, pp. 285–290. doi:[10.1007/978-3-540-76367-3_57](https://doi.org/10.1007/978-3-540-76367-3_57).
- [118] J. Haidenbauer, S. Petschauer, N. Kaiser, U. G. Meißner, A. Nogga, W. Weise, Hyperon-nucleon interaction at next-to-leading order in chiral effective field theory, Nucl. Phys. A915 (2013) 24–58. doi:[10.1016/j.nuclphysa.2013.06.008](https://doi.org/10.1016/j.nuclphysa.2013.06.008). arXiv:[1304.5339](https://arxiv.org/abs/1304.5339).
- [119] J. Haidenbauer, U.-G. Meißner, S. Petschauer, Strangeness $S = ?2$ baryon-baryon interaction at next-to-leading order in chiral effective field theory, Nucl. Phys. A954 (2016) 273–293. doi:[10.1016/j.nuclphysa.2016.01.006](https://doi.org/10.1016/j.nuclphysa.2016.01.006). arXiv:[1511.05859](https://arxiv.org/abs/1511.05859).
- [120] S. Petschauer, N. Kaiser, J. Haidenbauer, U.-G. Meißner, W. Weise, Leading three-baryon forces from SU(3) chiral effective field theory, Phys. Rev. C93 (2016) 014001. doi:[10.1103/PhysRevC.93.014001](https://doi.org/10.1103/PhysRevC.93.014001). arXiv:[1511.02095](https://arxiv.org/abs/1511.02095).
- [121] U.-G. Meißner, J. Haidenbauer, Foundations of Strangeness Nuclear Physics derived from chiral Effective Field Theory, Int. J. Mod. Phys. E26 (2017) 1740019. doi:[10.1142/S0218301317400195](https://doi.org/10.1142/S0218301317400195). arXiv:[1603.06429](https://arxiv.org/abs/1603.06429).
- [122] J. Haidenbauer, S. Petschauer, N. Kaiser, U.-G. Meißner, W. Weise, Scattering of decuplet baryons in chiral effective field theory, Eur. Phys. J. C77 (2017) 760. doi:[10.1140/epjc/s10052-017-5309-4](https://doi.org/10.1140/epjc/s10052-017-5309-4). arXiv:[1708.08071](https://arxiv.org/abs/1708.08071).
- [123] J. Haidenbauer, U. G. Meißner, A. Nogga, Hyperon-nucleon interaction within chiral effective field theory revisited, Eur. Phys. J. A56 (2020) 91. doi:[10.1140/epja/s10050-020-00100-4](https://doi.org/10.1140/epja/s10050-020-00100-4). arXiv:[1906.11681](https://arxiv.org/abs/1906.11681).
- [124] A. Nogga, Light hypernuclei based on chiral and phenomenological interactions, Nucl. Phys. A914 (2013) 140–150. doi:[10.1016/j.nuclphysa.2013.02.053](https://doi.org/10.1016/j.nuclphysa.2013.02.053).
- [125] S. Petschauer, J. Haidenbauer, N. Kaiser, U.-G. Meißner, W. Weise, Density-dependent effective baryon?baryon interaction from chiral three-baryon forces, Nucl. Phys. A957 (2017) 347–378. doi:[10.1016/j.nuclphysa.2016.09.010](https://doi.org/10.1016/j.nuclphysa.2016.09.010). arXiv:[1607.04307](https://arxiv.org/abs/1607.04307).
- [126] J. Haidenbauer, U.-G. Meißner, A study of hyperons in nuclear matter based on chiral effective field theory, Nucl. Phys. A936 (2015) 29–44. doi:[10.1016/j.nuclphysa.2015.01.005](https://doi.org/10.1016/j.nuclphysa.2015.01.005). arXiv:[1411.3114](https://arxiv.org/abs/1411.3114).
- [127] S. Petschauer, J. Haidenbauer, N. Kaiser, U.-G. Meißner, W. Weise, Hyperons in nuclear matter from SU(3) chiral effective field theory, Eur. Phys. J. A52 (2016) 15. doi:[10.1140/epja/i2016-16015-4](https://doi.org/10.1140/epja/i2016-16015-4). arXiv:[1507.08808](https://arxiv.org/abs/1507.08808).
- [128] J. Haidenbauer, U. G. Meißner, N. Kaiser, W. Weise, Lambda-nuclear interactions and hyperon puzzle in neutron stars, Eur. Phys. J. A53 (2017) 121. doi:[10.1140/epja/i2017-12316-4](https://doi.org/10.1140/epja/i2017-12316-4). arXiv:[1612.03758](https://arxiv.org/abs/1612.03758).
- [129] R. Wirth, R. Roth, Induced Hyperon-Nucleon-Nucleon Interactions and the Hyperon Puzzle, Phys. Rev. Lett. 117 (2016) 182501. doi:[10.1103/PhysRevLett.117.182501](https://doi.org/10.1103/PhysRevLett.117.182501). arXiv:[1605.08677](https://arxiv.org/abs/1605.08677).
- [130] R. Wirth, R. Roth, Light Neutron-Rich Hypernuclei from the Importance-Truncated No-Core Shell Model, Phys. Lett. B779 (2018) 336–341. doi:[10.1016/j.physletb.2018.02.021](https://doi.org/10.1016/j.physletb.2018.02.021). arXiv:[1710.04880](https://arxiv.org/abs/1710.04880).
- [131] R. Wirth, D. Gazda, P. Navrátil, A. Calci, J. Langhammer, R. Roth, Ab Initio Description of p-Shell Hypernuclei, Phys. Rev. Lett. 113 (2014) 192502. doi:[10.1103/PhysRevLett.113.192502](https://doi.org/10.1103/PhysRevLett.113.192502). arXiv:[1403.3067](https://arxiv.org/abs/1403.3067).

- [132] R. Wirth, D. Gazda, P. Navrátil, R. Roth, Hypernuclear No-Core Shell Model, Phys. Rev. C97 (2018) 064315. doi:[10.1103/PhysRevC.97.064315](https://doi.org/10.1103/PhysRevC.97.064315). arXiv:[1712.05694](https://arxiv.org/abs/1712.05694).
- [133] R. Wirth, R. Roth, Similarity renormalization group evolution of hypernuclear Hamiltonians, Phys. Rev. C100 (2019) 044313. doi:[10.1103/PhysRevC.100.044313](https://doi.org/10.1103/PhysRevC.100.044313). arXiv:[1902.03324](https://arxiv.org/abs/1902.03324).
- [134] H. Djapo, B.-J. Schaefer, J. Wambach, On the appearance of hyperons in neutron stars, Phys. Rev. C81 (2010) 035803. doi:[10.1103/PhysRevC.81.035803](https://doi.org/10.1103/PhysRevC.81.035803). arXiv:[0811.2939](https://arxiv.org/abs/0811.2939).
- [135] D. Lonardoni, F. Pederiva, S. Gandolfi, Accurate determination of the interaction between Λ hyperons and nucleons from auxiliary field diffusion Monte Carlo calculations, Phys. Rev. C89 (2014) 014314. doi:[10.1103/PhysRevC.89.014314](https://doi.org/10.1103/PhysRevC.89.014314). arXiv:[1312.3844](https://arxiv.org/abs/1312.3844).
- [136] D. Lonardoni, F. Pederiva, S. Gandolfi, Auxiliary Field Diffusion Monte Carlo study of the Hyperon-Nucleon interaction in Λ -hypernuclei, Nucl. Phys. A914 (2013) 243–247. doi:[10.1016/j.nuclphysa.2012.12.001](https://doi.org/10.1016/j.nuclphysa.2012.12.001). arXiv:[1211.6381](https://arxiv.org/abs/1211.6381).
- [137] D. Lonardoni, S. Gandolfi, F. Pederiva, Effects of the two-body and three-body hyperon-nucleon interactions in Λ -hypernuclei, Phys. Rev. C87 (2013) 041303. doi:[10.1103/PhysRevC.87.041303](https://doi.org/10.1103/PhysRevC.87.041303). arXiv:[1301.7472](https://arxiv.org/abs/1301.7472).
- [138] D. Lonardoni, F. Pederiva, S. Gandolfi, From hypernuclei to the Inner Core of Neutron Stars: A Quantum Monte Carlo Study, J. Phys. Conf. Ser. 529 (2014) 012012. doi:[10.1088/1742-6596/529/1/012012](https://doi.org/10.1088/1742-6596/529/1/012012). arXiv:[1408.4492](https://arxiv.org/abs/1408.4492).
- [139] D. Lonardoni, A. Lovato, S. Gandolfi, F. Pederiva, Hyperon Puzzle: Hints from Quantum Monte Carlo Calculations, Phys. Rev. Lett. 114 (2015) 092301. doi:[10.1103/PhysRevLett.114.092301](https://doi.org/10.1103/PhysRevLett.114.092301). arXiv:[1407.4448](https://arxiv.org/abs/1407.4448).
- [140] D. Lonardoni, F. Pederiva, Medium-mass hypernuclei and the nucleon-isospin dependence of the three-body hyperon-nucleon-nucleon force (2017). arXiv:[1711.07521](https://arxiv.org/abs/1711.07521).
- [141] S. Gandolfi, D. Lonardoni, The equation of state of dense matter and the effect of Λ hyperons to neutron star structure, AIP Conf. Proc. 2130 (2019) 020019. doi:[10.1063/1.5118387](https://doi.org/10.1063/1.5118387).
- [142] S. Nishizaki, T. Takatsuka, Y. Yamamoto, Effective $Y\bar{N}$ and YY interactions and hyperon mixing in neutron star matter: $Y = \text{Lambda}$ case, Prog. Theor. Phys. 105 (2001) 607–626. doi:[10.1143/PTP.105.607](https://doi.org/10.1143/PTP.105.607).
- [143] S. Nishizaki, T. Takatsuka, Y. Yamamoto, Hyperon-mixed neutron star matter and neutron stars, Prog. Theor. Phys. 108 (2002) 703–718. doi:[10.1143/PTP.108.703](https://doi.org/10.1143/PTP.108.703).
- [144] T. Hell, W. Weise, Dense baryonic matter: constraints from recent neutron star observations, Phys. Rev. C90 (2014) 045801. doi:[10.1103/PhysRevC.90.045801](https://doi.org/10.1103/PhysRevC.90.045801). arXiv:[1402.4098](https://arxiv.org/abs/1402.4098).
- [145] I. Bombaci, The Hyperon Puzzle in Neutron Stars, JPS Conf. Proc. 17 (2017) 101002. doi:[10.7566/JPSCP.17.101002](https://doi.org/10.7566/JPSCP.17.101002). arXiv:[1601.05339](https://arxiv.org/abs/1601.05339).
- [146] P. Demorest, T. Pennucci, S. Ransom, M. Roberts, J. Hessels, Shapiro Delay Measurement of A Two Solar Mass Neutron Star, Nature 467 (2010) 1081–1083. doi:[10.1038/nature09466](https://doi.org/10.1038/nature09466). arXiv:[1010.5788](https://arxiv.org/abs/1010.5788).
- [147] J. Antoniadis, et al., A Massive Pulsar in a Compact Relativistic Binary, Science 340 (2013) 6131. doi:[10.1126/science.1233232](https://doi.org/10.1126/science.1233232). arXiv:[1304.6875](https://arxiv.org/abs/1304.6875).
- [148] E. Fonseca, et al., The NANOGrav Nine-year Data Set: Mass and Geometric Measurements of Binary Millisecond Pulsars, Astrophys. J. 832 (2016) 167. doi:[10.3847/0004-637X/832/2/167](https://doi.org/10.3847/0004-637X/832/2/167). arXiv:[1603.00545](https://arxiv.org/abs/1603.00545).
- [149] H. T. Cromartie, et al., Relativistic Shapiro delay measurements of an extremely massive millisecond pulsar, Nat. Astron. 4 (2019) 72–76. doi:[10.1038/s41550-019-0880-2](https://doi.org/10.1038/s41550-019-0880-2). arXiv:[1904.06759](https://arxiv.org/abs/1904.06759).
- [150] S. R. Beane, E. Chang, S. D. Cohen, W. Detmold, H. W. Lin, T. C. Luu, K. Orginos, A. Parreno, M. J. Savage, A. Walker-Loud, Hyperon-Nucleon Interactions and the Composition of Dense Nuclear Matter from Quantum Chromodynamics, Phys. Rev. Lett. 109 (2012) 172001. doi:[10.1103/PhysRevLett.109.172001](https://doi.org/10.1103/PhysRevLett.109.172001). arXiv:[1204.3606](https://arxiv.org/abs/1204.3606).
- [151] K. Sasaki (HAL QCD), Coupled channel approach to hyperonic interactions from lattice QCD, Nucl. Phys. A914 (2013) 231–237. doi:[10.1016/j.nuclphysa.2013.06.003](https://doi.org/10.1016/j.nuclphysa.2013.06.003).
- [152] D. Kasen, B. Metzger, J. Barnes, E. Quataert, E. Ramirez-Ruiz, Origin of the heavy elements in binary neutron-star mergers from a gravitational wave event, Nature (2017). doi:[10.1038/nature24453](https://doi.org/10.1038/nature24453). arXiv:[1710.05463](https://arxiv.org/abs/1710.05463), [Nature551,80(2017)].
- [153] F. K. Thielemann, M. Eichler, I. V. Panov, B. Wehmeyer, Neutron Star Mergers and Nucleosynthesis of Heavy Elements, Ann. Rev. Nucl. Part. Sci. 67 (2017) 253–274. doi:[10.1146/annurev-nucl-101916-123246](https://doi.org/10.1146/annurev-nucl-101916-123246). arXiv:[1710.02142](https://arxiv.org/abs/1710.02142).
- [154] J. J. Cowan, C. Sneden, J. E. Lawler, A. Aprahamian, M. Wiescher, K. Langanke, G. Martínez-Pinedo, F.-K. Thielemann, Origin of the heaviest elements: The rapid neutron-capture process, Rev. Mod. Phys. 93 (2021) 15002. doi:[10.1103/RevModPhys.93.015002](https://doi.org/10.1103/RevModPhys.93.015002). arXiv:[1901.01410](https://arxiv.org/abs/1901.01410).
- [155] H. Sakurai, Nuclear physics with RI Beam Factory, Front. Phys. (Beijing) 13 (2018) 132111. doi:[10.1007/s11467-018-0849-0](https://doi.org/10.1007/s11467-018-0849-0).

- [156] A. B. Balantekin, J. Carlson, D. J. Dean, G. M. Fuller, R. J. Furnstahl, M. Hjorth-Jensen, R. V. F. Janssens, B.-A. Li, W. Nazarewicz, F. M. Nunes, W. E. Ormand, S. Reddy, B. M. Sherrill, Nuclear Theory and Science of the Facility for Rare Isotope Beams, *Mod. Phys. Lett. A* 29 (2014) 1430010. doi:[10.1142/S0217732314300109](https://doi.org/10.1142/S0217732314300109). [arXiv:1401.6435](https://arxiv.org/abs/1401.6435).
- [157] C. J. Horowitz, et al., *r*-Process Nucleosynthesis: Connecting Rare-Isotope Beam Facilities with the Cosmos, *J. Phys. G* 46 (2019) 083001. doi:[10.1088/1361-6471/ab0849](https://doi.org/10.1088/1361-6471/ab0849). [arXiv:1805.04637](https://arxiv.org/abs/1805.04637).
- [158] C. Forssen, G. Hagen, M. Hjorth-Jensen, W. Nazarewicz, J. Rotureau, Living on the edge of stability, the limits of the nuclear landscape, *Phys. Scripta* T152 (2013) 014022. doi:[10.1088/0031-8949/2013/T152/014022](https://doi.org/10.1088/0031-8949/2013/T152/014022). [arXiv:1212.6364](https://arxiv.org/abs/1212.6364).
- [159] L. Neufcourt, Y. Cao, W. Nazarewicz, F. Viens, Bayesian approach to model-based extrapolation of nuclear observables, *Phys. Rev. C* 98 (2018) 034318. doi:[10.1103/PhysRevC.98.034318](https://doi.org/10.1103/PhysRevC.98.034318). [arXiv:1806.00552](https://arxiv.org/abs/1806.00552).
- [160] S. R. Stroberg, J. D. Holt, A. Schwenk, J. Simonis, *Ab Initio* Limits of Atomic Nuclei, *Phys. Rev. Lett.* 126 (2021) 022501. doi:[10.1103/PhysRevLett.126.022501](https://doi.org/10.1103/PhysRevLett.126.022501). [arXiv:1905.10475](https://arxiv.org/abs/1905.10475).
- [161] L. Neufcourt, Y. Cao, W. Nazarewicz, E. Olsen, F. Viens, Neutron drip line in the Ca region from Bayesian model averaging, *Phys. Rev. Lett.* 122 (2019) 062502. doi:[10.1103/PhysRevLett.122.062502](https://doi.org/10.1103/PhysRevLett.122.062502). [arXiv:1901.07632](https://arxiv.org/abs/1901.07632).
- [162] H. W. Hammer, C. Ji, D. Phillips, Effective field theory description of halo nuclei, *J. Phys. G* 44 (2017) 103002. doi:[10.1088/1361-6471/aa83db](https://doi.org/10.1088/1361-6471/aa83db). [arXiv:1702.08605](https://arxiv.org/abs/1702.08605).
- [163] L. Platter, Effective Field Theory for Halo Nuclei, *Few-Body Systems* 58 (2017) 105. doi:[10.1007/s00601-017-1263-9](https://doi.org/10.1007/s00601-017-1263-9).
- [164] S. Duane, A. D. Kennedy, B. J. Pendleton, D. Roweth, Hybrid Monte Carlo, *Phys. Lett.* B195 (1987) 216–222. doi:[10.1016/0370-2693\(87\)91197-X](https://doi.org/10.1016/0370-2693(87)91197-X).
- [165] M. C. Bañuls, K. Cichy, Review on Novel Methods for Lattice Gauge Theories, *Rept. Prog. Phys.* 83 (2020) 024401. doi:[10.1088/1361-6633/ab6311](https://doi.org/10.1088/1361-6633/ab6311). [arXiv:1910.00257](https://arxiv.org/abs/1910.00257).
- [166] P. F. Bedaque, A complex path around the sign problem, *EPJ Web Conf.* 175 (2018) 01020. doi:[10.1051/epjconf/201817501020](https://doi.org/10.1051/epjconf/201817501020). [arXiv:1711.05868](https://arxiv.org/abs/1711.05868).
- [167] P. A. Boyle, Machines and Algorithms, *PoS LATTICE2016* (2017) 013. doi:[10.22323/1.256.0013](https://doi.org/10.22323/1.256.0013). [arXiv:1702.00208](https://arxiv.org/abs/1702.00208).
- [168] M. A. Clark, R. Babich, K. Barros, R. C. Brower, C. Rebbi, Solving Lattice QCD systems of equations using mixed precision solvers on GPUs, *Comput. Phys. Commun.* 181 (2010) 1517–1528. doi:[10.1016/j.cpc.2010.05.002](https://doi.org/10.1016/j.cpc.2010.05.002). [arXiv:0911.3191](https://arxiv.org/abs/0911.3191), <https://github.com/lattice/quda>.
- [169] R. Babich, M. A. Clark, B. Joo, G. Shi, R. C. Brower, S. Gottlieb, Scaling Lattice QCD beyond 100 GPUs, in: SC11 International Conference for High Performance Computing, Networking, Storage and Analysis Seattle, Washington, November 12-18, 2011, 2011. [arXiv:1109.2935](https://arxiv.org/abs/1109.2935).
- [170] M. Luscher, Topology, the Wilson flow and the HMC algorithm, *PoS LATTICE2010* (2010) 015. doi:[10.22323/1.105.0015](https://doi.org/10.22323/1.105.0015). [arXiv:1009.5877](https://arxiv.org/abs/1009.5877).
- [171] S. Aoki, et al., Review of lattice results concerning low-energy particle physics, *Eur. Phys. J. C* 77 (2017) 112. doi:[10.1140/epjc/s10052-016-4509-7](https://doi.org/10.1140/epjc/s10052-016-4509-7). [arXiv:1607.00299](https://arxiv.org/abs/1607.00299).
- [172] M. Luscher, Volume Dependence of the Energy Spectrum in Massive Quantum Field Theories. 1. Stable Particle States, *Commun. Math. Phys.* 104 (1986) 177. doi:[10.1007/BF01211589](https://doi.org/10.1007/BF01211589).
- [173] G. Colangelo, S. Durr, C. Haefeli, Finite volume effects for meson masses and decay constants, *Nucl. Phys. B* 721 (2005) 136–174. doi:[10.1016/j.nuclphysb.2005.05.015](https://doi.org/10.1016/j.nuclphysb.2005.05.015). [arXiv:hep-lat/0503014](https://arxiv.org/abs/hep-lat/0503014).
- [174] H. B. Nielsen, M. Ninomiya, No Go Theorem for Regularizing Chiral Fermions, *Phys. Lett.* 105B (1981) 219–223. doi:[10.1016/0370-2693\(81\)91026-1](https://doi.org/10.1016/0370-2693(81)91026-1).
- [175] S. Chandrasekharan, U. J. Wiese, An Introduction to chiral symmetry on the lattice, *Prog. Part. Nucl. Phys.* 53 (2004) 373–418. doi:[10.1016/j.ppnp.2004.05.003](https://doi.org/10.1016/j.ppnp.2004.05.003). [arXiv:hep-lat/0405024](https://arxiv.org/abs/hep-lat/0405024).
- [176] K. Symanzik, Continuum Limit and Improved Action in Lattice Theories. 1. Principles and phi**4 Theory, *Nucl. Phys. B* 226 (1983) 187–204. doi:[10.1016/0550-3213\(83\)90468-6](https://doi.org/10.1016/0550-3213(83)90468-6).
- [177] K. Symanzik, Continuum Limit and Improved Action in Lattice Theories. 2. O(N) Nonlinear Sigma Model in Perturbation Theory, *Nucl. Phys. B* 226 (1983) 205–227. doi:[10.1016/0550-3213\(83\)90469-8](https://doi.org/10.1016/0550-3213(83)90469-8).
- [178] L. Maiani, G. Martinelli, M. L. Paciello, B. Taglienti, Scalar Densities and Baryon Mass Differences in Lattice QCD With Wilson Fermions, *Nucl. Phys. B* 293 (1987) 420. doi:[10.1016/0550-3213\(87\)90078-2](https://doi.org/10.1016/0550-3213(87)90078-2).
- [179] J. Bulava, M. Donnellan, R. Sommer, On the computation of hadron-to-hadron transition matrix elements in lattice QCD, *JHEP* 01 (2012) 140. doi:[10.1007/JHEP01\(2012\)140](https://doi.org/10.1007/JHEP01(2012)140). [arXiv:1108.3774](https://arxiv.org/abs/1108.3774).
- [180] G. M. de Divitiis, R. Petronzio, N. Tantalo, On the extraction of zero momentum form factors on the lattice, *Phys. Lett.* B718 (2012) 589–596. doi:[10.1016/j.physletb.2012.10.035](https://doi.org/10.1016/j.physletb.2012.10.035). [arXiv:1208.5914](https://arxiv.org/abs/1208.5914).

- [181] F. Bernardoni, J. Bulava, M. Donnellan, R. Sommer (ALPHA), Precision lattice QCD computation of the $B^*B\pi$ coupling, Phys. Lett. B740 (2015) 278–284. doi:[10.1016/j.physletb.2014.11.051](https://doi.org/10.1016/j.physletb.2014.11.051). arXiv:[1404.6951](https://arxiv.org/abs/1404.6951).
- [182] A. J. Chambers, et al. (CSSM, QCDSF/UKQCD), Feynman-Hellmann approach to the spin structure of hadrons, Phys. Rev. D90 (2014) 014510. doi:[10.1103/PhysRevD.90.014510](https://doi.org/10.1103/PhysRevD.90.014510). arXiv:[1405.3019](https://arxiv.org/abs/1405.3019).
- [183] A. J. Chambers, et al., Disconnected contributions to the spin of the nucleon, Phys. Rev. D92 (2015) 114517. doi:[10.1103/PhysRevD.92.114517](https://doi.org/10.1103/PhysRevD.92.114517). arXiv:[1508.06856](https://arxiv.org/abs/1508.06856).
- [184] C. Bouchard, C. C. Chang, T. Kurth, K. Orginos, A. Walker-Loud, On the Feynman-Hellmann Theorem in Quantum Field Theory and the Calculation of Matrix Elements, Phys. Rev. D96 (2017) 014504. doi:[10.1103/PhysRevD.96.014504](https://doi.org/10.1103/PhysRevD.96.014504). arXiv:[1612.06963](https://arxiv.org/abs/1612.06963).
- [185] G. P. Lepage, The Analysis of Algorithms for Lattice Field Theory, in: Boulder ASI 1989:97-120, 1989, pp. 97–120.
- [186] G. S. Bali, B. Lang, B. U. Musch, A. Schäfer, Novel quark smearing for hadrons with high momenta in lattice QCD, Phys. Rev. D93 (2016) 094515. doi:[10.1103/PhysRevD.93.094515](https://doi.org/10.1103/PhysRevD.93.094515). arXiv:[1602.05525](https://arxiv.org/abs/1602.05525).
- [187] S. R. Beane, W. Detmold, T. C. Luu, K. Orginos, A. Parreno, M. J. Savage, A. Torok, A. Walker-Loud, High Statistics Analysis using Anisotropic Clover Lattices: (I) Single Hadron Correlation Functions, Phys. Rev. D79 (2009) 114502. doi:[10.1103/PhysRevD.79.114502](https://doi.org/10.1103/PhysRevD.79.114502). arXiv:[0903.2990](https://arxiv.org/abs/0903.2990).
- [188] S. R. Beane, W. Detmold, T. C. Luu, K. Orginos, A. Parreno, M. J. Savage, A. Torok, A. Walker-Loud, High Statistics Analysis using Anisotropic Clover Lattices. II. Three-Baryon Systems, Phys. Rev. D 80 (2009) 074501. doi:[10.1103/PhysRevD.80.074501](https://doi.org/10.1103/PhysRevD.80.074501). arXiv:[0905.0466](https://arxiv.org/abs/0905.0466).
- [189] S. R. Beane, W. Detmold, H.-W. Lin, T. C. Luu, K. Orginos, M. J. Savage, A. Torok, A. Walker-Loud (NPLQCD), High Statistics Analysis using Anisotropic Clover Lattices: (III) Baryon-Baryon Interactions, Phys. Rev. D81 (2010) 054505. doi:[10.1103/PhysRevD.81.054505](https://doi.org/10.1103/PhysRevD.81.054505). arXiv:[0912.4243](https://arxiv.org/abs/0912.4243).
- [190] T. Yamazaki, Y. Kuramashi, A. Ukawa (PACS-CS), Helium Nuclei in Quenched Lattice QCD, Phys. Rev. D81 (2010) 111504. doi:[10.1103/PhysRevD.81.111504](https://doi.org/10.1103/PhysRevD.81.111504). arXiv:[0912.1383](https://arxiv.org/abs/0912.1383).
- [191] T. Doi, M. G. Endres, Unified contraction algorithm for multi-baryon correlators on the lattice, Comput. Phys. Commun. 184 (2013) 117. doi:[10.1016/j.cpc.2012.09.004](https://doi.org/10.1016/j.cpc.2012.09.004). arXiv:[1205.0585](https://arxiv.org/abs/1205.0585).
- [192] W. Detmold, K. Orginos, Nuclear correlation functions in lattice QCD, Phys. Rev. D87 (2013) 114512. doi:[10.1103/PhysRevD.87.114512](https://doi.org/10.1103/PhysRevD.87.114512). arXiv:[1207.1452](https://arxiv.org/abs/1207.1452).
- [193] J. Günther, B. C. Toth, L. Varnhorst, Recursive approach to determine correlation functions in multibaryon systems, Phys. Rev. D87 (2013) 094513. doi:[10.1103/PhysRevD.87.094513](https://doi.org/10.1103/PhysRevD.87.094513). arXiv:[1301.4895](https://arxiv.org/abs/1301.4895).
- [194] S. Beane, P. Bedaque, K. Orginos, M. Savage, Nucleon-nucleon scattering from fully-dynamical lattice QCD, Phys. Rev. Lett. 97 (2006) 012001. doi:[10.1103/PhysRevLett.97.012001](https://doi.org/10.1103/PhysRevLett.97.012001). arXiv:[hep-lat/0602010](https://arxiv.org/abs/hep-lat/0602010).
- [195] N. Ishii, S. Aoki, T. Hatsuda, The Nuclear Force from Lattice QCD, Phys. Rev. Lett. 99 (2007) 022001. doi:[10.1103/PhysRevLett.99.022001](https://doi.org/10.1103/PhysRevLett.99.022001). arXiv:[nucl-th/0611096](https://arxiv.org/abs/nucl-th/0611096).
- [196] S. R. Beane, et al. (NPLQCD), Evidence for a Bound H-dibaryon from Lattice QCD, Phys. Rev. Lett. 106 (2011) 162001. doi:[10.1103/PhysRevLett.106.162001](https://doi.org/10.1103/PhysRevLett.106.162001). arXiv:[1012.3812](https://arxiv.org/abs/1012.3812).
- [197] T. Inoue, N. Ishii, S. Aoki, T. Doi, T. Hatsuda, Y. Ikeda, K. Murano, H. Nemura, K. Sasaki (HAL QCD), Bound H-dibaryon in Flavor SU(3) Limit of Lattice QCD, Phys. Rev. Lett. 106 (2011) 162002. doi:[10.1103/PhysRevLett.106.162002](https://doi.org/10.1103/PhysRevLett.106.162002). arXiv:[1012.5928](https://arxiv.org/abs/1012.5928).
- [198] R. L. Jaffe, Perhaps a Stable Dihyperon, Phys. Rev. Lett. 38 (1977) 195–198. doi:[10.1103/PhysRevLett.38.195](https://doi.org/10.1103/PhysRevLett.38.195), [Erratum: Phys. Rev. Lett. 38, 617 (1977)].
- [199] DOE Office of Nuclear Physics and Office of Advanced Scientific Computing Research, Scientific Grand Challenges: Forefront questions in nuclear science and the role of computing at the extreme scale, 2009. URL: https://extremecomputing.labworks.org/nuclearphysics/PNNL_18739_onlineversion_opt.pdf.
- [200] T. Yamazaki, K.-i. Ishikawa, Y. Kuramashi, A. Ukawa, Study of quark mass dependence of binding energy for light nuclei in 2+1 flavor lattice QCD, Phys. Rev. D92 (2015) 014501. doi:[10.1103/PhysRevD.92.014501](https://doi.org/10.1103/PhysRevD.92.014501). arXiv:[1502.04182](https://arxiv.org/abs/1502.04182).
- [201] E. Epelbaum, U.-G. Meißner, W. Gloeckle, Nuclear forces in the chiral limit, Nucl. Phys. A 714 (2003) 535–574. doi:[10.1016/S0375-9474\(02\)01393-3](https://doi.org/10.1016/S0375-9474(02)01393-3). arXiv:[nucl-th/0207089](https://arxiv.org/abs/nucl-th/0207089).
- [202] S. R. Beane, M. J. Savage, The Quark mass dependence of two nucleon systems, Nucl. Phys. A 717 (2003) 91–103. doi:[10.1016/S0375-9474\(02\)01586-5](https://doi.org/10.1016/S0375-9474(02)01586-5). arXiv:[nucl-th/0208021](https://arxiv.org/abs/nucl-th/0208021).
- [203] DOE Exascale Requirements Review: Nuclear Physics, 2016. URL: <https://exascaleage.org/np/>.
- [204] S. Durr, et al., Ab-Initio Determination of Light Hadron Masses, Science 322 (2008) 1224–1227. doi:[10.1126/science.1163233](https://doi.org/10.1126/science.1163233). arXiv:[0906.3599](https://arxiv.org/abs/0906.3599).
- [205] S. Borsanyi, et al., Ab initio calculation of the neutron-proton mass difference, Science 347 (2015) 1452–1455. doi:[10.1126/science.1257050](https://doi.org/10.1126/science.1257050). arXiv:[1406.4088](https://arxiv.org/abs/1406.4088).

- [206] T. Bhattacharya, V. Cirigliano, S. Cohen, R. Gupta, A. Joseph, H.-W. Lin, B. Yoon (PNDME), Iso-vector and Iso-scalar Tensor Charges of the Nucleon from Lattice QCD, Phys. Rev. D92 (2015) 094511. doi:[10.1103/PhysRevD.92.094511](https://doi.org/10.1103/PhysRevD.92.094511). [arXiv:1506.06411](https://arxiv.org/abs/1506.06411).
- [207] T. Bhattacharya, V. Cirigliano, S. Cohen, R. Gupta, H.-W. Lin, B. Yoon, Axial, Scalar and Tensor Charges of the Nucleon from 2+1+1-flavor Lattice QCD, Phys. Rev. D94 (2016) 054508. doi:[10.1103/PhysRevD.94.054508](https://doi.org/10.1103/PhysRevD.94.054508). [arXiv:1606.07049](https://arxiv.org/abs/1606.07049).
- [208] R. Gupta, B. Yoon, T. Bhattacharya, V. Cirigliano, Y.-C. Jang, H.-W. Lin, Flavor diagonal tensor charges of the nucleon from (2+1+1)-flavor lattice QCD, Phys. Rev. D98 (2018) 091501. doi:[10.1103/PhysRevD.98.091501](https://doi.org/10.1103/PhysRevD.98.091501). [arXiv:1808.07597](https://arxiv.org/abs/1808.07597).
- [209] T. Harris, G. von Hippel, P. Junnarkar, H. B. Meyer, K. Ottnad, J. Wilhelm, H. Wittig, L. Wrang, Nucleon isovector charges and twist-2 matrix elements with $N_f = 2 + 1$ dynamical Wilson quarks, Phys. Rev. D100 (2019) 034513. doi:[10.1103/PhysRevD.100.034513](https://doi.org/10.1103/PhysRevD.100.034513). [arXiv:1905.01291](https://arxiv.org/abs/1905.01291).
- [210] Y.-C. Jang, R. Gupta, H.-W. Lin, B. Yoon, T. Bhattacharya, Nucleon electromagnetic form factors in the continuum limit from (2+1+1)-flavor lattice QCD, Phys. Rev. D101 (2020) 014507. doi:[10.1103/PhysRevD.101.014507](https://doi.org/10.1103/PhysRevD.101.014507). [arXiv:1906.07217](https://arxiv.org/abs/1906.07217).
- [211] 2016. Science Talk 1: Cold Nuclear Physics, USQCD Annual Progress Review to the US DOE, <http://www.usqcd.org/reviews/June2016Review/agenda.html>; Nuclear Physics Exascale Requirements Review, <https://science.energy.gov/~/media/ascr/pdf/programdocuments/docs/2017/DOE-ExascaleReport-NP-Final.pdf>.
- [212] C. Chang, L. Del Debbio, A. Nicholson, S. Syritsyn, P. Vranas, A. Walker-Loud, J. Zanotti, Determination of $g_A(0)$ and $g_A(q^2)$ from Lattice QCD (????). [arXiv:Invited contribution to the Annual Review of Nuclear and Particle Science](https://arxiv.org/abs/1903.06487).
- [213] K. Orginos, A. Radyushkin, J. Karpie, S. Zafeiropoulos, Lattice QCD exploration of parton pseudo-distribution functions, Phys. Rev. D 96 (2017) 094503. doi:[10.1103/PhysRevD.96.094503](https://doi.org/10.1103/PhysRevD.96.094503). [arXiv:1706.05373](https://arxiv.org/abs/1706.05373).
- [214] N. Hasan, J. Green, S. Meinel, M. Engelhardt, S. Krieg, J. Negele, A. Pochinsky, S. Syritsyn, Nucleon axial, scalar, and tensor charges using lattice QCD at the physical pion mass, Phys. Rev. D 99 (2019) 114505. doi:[10.1103/PhysRevD.99.114505](https://doi.org/10.1103/PhysRevD.99.114505). [arXiv:1903.06487](https://arxiv.org/abs/1903.06487).
- [215] C. Alexandrou, S. Bacchio, M. Constantinou, J. Finkenrath, K. Hadjyiannakou, K. Jansen, G. Koutsou, A. Vaquero Aviles-Casco, Nucleon axial, tensor, and scalar charges and σ -terms in lattice QCD, Phys. Rev. D 102 (2020) 054517. doi:[10.1103/PhysRevD.102.054517](https://doi.org/10.1103/PhysRevD.102.054517). [arXiv:1909.00485](https://arxiv.org/abs/1909.00485).
- [216] W. Detmold, C.-J. Lin, S. Meinel, Axial couplings and strong decay widths of heavy hadrons, Phys. Rev. Lett. 108 (2012) 172003. doi:[10.1103/PhysRevLett.108.172003](https://doi.org/10.1103/PhysRevLett.108.172003). [arXiv:1109.2480](https://arxiv.org/abs/1109.2480).
- [217] T. Bhattacharya, R. Gupta, B. Yoon, Recent results of nucleon structure & matrix element calculations, PoS LATTICE2019 (2020) 247. doi:[10.22323/1.363.0247](https://doi.org/10.22323/1.363.0247). [arXiv:2003.08490](https://arxiv.org/abs/2003.08490).
- [218] A. Walker-Loud, CalLat elastic nucleon structure, 1, in: 37th International Symposium on Lattice Field Theory, 2020.
- [219] Y.-C. Jang, R. Gupta, B. Yoon, T. Bhattacharya, Axial Vector Form Factors from Lattice QCD that Satisfy the PCAC Relation, Phys. Rev. Lett. 124 (2020) 072002. doi:[10.1103/PhysRevLett.124.072002](https://doi.org/10.1103/PhysRevLett.124.072002). [arXiv:1905.06470](https://arxiv.org/abs/1905.06470).
- [220] Y.-C. Jang, R. Gupta, T. Bhattacharya, S. Park, B. Yoon, H.-W. Lin, Nucleon Axial Form Factors from Clover Fermion on 2+1+1-flavor HISQ Lattice, PoS LATTICE2019 (2020) 131. doi:[10.22323/1.363.0131](https://doi.org/10.22323/1.363.0131). [arXiv:2001.11592](https://arxiv.org/abs/2001.11592).
- [221] O. Bär, Three-particle $N\pi\pi$ state contribution to the nucleon two-point function in lattice QCD, Phys. Rev. D 97 (2018) 094507. doi:[10.1103/PhysRevD.97.094507](https://doi.org/10.1103/PhysRevD.97.094507). [arXiv:1802.10442](https://arxiv.org/abs/1802.10442).
- [222] G. S. Bali, et al., Nucleon mass and sigma term from lattice QCD with two light fermion flavors, Nucl. Phys. B866 (2013) 1–25. doi:[10.1016/j.nuclphysb.2012.08.009](https://doi.org/10.1016/j.nuclphysb.2012.08.009). [arXiv:1206.7034](https://arxiv.org/abs/1206.7034).
- [223] S. Durr, et al., Lattice computation of the nucleon scalar quark contents at the physical point, Phys. Rev. Lett. 116 (2016) 172001. doi:[10.1103/PhysRevLett.116.172001](https://doi.org/10.1103/PhysRevLett.116.172001). [arXiv:1510.08013](https://arxiv.org/abs/1510.08013).
- [224] Y.-B. Yang, A. Alexandru, T. Draper, J. Liang, K.-F. Liu (xQCD), πN and strangeness sigma terms at the physical point with chiral fermions, Phys. Rev. D94 (2016) 054503. doi:[10.1103/PhysRevD.94.054503](https://doi.org/10.1103/PhysRevD.94.054503). [arXiv:1511.09089](https://arxiv.org/abs/1511.09089).
- [225] G. S. Bali, S. Collins, D. Richtmann, A. Schäfer, W. Söldner, A. Sternbeck (RQCD), Direct determinations of the nucleon and pion σ terms at nearly physical quark masses, Phys. Rev. D93 (2016) 094504. doi:[10.1103/PhysRevD.93.094504](https://doi.org/10.1103/PhysRevD.93.094504). [arXiv:1603.00827](https://arxiv.org/abs/1603.00827).
- [226] S. Borsanyi, Z. Fodor, C. Hoelbling, L. Lellouch, K. Szabo, C. Torrero, L. Varnhorst, Ab-initio calculation of the proton and the neutron's scalar couplings for new physics searches (2020). [arXiv:2007.03319](https://arxiv.org/abs/2007.03319).

- [227] M. Hoferichter, J. Ruiz de Elvira, B. Kubis, U.-G. Meißner, High-Precision Determination of the Pion-Nucleon σ Term from Roy-Steiner Equations, Phys. Rev. Lett. 115 (2015) 092301. doi:[10.1103/PhysRevLett.115.092301](https://doi.org/10.1103/PhysRevLett.115.092301). arXiv:[1506.04142](https://arxiv.org/abs/1506.04142).
- [228] M. Hoferichter, J. Ruiz de Elvira, B. Kubis, U.-G. Meißner, Remarks on the pion-nucleon σ -term, Phys. Lett. B760 (2016) 74–78. doi:[10.1016/j.physletb.2016.06.038](https://doi.org/10.1016/j.physletb.2016.06.038). arXiv:[1602.07688](https://arxiv.org/abs/1602.07688).
- [229] L. Maiani, M. Testa, Final state interactions from Euclidean correlation functions, Phys. Lett. B245 (1990) 585–590. doi:[10.1016/0370-2693\(90\)90695-3](https://doi.org/10.1016/0370-2693(90)90695-3).
- [230] M. Lüscher, Volume Dependence of the Energy Spectrum in Massive Quantum Field Theories. 2. Scattering States, Commun. Math. Phys. 105 (1986) 153–188. doi:[10.1007/BF01211097](https://doi.org/10.1007/BF01211097).
- [231] M. Lüscher, Two particle states on a torus and their relation to the scattering matrix, Nucl. Phys. B354 (1991) 531–578. doi:[10.1016/0550-3213\(91\)90366-6](https://doi.org/10.1016/0550-3213(91)90366-6).
- [232] S. R. Beane, P. F. Bedaque, A. Parreno, M. J. Savage, Exploring hyperons and hypernuclei with lattice QCD, Nucl. Phys. A747 (2005) 55–74. doi:[10.1016/j.nuclphysa.2004.09.081](https://doi.org/10.1016/j.nuclphysa.2004.09.081). arXiv:[nucl-th/0311027](https://arxiv.org/abs/nucl-th/0311027).
- [233] S. R. Beane, P. F. Bedaque, A. Parreno, M. J. Savage, Two nucleons on a lattice, Phys. Lett. B585 (2004) 106–114. doi:[10.1016/j.physletb.2004.02.007](https://doi.org/10.1016/j.physletb.2004.02.007). arXiv:[hep-lat/0312004](https://arxiv.org/abs/hep-lat/0312004).
- [234] N. Ishizuka, Derivation of Lüscher's finite size formula for N pi and NN system, PoS LAT2009 (2009) 119. doi:[10.22323/1.091.0119](https://doi.org/10.22323/1.091.0119). arXiv:[0910.2772](https://arxiv.org/abs/0910.2772).
- [235] T. Luu, M. J. Savage, Extracting Scattering Phase-Shifts in Higher Partial-Waves from Lattice QCD Calculations, Phys. Rev. D83 (2011) 114508. doi:[10.1103/PhysRevD.83.114508](https://doi.org/10.1103/PhysRevD.83.114508). arXiv:[1101.3347](https://arxiv.org/abs/1101.3347).
- [236] L. Leskovec, S. Prelovsek, Scattering phase shifts for two particles of different mass and non-zero total momentum in lattice QCD, Phys. Rev. D85 (2012) 114507. doi:[10.1103/PhysRevD.85.114507](https://doi.org/10.1103/PhysRevD.85.114507). arXiv:[1202.2145](https://arxiv.org/abs/1202.2145).
- [237] N. Li, C. Liu, Generalized Lüscher formula in multichannel baryon-meson scattering, Phys. Rev. D87 (2013) 014502. doi:[10.1103/PhysRevD.87.014502](https://doi.org/10.1103/PhysRevD.87.014502). arXiv:[1209.2201](https://arxiv.org/abs/1209.2201).
- [238] R. A. Briceño, Z. Davoudi, T. C. Luu, Two-Nucleon Systems in a Finite Volume: (I) Quantization Conditions, Phys. Rev. D88 (2013) 034502. doi:[10.1103/PhysRevD.88.034502](https://doi.org/10.1103/PhysRevD.88.034502). arXiv:[1305.4903](https://arxiv.org/abs/1305.4903).
- [239] R. A. Briceño, Z. Davoudi, T. Luu, M. J. Savage, Two-nucleon systems in a finite volume. II. $^3S_1 - ^3D_1$ coupled channels and the deuteron, Phys. Rev. D88 (2013) 114507. doi:[10.1103/PhysRevD.88.114507](https://doi.org/10.1103/PhysRevD.88.114507). arXiv:[1309.3556](https://arxiv.org/abs/1309.3556).
- [240] K. Rummukainen, S. A. Gottlieb, Resonance scattering phase shifts on a nonrest frame lattice, Nucl. Phys. B450 (1995) 397–436. doi:[10.1016/0550-3213\(95\)00313-H](https://doi.org/10.1016/0550-3213(95)00313-H). arXiv:[hep-lat/9503028](https://arxiv.org/abs/hep-lat/9503028).
- [241] X. Li, C. Liu, Two particle states in an asymmetric box, Phys. Lett. B587 (2004) 100–104. doi:[10.1016/j.physletb.2004.02.068](https://doi.org/10.1016/j.physletb.2004.02.068). arXiv:[hep-lat/0311035](https://arxiv.org/abs/hep-lat/0311035).
- [242] X. Feng, X. Li, C. Liu, Two particle states in an asymmetric box and the elastic scattering phases, Phys. Rev. D70 (2004) 014505. doi:[10.1103/PhysRevD.70.014505](https://doi.org/10.1103/PhysRevD.70.014505). arXiv:[hep-lat/0404001](https://arxiv.org/abs/hep-lat/0404001).
- [243] C. h. Kim, C. T. Sachrajda, S. R. Sharpe, Finite-volume effects for two-hadron states in moving frames, Nucl. Phys. B727 (2005) 218–243. doi:[10.1016/j.nuclphysb.2005.08.029](https://doi.org/10.1016/j.nuclphysb.2005.08.029). arXiv:[hep-lat/0507006](https://arxiv.org/abs/hep-lat/0507006).
- [244] S. Bour, S. Koenig, D. Lee, H. W. Hammer, U.-G. Meißner, Topological phases for bound states moving in a finite volume, Phys. Rev. D84 (2011) 091503. doi:[10.1103/PhysRevD.84.091503](https://doi.org/10.1103/PhysRevD.84.091503). arXiv:[1107.1272](https://arxiv.org/abs/1107.1272).
- [245] Z. Davoudi, M. J. Savage, Improving the Volume Dependence of Two-Body Binding Energies Calculated with Lattice QCD, Phys. Rev. D84 (2011) 114502. doi:[10.1103/PhysRevD.84.114502](https://doi.org/10.1103/PhysRevD.84.114502). arXiv:[1108.5371](https://arxiv.org/abs/1108.5371).
- [246] R. A. Briceno, Z. Davoudi, Moving multichannel systems in a finite volume with application to proton-proton fusion, Phys. Rev. D 88 (2013) 094507. doi:[10.1103/PhysRevD.88.094507](https://doi.org/10.1103/PhysRevD.88.094507). arXiv:[1204.1110](https://arxiv.org/abs/1204.1110).
- [247] F. X. Lee, A. Alexandru, Scattering phase-shift formulas for mesons and baryons in elongated boxes, Phys. Rev. D96 (2017) 054508. doi:[10.1103/PhysRevD.96.054508](https://doi.org/10.1103/PhysRevD.96.054508). arXiv:[1706.00262](https://arxiv.org/abs/1706.00262).
- [248] R. A. Briceño, Two-particle multichannel systems in a finite volume with arbitrary spin, Phys. Rev. D89 (2014) 074507. doi:[10.1103/PhysRevD.89.074507](https://doi.org/10.1103/PhysRevD.89.074507). arXiv:[1401.3312](https://arxiv.org/abs/1401.3312).
- [249] K. Polejaeva, A. Rusetsky, Three particles in a finite volume, Eur. Phys. J. A48 (2012) 67. doi:[10.1140/epja/i2012-12067-8](https://doi.org/10.1140/epja/i2012-12067-8). arXiv:[1203.1241](https://arxiv.org/abs/1203.1241).
- [250] R. A. Briceno, Z. Davoudi, Three-particle scattering amplitudes from a finite volume formalism, Phys. Rev. D 87 (2013) 094507. doi:[10.1103/PhysRevD.87.094507](https://doi.org/10.1103/PhysRevD.87.094507). arXiv:[1212.3398](https://arxiv.org/abs/1212.3398).
- [251] M. T. Hansen, S. R. Sharpe, Relativistic, model-independent, three-particle quantization condition, Phys. Rev. D90 (2014) 116003. doi:[10.1103/PhysRevD.90.116003](https://doi.org/10.1103/PhysRevD.90.116003). arXiv:[1408.5933](https://arxiv.org/abs/1408.5933).
- [252] M. T. Hansen, S. R. Sharpe, Expressing the three-particle finite-volume spectrum in terms of the three-to-three scattering amplitude, Phys. Rev. D92 (2015) 114509. doi:[10.1103/PhysRevD.92.114509](https://doi.org/10.1103/PhysRevD.92.114509). arXiv:[1504.04248](https://arxiv.org/abs/1504.04248).
- [253] R. A. Briceño, M. T. Hansen, S. R. Sharpe, Relating the finite-volume spectrum and the two-and-three-particle S matrix for relativistic systems of identical scalar particles, Phys. Rev. D95 (2017) 074510. doi:[10.1103/PhysRevD.95.074510](https://doi.org/10.1103/PhysRevD.95.074510).

- [1103/PhysRevD.95.074510. arXiv:1701.07465.](#)
- [254] H.-W. Hammer, J.-Y. Pang, A. Rusetsky, Three-particle quantization condition in a finite volume: 1. The role of the three-particle force, JHEP 09 (2017) 109. doi:[10.1007/JHEP09\(2017\)109](#). [arXiv:1706.07700](#).
- [255] H. W. Hammer, J. Y. Pang, A. Rusetsky, Three particle quantization condition in a finite volume: 2. general formalism and the analysis of data, JHEP 10 (2017) 115. doi:[10.1007/JHEP10\(2017\)115](#). [arXiv:1707.02176](#).
- [256] M. Mai, M. Döring, Three-body Unitarity in the Finite Volume, Eur. Phys. J. A 53 (2017) 240. doi:[10.1140/epja/i2017-12440-1](#). [arXiv:1709.08222](#).
- [257] M. Döring, H.-W. Hammer, M. Mai, J. Y. Pang, A. Rusetsky, J. Wu, Three-body spectrum in a finite volume: the role of cubic symmetry, Phys. Rev. D97 (2018) 114508. doi:[10.1103/PhysRevD.97.114508](#). [arXiv:1802.03362](#).
- [258] M. T. Hansen, F. Romero-López, S. R. Sharpe, Generalizing the relativistic quantization condition to include all three-pion isospin channels, JHEP 07 (2020) 047. doi:[10.1007/JHEP07\(2020\)047](#). [arXiv:2003.10974](#), [Erratum: JHEP 02, 014 (2021)].
- [259] V. Bernard, U.-G. Meißner, A. Rusetsky, The Delta-resonance in a finite volume, Nucl. Phys. B788 (2008) 1–20. doi:[10.1016/j.nuclphysb.2007.07.030](#). [arXiv:hep-lat/0702012](#).
- [260] J. M. M. Hall, A. C. P. Hsu, D. B. Leinweber, A. W. Thomas, R. D. Young, Finite-volume matrix Hamiltonian model for a $\Delta \rightarrow N\pi$ system, Phys. Rev. D87 (2013) 094510. doi:[10.1103/PhysRevD.87.094510](#). [arXiv:1303.4157](#).
- [261] J.-J. Wu, T. S. H. Lee, A. W. Thomas, R. D. Young, Finite-volume Hamiltonian method for coupled-channels interactions in lattice QCD, Phys. Rev. C90 (2014) 055206. doi:[10.1103/PhysRevC.90.055206](#). [arXiv:1402.4868](#).
- [262] R. A. Briceno, J. J. Dudek, R. D. Young, Scattering processes and resonances from lattice QCD, Rev. Mod. Phys. 90 (2018) 025001. doi:[10.1103/RevModPhys.90.025001](#). [arXiv:1706.06223](#).
- [263] A. Torok, S. R. Beane, W. Detmold, T. C. Luu, K. Orginos, A. Parreno, M. J. Savage, A. Walker-Loud, Meson-Baryon Scattering Lengths from Mixed-Action Lattice QCD, Phys. Rev. D81 (2010) 074506. doi:[10.1103/PhysRevD.81.074506](#). [arXiv:0907.1913](#).
- [264] C. B. Lang, V. Verduci, Scattering in the πN negative parity channel in lattice QCD, Phys. Rev. D87 (2013) 054502. doi:[10.1103/PhysRevD.87.054502](#). [arXiv:1212.5055](#).
- [265] D. Mohler, Review of lattice studies of resonances, PoS LATTICE2012 (2012) 003. doi:[10.22323/1.164.0003](#). [arXiv:1211.6163](#).
- [266] W. Detmold, A. Nicholson, Low energy scattering phase shifts for meson-baryon systems, Phys. Rev. D93 (2016) 114511. doi:[10.1103/PhysRevD.93.114511](#). [arXiv:1511.02275](#).
- [267] C. B. Lang, L. Leskovec, M. Padmanath, S. Prelovsek, Pion-nucleon scattering in the Roper channel from lattice QCD, Phys. Rev. D95 (2017) 014510. doi:[10.1103/PhysRevD.95.014510](#). [arXiv:1610.01422](#).
- [268] C. W. Andersen, J. Bulava, B. Hörrz, C. Morningstar, Elastic $I = 3/2p$ -wave nucleon-pion scattering amplitude and the $\Delta(1232)$ resonance from $N_f=2+1$ lattice QCD, Phys. Rev. D97 (2018) 014506. doi:[10.1103/PhysRevD.97.014506](#). [arXiv:1710.01557](#).
- [269] S. Paul, et al., Towards the P-wave nucleon-pion scattering amplitude in the $\Delta(1232)$ channel, PoS LATTICE2018 (2018) 089. doi:[10.22323/1.334.0089](#). [arXiv:1812.01059](#).
- [270] T. Khan, D. G. Richards, F. Winter, Positive-parity Baryon Spectra on Isotropic Lattice, PoS LATTICE2018 (2019) 312. doi:[10.22323/1.334.0312](#).
- [271] S. R. Beane, E. Chang, W. Detmold, H. W. Lin, T. C. Luu, K. Orginos, A. Parreno, M. J. Savage, A. Torok, A. Walker-Loud (NPLQCD), The Deuteron and Exotic Two-Body Bound States from Lattice QCD, Phys. Rev. D85 (2012) 054511. doi:[10.1103/PhysRevD.85.054511](#). [arXiv:1109.2889](#).
- [272] S. R. Beane, E. Chang, S. D. Cohen, W. Detmold, H. W. Lin, T. C. Luu, K. Orginos, A. Parreno, M. J. Savage, A. Walker-Loud (NPLQCD), Light Nuclei and Hypernuclei from Quantum Chromodynamics in the Limit of SU(3) Flavor Symmetry, Phys. Rev. D87 (2013) 034506. doi:[10.1103/PhysRevD.87.034506](#). [arXiv:1206.5219](#).
- [273] T. Yamazaki, K.-i. Ishikawa, Y. Kuramashi, A. Ukawa, Helium nuclei, deuteron and dineutron in 2+1 flavor lattice QCD, Phys. Rev. D86 (2012) 074514. doi:[10.1103/PhysRevD.86.074514](#). [arXiv:1207.4277](#).
- [274] S. R. Beane, et al. (NPLQCD), Nucleon-Nucleon Scattering Parameters in the Limit of SU(3) Flavor Symmetry, Phys. Rev. C88 (2013) 024003. doi:[10.1103/PhysRevC.88.024003](#). [arXiv:1301.5790](#).
- [275] K. Orginos, A. Parreno, M. J. Savage, S. R. Beane, E. Chang, W. Detmold, Two nucleon systems at $m_\pi \sim 450$ MeV from lattice QCD, Phys. Rev. D92 (2015) 114512. doi:[10.1103/PhysRevD.92.114512](#). [arXiv:1508.07583](#).
- [276] E. Berkowitz, T. Kurth, A. Nicholson, B. Joo, E. Rinaldi, M. Strother, P. M. Vranas, A. Walker-Loud, Two-Nucleon Higher Partial-Wave Scattering from Lattice QCD, Phys. Lett. B765 (2017) 285–292. doi:[10.1016/j.jhep.2017.08.001](#).

- [physletb](#).2016.12.024. [arXiv:1508.00886](#).
- [277] M. L. Wagman, F. Winter, E. Chang, Z. Davoudi, W. Detmold, K. Orginos, M. J. Savage, P. E. Shanahan, Baryon-Baryon Interactions and Spin-Flavor Symmetry from Lattice Quantum Chromodynamics, *Phys. Rev. D*96 (2017) 114510. doi:[10.1103/PhysRevD.96.114510](#). [arXiv:1706.06550](#).
- [278] E. Berkowitz, et al., Progress in Multibaryon Spectroscopy, *PoS LATTICE2018* (2018) 003. doi:[10.22323/1.334.0003](#). [arXiv:1902.09416](#).
- [279] S. R. Beane, P. F. Bedaque, T. C. Luu, K. Orginos, E. Pallante, A. Parreno, M. J. Savage (NPLQCD), Hyperon-Nucleon Scattering from Fully-Dynamical Lattice QCD, *Nucl. Phys.* A794 (2007) 62–72. doi:[10.1016/j.nuclphysa.2007.07.006](#). [arXiv:hep-lat/0612026](#).
- [280] H. Nemura, N. Ishii, S. Aoki, T. Hatsuda, Hyperon-nucleon force from lattice QCD, *Phys. Lett.* B673 (2009) 136–141. doi:[10.1016/j.physletb.2009.02.003](#). [arXiv:0806.1094](#).
- [281] A. Francis, J. R. Green, P. M. Junnarkar, C. Miao, T. D. Rae, H. Wittig, Lattice QCD study of the H dibaryon using hexaquark and two-baryon interpolators, *Phys. Rev. D*99 (2019) 074505. doi:[10.1103/PhysRevD.99.074505](#). [arXiv:1805.03966](#).
- [282] S. Aoki, T. Hatsuda, N. Ishii, Theoretical Foundation of the Nuclear Force in QCD and its applications to Central and Tensor Forces in Quenched Lattice QCD Simulations, *Prog. Theor. Phys.* 123 (2010) 89–128. doi:[10.1143/PTP.123.89](#). [arXiv:0909.5585](#).
- [283] K. Murano, N. Ishii, S. Aoki, T. Hatsuda, Nucleon-Nucleon Potential and its Non-locality in Lattice QCD, *Prog. Theor. Phys.* 125 (2011) 1225–1240. doi:[10.1143/PTP.125.1225](#). [arXiv:1103.0619](#).
- [284] S. Aoki, N. Ishii, T. Doi, T. Hatsuda, Y. Ikeda, T. Inoue, K. Murano, H. Nemura, K. Sasaki (HAL QCD), Extraction of Hadron Interactions above Inelastic Threshold in Lattice QCD, *Proc. Japan Acad. B* 87 (2011) 509–517. doi:[10.2183/pjab.87.509](#). [arXiv:1106.2281](#).
- [285] N. Ishii, S. Aoki, T. Doi, T. Hatsuda, Y. Ikeda, T. Inoue, K. Murano, H. Nemura, K. Sasaki (HAL QCD), Hadron-hadron interactions from imaginary-time Nambu-Bethe-Salpeter wave function on the lattice, *Phys. Lett. B*712 (2012) 437–441. doi:[10.1016/j.physletb.2012.04.076](#). [arXiv:1203.3642](#).
- [286] S. Aoki, T. Doi, T. Hatsuda, Y. Ikeda, T. Inoue, N. Ishii, K. Murano, H. Nemura, K. Sasaki (HAL QCD), Lattice QCD approach to Nuclear Physics, *PTEP* 2012 (2012) 01A105. doi:[10.1093/ptep/pts010](#). [arXiv:1206.5088](#).
- [287] S. Aoki, B. Charron, T. Doi, T. Hatsuda, T. Inoue, N. Ishii, Construction of energy-independent potentials above inelastic thresholds in quantum field theories, *Phys. Rev. D* 87 (2013) 034512. doi:[10.1103/PhysRevD.87.034512](#). [arXiv:1212.4896](#).
- [288] S. Aoki, Nucleon-nucleon interactions via Lattice QCD: Methodology, *Eur. Phys. J. A*49 (2013) 81. doi:[10.1140/epja/i2013-13081-0](#). [arXiv:1309.4150](#).
- [289] T. Iritani, S. Aoki, T. Doi, S. Gongyo, T. Hatsuda, Y. Ikeda, T. Inoue, N. Ishii, H. Nemura, K. Sasaki (HAL QCD), Systematics of the HAL QCD Potential at Low Energies in Lattice QCD, *Phys. Rev. D*99 (2019) 014514. doi:[10.1103/PhysRevD.99.014514](#). [arXiv:1805.02365](#).
- [290] J. Bulava, M. T. Hansen, Scattering amplitudes from finite-volume spectral functions, *Phys. Rev. D* 100 (2019) 034521. doi:[10.1103/PhysRevD.100.034521](#). [arXiv:1903.11735](#).
- [291] S. Aoki, et al. (CP-PACS), I=2 pion scattering length from two-pion wave functions, *Phys. Rev. D*71 (2005) 094504. doi:[10.1103/PhysRevD.71.094504](#). [arXiv:hep-lat/0503025](#).
- [292] T. Inoue, N. Ishii, S. Aoki, T. Doi, T. Hatsuda, Y. Ikeda, K. Murano, H. Nemura, K. Sasaki (HAL QCD), Baryon-Baryon Interactions in the Flavor SU(3) Limit from Full QCD Simulations on the Lattice, *Prog. Theor. Phys.* 124 (2010) 591–603. doi:[10.1143/PTP.124.591](#). [arXiv:1007.3559](#).
- [293] F. Etminan, H. Nemura, S. Aoki, T. Doi, T. Hatsuda, Y. Ikeda, T. Inoue, N. Ishii, K. Murano, K. Sasaki (HAL QCD), Spin-2 $N\Omega$ dibaryon from Lattice QCD, *Nucl. Phys. A* 928 (2014) 89–98. doi:[10.1016/j.nuclphysa.2014.05.014](#). [arXiv:1403.7284](#).
- [294] K. Sasaki, S. Aoki, T. Doi, T. Hatsuda, Y. Ikeda, T. Inoue, N. Ishii, K. Murano (HAL QCD), Coupled-channel approach to strangeness $S = -2$ baryon–bayron interactions in lattice QCD, *PTEP* 2015 (2015) 113B01. doi:[10.1093/ptep/ptv144](#). [arXiv:1504.01717](#).
- [295] K. Murano, N. Ishii, S. Aoki, T. Doi, T. Hatsuda, Y. Ikeda, T. Inoue, H. Nemura, K. Sasaki (HAL QCD), Spin-orbit force from lattice QCD, *Phys. Lett. B* 735 (2014) 19–24. doi:[10.1016/j.physletb.2014.05.061](#). [arXiv:1305.2293](#).
- [296] T. Doi, S. Aoki, T. Hatsuda, Y. Ikeda, T. Inoue, N. Ishii, K. Murano, H. Nemura, K. Sasaki (HAL QCD), Exploring Three-Nucleon Forces in Lattice QCD, *Prog. Theor. Phys.* 127 (2012) 723–738. doi:[10.1143/PTP.127.723](#). [arXiv:1106.2276](#).
- [297] S. Gongyo, et al., Most Strange Dibaryon from Lattice QCD, *Phys. Rev. Lett.* 120 (2018) 212001. doi:[10.1103/PhysRevLett.120.212001](#). [arXiv:1709.00654](#).

- [298] K. Sasaki, et al., $\Lambda\Lambda$ and $N\Xi$ interactions from Lattice QCD near the physical point, Nucl. Phys. A (2019) 121737. doi:[10.1016/j.nuclphysa.2020.121737](https://doi.org/10.1016/j.nuclphysa.2020.121737). arXiv:[1912.08630](https://arxiv.org/abs/1912.08630).
- [299] T. Iritani, et al. (HAL QCD), $N\Omega$ dibaryon from lattice QCD near the physical point, Phys. Lett. B 792 (2019) 284–289. doi:[10.1016/j.physletb.2019.03.050](https://doi.org/10.1016/j.physletb.2019.03.050). arXiv:[1810.03416](https://arxiv.org/abs/1810.03416).
- [300] T. Doi, et al., Baryon interactions from lattice QCD with physical quark masses – Nuclear forces and $\Xi\Xi$ forces –, EPJ Web Conf. 175 (2018) 05009. doi:[10.1051/epjconf/201817505009](https://doi.org/10.1051/epjconf/201817505009). arXiv:[1711.01952](https://arxiv.org/abs/1711.01952).
- [301] C. J. D. Lin, G. Martinelli, C. T. Sachrajda, M. Testa, $K \rightarrow \pi\pi$ decays in a finite volume, Nucl. Phys. B619 (2001) 467–498. doi:[10.1016/S0550-3213\(01\)00495-3](https://doi.org/10.1016/S0550-3213(01)00495-3). arXiv:[hep-lat/0104006](https://arxiv.org/abs/hep-lat/0104006).
- [302] E. Berkowitz, A. Nicholson, C. C. Chang, E. Rinaldi, M. A. Clark, B. Joó, T. Kurth, P. Vranas, A. Walker-Loud, Calm Multi-Baryon Operators, EPJ Web Conf. 175 (2018) 05029. doi:[10.1051/epjconf/201817505029](https://doi.org/10.1051/epjconf/201817505029). arXiv:[1710.05642](https://arxiv.org/abs/1710.05642).
- [303] T. Inoue, S. Aoki, T. Doi, T. Hatsuda, Y. Ikeda, N. Ishii, K. Murano, H. Nemura, K. Sasaki (HAL QCD), Two-Baryon Potentials and H-Dibaryon from 3-flavor Lattice QCD Simulations, Nucl. Phys. A881 (2012) 28–43. doi:[10.1016/j.nuclphysa.2012.02.008](https://doi.org/10.1016/j.nuclphysa.2012.02.008). arXiv:[1112.5926](https://arxiv.org/abs/1112.5926).
- [304] T. Iritani, et al., Mirage in Temporal Correlation functions for Baryon-Baryon Interactions in Lattice QCD, JHEP 10 (2016) 101. doi:[10.1007/JHEP10\(2016\)101](https://doi.org/10.1007/JHEP10(2016)101). arXiv:[1607.06371](https://arxiv.org/abs/1607.06371).
- [305] T. Iritani, S. Aoki, T. Doi, T. Hatsuda, Y. Ikeda, T. Inoue, N. Ishii, H. Nemura, K. Sasaki (HAL QCD), Consistency between Lüscher's finite volume method and HAL QCD method for two-baryon systems in lattice QCD, JHEP 03 (2019) 007. doi:[10.1007/JHEP03\(2019\)007](https://doi.org/10.1007/JHEP03(2019)007). arXiv:[1812.08539](https://arxiv.org/abs/1812.08539).
- [306] T. Yamazaki, K.-I. Ishikawa, Y. Kuramashi, A. Ukawa (PACS), Systematic study of operator dependence in nucleus calculation at large quark mass, PoS LATTICE2016 (2017) 108. doi:[10.22323/1.256.0108](https://doi.org/10.22323/1.256.0108). arXiv:[1702.00541](https://arxiv.org/abs/1702.00541).
- [307] T. Yamazaki, K.-i. Ishikawa, Y. Kuramashi (PACS), Comparison of different source calculations in two-nucleon channel at large quark mass, EPJ Web Conf. 175 (2018) 05019. doi:[10.1051/epjconf/201817505019](https://doi.org/10.1051/epjconf/201817505019). arXiv:[1710.08066](https://arxiv.org/abs/1710.08066).
- [308] D. J. Wilson, R. A. Briceno, J. J. Dudek, R. G. Edwards, C. E. Thomas, Coupled $\pi\pi, K\bar{K}$ scattering in P -wave and the ρ resonance from lattice QCD, Phys. Rev. D92 (2015) 094502. doi:[10.1103/PhysRevD.92.094502](https://doi.org/10.1103/PhysRevD.92.094502). arXiv:[1507.02599](https://arxiv.org/abs/1507.02599).
- [309] T. Iritani, S. Aoki, T. Doi, T. Hatsuda, Y. Ikeda, T. Inoue, N. Ishii, H. Nemura, K. Sasaki, Are two nucleons bound in lattice QCD for heavy quark masses? Consistency check with Lüscher's finite volume formula, Phys. Rev. D96 (2017) 034521. doi:[10.1103/PhysRevD.96.034521](https://doi.org/10.1103/PhysRevD.96.034521). arXiv:[1703.07210](https://arxiv.org/abs/1703.07210).
- [310] S. R. Beane, et al., Comment on "are two nucleons bound in lattice qcd for heavy quark masses? - sanity check with lüscher's finite volume formula -" (2017). arXiv:[1705.09239](https://arxiv.org/abs/1705.09239).
- [311] R. Briceño, private communication, ????
- [312] T. Yamazaki, Y. Kuramashi, A. Ukawa (PACS-CS), Two-Nucleon Bound States in Quenched Lattice QCD, Phys. Rev. D84 (2011) 054506. doi:[10.1103/PhysRevD.84.054506](https://doi.org/10.1103/PhysRevD.84.054506). arXiv:[1105.1418](https://arxiv.org/abs/1105.1418).
- [313] V. Baru, E. Epelbaum, A. A. Filin, J. Gegelia, Low-energy theorems for nucleon-nucleon scattering at unphysical pion masses, Phys. Rev. C92 (2015) 014001. doi:[10.1103/PhysRevC.92.014001](https://doi.org/10.1103/PhysRevC.92.014001). arXiv:[1504.07852](https://arxiv.org/abs/1504.07852).
- [314] V. Baru, E. Epelbaum, A. A. Filin, Low-energy theorems for nucleon-nucleon scattering at $M_\pi = 450$ MeV, Phys. Rev. C94 (2016) 014001. doi:[10.1103/PhysRevC.94.014001](https://doi.org/10.1103/PhysRevC.94.014001). arXiv:[1604.02551](https://arxiv.org/abs/1604.02551).
- [315] J. J. Dudek, R. G. Edwards, C. E. Thomas (Hadron Spectrum), Energy dependence of the ρ resonance in $\pi\pi$ elastic scattering from lattice QCD, Phys. Rev. D87 (2013) 034505. doi:[10.1103/PhysRevD.87.034505](https://doi.org/10.1103/PhysRevD.87.034505), [10.1103/PhysRevD.90.099902](https://doi.org/10.1103/PhysRevD.90.099902). arXiv:[1212.0830](https://arxiv.org/abs/1212.0830), [Erratum: Phys. Rev.D90,no.9,099902(2014)].
- [316] O. Bär, Nucleon-pion-state contribution in lattice calculations of the nucleon charges g_A, g_T and g_S , Phys. Rev. D 94 (2016) 054505. doi:[10.1103/PhysRevD.94.054505](https://doi.org/10.1103/PhysRevD.94.054505). arXiv:[1606.09385](https://arxiv.org/abs/1606.09385).
- [317] O. Bar, Chiral perturbation theory and nucleon-pion-state contaminations in lattice QCD, Int. J. Mod. Phys. A 32 (2017) 1730011. doi:[10.1142/S0217751X17300113](https://doi.org/10.1142/S0217751X17300113). arXiv:[1705.02806](https://arxiv.org/abs/1705.02806).
- [318] M. T. Hansen, H. B. Meyer, On the effect of excited states in lattice calculations of the nucleon axial charge, Nucl. Phys. B 923 (2017) 558–587. doi:[10.1016/j.nuclphysb.2017.08.017](https://doi.org/10.1016/j.nuclphysb.2017.08.017). arXiv:[1610.03843](https://arxiv.org/abs/1610.03843).
- [319] D. Kawai (HAL QCD), ρ resonance from the $I = 1$ $\pi\pi$ potential in lattice QCD, EPJ Web Conf. 175 (2018) 05007. doi:[10.1051/epjconf/201817505007](https://doi.org/10.1051/epjconf/201817505007).
- [320] Y. Akahoshi, S. Aoki, T. Aoyama, T. Doi, T. Miyamoto, K. Sasaki, The HAL QCD potential in $I = 1$ $\pi\pi$ system with the ρ meson bound state, PTEP 2020 (2020) 073B07. doi:[10.1093/ptep/ptaa087](https://doi.org/10.1093/ptep/ptaa087). arXiv:[2004.01356](https://arxiv.org/abs/2004.01356).
- [321] K. Murakami, Y. Akahoshi, S. Aoki (LATTICE-HALQCD), S-wave kaon-nucleon potentials with all-to-all propagators in the HAL QCD method, PTEP 2020 (2020) 093B03. doi:[10.1093/ptep/ptaa118](https://doi.org/10.1093/ptep/ptaa118). arXiv:[2006.01383](https://arxiv.org/abs/2006.01383).

- [322] T. Yamazaki, Y. Kuramashi, Relation between scattering amplitude and Bethe-Salpeter wave function in quantum field theory, Phys. Rev. D 96 (2017) 114511. doi:[10.1103/PhysRevD.96.114511](https://doi.org/10.1103/PhysRevD.96.114511). arXiv:[1709.09779](https://arxiv.org/abs/1709.09779).
- [323] Z. Davoudi, Lattice QCD input for nuclear structure and reactions, EPJ Web Conf. 175 (2018) 01022. doi:[10.1051/epjconf/201817501022](https://doi.org/10.1051/epjconf/201817501022). arXiv:[1711.02020](https://arxiv.org/abs/1711.02020).
- [324] S. Aoki, T. Doi, T. Hatsuda, N. Ishii, Comment on “Relation between scattering amplitude and Bethe-Salpeter wave function in quantum field theory”, Phys. Rev. D 98 (2018) 038501. doi:[10.1103/PhysRevD.98.038501](https://doi.org/10.1103/PhysRevD.98.038501). arXiv:[1711.09344](https://arxiv.org/abs/1711.09344).
- [325] Y. Namekawa, T. Yamazaki, Scattering amplitude from Bethe-Salpeter wave function inside the interaction range, Phys. Rev. D 98 (2018) 011501. doi:[10.1103/PhysRevD.98.011501](https://doi.org/10.1103/PhysRevD.98.011501). arXiv:[1712.10141](https://arxiv.org/abs/1712.10141).
- [326] T. Yamazaki, Y. Kuramashi, Reply to “Comment on ‘Relation between scattering amplitude and Bethe-Salpeter wave function in quantum field theory’”, Phys. Rev. D 98 (2018) 038502. doi:[10.1103/PhysRevD.98.038502](https://doi.org/10.1103/PhysRevD.98.038502). arXiv:[1808.06299](https://arxiv.org/abs/1808.06299).
- [327] A. Nicholson, et al., Symmetries and Interactions from Lattice QCD, in: 13th Conference on the Intersections of Particle and Nuclear Physics, 2018. arXiv:[1812.11127](https://arxiv.org/abs/1812.11127).
- [328] M. Peardon, J. Bulava, J. Foley, C. Morningstar, J. Dudek, R. G. Edwards, B. Joo, H.-W. Lin, D. G. Richards, K. J. Juge (Hadron Spectrum), A Novel quark-field creation operator construction for hadronic physics in lattice QCD, Phys. Rev. D80 (2009) 054506. doi:[10.1103/PhysRevD.80.054506](https://doi.org/10.1103/PhysRevD.80.054506). arXiv:[0905.2160](https://arxiv.org/abs/0905.2160).
- [329] C. Morningstar, J. Bulava, J. Foley, K. J. Juge, D. Lenkner, M. Peardon, C. H. Wong, Improved stochastic estimation of quark propagation with Laplacian Heaviside smearing in lattice QCD, Phys. Rev. D83 (2011) 114505. doi:[10.1103/PhysRevD.83.114505](https://doi.org/10.1103/PhysRevD.83.114505). arXiv:[1104.3870](https://arxiv.org/abs/1104.3870).
- [330] B. Blossier, M. Della Morte, G. von Hippel, T. Mendes, R. Sommer, On the generalized eigenvalue method for energies and matrix elements in lattice field theory, JHEP 04 (2009) 094. doi:[10.1088/1126-6708/2009/04/094](https://doi.org/10.1088/1126-6708/2009/04/094). arXiv:[0902.1265](https://arxiv.org/abs/0902.1265).
- [331] S. Prelovsek, L. Leskovec, C. B. Lang, D. Mohler, K π Scattering and the K^* Decay width from Lattice QCD, Phys. Rev. D88 (2013) 054508. doi:[10.1103/PhysRevD.88.054508](https://doi.org/10.1103/PhysRevD.88.054508). arXiv:[1307.0736](https://arxiv.org/abs/1307.0736).
- [332] S. Prelovsek, L. Leskovec, Evidence for $X(3872)$ from DD^* scattering on the lattice, Phys. Rev. Lett. 111 (2013) 192001. doi:[10.1103/PhysRevLett.111.192001](https://doi.org/10.1103/PhysRevLett.111.192001). arXiv:[1307.5172](https://arxiv.org/abs/1307.5172).
- [333] G. S. Bali, S. Collins, A. Cox, G. Donald, M. Göckeler, C. B. Lang, A. Schäfer (RQCD), ρ and K^* resonances on the lattice at nearly physical quark masses and $N_f = 2$, Phys. Rev. D93 (2016) 054509. doi:[10.1103/PhysRevD.93.054509](https://doi.org/10.1103/PhysRevD.93.054509). arXiv:[1512.08678](https://arxiv.org/abs/1512.08678).
- [334] R. A. Briceno, J. J. Dudek, R. G. Edwards, D. J. Wilson, Isoscalar $\pi\pi$ scattering and the σ meson resonance from QCD, Phys. Rev. Lett. 118 (2017) 022002. doi:[10.1103/PhysRevLett.118.022002](https://doi.org/10.1103/PhysRevLett.118.022002). arXiv:[1607.05900](https://arxiv.org/abs/1607.05900).
- [335] R. A. Briceno, J. J. Dudek, R. G. Edwards, D. J. Wilson, Isoscalar $\pi\pi, K\bar{K}, \eta\eta$ scattering and the σ, f_0, f_2 mesons from QCD, Phys. Rev. D97 (2018) 054513. doi:[10.1103/PhysRevD.97.054513](https://doi.org/10.1103/PhysRevD.97.054513). arXiv:[1708.06667](https://arxiv.org/abs/1708.06667).
- [336] G. S. Bali, S. Collins, A. Cox, A. Schäfer, Masses and decay constants of the $D_{s0}^*(2317)$ and $D_{s1}(2460)$ from $N_f = 2$ lattice QCD close to the physical point, Phys. Rev. D96 (2017) 074501. doi:[10.1103/PhysRevD.96.074501](https://doi.org/10.1103/PhysRevD.96.074501). arXiv:[1706.01247](https://arxiv.org/abs/1706.01247).
- [337] C. Alexandrou, L. Leskovec, S. Meinel, J. Negele, S. Paul, M. Petschlies, A. Pochinsky, G. Rendon, S. Syritsyn, P -wave $\pi\pi$ scattering and the ρ resonance from lattice QCD, Phys. Rev. D96 (2017) 034525. doi:[10.1103/PhysRevD.96.034525](https://doi.org/10.1103/PhysRevD.96.034525). arXiv:[1704.05439](https://arxiv.org/abs/1704.05439).
- [338] G. K. C. Cheung, C. E. Thomas, J. J. Dudek, R. G. Edwards (Hadron Spectrum), Tetraquark operators in lattice QCD and exotic flavour states in the charm sector, JHEP 11 (2017) 033. doi:[10.1007/JHEP11\(2017\)033](https://doi.org/10.1007/JHEP11(2017)033). arXiv:[1709.01417](https://arxiv.org/abs/1709.01417).
- [339] C. Culver, M. Mai, A. Alexandru, M. Döring, F. X. Lee, Pion scattering in the isospin $I = 2$ channel from elongated lattices, Phys. Rev. D100 (2019) 034509. doi:[10.1103/PhysRevD.100.034509](https://doi.org/10.1103/PhysRevD.100.034509). arXiv:[1905.10202](https://arxiv.org/abs/1905.10202).
- [340] A. J. Woss, C. E. Thomas, J. J. Dudek, R. G. Edwards, D. J. Wilson, b_1 resonance in coupled $\pi\omega, \pi\phi$ scattering from lattice QCD, Phys. Rev. D100 (2019) 054506. doi:[10.1103/PhysRevD.100.054506](https://doi.org/10.1103/PhysRevD.100.054506). arXiv:[1904.04136](https://arxiv.org/abs/1904.04136).
- [341] B. Hörz, A. Hanlon, Two- and three-pion finite-volume spectra at maximal isospin from lattice QCD, Phys. Rev. Lett. 123 (2019) 142002. doi:[10.1103/PhysRevLett.123.142002](https://doi.org/10.1103/PhysRevLett.123.142002). arXiv:[1905.04277](https://arxiv.org/abs/1905.04277).
- [342] J.-W. Chen, Connecting the quenched and unquenched worlds via the large $N(c)$ world, Phys. Lett. B 543 (2002) 183–188. doi:[10.1016/S0370-2693\(02\)02461-9](https://doi.org/10.1016/S0370-2693(02)02461-9). arXiv:[hep-lat/0205014](https://arxiv.org/abs/hep-lat/0205014).
- [343] S. R. Beane, M. J. Savage, Partially quenched nucleon nucleon scattering, Phys. Rev. D 67 (2003) 054502. doi:[10.1103/PhysRevD.67.054502](https://doi.org/10.1103/PhysRevD.67.054502). arXiv:[hep-lat/0210046](https://arxiv.org/abs/hep-lat/0210046).
- [344] L. Lellouch, M. Lüscher, Weak transition matrix elements from finite volume correlation functions, Commun. Math. Phys. 219 (2001) 31–44. doi:[10.1007/s002200100410](https://doi.org/10.1007/s002200100410). arXiv:[hep-lat/0003023](https://arxiv.org/abs/hep-lat/0003023).

- [345] W. Detmold, M. J. Savage, Electroweak matrix elements in the two nucleon sector from lattice QCD, Nucl. Phys. A 743 (2004) 170–193. doi:[10.1016/j.nuclphysa.2004.07.007](https://doi.org/10.1016/j.nuclphysa.2004.07.007). arXiv:[hep-lat/0403005](https://arxiv.org/abs/hep-lat/0403005).
- [346] V. Bernard, D. Hoja, U. G. Meißner, A. Rusetsky, Matrix elements of unstable states, JHEP 09 (2012) 023. doi:[10.1007/JHEP09\(2012\)023](https://doi.org/10.1007/JHEP09(2012)023). arXiv:[1205.4642](https://arxiv.org/abs/1205.4642).
- [347] R. A. Briceño, M. T. Hansen, A. Walker-Loud, Multichannel $1 \rightarrow 2$ transition amplitudes in a finite volume, Phys. Rev. D91 (2015) 034501. doi:[10.1103/PhysRevD.91.034501](https://doi.org/10.1103/PhysRevD.91.034501). arXiv:[1406.5965](https://arxiv.org/abs/1406.5965).
- [348] R. A. Briceño, M. T. Hansen, Multichannel $0 \rightarrow 2$ and $1 \rightarrow 2$ transition amplitudes for arbitrary spin particles in a finite volume, Phys. Rev. D92 (2015) 074509. doi:[10.1103/PhysRevD.92.074509](https://doi.org/10.1103/PhysRevD.92.074509). arXiv:[1502.04314](https://arxiv.org/abs/1502.04314).
- [349] R. A. Briceño, M. T. Hansen, Relativistic, model-independent, multichannel $2 \rightarrow 2$ transition amplitudes in a finite volume, Phys. Rev. D94 (2016) 013008. doi:[10.1103/PhysRevD.94.013008](https://doi.org/10.1103/PhysRevD.94.013008). arXiv:[1509.08507](https://arxiv.org/abs/1509.08507).
- [350] A. Baroni, R. A. Briceño, M. T. Hansen, F. G. Ortega-Gama, Form factors of two-hadron states from a covariant finite-volume formalism, Phys. Rev. D 100 (2019) 034511. doi:[10.1103/PhysRevD.100.034511](https://doi.org/10.1103/PhysRevD.100.034511). arXiv:[1812.10504](https://arxiv.org/abs/1812.10504).
- [351] R. A. Briceño, M. T. Hansen, A. W. Jackura, Consistency checks for two-body finite-volume matrix elements: I. Conserved currents and bound states, Phys. Rev. D 100 (2019) 114505. doi:[10.1103/PhysRevD.100.114505](https://doi.org/10.1103/PhysRevD.100.114505). arXiv:[1909.10357](https://arxiv.org/abs/1909.10357).
- [352] R. A. Briceño, Z. Davoudi, M. T. Hansen, M. R. Schindler, A. Baroni, Long-range electroweak amplitudes of single hadrons from Euclidean finite-volume correlation functions, Phys. Rev. D 101 (2020) 014509. doi:[10.1103/PhysRevD.101.014509](https://doi.org/10.1103/PhysRevD.101.014509). arXiv:[1911.04036](https://arxiv.org/abs/1911.04036).
- [353] R. A. Briceño, M. T. Hansen, A. W. Jackura, Consistency checks for two-body finite-volume matrix elements: II. Perturbative systems, Phys. Rev. D 101 (2020) 094508. doi:[10.1103/PhysRevD.101.094508](https://doi.org/10.1103/PhysRevD.101.094508). arXiv:[2002.00023](https://arxiv.org/abs/2002.00023).
- [354] S. Beane, E. Chang, S. Cohen, W. Detmold, H. Lin, K. Orginos, A. Parreño, M. Savage, B. Tiburzi, Magnetic moments of light nuclei from lattice quantum chromodynamics, Phys. Rev. Lett. 113 (2014) 252001. doi:[10.1103/PhysRevLett.113.252001](https://doi.org/10.1103/PhysRevLett.113.252001). arXiv:[1409.3556](https://arxiv.org/abs/1409.3556).
- [355] S. R. Beane, E. Chang, W. Detmold, K. Orginos, A. Parreño, M. J. Savage, B. C. Tiburzi (NPLQCD), Ab initio Calculation of the $\text{np} \rightarrow \text{d}\gamma$ Radiative Capture Process, Phys. Rev. Lett. 115 (2015) 132001. doi:[10.1103/PhysRevLett.115.132001](https://doi.org/10.1103/PhysRevLett.115.132001). arXiv:[1505.02422](https://arxiv.org/abs/1505.02422).
- [356] P. E. Shanahan, B. C. Tiburzi, M. L. Wagman, F. Winter, E. Chang, Z. Davoudi, W. Detmold, K. Orginos, M. J. Savage, Isotensor Axial Polarizability and Lattice QCD Input for Nuclear Double- β Decay Phenomenology, Phys. Rev. Lett. 119 (2017) 062003. doi:[10.1103/PhysRevLett.119.062003](https://doi.org/10.1103/PhysRevLett.119.062003). arXiv:[1701.03456](https://arxiv.org/abs/1701.03456).
- [357] B. C. Tiburzi, M. L. Wagman, F. Winter, E. Chang, Z. Davoudi, W. Detmold, K. Orginos, M. J. Savage, P. E. Shanahan, Double- β Decay Matrix Elements from Lattice Quantum Chromodynamics, Phys. Rev. D96 (2017) 054505. doi:[10.1103/PhysRevD.96.054505](https://doi.org/10.1103/PhysRevD.96.054505). arXiv:[1702.02929](https://arxiv.org/abs/1702.02929).
- [358] F. Winter, W. Detmold, A. S. Gambhir, K. Orginos, M. J. Savage, P. E. Shanahan, M. L. Wagman, First lattice QCD study of the gluonic structure of light nuclei, Phys. Rev. D 96 (2017) 094512. doi:[10.1103/PhysRevD.96.094512](https://doi.org/10.1103/PhysRevD.96.094512). arXiv:[1709.00395](https://arxiv.org/abs/1709.00395).
- [359] C. Alexandrou, M. Constantinou, K. Hadjyiannakou, K. Jansen, C. Kallidonis, G. Koutsou, A. Vaquero Aviles-Casco, Nucleon axial form factors using $N_f = 2$ twisted mass fermions with a physical value of the pion mass, Phys. Rev. D96 (2017) 054507. doi:[10.1103/PhysRevD.96.054507](https://doi.org/10.1103/PhysRevD.96.054507). arXiv:[1705.03399](https://arxiv.org/abs/1705.03399).
- [360] S. Capitani, M. Della Morte, D. Djukanovic, G. M. von Hippel, J. Hua, B. Jäger, P. M. Junnarkar, H. B. Meyer, T. D. Rae, H. Wittig, Isovector axial form factors of the nucleon in two-flavor lattice QCD, Int. J. Mod. Phys. A34 (2019) 1950009. doi:[10.1142/S0217751X1950009X](https://doi.org/10.1142/S0217751X1950009X). arXiv:[1705.06186](https://arxiv.org/abs/1705.06186).
- [361] K.-I. Ishikawa, Y. Kuramashi, S. Sasaki, N. Tsukamoto, A. Ukawa, T. Yamazaki (PACS), Nucleon form factors on a large volume lattice near the physical point in 2+1 flavor QCD, Phys. Rev. D98 (2018) 074510. doi:[10.1103/PhysRevD.98.074510](https://doi.org/10.1103/PhysRevD.98.074510). arXiv:[1807.03974](https://arxiv.org/abs/1807.03974).
- [362] E. Shintani, K.-I. Ishikawa, Y. Kuramashi, S. Sasaki, T. Yamazaki, Nucleon form factors and root-mean-square radii on a $(10.8 \text{ fm})^4$ lattice at the physical point, Phys. Rev. D99 (2019) 014510. doi:[10.1103/PhysRevD.99.014510](https://doi.org/10.1103/PhysRevD.99.014510). arXiv:[1811.07292](https://arxiv.org/abs/1811.07292).
- [363] R. Gupta, Y.-C. Jang, H.-W. Lin, B. Yoon, T. Bhattacharya, Axial Vector Form Factors of the Nucleon from Lattice QCD, Phys. Rev. D96 (2017) 114503. doi:[10.1103/PhysRevD.96.114503](https://doi.org/10.1103/PhysRevD.96.114503). arXiv:[1705.06834](https://arxiv.org/abs/1705.06834).
- [364] O. Bär, Nucleon-pion-state contribution to nucleon two-point correlation functions, Phys. Rev. D 92 (2015) 074504. doi:[10.1103/PhysRevD.92.074504](https://doi.org/10.1103/PhysRevD.92.074504). arXiv:[1503.03649](https://arxiv.org/abs/1503.03649).
- [365] O. Bar, $N\pi$ states and the projection method for the nucleon axial and pseudoscalar form factors, Phys. Rev. D 101 (2020) 034515. doi:[10.1103/PhysRevD.101.034515](https://doi.org/10.1103/PhysRevD.101.034515). arXiv:[1912.05873](https://arxiv.org/abs/1912.05873).

- [366] G. S. Bali, S. Collins, M. Gruber, A. Schäfer, P. Wein, T. Wurm, Solving the PCAC puzzle for nucleon axial and pseudoscalar form factors, *Phys. Lett.* B789 (2019) 666–674. doi:[10.1016/j.physletb.2018.12.053](https://doi.org/10.1016/j.physletb.2018.12.053). [arXiv:1810.05569](https://arxiv.org/abs/1810.05569).
- [367] G. S. Bali, L. Barca, S. Collins, M. Gruber, M. Löfller, A. Schäfer, W. Söldner, P. Wein, S. Weishäupl, T. Wurm (RQCD), Nucleon axial structure from lattice QCD, *JHEP* 05 (2020) 126. doi:[10.1007/JHEP05\(2020\)126](https://doi.org/10.1007/JHEP05(2020)126). [arXiv:1911.13150](https://arxiv.org/abs/1911.13150).
- [368] R. A. Briceño, J. J. Dudek, R. G. Edwards, C. J. Shultz, C. E. Thomas, D. J. Wilson, The $\pi\pi \rightarrow \pi\gamma^*$ amplitude and the resonant $\rho \rightarrow \pi\gamma^*$ transition from lattice QCD, *Phys. Rev.* D93 (2016) 114508. doi:[10.1103/PhysRevD.93.114508](https://doi.org/10.1103/PhysRevD.93.114508). [arXiv:1604.03530](https://arxiv.org/abs/1604.03530).
- [369] C. Alexandrou, L. Leskovec, S. Meinel, J. Negele, S. Paul, M. Petschlies, A. Pochinsky, G. Rendon, S. Syritsyn, $\pi\gamma \rightarrow \pi\pi$ transition and the ρ radiative decay width from lattice QCD, *Phys. Rev.* D98 (2018) 074502. doi:[10.1103/PhysRevD.98.074502](https://doi.org/10.1103/PhysRevD.98.074502). [arXiv:1807.08357](https://arxiv.org/abs/1807.08357).
- [370] C. G. Payne, S. Bacca, G. Hagen, W. Jiang, T. Papenbrock, Coherent elastic neutrino-nucleus scattering on ^{40}Ar from first principles, *Phys. Rev.* C100 (2019) 061304. doi:[10.1103/PhysRevC.100.061304](https://doi.org/10.1103/PhysRevC.100.061304). [arXiv:1908.09739](https://arxiv.org/abs/1908.09739).
- [371] S. Weinberg, Phenomenological Lagrangians, *Physica* A96 (1979) 327–340. doi:[10.1016/0378-4371\(79\)90223-1](https://doi.org/10.1016/0378-4371(79)90223-1).
- [372] S. Weinberg, Why the renormalization group is a good thing, 1981.
- [373] J. Gasser, H. Leutwyler, Chiral Perturbation Theory to One Loop, *Annals Phys.* 158 (1984) 142. doi:[10.1016/0003-4916\(84\)90242-2](https://doi.org/10.1016/0003-4916(84)90242-2).
- [374] J. Gasser, H. Leutwyler, Chiral Perturbation Theory: Expansions in the Mass of the Strange Quark, *Nucl. Phys.* B250 (1985) 465–516. doi:[10.1016/0550-3213\(85\)90492-4](https://doi.org/10.1016/0550-3213(85)90492-4).
- [375] W. Bietenholz, et al., Tuning the strange quark mass in lattice simulations, *Phys. Lett.* B690 (2010) 436–441. doi:[10.1016/j.physletb.2010.05.067](https://doi.org/10.1016/j.physletb.2010.05.067). [arXiv:1003.1114](https://arxiv.org/abs/1003.1114).
- [376] W. Bietenholz, et al., Flavour blindness and patterns of flavour symmetry breaking in lattice simulations of up, down and strange quarks, *Phys. Rev.* D84 (2011) 054509. doi:[10.1103/PhysRevD.84.054509](https://doi.org/10.1103/PhysRevD.84.054509). [arXiv:1102.5300](https://arxiv.org/abs/1102.5300).
- [377] M. Bruno, et al., Simulation of QCD with $N_f = 2 + 1$ flavors of non-perturbatively improved Wilson fermions, *JHEP* 02 (2015) 043. doi:[10.1007/JHEP02\(2015\)043](https://doi.org/10.1007/JHEP02(2015)043). [arXiv:1411.3982](https://arxiv.org/abs/1411.3982).
- [378] S. R. Beane, W. Detmold, P. M. Junnarkar, T. C. Luu, K. Orginos, A. Parreno, M. J. Savage, A. Torok, A. Walker-Loud, SU(2) Low-Energy Constants from Mixed-Action Lattice QCD, *Phys. Rev.* D86 (2012) 094509. doi:[10.1103/PhysRevD.86.094509](https://doi.org/10.1103/PhysRevD.86.094509). [arXiv:1108.1380](https://arxiv.org/abs/1108.1380).
- [379] S. Borsanyi, S. Durr, Z. Fodor, S. Krieg, A. Schafer, E. E. Scholz, K. K. Szabo, SU(2) chiral perturbation theory low-energy constants from 2+1 flavor staggered lattice simulations, *Phys. Rev.* D88 (2013) 014513. doi:[10.1103/PhysRevD.88.014513](https://doi.org/10.1103/PhysRevD.88.014513). [arXiv:1205.0788](https://arxiv.org/abs/1205.0788).
- [380] P. A. Boyle, et al., Low energy constants of SU(2) partially quenched chiral perturbation theory from $N_f=2+1$ domain wall QCD, *Phys. Rev.* D93 (2016) 054502. doi:[10.1103/PhysRevD.93.054502](https://doi.org/10.1103/PhysRevD.93.054502). [arXiv:1511.01950](https://arxiv.org/abs/1511.01950).
- [381] S. Dürr, Validity of ChPT - is $M_\pi=135$ MeV small enough ?, PoS LATTICE2014 (2015) 006. doi:[10.22323/1.214.0006](https://doi.org/10.22323/1.214.0006). [arXiv:1412.6434](https://arxiv.org/abs/1412.6434).
- [382] C. Bernard, Effective Field Theories and Lattice QCD, PoS CD15 (2015) 004. doi:[10.22323/1.253.0004](https://doi.org/10.22323/1.253.0004). [arXiv:1510.02180](https://arxiv.org/abs/1510.02180).
- [383] A. Roessl, Pion kaon scattering near the threshold in chiral SU(2) perturbation theory, *Nucl. Phys.* B555 (1999) 507–539. doi:[10.1016/S0550-3213\(99\)00336-3](https://doi.org/10.1016/S0550-3213(99)00336-3). [arXiv:hep-ph/9904230](https://arxiv.org/abs/hep-ph/9904230).
- [384] C. Allton, et al. (RBC-UKQCD), Physical Results from 2+1 Flavor Domain Wall QCD and SU(2) Chiral Perturbation Theory, *Phys. Rev.* D78 (2008) 114509. doi:[10.1103/PhysRevD.78.114509](https://doi.org/10.1103/PhysRevD.78.114509). [arXiv:0804.0473](https://arxiv.org/abs/0804.0473).
- [385] T. Bae, et al. (SWME), Neutral kaon mixing from new physics: matrix elements in $N_f = 2 + 1$ lattice QCD, *Phys. Rev.* D88 (2013) 071503. doi:[10.1103/PhysRevD.88.071503](https://doi.org/10.1103/PhysRevD.88.071503). [arXiv:1309.2040](https://arxiv.org/abs/1309.2040).
- [386] P. F. Bedaque, U. van Kolck, Effective field theory for few nucleon systems, *Ann. Rev. Nucl. Part. Sci.* 52 (2002) 339–396. doi:[10.1146/annurev.nucl.52.050102.090637](https://doi.org/10.1146/annurev.nucl.52.050102.090637). [arXiv:nucl-th/0203055](https://arxiv.org/abs/nucl-th/0203055).
- [387] E. Epelbaum, H.-W. Hammer, U.-G. Meißner, Modern Theory of Nuclear Forces, *Rev. Mod. Phys.* 81 (2009) 1773–1825. doi:[10.1103/RevModPhys.81.1773](https://doi.org/10.1103/RevModPhys.81.1773). [arXiv:0811.1338](https://arxiv.org/abs/0811.1338).
- [388] R. Machleidt, D. R. Entem, Chiral effective field theory and nuclear forces, *Phys. Rept.* 503 (2011) 1–75. doi:[10.1016/j.physrep.2011.02.001](https://doi.org/10.1016/j.physrep.2011.02.001). [arXiv:1105.2919](https://arxiv.org/abs/1105.2919).
- [389] H. W. Hammer, S. König, U. van Kolck, Nuclear effective field theory: status and perspectives, *Rev. Mod. Phys.* 92 (2020) 025004. doi:[10.1103/RevModPhys.92.025004](https://doi.org/10.1103/RevModPhys.92.025004). [arXiv:1906.12122](https://arxiv.org/abs/1906.12122).
- [390] I. Tews, Z. Davoudi, A. Ekström, J. D. Holt, J. E. Lynn, New Ideas in Constraining Nuclear Forces, *J. Phys. G* 47 (2020) 103001. doi:[10.1088/1361-6471/ab9079](https://doi.org/10.1088/1361-6471/ab9079). [arXiv:2001.03334](https://arxiv.org/abs/2001.03334).

- [391] B. R. Barrett, P. Navratil, J. P. Vary, Ab initio no core shell model, *Prog. Part. Nucl. Phys.* 69 (2013) 131–181. doi:[10.1016/j.ppnp.2012.10.003](https://doi.org/10.1016/j.ppnp.2012.10.003).
- [392] J. E. Lynn, I. Tews, S. Gandolfi, A. Lovato, Quantum Monte Carlo Methods in Nuclear Physics: Recent Advances, *Ann. Rev. Nucl. Part. Sci.* 69 (2019) 279–305. doi:[10.1146/annurev-nucl-101918-023600](https://doi.org/10.1146/annurev-nucl-101918-023600). [arXiv:1901.04868](https://arxiv.org/abs/1901.04868).
- [393] J. Carlson, S. Gandolfi, F. Pederiva, S. C. Pieper, R. Schiavilla, K. E. Schmidt, R. B. Wiringa, Quantum Monte Carlo methods for nuclear physics, *Rev. Mod. Phys.* 87 (2015) 1067. doi:[10.1103/RevModPhys.87.1067](https://doi.org/10.1103/RevModPhys.87.1067). [arXiv:1412.3081](https://arxiv.org/abs/1412.3081).
- [394] W. Dickhoff, C. Barbieri, Selfconsistent Green’s function method for nuclei and nuclear matter, *Prog. Part. Nucl. Phys.* 52 (2004) 377–496. doi:[10.1016/j.ppnp.2004.02.038](https://doi.org/10.1016/j.ppnp.2004.02.038). [arXiv:nucl-th/0402034](https://arxiv.org/abs/nucl-th/0402034).
- [395] C. Barbieri, A. Carbone, Self-consistent Green’s function approaches, volume 936, 2017, pp. 571–644. doi:[10.1007/978-3-319-53336-0_11](https://doi.org/10.1007/978-3-319-53336-0_11). [arXiv:1611.03923](https://arxiv.org/abs/1611.03923).
- [396] D. Lee, Lattice methods and the nuclear few- and many-body problem, volume 936, 2017, pp. 237–261. doi:[10.1007/978-3-319-53336-0_6](https://doi.org/10.1007/978-3-319-53336-0_6). [arXiv:1609.00421](https://arxiv.org/abs/1609.00421).
- [397] T. A. Lähde, U.-G. Meißner, Nuclear Lattice Effective Field Theory: An introduction, volume 957, Springer, 2019. doi:[10.1007/978-3-030-14189-9](https://doi.org/10.1007/978-3-030-14189-9).
- [398] J. Gasser, M. E. Sainio, A. Svarc, Nucleons with Chiral Loops, *Nucl. Phys.* B307 (1988) 779–853. doi:[10.1016/0550-3213\(88\)90108-3](https://doi.org/10.1016/0550-3213(88)90108-3).
- [399] E. E. Jenkins, A. V. Manohar, Baryon chiral perturbation theory using a heavy fermion Lagrangian, *Phys. Lett.* B255 (1991) 558–562. doi:[10.1016/0370-2693\(91\)90266-S](https://doi.org/10.1016/0370-2693(91)90266-S).
- [400] H. Georgi, An Effective Field Theory for Heavy Quarks at Low-energies, *Phys. Lett.* B240 (1990) 447–450. doi:[10.1016/0370-2693\(90\)91128-X](https://doi.org/10.1016/0370-2693(90)91128-X).
- [401] M. E. Luke, A. V. Manohar, Reparametrization invariance constraints on heavy particle effective field theories, *Phys. Lett.* B286 (1992) 348–354. doi:[10.1016/0370-2693\(92\)91786-9](https://doi.org/10.1016/0370-2693(92)91786-9). [arXiv:hep-ph/9205228](https://arxiv.org/abs/hep-ph/9205228).
- [402] A. Walker-Loud, et al., Light hadron spectroscopy using domain wall valence quarks on an Asqtad sea, *Phys. Rev.* D79 (2009) 054502. doi:[10.1103/PhysRevD.79.054502](https://doi.org/10.1103/PhysRevD.79.054502). [arXiv:0806.4549](https://arxiv.org/abs/0806.4549).
- [403] K. I. Ishikawa, et al. (PACS-CS), SU(2) and SU(3) chiral perturbation theory analyses on baryon masses in 2+1 flavor lattice QCD, *Phys. Rev.* D80 (2009) 054502. doi:[10.1103/PhysRevD.80.054502](https://doi.org/10.1103/PhysRevD.80.054502). [arXiv:0905.0962](https://arxiv.org/abs/0905.0962).
- [404] G. ’t Hooft, A Planar Diagram Theory for Strong Interactions, *Nucl. Phys.* B72 (1974) 461. doi:[10.1016/0550-3213\(74\)90154-0](https://doi.org/10.1016/0550-3213(74)90154-0), [,337(1973)].
- [405] E. Witten, Baryons in the 1/n Expansion, *Nucl. Phys.* B160 (1979) 57–115. doi:[10.1016/0550-3213\(79\)90232-3](https://doi.org/10.1016/0550-3213(79)90232-3).
- [406] R. F. Dashen, A. V. Manohar, Baryon - pion couplings from large N(c) QCD, *Phys. Lett.* B315 (1993) 425–430. doi:[10.1016/0370-2693\(93\)91635-Z](https://doi.org/10.1016/0370-2693(93)91635-Z). [arXiv:hep-ph/9307241](https://arxiv.org/abs/hep-ph/9307241).
- [407] R. F. Dashen, A. V. Manohar, 1/N(c) corrections to the baryon axial currents in QCD, *Phys. Lett.* B315 (1993) 438–440. doi:[10.1016/0370-2693\(93\)91637-3](https://doi.org/10.1016/0370-2693(93)91637-3). [arXiv:hep-ph/9307242](https://arxiv.org/abs/hep-ph/9307242).
- [408] E. E. Jenkins, Baryon hyperfine mass splittings in large N QCD, *Phys. Lett.* B315 (1993) 441–446. doi:[10.1016/0370-2693\(93\)91638-4](https://doi.org/10.1016/0370-2693(93)91638-4). [arXiv:hep-ph/9307244](https://arxiv.org/abs/hep-ph/9307244).
- [409] R. F. Dashen, E. E. Jenkins, A. V. Manohar, The 1/N(c) expansion for baryons, *Phys. Rev.* D49 (1994) 4713. doi:[10.1103/PhysRevD.51.2489](https://doi.org/10.1103/PhysRevD.51.2489), [10.1103/PhysRevD.49.4713](https://doi.org/10.1103/PhysRevD.49.4713). [arXiv:hep-ph/9310379](https://arxiv.org/abs/hep-ph/9310379), [Erratum: *Phys. Rev.* D51,2489(1995)].
- [410] E. E. Jenkins, Chiral Lagrangian for baryons in the 1/n(c) expansion, *Phys. Rev.* D53 (1996) 2625–2644. doi:[10.1103/PhysRevD.53.2625](https://doi.org/10.1103/PhysRevD.53.2625). [arXiv:hep-ph/9509433](https://arxiv.org/abs/hep-ph/9509433).
- [411] R. Flores-Mendieta, C. P. Hofmann, E. E. Jenkins, A. V. Manohar, On the structure of large N(c) cancellations in baryon chiral perturbation theory, *Phys. Rev.* D62 (2000) 034001. doi:[10.1103/PhysRevD.62.034001](https://doi.org/10.1103/PhysRevD.62.034001). [arXiv:hep-ph/0001218](https://arxiv.org/abs/hep-ph/0001218).
- [412] E. E. Jenkins, A. V. Manohar, J. W. Negele, A. Walker-Loud, A Lattice Test of 1/N(c) Baryon Mass Relations, *Phys. Rev.* D81 (2010) 014502. doi:[10.1103/PhysRevD.81.014502](https://doi.org/10.1103/PhysRevD.81.014502). [arXiv:0907.0529](https://arxiv.org/abs/0907.0529).
- [413] I. P. Fernando, J. L. Goity, Baryon spin-flavor structure from an analysis of lattice QCD results of the baryon spectrum, *Phys. Rev.* D91 (2015) 036005. doi:[10.1103/PhysRevD.91.036005](https://doi.org/10.1103/PhysRevD.91.036005). [arXiv:1410.1384](https://arxiv.org/abs/1410.1384).
- [414] A. Walker-Loud, Evidence for non-analytic light quark mass dependence in the baryon spectrum, *Phys. Rev.* D86 (2012) 074509. doi:[10.1103/PhysRevD.86.074509](https://doi.org/10.1103/PhysRevD.86.074509). [arXiv:1112.2658](https://arxiv.org/abs/1112.2658).
- [415] T. DeGrand, Lattice baryons in the 1/N expansion, *Phys. Rev.* D86 (2012) 034508. doi:[10.1103/PhysRevD.86.034508](https://doi.org/10.1103/PhysRevD.86.034508). [arXiv:1205.0235](https://arxiv.org/abs/1205.0235).
- [416] T. DeGrand, Lattice calculations of the spectroscopy of baryons with broken flavor SU(3) symmetry and 3, 5, or 7 colors, *Phys. Rev.* D89 (2014) 014506. doi:[10.1103/PhysRevD.89.014506](https://doi.org/10.1103/PhysRevD.89.014506). [arXiv:1308.4114](https://arxiv.org/abs/1308.4114).

- [417] T. DeGrand, Y. Liu, Lattice study of large N_c QCD, Phys. Rev. D94 (2016) 034506. doi:[10.1103/PhysRevD.95.019902](https://doi.org/10.1103/PhysRevD.95.019902), [10.1103/PhysRevD.94.034506](https://doi.org/10.1103/PhysRevD.94.034506). arXiv:[1606.01277](https://arxiv.org/abs/1606.01277), [Erratum: Phys. Rev.D95,no.1,019902(2017)].
- [418] B. C. Tiburzi, A. Walker-Loud, Hyperons in Two Flavor Chiral Perturbation Theory, Phys. Lett. B669 (2008) 246–253. doi:[10.1016/j.physletb.2008.09.054](https://doi.org/10.1016/j.physletb.2008.09.054). arXiv:[0808.0482](https://arxiv.org/abs/0808.0482).
- [419] F.-J. Jiang, B. C. Tiburzi, Hyperon Axial Charges in Two-Flavor Chiral Perturbation Theory, Phys. Rev. D80 (2009) 077501. doi:[10.1103/PhysRevD.80.077501](https://doi.org/10.1103/PhysRevD.80.077501). arXiv:[0905.0857](https://arxiv.org/abs/0905.0857).
- [420] F.-J. Jiang, B. C. Tiburzi, A. Walker-Loud, Kaon Thresholds and Two-Flavor Chiral Expansions for Hyperons, Phys. Lett. B695 (2011) 329–336. doi:[10.1016/j.physletb.2010.11.003](https://doi.org/10.1016/j.physletb.2010.11.003). arXiv:[0911.4721](https://arxiv.org/abs/0911.4721).
- [421] V. Bernard, N. Kaiser, J. Kambor, U. G. Meißner, Chiral structure of the nucleon, Nucl. Phys. B388 (1992) 315–345. doi:[10.1016/0550-3213\(92\)90615-I](https://doi.org/10.1016/0550-3213(92)90615-I).
- [422] V. Bernard, N. Kaiser, U.-G. Meißner, Chiral dynamics in nucleons and nuclei, Int. J. Mod. Phys. E4 (1995) 193–346. doi:[10.1142/S0218301395000092](https://doi.org/10.1142/S0218301395000092). arXiv:[hep-ph/9501384](https://arxiv.org/abs/hep-ph/9501384).
- [423] T. R. Hemmert, B. R. Holstein, J. Kambor, Systematic 1/M expansion for spin 3/2 particles in baryon chiral perturbation theory, Phys. Lett. B395 (1997) 89–95. doi:[10.1016/S0370-2693\(97\)00049-X](https://doi.org/10.1016/S0370-2693(97)00049-X). arXiv:[hep-ph/9606456](https://arxiv.org/abs/hep-ph/9606456).
- [424] T. R. Hemmert, B. R. Holstein, J. Kambor, Chiral Lagrangians and delta(1232) interactions: Formalism, J. Phys. G24 (1998) 1831–1859. doi:[10.1088/0954-3899/24/10/003](https://doi.org/10.1088/0954-3899/24/10/003). arXiv:[hep-ph/9712496](https://arxiv.org/abs/hep-ph/9712496).
- [425] V. Pascalutsa, D. R. Phillips, Effective theory of the delta(1232) in Compton scattering off the nucleon, Phys. Rev. C67 (2003) 055202. doi:[10.1103/PhysRevC.67.055202](https://doi.org/10.1103/PhysRevC.67.055202). arXiv:[nucl-th/0212024](https://arxiv.org/abs/nucl-th/0212024).
- [426] M. Beneke, A. P. Chapovsky, A. Signer, G. Zanderighi, Effective theory approach to unstable particle production, Phys. Rev. Lett. 93 (2004) 011602. doi:[10.1103/PhysRevLett.93.011602](https://doi.org/10.1103/PhysRevLett.93.011602). arXiv:[hep-ph/0312331](https://arxiv.org/abs/hep-ph/0312331).
- [427] H. W. Griesshammer, J. A. McGovern, D. R. Phillips, G. Feldman, Using effective field theory to analyse low-energy Compton scattering data from protons and light nuclei, Prog. Part. Nucl. Phys. 67 (2012) 841–897. doi:[10.1016/j.ppnp.2012.04.003](https://doi.org/10.1016/j.ppnp.2012.04.003). arXiv:[1203.6834](https://arxiv.org/abs/1203.6834).
- [428] T. Becher, H. Leutwyler, Baryon chiral perturbation theory in manifestly Lorentz invariant form, Eur. Phys. J. C9 (1999) 643–671. doi:[10.1007/PL00021673](https://doi.org/10.1007/PL00021673). arXiv:[hep-ph/9901384](https://arxiv.org/abs/hep-ph/9901384).
- [429] T. Fuchs, J. Gegelia, G. Japaridze, S. Scherer, Renormalization of relativistic baryon chiral perturbation theory and power counting, Phys. Rev. D68 (2003) 056005. doi:[10.1103/PhysRevD.68.056005](https://doi.org/10.1103/PhysRevD.68.056005). arXiv:[hep-ph/0302117](https://arxiv.org/abs/hep-ph/0302117).
- [430] M. R. Schindler, J. Gegelia, S. Scherer, Infrared regularization of baryon chiral perturbation theory reformulated, Phys. Lett. B586 (2004) 258–266. doi:[10.1016/j.physletb.2004.02.056](https://doi.org/10.1016/j.physletb.2004.02.056). arXiv:[hep-ph/0309005](https://arxiv.org/abs/hep-ph/0309005).
- [431] M. R. Schindler, J. Gegelia, S. Scherer, Infrared and extended on mass shell renormalization of two loop diagrams, Nucl. Phys. B682 (2004) 367–376. doi:[10.1016/j.nuclphysb.2004.01.027](https://doi.org/10.1016/j.nuclphysb.2004.01.027). arXiv:[hep-ph/0310207](https://arxiv.org/abs/hep-ph/0310207).
- [432] J. Martin Camalich, L. S. Geng, M. J. Vicente Vacas, The lowest-lying baryon masses in covariant SU(3)-flavor chiral perturbation theory, Phys. Rev. D82 (2010) 074504. doi:[10.1103/PhysRevD.82.074504](https://doi.org/10.1103/PhysRevD.82.074504). arXiv:[1003.1929](https://arxiv.org/abs/1003.1929).
- [433] X. L. Ren, L. S. Geng, J. Martin Camalich, J. Meng, H. Toki, Octet baryon masses in next-to-next-to-next-to-leading order covariant baryon chiral perturbation theory, JHEP 12 (2012) 073. doi:[10.1007/JHEP12\(2012\)073](https://doi.org/10.1007/JHEP12(2012)073). arXiv:[1209.3641](https://arxiv.org/abs/1209.3641).
- [434] J. F. Donoghue, B. R. Holstein, B. Borasoy, SU(3) baryon chiral perturbation theory and long distance regularization, Phys. Rev. D59 (1999) 036002. doi:[10.1103/PhysRevD.59.036002](https://doi.org/10.1103/PhysRevD.59.036002). arXiv:[hep-ph/9804281](https://arxiv.org/abs/hep-ph/9804281).
- [435] D. B. Leinweber, A. W. Thomas, K. Tsushima, S. V. Wright, Baryon masses from lattice QCD: Beyond the perturbative chiral regime, Phys. Rev. D61 (2000) 074502. doi:[10.1103/PhysRevD.61.074502](https://doi.org/10.1103/PhysRevD.61.074502). arXiv:[hep-lat/9906027](https://arxiv.org/abs/hep-lat/9906027).
- [436] D. B. Leinweber, A. W. Thomas, R. D. Young, Physical nucleon properties from lattice QCD, Phys. Rev. Lett. 92 (2004) 242002. doi:[10.1103/PhysRevLett.92.242002](https://doi.org/10.1103/PhysRevLett.92.242002). arXiv:[hep-lat/0302020](https://arxiv.org/abs/hep-lat/0302020).
- [437] A. Walker-Loud, New lessons from the nucleon mass, lattice QCD and heavy baryon chiral perturbation theory, PoS LATTICE2008 (2008) 005. doi:[10.22323/1.066.0005](https://doi.org/10.22323/1.066.0005). arXiv:[0810.0663](https://arxiv.org/abs/0810.0663).
- [438] A. Walker-Loud, Baryons in/and Lattice QCD, PoS CD12 (2013) 017. doi:[10.22323/1.172.0017](https://doi.org/10.22323/1.172.0017). arXiv:[1304.6341](https://arxiv.org/abs/1304.6341).
- [439] A. Walker-Loud, Nuclear Physics Review, PoS LATTICE2013 (2014) 013. doi:[10.22323/1.187.0013](https://doi.org/10.22323/1.187.0013). arXiv:[1401.8259](https://arxiv.org/abs/1401.8259).
- [440] J. Kambor, M. Mojzis, Field redefinitions and wave function renormalization to $O(p^{**4})$ in heavy baryon chiral perturbation theory, JHEP 04 (1999) 031. doi:[10.1088/1126-6708/1999/04/031](https://doi.org/10.1088/1126-6708/1999/04/031). arXiv:[hep-ph/9901235](https://arxiv.org/abs/hep-ph/9901235).
- [441] V. Bernard, U.-G. Meißner, The Nucleon axial-vector coupling beyond one loop, Phys. Lett. B639 (2006) 278–282. doi:[10.1016/j.physletb.2006.06.018](https://doi.org/10.1016/j.physletb.2006.06.018). arXiv:[hep-lat/0605010](https://arxiv.org/abs/hep-lat/0605010).

- [442] B. C. Tiburzi, A. Walker-Loud, Strong isospin breaking in the nucleon and Delta masses, Nucl. Phys. A764 (2006) 274–302. doi:[10.1016/j.nuclphysa.2005.08.013](https://doi.org/10.1016/j.nuclphysa.2005.08.013). arXiv:[hep-lat/0501018](https://arxiv.org/abs/hep-lat/0501018).
- [443] A. Walker-Loud, Strong isospin breaking with twisted mass lattice QCD (2009). arXiv:[0904.2404](https://arxiv.org/abs/0904.2404).
- [444] D. A. Brantley, B. Joo, E. V. Mastropas, E. Mereghetti, H. Monge-Camacho, B. C. Tiburzi, A. Walker-Loud, Strong isospin violation and chiral logarithms in the baryon spectrum (2016). arXiv:[1612.07733](https://arxiv.org/abs/1612.07733).
- [445] W. C. Haxton, C. L. Song, Morphing the shell model into an effective theory, Phys. Rev. Lett. 84 (2000) 5484. doi:[10.1103/PhysRevLett.84.5484](https://doi.org/10.1103/PhysRevLett.84.5484). arXiv:[nucl-th/9907097](https://arxiv.org/abs/nucl-th/9907097).
- [446] W. C. Haxton, Harmonic-oscillator-based effective theory (2006). doi:[10.1142/9789812708250_0013](https://doi.org/10.1142/9789812708250_0013). arXiv:[nucl-th/0608017](https://arxiv.org/abs/nucl-th/0608017).
- [447] W. C. Haxton, The Form of the Effective Interaction in Harmonic-Oscillator-Based Effective Theory, Phys. Rev. C77 (2008) 034005. doi:[10.1103/PhysRevC.77.034005](https://doi.org/10.1103/PhysRevC.77.034005). arXiv:[0710.0289](https://arxiv.org/abs/0710.0289).
- [448] E. Epelbaum, Nuclear forces from chiral effective field theory, Prog. Part. Nucl. Phys. 67 (2012) 343–347. doi:[10.1016/j.ppnp.2011.12.041](https://doi.org/10.1016/j.ppnp.2011.12.041).
- [449] H.-W. Hammer, A. Nogga, A. Schwenk, Three-body forces: From cold atoms to nuclei, Rev. Mod. Phys. 85 (2013) 197. doi:[10.1103/RevModPhys.85.197](https://doi.org/10.1103/RevModPhys.85.197). arXiv:[1210.4273](https://arxiv.org/abs/1210.4273).
- [450] R. Machleidt, F. Sammarruca, Chiral EFT based nuclear forces: Achievements and challenges, Phys. Scripta 91 (2016) 083007. doi:[10.1088/0031-8949/91/8/083007](https://doi.org/10.1088/0031-8949/91/8/083007). arXiv:[1608.05978](https://arxiv.org/abs/1608.05978).
- [451] S. Weinberg, Nuclear forces from chiral Lagrangians, Phys. Lett. B251 (1990) 288–292. doi:[10.1016/0370-2693\(90\)90938-3](https://doi.org/10.1016/0370-2693(90)90938-3).
- [452] S. Weinberg, Effective chiral Lagrangians for nucleon - pion interactions and nuclear forces, Nucl. Phys. B363 (1991) 3–18. doi:[10.1016/0550-3213\(91\)90231-L](https://doi.org/10.1016/0550-3213(91)90231-L).
- [453] S. Weinberg, Three body interactions among nucleons and pions, Phys. Lett. B295 (1992) 114–121. doi:[10.1016/0370-2693\(92\)90099-P](https://doi.org/10.1016/0370-2693(92)90099-P). arXiv:[hep-ph/9209257](https://arxiv.org/abs/hep-ph/9209257).
- [454] E. Epelbaum, H. Krebs, U. G. Meißner, Improved chiral nucleon-nucleon potential up to next-to-next-to-next-to-leading order, Eur. Phys. J. A51 (2015) 53. doi:[10.1140/epja/i2015-15053-8](https://doi.org/10.1140/epja/i2015-15053-8). arXiv:[1412.0142](https://arxiv.org/abs/1412.0142).
- [455] J. A. Melendez, S. Wesolowski, R. J. Furnstahl, Bayesian truncation errors in chiral effective field theory: nucleon-nucleon observables, Phys. Rev. C96 (2017) 024003. doi:[10.1103/PhysRevC.96.024003](https://doi.org/10.1103/PhysRevC.96.024003). arXiv:[1704.03308](https://arxiv.org/abs/1704.03308).
- [456] G. P. Lepage, How to renormalize the Schrodinger equation, in: Nuclear physics. Proceedings, 8th Jorge Andre Swieca Summer School, Sao Jose dos Campos, Campos do Jordao, Brazil, January 26–February 7, 1997, 1997, pp. 135–180. arXiv:[nucl-th/9706029](https://arxiv.org/abs/nucl-th/9706029).
- [457] P. F. Bedaque, U. van Kolck, Nucleon deuteron scattering from an effective field theory, Phys. Lett. B428 (1998) 221–226. doi:[10.1016/S0370-2693\(98\)00430-4](https://doi.org/10.1016/S0370-2693(98)00430-4). arXiv:[nucl-th/9710073](https://arxiv.org/abs/nucl-th/9710073).
- [458] U. van Kolck, Effective field theory of short range forces, Nucl. Phys. A645 (1999) 273–302. doi:[10.1016/S0375-9474\(98\)00612-5](https://doi.org/10.1016/S0375-9474(98)00612-5). arXiv:[nucl-th/9808007](https://arxiv.org/abs/nucl-th/9808007).
- [459] P. F. Bedaque, H. W. Hammer, U. van Kolck, Effective theory for neutron deuteron scattering: Energy dependence, Phys. Rev. C58 (1998) R641–R644. doi:[10.1103/PhysRevC.58.R641](https://doi.org/10.1103/PhysRevC.58.R641). arXiv:[nucl-th/9802057](https://arxiv.org/abs/nucl-th/9802057).
- [460] J.-W. Chen, G. Rupak, M. J. Savage, Nucleon-nucleon effective field theory without pions, Nucl. Phys. A653 (1999) 386–412. doi:[10.1016/S0375-9474\(99\)00298-5](https://doi.org/10.1016/S0375-9474(99)00298-5). arXiv:[nucl-th/9902056](https://arxiv.org/abs/nucl-th/9902056).
- [461] X. Kong, F. Ravndal, Coulomb effects in low-energy proton proton scattering, Nucl. Phys. A665 (2000) 137–163. doi:[10.1016/S0375-9474\(99\)00406-6](https://doi.org/10.1016/S0375-9474(99)00406-6). arXiv:[hep-ph/9903523](https://arxiv.org/abs/hep-ph/9903523).
- [462] P. F. Bedaque, H. W. Hammer, U. van Kolck, The Three boson system with short range interactions, Nucl. Phys. A646 (1999) 444–466. doi:[10.1016/S0375-9474\(98\)00650-2](https://doi.org/10.1016/S0375-9474(98)00650-2). arXiv:[nucl-th/9811046](https://arxiv.org/abs/nucl-th/9811046).
- [463] P. F. Bedaque, H. W. Hammer, U. van Kolck, Renormalization of the three-body system with short range interactions, Phys. Rev. Lett. 82 (1999) 463–467. doi:[10.1103/PhysRevLett.82.463](https://doi.org/10.1103/PhysRevLett.82.463). arXiv:[nucl-th/9809025](https://arxiv.org/abs/nucl-th/9809025).
- [464] P. F. Bedaque, G. Rupak, H. W. Grießhammer, H.-W. Hammer, Low-energy expansion in the three-body system to all orders and the triton channel, Nucl. Phys. A714 (2003) 589–610. doi:[10.1016/S0375-9474\(02\)01402-1](https://doi.org/10.1016/S0375-9474(02)01402-1). arXiv:[nucl-th/0207034](https://arxiv.org/abs/nucl-th/0207034).
- [465] L. Platter, H. W. Hammer, U.-G. Meißner, On the correlation between the binding energies of the triton and the alpha-particle, Phys. Lett. B607 (2005) 254–258. doi:[10.1016/j.physletb.2004.12.068](https://doi.org/10.1016/j.physletb.2004.12.068). arXiv:[nucl-th/0409040](https://arxiv.org/abs/nucl-th/0409040).
- [466] J. Vanasse, Fully Perturbative Calculation of nd Scattering to Next-to-next-to-leading-order, Phys. Rev. C88 (2013) 044001. doi:[10.1103/PhysRevC.88.044001](https://doi.org/10.1103/PhysRevC.88.044001). arXiv:[1305.0283](https://arxiv.org/abs/1305.0283).
- [467] S. König, H. W. Grießhammer, H.-W. Hammer, U. van Kolck, Effective theory of ^3H and ^3He , J. Phys. G43 (2016) 055106. doi:[10.1088/0954-3899/43/5/055106](https://doi.org/10.1088/0954-3899/43/5/055106). arXiv:[1508.05085](https://arxiv.org/abs/1508.05085).

- [468] L. Contessi, A. Lovato, F. Pederiva, A. Roggero, J. Kirscher, U. van Kolck, Ground-state properties of ^4He and ^{16}O extrapolated from lattice QCD with pionless EFT, Phys. Lett. B772 (2017) 839–848. doi:[10.1016/j.physletb.2017.07.048](https://doi.org/10.1016/j.physletb.2017.07.048). [arXiv:1701.06516](https://arxiv.org/abs/1701.06516).
- [469] A. Bansal, S. Binder, A. Ekström, G. Hagen, G. R. Jansen, T. Papenbrock, Pion-less effective field theory for atomic nuclei and lattice nuclei, Phys. Rev. C98 (2018) 054301. doi:[10.1103/PhysRevC.98.054301](https://doi.org/10.1103/PhysRevC.98.054301). [arXiv:1712.10246](https://arxiv.org/abs/1712.10246).
- [470] J. Vanasse, Triton charge radius to next-to-next-to-leading order in pionless effective field theory, Phys. Rev. C95 (2017) 024002. doi:[10.1103/PhysRevC.95.024002](https://doi.org/10.1103/PhysRevC.95.024002). [arXiv:1512.03805](https://arxiv.org/abs/1512.03805).
- [471] J. Vanasse, Charge and Magnetic Properties of Three-Nucleon Systems in Pionless Effective Field Theory, Phys. Rev. C98 (2018) 034003. doi:[10.1103/PhysRevC.98.034003](https://doi.org/10.1103/PhysRevC.98.034003). [arXiv:1706.02665](https://arxiv.org/abs/1706.02665).
- [472] D. B. Kaplan, M. J. Savage, R. P. Springer, M. B. Wise, An Effective field theory calculation of the parity violating asymmetry in (polarized) $n + p \rightarrow d + \gamma$, Phys. Lett. B449 (1999) 1–5. doi:[10.1016/S0370-2693\(99\)00032-5](https://doi.org/10.1016/S0370-2693(99)00032-5). [arXiv:nucl-th/9807081](https://arxiv.org/abs/nucl-th/9807081).
- [473] S. Ando, J. W. Shin, C. H. Hyun, S. W. Hong, K. Kubodera, Proton-proton fusion in pionless effective theory, Phys. Lett. B668 (2008) 187–192. doi:[10.1016/j.physletb.2008.08.040](https://doi.org/10.1016/j.physletb.2008.08.040). [arXiv:0801.4330](https://arxiv.org/abs/0801.4330).
- [474] H. De-Leon, L. Platter, D. Gazit, Tritium β -decay in pionless effective field theory, Phys. Rev. C100 (2019) 055502. doi:[10.1103/PhysRevC.100.055502](https://doi.org/10.1103/PhysRevC.100.055502). [arXiv:1611.10004](https://arxiv.org/abs/1611.10004).
- [475] D. R. Phillips, M. R. Schindler, R. P. Springer, An Effective-field-theory analysis of low-energy parity-violation in nucleon-nucleon scattering, Nucl. Phys. A822 (2009) 1–19. doi:[10.1016/j.nuclphysa.2009.02.011](https://doi.org/10.1016/j.nuclphysa.2009.02.011). [arXiv:0812.2073](https://arxiv.org/abs/0812.2073).
- [476] M. R. Schindler, R. P. Springer, Two parity violating asymmetries from $n + p \rightarrow d + \gamma$ in pionless effective field theories, Nucl. Phys. A846 (2010) 51–62. doi:[10.1016/j.nuclphysa.2010.06.002](https://doi.org/10.1016/j.nuclphysa.2010.06.002). [arXiv:0907.5358](https://arxiv.org/abs/0907.5358).
- [477] M. R. Schindler, R. P. Springer, The Theory of Parity Violation in Few-Nucleon Systems, Prog. Part. Nucl. Phys. 72 (2013) 1–43. doi:[10.1016/j.ppnp.2013.05.002](https://doi.org/10.1016/j.ppnp.2013.05.002). [arXiv:1305.4190](https://arxiv.org/abs/1305.4190).
- [478] E. Chang, W. Detmold, K. Orginos, A. Parreno, M. J. Savage, B. C. Tiburzi, S. R. Beane (NPLQCD), Magnetic structure of light nuclei from lattice QCD, Phys. Rev. D92 (2015) 114502. doi:[10.1103/PhysRevD.92.114502](https://doi.org/10.1103/PhysRevD.92.114502). [arXiv:1506.05518](https://arxiv.org/abs/1506.05518).
- [479] E. Epelbaum, Nuclear Chiral EFT in the Precision Era, PoS CD15 (2016) 014. doi:[10.22323/1.253.0014](https://doi.org/10.22323/1.253.0014). [arXiv:1510.07036](https://arxiv.org/abs/1510.07036).
- [480] A. Manohar, H. Georgi, Chiral Quarks and the Nonrelativistic Quark Model, Nucl. Phys. B234 (1984) 189–212. doi:[10.1016/0550-3213\(84\)90231-1](https://doi.org/10.1016/0550-3213(84)90231-1).
- [481] C. Ordonez, U. van Kolck, Chiral lagrangians and nuclear forces, Phys. Lett. B291 (1992) 459–464. doi:[10.1016/0370-2693\(92\)91404-W](https://doi.org/10.1016/0370-2693(92)91404-W).
- [482] C. Ordonez, L. Ray, U. van Kolck, Nucleon-nucleon potential from an effective chiral Lagrangian, Phys. Rev. Lett. 72 (1994) 1982–1985. doi:[10.1103/PhysRevLett.72.1982](https://doi.org/10.1103/PhysRevLett.72.1982).
- [483] C. Ordonez, L. Ray, U. van Kolck, The Two nucleon potential from chiral Lagrangians, Phys. Rev. C53 (1996) 2086–2105. doi:[10.1103/PhysRevC.53.2086](https://doi.org/10.1103/PhysRevC.53.2086). [arXiv:hep-ph/9511380](https://arxiv.org/abs/hep-ph/9511380).
- [484] E. Epelbaum, W. Gloeckle, U.-G. Meißner, Nuclear forces from chiral Lagrangians using the method of unitary transformation. 1. Formalism, Nucl. Phys. A637 (1998) 107–134. doi:[10.1016/S0375-9474\(98\)00220-6](https://doi.org/10.1016/S0375-9474(98)00220-6). [arXiv:nucl-th/9801064](https://arxiv.org/abs/nucl-th/9801064).
- [485] D. R. Entem, R. Machleidt, Accurate charge dependent nucleon-nucleon potential at fourth order of chiral perturbation theory, Phys. Rev. C68 (2003) 041001. doi:[10.1103/PhysRevC.68.041001](https://doi.org/10.1103/PhysRevC.68.041001). [arXiv:nucl-th/0304018](https://arxiv.org/abs/nucl-th/0304018).
- [486] E. Epelbaum, W. Glockle, U.-G. Meißner, The Two-nucleon system at next-to-next-to-next-to-leading order, Nucl. Phys. A747 (2005) 362–424. doi:[10.1016/j.nuclphysa.2004.09.107](https://doi.org/10.1016/j.nuclphysa.2004.09.107). [arXiv:nucl-th/0405048](https://arxiv.org/abs/nucl-th/0405048).
- [487] D. R. Entem, R. Machleidt, Y. Nosyk, High-quality two-nucleon potentials up to fifth order of the chiral expansion, Phys. Rev. C96 (2017) 024004. doi:[10.1103/PhysRevC.96.024004](https://doi.org/10.1103/PhysRevC.96.024004). [arXiv:1703.05454](https://arxiv.org/abs/1703.05454).
- [488] P. Reinert, H. Krebs, E. Epelbaum, Semilocal momentum-space regularized chiral two-nucleon potentials up to fifth order, Eur. Phys. J. A54 (2018) 86. doi:[10.1140/epja/i2018-12516-4](https://doi.org/10.1140/epja/i2018-12516-4). [arXiv:1711.08821](https://arxiv.org/abs/1711.08821).
- [489] N. Barnea, L. Contessi, D. Gazit, F. Pederiva, U. van Kolck, Effective Field Theory for Lattice Nuclei, Phys. Rev. Lett. 114 (2015) 052501. doi:[10.1103/PhysRevLett.114.052501](https://doi.org/10.1103/PhysRevLett.114.052501). [arXiv:1311.4966](https://arxiv.org/abs/1311.4966).
- [490] J. Kirscher, N. Barnea, D. Gazit, F. Pederiva, U. van Kolck, Spectra and Scattering of Light Lattice Nuclei from Effective Field Theory, Phys. Rev. C92 (2015) 054002. doi:[10.1103/PhysRevC.92.054002](https://doi.org/10.1103/PhysRevC.92.054002). [arXiv:1506.09048](https://arxiv.org/abs/1506.09048).
- [491] S. Gandolfi, A. Gezerlis, J. Carlson, Neutron Matter from Low to High Density, Ann. Rev. Nucl. Part. Sci. 65 (2015) 303–328. doi:[10.1146/annurev-nucl-102014-021957](https://doi.org/10.1146/annurev-nucl-102014-021957). [arXiv:1501.05675](https://arxiv.org/abs/1501.05675).
- [492] P. Klos, J. E. Lynn, I. Tews, S. Gandolfi, A. Gezerlis, H. W. Hammer, M. Hoferichter, A. Schwenk, Quantum Monte Carlo calculations of two neutrons in finite volume, Phys. Rev. C94 (2016) 054005. doi:[10.1103/PhysRevC.94.054005](https://doi.org/10.1103/PhysRevC.94.054005).

- [PhysRevC.94.054005](#). [arXiv:1604.01387](#).
- [493] S. Gandolfi, H. W. Hammer, P. Klos, J. E. Lynn, A. Schwenk, Is a Trineutron Resonance Lower in Energy than a Tetraneutron Resonance?, *Phys. Rev. Lett.* 118 (2017) 232501. doi:[10.1103/PhysRevLett.118.232501](#). [arXiv:1612.01502](#).
- [494] A. Gardestig, Extracting the neutron-neutron scattering length - recent developments, *J. Phys. G* 36 (2009) 053001. doi:[10.1088/0954-3899/36/5/053001](#). [arXiv:0904.2787](#).
- [495] H. Muller, S. Koonin, R. Seki, U. van Kolck, Nuclear matter on a lattice, *Phys. Rev. C* 61 (2000) 044320. doi:[10.1103/PhysRevC.61.044320](#). [arXiv:nucl-th/9910038](#).
- [496] D. Lee, B. Borasoy, T. Schäfer, Nuclear lattice simulations with chiral effective field theory, *Phys. Rev. C* 70 (2004) 014007. doi:[10.1103/PhysRevC.70.014007](#). [arXiv:nucl-th/0402072](#).
- [497] F. Hoyle, On Nuclear Reactions Occuring in Very Hot Stars. 1. The Synthesis of Elements from Carbon to Nickel, *Astrophys. J. Suppl.* 1 (1954) 121–146. doi:[10.1086/190005](#).
- [498] M. E. Burbidge, G. Burbidge, W. A. Fowler, F. Hoyle, Synthesis of the elements in stars, *Rev. Mod. Phys.* 29 (1957) 547–650. doi:[10.1103/RevModPhys.29.547](#).
- [499] E. Epelbaum, H. Krebs, D. Lee, U.-G. Meißner, Ab initio calculation of the Hoyle state, *Phys. Rev. Lett.* 106 (2011) 192501. doi:[10.1103/PhysRevLett.106.192501](#). [arXiv:1101.2547](#).
- [500] E. Epelbaum, H. Krebs, T. A. Lähde, D. Lee, U.-G. Meißner, G. Rupak, Ab Initio Calculation of the Spectrum and Structure of ^{16}O , *Phys. Rev. Lett.* 112 (2014) 102501. doi:[10.1103/PhysRevLett.112.102501](#). [arXiv:1312.7703](#).
- [501] E. Epelbaum, H. Krebs, U. G. Meißner, Precision nucleon-nucleon potential at fifth order in the chiral expansion, *Phys. Rev. Lett.* 115 (2015) 122301. doi:[10.1103/PhysRevLett.115.122301](#). [arXiv:1412.4623](#).
- [502] S. Binder, A. Calci, E. Epelbaum, R. J. Furnstahl, J. Golak, K. Hebeler, H. Kamada, H. Krebs, J. Langhammer, S. Liebig, P. Maris, U.-G. Meißner, D. Minossi, A. Nogga, H. Potter, R. Roth, R. Skibiński, K. Topolnicki, J. P. Vary, H. Witała (LENPIC), Few-nucleon systems with state-of-the-art chiral nucleon-nucleon forces, *Phys. Rev. C* 93 (2016) 044002. doi:[10.1103/PhysRevC.93.044002](#). [arXiv:1505.07218](#).
- [503] J. E. Lynn, I. Tews, J. Carlson, S. Gandolfi, A. Gezerlis, K. E. Schmidt, A. Schwenk, Chiral Three-Nucleon Interactions in Light Nuclei, Neutron- α Scattering, and Neutron Matter, *Phys. Rev. Lett.* 116 (2016) 062501. doi:[10.1103/PhysRevLett.116.062501](#). [arXiv:1509.03470](#).
- [504] J. E. Lynn, I. Tews, J. Carlson, S. Gandolfi, A. Gezerlis, K. E. Schmidt, A. Schwenk, Quantum Monte Carlo calculations of light nuclei with local chiral two- and three-nucleon interactions, *Phys. Rev. C* 96 (2017) 054007. doi:[10.1103/PhysRevC.96.054007](#). [arXiv:1706.07668](#).
- [505] D. Lonardoni, J. Carlson, S. Gandolfi, J. E. Lynn, K. E. Schmidt, A. Schwenk, X. Wang, Properties of nuclei up to $A = 16$ using local chiral interactions, *Phys. Rev. Lett.* 120 (2018) 122502. doi:[10.1103/PhysRevLett.120.122502](#). [arXiv:1709.09143](#).
- [506] S. Binder, A. Calci, E. Epelbaum, R. J. Furnstahl, J. Golak, K. Hebeler, T. Hüther, H. Kamada, H. Krebs, P. Maris, U.-G. Meißner, A. Nogga, R. Roth, R. Skibiński, K. Topolnicki, J. P. Vary, K. Vobig, H. Witała (LENPIC), Few-nucleon and many-nucleon systems with semilocal coordinate-space regularized chiral nucleon-nucleon forces, *Phys. Rev. C* 98 (2018) 014002. doi:[10.1103/PhysRevC.98.014002](#). [arXiv:1802.08584](#).
- [507] E. Epelbaum, J. Golak, K. Hebeler, T. Hüther, H. Kamada, H. Krebs, P. Maris, U.-G. Meißner, A. Nogga, R. Roth, R. Skibiński, K. Topolnicki, J. P. Vary, K. Vobig, H. Witała (LENPIC), Few- and many-nucleon systems with semilocal coordinate-space regularized chiral two- and three-body forces, *Phys. Rev. C* 99 (2019) 024313. doi:[10.1103/PhysRevC.99.024313](#). [arXiv:1807.02848](#).
- [508] C. Drischler, T. Krüger, K. Hebeler, A. Schwenk, Pairing in neutron matter: New uncertainty estimates and three-body forces, *Phys. Rev. C* 95 (2017) 024302. doi:[10.1103/PhysRevC.95.024302](#). [arXiv:1610.05213](#).
- [509] C. Drischler, K. Hebeler, A. Schwenk, Chiral interactions up to next-to-next-to-next-to-leading order and nuclear saturation, *Phys. Rev. Lett.* 122 (2019) 042501. doi:[10.1103/PhysRevLett.122.042501](#). [arXiv:1710.08220](#).
- [510] S. Wesolowski, N. Klco, R. J. Furnstahl, D. R. Phillips, A. Thapaliya, Bayesian parameter estimation for effective field theories, *J. Phys. G* 43 (2016) 074001. doi:[10.1088/0954-3899/43/7/074001](#). [arXiv:1511.03618](#).
- [511] S. Wesolowski, R. J. Furnstahl, J. A. Melendez, D. R. Phillips, Exploring Bayesian parameter estimation for chiral effective field theory using nucleon-nucleon phase shifts, *J. Phys. G* 46 (2019) 045102. doi:[10.1088/1361-6471/aaf5fc](#). [arXiv:1808.08211](#).
- [512] R. J. Furnstahl, N. Klco, D. R. Phillips, S. Wesolowski, Quantifying truncation errors in effective field theory, *Phys. Rev. C* 92 (2015) 024005. doi:[10.1103/PhysRevC.92.024005](#). [arXiv:1506.01343](#).
- [513] J. A. Melendez, R. J. Furnstahl, D. R. Phillips, M. T. Pratola, S. Wesolowski, Quantifying Correlated Truncation Errors in Effective Field Theory, *Phys. Rev. C* 100 (2019) 044001. doi:[10.1103/PhysRevC.100.044001](#).

[arXiv:1904.10581](#).

- [514] R. J. Furnstahl, D. R. Phillips, S. Wesolowski, A recipe for EFT uncertainty quantification in nuclear physics, *J. Phys. G* 42 (2015) 034028. doi:[10.1088/0954-3899/42/3/034028](https://doi.org/10.1088/0954-3899/42/3/034028). [arXiv:1407.0657](#).
- [515] A. Dyhdalo, R. J. Furnstahl, K. Hebeler, I. Tews, Regulator Artifacts in Uniform Matter for Chiral Interactions, *Phys. Rev. C* 94 (2016) 034001. doi:[10.1103/PhysRevC.94.034001](https://doi.org/10.1103/PhysRevC.94.034001). [arXiv:1602.08038](#).
- [516] A. Ekström, et al., Optimized Chiral Nucleon-Nucleon Interaction at Next-to-Next-to-Leading Order, *Phys. Rev. Lett.* 110 (2013) 192502. doi:[10.1103/PhysRevLett.110.192502](https://doi.org/10.1103/PhysRevLett.110.192502). [arXiv:1303.4674](#).
- [517] B. D. Carlsson, A. Ekström, C. Forssén, D. F. Strömborg, G. R. Jansen, O. Lilja, M. Lindby, B. A. Mattsson, K. A. Wendt, Uncertainty analysis and order-by-order optimization of chiral nuclear interactions, *Phys. Rev. X* 6 (2016) 011019. doi:[10.1103/PhysRevX.6.011019](https://doi.org/10.1103/PhysRevX.6.011019). [arXiv:1506.02466](#).
- [518] D. R. Entem, N. Kaiser, R. Machleidt, Y. Nosyk, Peripheral nucleon-nucleon scattering at fifth order of chiral perturbation theory, *Phys. Rev. C* 91 (2015) 014002. doi:[10.1103/PhysRevC.91.014002](https://doi.org/10.1103/PhysRevC.91.014002). [arXiv:1411.5335](#).
- [519] A. Gezerlis, I. Tews, E. Epelbaum, S. Gandolfi, K. Hebeler, A. Nogga, A. Schwenk, Quantum Monte Carlo Calculations with Chiral Effective Field Theory Interactions, *Phys. Rev. Lett.* 111 (2013) 032501. doi:[10.1103/PhysRevLett.111.032501](https://doi.org/10.1103/PhysRevLett.111.032501). [arXiv:1303.6243](#).
- [520] A. Gezerlis, I. Tews, E. Epelbaum, M. Freunek, S. Gandolfi, K. Hebeler, A. Nogga, A. Schwenk, Local chiral effective field theory interactions and quantum Monte Carlo applications, *Phys. Rev. C* 90 (2014) 054323. doi:[10.1103/PhysRevC.90.054323](https://doi.org/10.1103/PhysRevC.90.054323). [arXiv:1406.0454](#).
- [521] J. Hoppe, C. Drischler, R. J. Furnstahl, K. Hebeler, A. Schwenk, Weinberg eigenvalues for chiral nucleon-nucleon interactions, *Phys. Rev. C* 96 (2017) 054002. doi:[10.1103/PhysRevC.96.054002](https://doi.org/10.1103/PhysRevC.96.054002). [arXiv:1707.06438](#).
- [522] D. B. Kaplan, M. J. Savage, M. B. Wise, Nucleon - nucleon scattering from effective field theory, *Nucl. Phys. B* 478 (1996) 629–659. doi:[10.1016/0550-3213\(96\)00357-4](https://doi.org/10.1016/0550-3213(96)00357-4). [arXiv:nucl-th/9605002](#).
- [523] D. B. Kaplan, M. J. Savage, M. B. Wise, A New expansion for nucleon-nucleon interactions, *Phys. Lett. B* 424 (1998) 390–396. doi:[10.1016/S0370-2693\(98\)00210-X](https://doi.org/10.1016/S0370-2693(98)00210-X). [arXiv:nucl-th/9801034](#).
- [524] D. B. Kaplan, M. J. Savage, M. B. Wise, Two nucleon systems from effective field theory, *Nucl. Phys. B* 534 (1998) 329–355. doi:[10.1016/S0550-3213\(98\)00440-4](https://doi.org/10.1016/S0550-3213(98)00440-4). [arXiv:nucl-th/9802075](#).
- [525] X. Kong, F. Ravndal, Proton proton scattering lengths from effective field theory, *Phys. Lett. B* 450 (1999) 320–324. doi:[10.1016/S0370-2693\(99\)00619-X](https://doi.org/10.1016/S0370-2693(99)00619-X), [10.1016/S0370-2693\(99\)00144-6](https://doi.org/10.1016/S0370-2693(99)00144-6). [arXiv:nucl-th/9811076](#), [Erratum: *Phys. Lett.B*458,565(1999)].
- [526] V. Cirigliano, W. Dekens, E. Mereghetti, A. Walker-Loud, Neutrinoless double- β decay in effective field theory: The light-Majorana neutrino-exchange mechanism, *Phys. Rev. C* 97 (2018) 065501. doi:[10.1103/PhysRevC.97.065501](https://doi.org/10.1103/PhysRevC.97.065501), [10.1103/PhysRevC.100.019903](https://doi.org/10.1103/PhysRevC.100.019903). [arXiv:1710.01729](#), [Erratum: *Phys. Rev.C*100,no.1,019903(2019)].
- [527] V. Cirigliano, W. Dekens, J. De Vries, M. L. Graesser, E. Mereghetti, S. Pastore, U. Van Kolck, New Leading Contribution to Neutrinoless Double- β Decay, *Phys. Rev. Lett.* 120 (2018) 202001. doi:[10.1103/PhysRevLett.120.202001](https://doi.org/10.1103/PhysRevLett.120.202001). [arXiv:1802.10097](#).
- [528] S. Fleming, T. Mehen, I. W. Stewart, NNLO corrections to nucleon-nucleon scattering and perturbative pions, *Nucl. Phys. A* 677 (2000) 313–366. doi:[10.1016/S0375-9474\(00\)00221-9](https://doi.org/10.1016/S0375-9474(00)00221-9). [arXiv:nucl-th/9911001](#).
- [529] D. B. Kaplan, Convergence of nuclear effective field theory with perturbative pions, *Phys. Rev. C* 102 (2020) 034004. doi:[10.1103/PhysRevC.102.034004](https://doi.org/10.1103/PhysRevC.102.034004). [arXiv:1905.07485](#).
- [530] S. R. Beane, P. F. Bedaque, M. J. Savage, U. van Kolck, Towards a perturbative theory of nuclear forces, *Nucl. Phys. A* 700 (2002) 377–402. doi:[10.1016/S0375-9474\(01\)01324-0](https://doi.org/10.1016/S0375-9474(01)01324-0). [arXiv:nucl-th/0104030](#).
- [531] A. Nogga, R. G. E. Timmermans, U. van Kolck, Renormalization of one-pion exchange and power counting, *Phys. Rev. C* 72 (2005) 054006. doi:[10.1103/PhysRevC.72.054006](https://doi.org/10.1103/PhysRevC.72.054006). [arXiv:nucl-th/0506005](#).
- [532] M. Pavon Valderrama, E. Ruiz Arriola, Renormalization of NN interaction with chiral two pion exchange potential: Non-central phases, *Phys. Rev. C* 74 (2006) 064004. doi:[10.1103/PhysRevC.74.064004](https://doi.org/10.1103/PhysRevC.74.064004), [10.1103/PhysRevC.75.059905](https://doi.org/10.1103/PhysRevC.75.059905). [arXiv:nucl-th/0507075](#), [Erratum: *Phys. Rev.C*75,059905(2007)].
- [533] M. C. Birse, Power counting with one-pion exchange, *Phys. Rev. C* 74 (2006) 014003. doi:[10.1103/PhysRevC.74.014003](https://doi.org/10.1103/PhysRevC.74.014003). [arXiv:nucl-th/0507077](#).
- [534] S. Wu, B. Long, Perturbative NN scattering in chiral effective field theory, *Phys. Rev. C* 99 (2019) 024003. doi:[10.1103/PhysRevC.99.024003](https://doi.org/10.1103/PhysRevC.99.024003). [arXiv:1807.04407](#).
- [535] E. Epelbaum, J. Gegelia, Weinberg's approach to nucleon–nucleon scattering revisited, *Phys. Lett. B* 716 (2012) 338–344. doi:[10.1016/j.physletb.2012.08.025](https://doi.org/10.1016/j.physletb.2012.08.025). [arXiv:1207.2420](#).
- [536] X.-L. Ren, K.-W. Li, L.-S. Geng, B.-W. Long, P. Ring, J. Meng, Leading order relativistic chiral nucleon-nucleon interaction, *Chin. Phys. C* 42 (2018) 014103. doi:[10.1088/1674-1137/42/1/014103](https://doi.org/10.1088/1674-1137/42/1/014103). [arXiv:1611.08475](#).
- [537] M. P. Valderrama, Perturbative renormalizability of chiral two pion exchange in nucleon-nucleon scattering, *Phys. Rev. C* 83 (2011) 024003. doi:[10.1103/PhysRevC.83.024003](https://doi.org/10.1103/PhysRevC.83.024003). [arXiv:0912.0699](#).

- [538] B. Long, C. J. Yang, Renormalizing Chiral Nuclear Forces: Triplet Channels, Phys. Rev. C85 (2012) 034002. doi:[10.1103/PhysRevC.85.034002](https://doi.org/10.1103/PhysRevC.85.034002). arXiv:[1111.3993](https://arxiv.org/abs/1111.3993).
- [539] B. Long, C. J. Yang, Short-range nuclear forces in singlet channels, Phys. Rev. C86 (2012) 024001. doi:[10.1103/PhysRevC.86.024001](https://doi.org/10.1103/PhysRevC.86.024001). arXiv:[1202.4053](https://arxiv.org/abs/1202.4053).
- [540] Y.-H. Song, R. Lazauskas, U. van Kolck, Triton binding energy and neutron-deuteron scattering up to next-to-leading order in chiral effective field theory, Phys. Rev. C96 (2017) 024002. doi:[10.1103/PhysRevC.96.024002](https://doi.org/10.1103/PhysRevC.96.024002), [10.1103/PhysRevC.100.019901](https://doi.org/10.1103/PhysRevC.100.019901). arXiv:[1612.09090](https://arxiv.org/abs/1612.09090), [erratum: Phys. Rev.C100,no.1,019901(2019)].
- [541] M. Pavón Valderrama, D. R. Phillips, Power Counting of Contact-Range Currents in Effective Field Theory, Phys. Rev. Lett. 114 (2015) 082502. doi:[10.1103/PhysRevLett.114.082502](https://doi.org/10.1103/PhysRevLett.114.082502). arXiv:[1407.0437](https://arxiv.org/abs/1407.0437).
- [542] M. Hoferichter, J. Ruiz de Elvira, B. Kubis, U.-G. Meißner, Matching pion-nucleon Roy-Steiner equations to chiral perturbation theory, Phys. Rev. Lett. 115 (2015) 192301. doi:[10.1103/PhysRevLett.115.192301](https://doi.org/10.1103/PhysRevLett.115.192301). arXiv:[1507.07552](https://arxiv.org/abs/1507.07552).
- [543] M. Hoferichter, J. Ruiz de Elvira, B. Kubis, U.-G. Meißner, Roy-Steiner-equation analysis of pion-nucleon scattering, Phys. Rept. 625 (2016) 1–88. doi:[10.1016/j.physrep.2016.02.002](https://doi.org/10.1016/j.physrep.2016.02.002). arXiv:[1510.06039](https://arxiv.org/abs/1510.06039).
- [544] V. Bernard, N. Kaiser, U.-G. Meißner, Aspects of chiral pion-nucleon physics, Nucl. Phys. A615 (1997) 483–500. doi:[10.1016/S0375-9474\(97\)00021-3](https://doi.org/10.1016/S0375-9474(97)00021-3). arXiv:[hep-ph/9611253](https://arxiv.org/abs/hep-ph/9611253).
- [545] E. Epelbaum, U. G. Meißner, W. Gloeckle, C. Elster, Resonance saturation for four nucleon operators, Phys. Rev. C65 (2002) 044001. doi:[10.1103/PhysRevC.65.044001](https://doi.org/10.1103/PhysRevC.65.044001). arXiv:[nucl-th/0106007](https://arxiv.org/abs/nucl-th/0106007).
- [546] H. Krebs, E. Epelbaum, U.-G. Meißner, Nuclear forces with Delta-excitations up to next-to-next-to-leading order. I. Peripheral nucleon-nucleon waves, Eur. Phys. J. A32 (2007) 127–137. doi:[10.1140/epja/i2007-10372-y](https://doi.org/10.1140/epja/i2007-10372-y). arXiv:[nucl-th/0703087](https://arxiv.org/abs/nucl-th/0703087).
- [547] E. Epelbaum, H. Krebs, U.-G. Meißner, Delta-excitations and the three-nucleon force, Nucl. Phys. A806 (2008) 65–78. doi:[10.1016/j.nuclphysa.2008.02.305](https://doi.org/10.1016/j.nuclphysa.2008.02.305). arXiv:[0712.1969](https://arxiv.org/abs/0712.1969).
- [548] H. Krebs, A. M. Gasparyan, E. Epelbaum, Three-nucleon force in chiral EFT with explicit $\Delta(1232)$ degrees of freedom: Longest-range contributions at fourth order, Phys. Rev. C98 (2018) 014003. doi:[10.1103/PhysRevC.98.014003](https://doi.org/10.1103/PhysRevC.98.014003). arXiv:[1803.09613](https://arxiv.org/abs/1803.09613).
- [549] K. Hebeler, S. K. Bogner, R. J. Furnstahl, A. Nogga, A. Schwenk, Improved nuclear matter calculations from chiral low-momentum interactions, Phys. Rev. C83 (2011) 031301. doi:[10.1103/PhysRevC.83.031301](https://doi.org/10.1103/PhysRevC.83.031301). arXiv:[1012.3381](https://arxiv.org/abs/1012.3381).
- [550] P. Klos, A. Carbone, K. Hebeler, J. Menéndez, A. Schwenk, Uncertainties in constraining low-energy constants from ^3H β decay, Eur. Phys. J. A53 (2017) 168. doi:[10.1140/epja/i2018-12530-6](https://doi.org/10.1140/epja/i2018-12530-6), [10.1140/epja/i2017-12357-7](https://doi.org/10.1140/epja/i2017-12357-7). arXiv:[1612.08010](https://arxiv.org/abs/1612.08010), [Erratum: Eur. Phys. J.A54,no.5,76(2018)].
- [551] E. Epelbaum, et al., Towards high-order calculations of three-nucleon scattering in chiral effective field theory, Eur. Phys. J. A56 (2020) 92. doi:[10.1140/epja/s10050-020-00102-2](https://doi.org/10.1140/epja/s10050-020-00102-2). arXiv:[1907.03608](https://arxiv.org/abs/1907.03608).
- [552] H. Krebs, A. Gasparyan, E. Epelbaum, Chiral three-nucleon force at $N^4\text{LO}$ I: Longest-range contributions, Phys. Rev. C85 (2012) 054006. doi:[10.1103/PhysRevC.85.054006](https://doi.org/10.1103/PhysRevC.85.054006). arXiv:[1203.0067](https://arxiv.org/abs/1203.0067).
- [553] L. Girlanda, A. Kievsky, M. Viviani, Subleading contributions to the three-nucleon contact interaction, Phys. Rev. C84 (2011) 014001. doi:[10.1103/PhysRevC.84.014001](https://doi.org/10.1103/PhysRevC.84.014001). arXiv:[1102.4799](https://arxiv.org/abs/1102.4799).
- [554] H. Krebs, A. Gasparyan, E. Epelbaum, Chiral three-nucleon force at $N^4\text{LO}$ II: Intermediate-range contributions, Phys. Rev. C87 (2013) 054007. doi:[10.1103/PhysRevC.87.054007](https://doi.org/10.1103/PhysRevC.87.054007). arXiv:[1302.2872](https://arxiv.org/abs/1302.2872).
- [555] A. Ekström, B. D. Carlsson, K. A. Wendt, C. Forssén, M. Hjorth-Jensen, R. Machleidt, S. M. Wild, Statistical uncertainties of a chiral interaction at next-to-next-to leading order, J. Phys. G42 (2015) 034003. doi:[10.1088/0954-3899/42/3/034003](https://doi.org/10.1088/0954-3899/42/3/034003). arXiv:[1406.6895](https://arxiv.org/abs/1406.6895).
- [556] M. Piarulli, L. Girlanda, R. Schiavilla, R. Navarro Pérez, J. E. Amaro, E. Ruiz Arriola, Minimally nonlocal nucleon-nucleon potentials with chiral two-pion exchange including Δ resonances, Phys. Rev. C91 (2015) 024003. doi:[10.1103/PhysRevC.91.024003](https://doi.org/10.1103/PhysRevC.91.024003). arXiv:[1412.6446](https://arxiv.org/abs/1412.6446).
- [557] M. Piarulli, L. Girlanda, R. Schiavilla, A. Kievsky, A. Lovato, L. E. Marcucci, S. C. Pieper, M. Viviani, R. B. Wiringa, Local chiral potentials with Δ -intermediate states and the structure of light nuclei, Phys. Rev. C94 (2016) 054007. doi:[10.1103/PhysRevC.94.054007](https://doi.org/10.1103/PhysRevC.94.054007). arXiv:[1606.06335](https://arxiv.org/abs/1606.06335).
- [558] A. Ekström, G. Hagen, T. D. Morris, T. Papenbrock, P. D. Schwartz, Δ isobars and nuclear saturation, Phys. Rev. C97 (2018) 024332. doi:[10.1103/PhysRevC.97.024332](https://doi.org/10.1103/PhysRevC.97.024332). arXiv:[1707.09028](https://arxiv.org/abs/1707.09028).
- [559] D. R. Entem, N. Kaiser, R. Machleidt, Y. Nosyk, Dominant contributions to the nucleon-nucleon interaction at sixth order of chiral perturbation theory, Phys. Rev. C92 (2015) 064001. doi:[10.1103/PhysRevC.92.064001](https://doi.org/10.1103/PhysRevC.92.064001). arXiv:[1505.03562](https://arxiv.org/abs/1505.03562).
- [560] S. K. Bogner, R. J. Furnstahl, R. J. Perry, Similarity Renormalization Group for Nucleon-Nucleon Interactions, Phys. Rev. C75 (2007) 061001. doi:[10.1103/PhysRevC.75.061001](https://doi.org/10.1103/PhysRevC.75.061001). arXiv:[nucl-th/0611045](https://arxiv.org/abs/nucl-th/0611045).

- [561] K. Hebeler, Momentum space evolution of chiral three-nucleon forces, Phys. Rev. C85 (2012) 021002. doi:[10.1103/PhysRevC.85.021002](https://doi.org/10.1103/PhysRevC.85.021002). arXiv:[1201.0169](https://arxiv.org/abs/1201.0169).
- [562] R. J. Furnstahl, K. Hebeler, New applications of renormalization group methods in nuclear physics, Rept. Prog. Phys. 76 (2013) 126301. doi:[10.1088/0034-4885/76/12/126301](https://doi.org/10.1088/0034-4885/76/12/126301). arXiv:[1305.3800](https://arxiv.org/abs/1305.3800).
- [563] G. Hagen, et al., Neutron and weak-charge distributions of the ^{48}Ca nucleus, Nature Phys. 12 (2015) 186–190. doi:[10.1038/nphys3529](https://doi.org/10.1038/nphys3529). arXiv:[1509.07169](https://arxiv.org/abs/1509.07169).
- [564] S. Pastore, L. Girlanda, R. Schiavilla, M. Viviani, R. B. Wiringa, Electromagnetic Currents and Magnetic Moments in (chi)EFT, Phys. Rev. C80 (2009) 034004. doi:[10.1103/PhysRevC.80.034004](https://doi.org/10.1103/PhysRevC.80.034004). arXiv:[0906.1800](https://arxiv.org/abs/0906.1800).
- [565] H. Krebs, E. Epelbaum, U.-G. Meißner, Nuclear Electromagnetic Currents to Fourth Order in Chiral Effective Field Theory, Few Body Syst. 60 (2019) 31. doi:[10.1007/s00601-019-1500-5](https://doi.org/10.1007/s00601-019-1500-5). arXiv:[1902.06839](https://arxiv.org/abs/1902.06839).
- [566] S. Pastore, S. C. Pieper, R. Schiavilla, R. B. Wiringa, Quantum Monte Carlo calculations of electromagnetic moments and transitions in $A \leq 9$ nuclei with meson-exchange currents derived from chiral effective field theory, Phys. Rev. C87 (2013) 035503. doi:[10.1103/PhysRevC.87.035503](https://doi.org/10.1103/PhysRevC.87.035503). arXiv:[1212.3375](https://arxiv.org/abs/1212.3375).
- [567] S. Pastore, A. Baroni, J. Carlson, S. Gandolfi, S. C. Pieper, R. Schiavilla, R. B. Wiringa, Quantum Monte Carlo calculations of weak transitions in $A = 6$?10 nuclei, Phys. Rev. C97 (2018) 022501. doi:[10.1103/PhysRevC.97.022501](https://doi.org/10.1103/PhysRevC.97.022501). arXiv:[1709.03592](https://arxiv.org/abs/1709.03592).
- [568] P. Gysbers, et al., Discrepancy between experimental and theoretical β -decay rates resolved from first principles, Nature Phys. 15 (2019) 428–431. doi:[10.1038/s41567-019-0450-7](https://doi.org/10.1038/s41567-019-0450-7). arXiv:[1903.00047](https://arxiv.org/abs/1903.00047).
- [569] C. Körber, A. Nogga, J. de Vries, First-principle calculations of Dark Matter scattering off light nuclei, Phys. Rev. C96 (2017) 035805. doi:[10.1103/PhysRevC.96.035805](https://doi.org/10.1103/PhysRevC.96.035805). arXiv:[1704.01150](https://arxiv.org/abs/1704.01150).
- [570] L. Andreoli, V. Cirigliano, S. Gandolfi, F. Pederiva, Quantum Monte Carlo calculations of dark matter scattering off light nuclei, Phys. Rev. C99 (2019) 025501. doi:[10.1103/PhysRevC.99.025501](https://doi.org/10.1103/PhysRevC.99.025501). arXiv:[1811.01843](https://arxiv.org/abs/1811.01843).
- [571] M. Hoferichter, P. Klos, J. Menéndez, A. Schwenk, Analysis strategies for general spin-independent WIMP-nucleus scattering, Phys. Rev. D94 (2016) 063505. doi:[10.1103/PhysRevD.94.063505](https://doi.org/10.1103/PhysRevD.94.063505). arXiv:[1605.08043](https://arxiv.org/abs/1605.08043).
- [572] M. Hoferichter, P. Klos, J. Menéndez, A. Schwenk, Nuclear structure factors for general spin-independent WIMP-nucleus scattering, Phys. Rev. D99 (2019) 055031. doi:[10.1103/PhysRevD.99.055031](https://doi.org/10.1103/PhysRevD.99.055031). arXiv:[1812.05617](https://arxiv.org/abs/1812.05617).
- [573] J. de Vries, U.-G. Meißner, E. Epelbaum, N. Kaiser, Parity violation in proton-proton scattering from chiral effective field theory, Eur. Phys. J. A49 (2013) 149. doi:[10.1140/epja/i2013-13149-9](https://doi.org/10.1140/epja/i2013-13149-9). arXiv:[1309.4711](https://arxiv.org/abs/1309.4711).
- [574] M. Viviani, A. Baroni, L. Girlanda, A. Kievsky, L. E. Marcucci, R. Schiavilla, Chiral effective field theory analysis of hadronic parity violation in few-nucleon systems, Phys. Rev. C89 (2014) 064004. doi:[10.1103/PhysRevC.89.064004](https://doi.org/10.1103/PhysRevC.89.064004). arXiv:[1403.2267](https://arxiv.org/abs/1403.2267).
- [575] C. M. Maekawa, E. Mereghetti, J. de Vries, U. van Kolck, The Time-Reversal- and Parity-Violating Nuclear Potential in Chiral Effective Theory, Nucl. Phys. A872 (2011) 117–160. doi:[10.1016/j.nuclphysa.2011.09.020](https://doi.org/10.1016/j.nuclphysa.2011.09.020). arXiv:[1106.6119](https://arxiv.org/abs/1106.6119).
- [576] J. de Vries, E. Mereghetti, R. G. E. Timmermans, U. van Kolck, The Effective Chiral Lagrangian From Dimension-Six Parity and Time-Reversal Violation, Annals Phys. 338 (2013) 50–96. doi:[10.1016/j.aop.2013.05.022](https://doi.org/10.1016/j.aop.2013.05.022). arXiv:[1212.0990](https://arxiv.org/abs/1212.0990).
- [577] J. Bsaisou, J. de Vries, C. Hanhart, S. Liebig, U.-G. Meißner, D. Minossi, A. Nogga, A. Wirzba, Nuclear Electric Dipole Moments in Chiral Effective Field Theory, JHEP 03 (2015) 104. doi:[10.1007/JHEP03\(2015\)104](https://doi.org/10.1007/JHEP03(2015)104), [10.1007/JHEP05\(2015\)083](https://doi.org/10.1007/JHEP05(2015)083). arXiv:[1411.5804](https://arxiv.org/abs/1411.5804), [Erratum: JHEP05,083(2015)].
- [578] J. Bsaisou, U.-G. Meißner, A. Nogga, A. Wirzba, P- and T-Violating Lagrangians in Chiral Effective Field Theory and Nuclear Electric Dipole Moments, Annals Phys. 359 (2015) 317–370. doi:[10.1016/j.aop.2015.04.031](https://doi.org/10.1016/j.aop.2015.04.031). arXiv:[1412.5471](https://arxiv.org/abs/1412.5471).
- [579] A. Gnech, M. Viviani, Time Reversal Violation in Light Nuclei, Phys. Rev. C101 (2020) 024004. doi:[10.1103/PhysRevC.101.024004](https://doi.org/10.1103/PhysRevC.101.024004). arXiv:[1906.09021](https://arxiv.org/abs/1906.09021).
- [580] G. Barton, Notes on the static parity nonconserving internucleon potential, Nuovo Cim. 19 (1961) 512–527. doi:[10.1007/BF02733247](https://doi.org/10.1007/BF02733247).
- [581] I. S. Towner, A. C. Hayes, P, T violating nuclear matrix elements in the one meson exchange approximation, Phys. Rev. C49 (1994) 2391–2397. doi:[10.1103/PhysRevC.49.2391](https://doi.org/10.1103/PhysRevC.49.2391). arXiv:[nucl-th/9402026](https://arxiv.org/abs/nucl-th/9402026).
- [582] W. C. Haxton, T. Luu, The Canonical nuclear many body problem as an effective theory, Nucl. Phys. A690 (2001) 15–28. doi:[10.1016/S0375-9474\(01\)00927-7](https://doi.org/10.1016/S0375-9474(01)00927-7). arXiv:[nucl-th/0101022](https://arxiv.org/abs/nucl-th/0101022).
- [583] W. C. Haxton, T. Luu, Perturbative effective theory in an oscillator basis?, Phys. Rev. Lett. 89 (2002) 182503. doi:[10.1103/PhysRevLett.89.182503](https://doi.org/10.1103/PhysRevLett.89.182503). arXiv:[nucl-th/0204072](https://arxiv.org/abs/nucl-th/0204072).
- [584] T. C. Luu, S. Bogner, W. C. Haxton, P. Navratil, Effective interactions for the three-body problem, Phys. Rev. C70 (2004) 014316. doi:[10.1103/PhysRevC.70.014316](https://doi.org/10.1103/PhysRevC.70.014316). arXiv:[nucl-th/0404028](https://arxiv.org/abs/nucl-th/0404028).

- [585] K. S. McElvain, W. C. Haxton, Nuclear physics without high-momentum potentials: Constructing the nuclear effective interaction directly from scattering observables, *Phys. Lett.* B797 (2019) 134880. doi:[10.1016/j.physletb.2019.134880](https://doi.org/10.1016/j.physletb.2019.134880). arXiv:[1902.03543](https://arxiv.org/abs/1902.03543).
- [586] A. de Shalit, I. Talmi, Nuclear Shell Theory, Academic Press Inc., New York and London, 1963.
- [587] H. A. Bethe, Nuclear Many-Body Problem, *Phys. Rev.* 103 (1956) 1353–1390. URL: <https://doi.org/10.1103/PhysRev.103.1353>. doi:[10.1103/PhysRev.103.1353](https://doi.org/10.1103/PhysRev.103.1353).
- [588] T. Kuo, Structure of finite nuclei and the free nucleon-nucleon interaction: An application to O-18 and F-18, *Nucl. Phys.* 85 (1966) 40–86. doi:[10.1016/0029-5582\(66\)90131-3](https://doi.org/10.1016/0029-5582(66)90131-3).
- [589] B. R. Barrett, M. W. Kirson, Higher-order terms and the apparent non-convergence of the perturbation expansion for the effective interaction in finite nuclei, *Nucl. Phys.* A148 (1970) 145–180. doi:[10.1016/0375-9474\(72\)90813-5](https://doi.org/10.1016/0375-9474(72)90813-5), [10.1016/0375-9474\(70\)90617-2](https://doi.org/10.1016/0375-9474(70)90617-2), [Erratum: *Nucl. Phys.* A196, 638 (1972)].
- [590] T. Schucan, H. Weidenmüller, The effective interaction in nuclei and its perturbation expansion: An algebraic approach, *Annals of Physics* 73 (1972) 108–135. URL: <http://www.sciencedirect.com/science/article/pii/0003491672903156>. doi:[10.1016/0003-4916\(72\)90315-6](https://doi.org/10.1016/0003-4916(72)90315-6).
- [591] T. H. Schucan, H. A. Weidenmüller, Perturbation theory for the effective interaction in nuclei, *Annals of Physics* 76 (1973) 483–509. URL: <http://www.sciencedirect.com/science/article/pii/0003491673900444>. doi:[10.1016/0003-4916\(73\)90044-4](https://doi.org/10.1016/0003-4916(73)90044-4).
- [592] S. D. Glazek, K. G. Wilson, Perturbative renormalization group for Hamiltonians, *Phys. Rev.* D49 (1994) 4214–4218. doi:[10.1103/PhysRevD.49.4214](https://doi.org/10.1103/PhysRevD.49.4214).
- [593] S. D. Glazek, K. G. Wilson, Renormalization of Hamiltonians, *Phys. Rev.* D48 (1993) 5863–5872. doi:[10.1103/PhysRevD.48.5863](https://doi.org/10.1103/PhysRevD.48.5863).
- [594] E. D. Jurgenson, S. K. Bogner, R. J. Furnstahl, R. J. Perry, Decoupling in the Similarity Renormalization Group for Nucleon-Nucleon Forces, *Phys. Rev.* C78 (2008) 014003. doi:[10.1103/PhysRevC.78.014003](https://doi.org/10.1103/PhysRevC.78.014003). arXiv:[0711.4252](https://arxiv.org/abs/0711.4252).
- [595] S. D. Glazek, M. Wieckowski, Large momentum convergence of Hamiltonian bound state dynamics of effective fermions in quantum field theory, *Phys. Rev.* D 66 (2002) 016001. doi:[10.1103/PhysRevD.66.016001](https://doi.org/10.1103/PhysRevD.66.016001). arXiv:[hep-th/0204171](https://arxiv.org/abs/hep-th/0204171).
- [596] H. Hergert, S. K. Bogner, T. D. Morris, A. Schwenk, K. Tsukiyama, The In-Medium Similarity Renormalization Group: A Novel Ab Initio Method for Nuclei, *Phys. Rept.* 621 (2016) 165–222. doi:[10.1016/j.physrep.2015.12.007](https://doi.org/10.1016/j.physrep.2015.12.007). arXiv:[1512.06956](https://arxiv.org/abs/1512.06956).
- [597] I. Stetcu, B. R. Barrett, U. van Kolck, No-core shell model in an effective-field-theory framework, *Phys. Lett.* B653 (2007) 358–362. doi:[10.1016/j.physletb.2007.07.065](https://doi.org/10.1016/j.physletb.2007.07.065). arXiv:[nucl-th/0609023](https://arxiv.org/abs/nucl-th/0609023).
- [598] C. J. Yang, Chiral potential renormalized in harmonic-oscillator space, *Phys. Rev.* C94 (2016) 064004. doi:[10.1103/PhysRevC.94.064004](https://doi.org/10.1103/PhysRevC.94.064004). arXiv:[1610.01350](https://arxiv.org/abs/1610.01350).
- [599] A. Nogga, S. K. Bogner, A. Schwenk, Low-momentum interaction in few-nucleon systems, *Phys. Rev.* C70 (2004) 061002. doi:[10.1103/PhysRevC.70.061002](https://doi.org/10.1103/PhysRevC.70.061002). arXiv:[nucl-th/0405016](https://arxiv.org/abs/nucl-th/0405016).
- [600] S. K. Bogner, A. Schwenk, R. J. Furnstahl, A. Nogga, Is nuclear matter perturbative with low-momentum interactions?, *Nucl. Phys.* A763 (2005) 59–79. doi:[10.1016/j.nuclphysa.2005.08.024](https://doi.org/10.1016/j.nuclphysa.2005.08.024). arXiv:[nucl-th/0504043](https://arxiv.org/abs/nucl-th/0504043).
- [601] S. K. Bogner, R. J. Furnstahl, Variational calculations of nuclei with low-momentum potentials, *Phys. Lett.* B632 (2006) 501–506. doi:[10.1016/j.physletb.2005.10.094](https://doi.org/10.1016/j.physletb.2005.10.094). arXiv:[nucl-th/0508022](https://arxiv.org/abs/nucl-th/0508022).
- [602] S. K. Bogner, R. J. Furnstahl, Variational calculations using low-momentum potentials with smooth cutoffs, *Phys. Lett.* B639 (2006) 237–241. doi:[10.1016/j.physletb.2006.06.037](https://doi.org/10.1016/j.physletb.2006.06.037). arXiv:[nucl-th/0602017](https://arxiv.org/abs/nucl-th/0602017).
- [603] S. K. Bogner, R. J. Furnstahl, S. Ramanan, A. Schwenk, Convergence of the Born series with low-momentum interactions, *Nucl. Phys.* A773 (2006) 203–220. doi:[10.1016/j.nuclphysa.2006.05.004](https://doi.org/10.1016/j.nuclphysa.2006.05.004). arXiv:[nucl-th/0602060](https://arxiv.org/abs/nucl-th/0602060).
- [604] I. Stetcu, J. Rotureau, B. R. Barrett, U. van Kolck, Effective interactions for light nuclei: An Effective (field theory) approach, *J. Phys.* G37 (2010) 064033. doi:[10.1088/0954-3899/37/6/064033](https://doi.org/10.1088/0954-3899/37/6/064033). arXiv:[0912.3015](https://arxiv.org/abs/0912.3015).
- [605] J. Rotureau, I. Stetcu, B. R. Barrett, U. van Kolck, Two and Three Nucleons in a Trap and the Continuum Limit, *Phys. Rev.* C85 (2012) 034003. doi:[10.1103/PhysRevC.85.034003](https://doi.org/10.1103/PhysRevC.85.034003). arXiv:[1112.0267](https://arxiv.org/abs/1112.0267).
- [606] K. S. McElvain, Harmonic Oscillator Based Effective Theory, Connecting LQCD to Nuclear Structure, Ph.D. thesis, University of California, Berkeley, 2017.
- [607] W. C. Haxton, K. S. McElvain, In preparation, 2020.
- [608] R. B. Wiringa, V. G. J. Stoks, R. Schiavilla, An Accurate nucleon-nucleon potential with charge independence breaking, *Phys. Rev.* C51 (1995) 38–51. doi:[10.1103/PhysRevC.51.38](https://doi.org/10.1103/PhysRevC.51.38). arXiv:[nucl-th/9408016](https://arxiv.org/abs/nucl-th/9408016).
- [609] T. Schucan, H. Weidenmüller, The effective interaction in nuclei and its perturbation expansion: An algebraic approach, *Ann. Phys.* 73 (1972) 108–135. doi:[10.1016/0003-4916\(72\)90315-6](https://doi.org/10.1016/0003-4916(72)90315-6).

- [610] T. H. Schucan, H. A. Weidenmüller, Perturbation theory for the effective interaction in nuclei, *Ann. Phys.* 76 (1973) 483–509. doi:[10.1016/0003-4916\(73\)90044-4](https://doi.org/10.1016/0003-4916(73)90044-4).
- [611] L. Gomes, J. Walecka, V. Weisskopf, Properties of nuclear matter, *Annals Phys.* 3 (1958) 241–274. doi:[10.1016/0003-4916\(58\)90019-8](https://doi.org/10.1016/0003-4916(58)90019-8).
- [612] F. Coester, H. Kümmel, Short-range correlations in nuclear wave functions, *Nuclear Physics* 17 (1960) 477 – 485. URL: <http://www.sciencedirect.com/science/article/pii/0029558260901401>. doi:[https://doi.org/10.1016/0029-5582\(60\)90140-1](https://doi.org/10.1016/0029-5582(60)90140-1).
- [613] D. Zheng, B. Barrett, J. Vary, W. Haxton, C. Song, Large basis shell model studies of light nuclei with a multivalued G matrix effective interaction, *Phys. Rev. C* 52 (1995) 2488–2498. doi:[10.1103/PhysRevC.52.2488](https://doi.org/10.1103/PhysRevC.52.2488). [arXiv:nucl-th/9507011](https://arxiv.org/abs/nucl-th/9507011).
- [614] W. Haxton, K. McElvain, Work in progress, 2020.
- [615] P. F. Bedaque, I. Sato, A. Walker-Loud, Finite volume corrections to pi-pi scattering, *Phys. Rev. D* 73 (2006) 074501. doi:[10.1103/PhysRevD.73.074501](https://doi.org/10.1103/PhysRevD.73.074501). [arXiv:hep-lat/0601033](https://arxiv.org/abs/hep-lat/0601033).
- [616] I. Sato, P. F. Bedaque, Fitting two nucleons inside a box: Exponentially suppressed corrections to the Luscher's formula, *Phys. Rev. D* 76 (2007) 034502. doi:[10.1103/PhysRevD.76.034502](https://doi.org/10.1103/PhysRevD.76.034502). [arXiv:hep-lat/0702021](https://arxiv.org/abs/hep-lat/0702021).
- [617] G. Racah, On the symmetry of particle and antiparticle, *Nuovo Cim.* 14 (1937) 322–328. doi:[10.1007/BF02961321](https://doi.org/10.1007/BF02961321).
- [618] W. H. Fury, On transition probabilities in double beta-disintegration, *Phys. Rev.* 56 (1939) 1184–1193. doi:[10.1103/PhysRev.56.1184](https://doi.org/10.1103/PhysRev.56.1184).
- [619] M. Tanabashi, et al. (Particle Data Group), Review of Particle Physics, *Phys. Rev. D* 98 (2018) 030001. doi:[10.1103/PhysRevD.98.030001](https://doi.org/10.1103/PhysRevD.98.030001).
- [620] M. Aker, et al. (KATRIN), Improved Upper Limit on the Neutrino Mass from a Direct Kinematic Method by KATRIN, *Phys. Rev. Lett.* 123 (2019) 221802. doi:[10.1103/PhysRevLett.123.221802](https://doi.org/10.1103/PhysRevLett.123.221802). [arXiv:1909.06048](https://arxiv.org/abs/1909.06048).
- [621] S. R. Elliott, A. A. Hahn, M. K. Moe, Direct Evidence for Two Neutrino Double Beta Decay in ^{82}Se , *Phys. Rev. Lett.* 59 (1987) 2020–2023. doi:[10.1103/PhysRevLett.59.2020](https://doi.org/10.1103/PhysRevLett.59.2020), [,989(1987)].
- [622] J. Argyriades, et al. (NEMO-3), Measurement of the two neutrino double beta decay half-life of Zr-96 with the NEMO-3 detector, *Nucl. Phys. A* 847 (2010) 168–179. doi:[10.1016/j.nuclphysa.2010.07.009](https://doi.org/10.1016/j.nuclphysa.2010.07.009). [arXiv:0906.2694](https://arxiv.org/abs/0906.2694).
- [623] N. Ackerman, et al. (EXO-200), Observation of Two-Neutrino Double-Beta Decay in ^{136}Xe with EXO-200, *Phys. Rev. Lett.* 107 (2011) 212501. doi:[10.1103/PhysRevLett.107.212501](https://doi.org/10.1103/PhysRevLett.107.212501). [arXiv:1108.4193](https://arxiv.org/abs/1108.4193).
- [624] M. Agostini, et al. (GERDA), Measurement of the half-life of the two-neutrino double beta decay of Ge-76 with the Gerda experiment, *J. Phys. G* 40 (2013) 035110. doi:[10.1088/0954-3899/40/3/035110](https://doi.org/10.1088/0954-3899/40/3/035110). [arXiv:1212.3210](https://arxiv.org/abs/1212.3210).
- [625] C. Alduino, et al. (CUORE), Measurement of the two-neutrino double-beta decay half-life of ^{130}Te with the CUORE-0 experiment, *Eur. Phys. J. C* 77 (2017) 13. doi:[10.1140/epjc/s10052-016-4498-6](https://doi.org/10.1140/epjc/s10052-016-4498-6). [arXiv:1609.01666](https://arxiv.org/abs/1609.01666).
- [626] R. Arnold, et al. (NEMO-3), Measurement of the double-beta decay half-life and search for the neutrinoless double-beta decay of ^{48}Ca with the NEMO-3 detector, *Phys. Rev. D* 93 (2016) 112008. doi:[10.1103/PhysRevD.93.112008](https://doi.org/10.1103/PhysRevD.93.112008). [arXiv:1604.01710](https://arxiv.org/abs/1604.01710).
- [627] A. Gando, et al. (KamLAND-Zen), Precision measurement of the ^{136}Xe two-neutrino $\beta\beta$ spectrum in KamLAND-Zen and its impact on the quenching of nuclear matrix elements, *Phys. Rev. Lett.* 122 (2019) 192501. doi:[10.1103/PhysRevLett.122.192501](https://doi.org/10.1103/PhysRevLett.122.192501). [arXiv:1901.03871](https://arxiv.org/abs/1901.03871).
- [628] R. Arnold, et al., Final results on ^{82}Se double beta decay to the ground state of ^{82}Kr from the NEMO-3 experiment, *Eur. Phys. J. C* 78 (2018) 821. doi:[10.1140/epjc/s10052-018-6295-x](https://doi.org/10.1140/epjc/s10052-018-6295-x). [arXiv:1806.05553](https://arxiv.org/abs/1806.05553).
- [629] R. Arnold, et al. (NEMO-3), Detailed studies of ^{100}Mo two-neutrino double beta decay in NEMO-3, *Eur. Phys. J. C* 79 (2019) 440. doi:[10.1140/epjc/s10052-019-6948-4](https://doi.org/10.1140/epjc/s10052-019-6948-4). [arXiv:1903.08084](https://arxiv.org/abs/1903.08084).
- [630] J. Schechter, J. W. F. Valle, Neutrino Masses in SU(2) \times U(1) Theories, *Phys. Rev. D* 22 (1980) 2227. doi:[10.1103/PhysRevD.22.2227](https://doi.org/10.1103/PhysRevD.22.2227).
- [631] M. Fukugita, T. Yanagida, Baryogenesis Without Grand Unification, *Phys. Lett. B* 174 (1986) 45–47. doi:[10.1016/0370-2693\(86\)91126-3](https://doi.org/10.1016/0370-2693(86)91126-3).
- [632] F. F. Deppisch, L. Graf, J. Harz, W.-C. Huang, Neutrinoless Double Beta Decay and the Baryon Asymmetry of the Universe, *Phys. Rev. D* 98 (2018) 055029. doi:[10.1103/PhysRevD.98.055029](https://doi.org/10.1103/PhysRevD.98.055029). [arXiv:1711.10432](https://arxiv.org/abs/1711.10432).
- [633] A. Giuliani, J. J. Gomez Cadenas, S. Pascoli, E. Previtali, R. Saakyan, K. Schaeffner, S. Schoenert, Double Beta Decay APPEC Committee Report (2019). [arXiv:1910.04688](https://arxiv.org/abs/1910.04688).
- [634] J. Menendez, A. Poves, E. Caurier, F. Nowacki, Disassembling the Nuclear Matrix Elements of the Neutrinoless beta beta Decay, *Nucl. Phys. A* 818 (2009) 139–151. doi:[10.1016/j.nuclphysa.2008.12.005](https://doi.org/10.1016/j.nuclphysa.2008.12.005). [arXiv:0801.3760](https://arxiv.org/abs/0801.3760).

- [635] T. R. Rodriguez, G. Martinez-Pinedo, Energy density functional study of nuclear matrix elements for neutrinoless $\beta\beta$ decay, Phys. Rev. Lett. 105 (2010) 252503. doi:[10.1103/PhysRevLett.105.252503](https://doi.org/10.1103/PhysRevLett.105.252503). arXiv:[1008.5260](https://arxiv.org/abs/1008.5260).
- [636] A. Meroni, S. T. Petcov, F. Simkovic, Multiple cp non-conserving mechanisms of $(\beta\beta)_{0\nu}$ -decay and nuclei with largely different nuclear matrix elements, JHEP 02 (2013) 025. doi:[10.1007/JHEP02\(2013\)025](https://doi.org/10.1007/JHEP02(2013)025). arXiv:[1212.1331](https://arxiv.org/abs/1212.1331).
- [637] F. Šimkovic, V. Rodin, A. Faessler, P. Vogel, $0\nu\beta\beta$ and $2\nu\beta\beta$ nuclear matrix elements, quasiparticle random-phase approximation, and isospin symmetry restoration, Phys. Rev. C87 (2013) 045501. doi:[10.1103/PhysRevC.87.045501](https://doi.org/10.1103/PhysRevC.87.045501). arXiv:[1302.1509](https://arxiv.org/abs/1302.1509).
- [638] M. T. Mustonen, J. Engel, Large-scale calculations of the double- β decay of ^{76}Ge , ^{130}Te , ^{136}Xe , and ^{150}Nd in the deformed self-consistent Skyrme quasiparticle random-phase approximation, Phys. Rev. C87 (2013) 064302. doi:[10.1103/PhysRevC.87.064302](https://doi.org/10.1103/PhysRevC.87.064302). arXiv:[1301.6997](https://arxiv.org/abs/1301.6997).
- [639] N. Lopez Vaquero, T. R. Rodríguez, J. L. Egido, Shape and pairing fluctuations effects on neutrinoless double beta decay nuclear matrix elements, Phys. Rev. Lett. 111 (2013) 142501. doi:[10.1103/PhysRevLett.111.142501](https://doi.org/10.1103/PhysRevLett.111.142501). arXiv:[1401.0650](https://arxiv.org/abs/1401.0650).
- [640] J. M. Yao, L. S. Song, K. Hagino, P. Ring, J. Meng, Systematic study of nuclear matrix elements in neutrinoless double- β decay with a beyond-mean-field covariant density functional theory, Phys. Rev. C91 (2015) 024316. doi:[10.1103/PhysRevC.91.024316](https://doi.org/10.1103/PhysRevC.91.024316). arXiv:[1410.6326](https://arxiv.org/abs/1410.6326).
- [641] A. Neacsu, M. Horoi, Shell model studies of the ^{130}Te neutrinoless double-beta decay, Phys. Rev. C91 (2015) 024309. doi:[10.1103/PhysRevC.91.024309](https://doi.org/10.1103/PhysRevC.91.024309). arXiv:[1411.4313](https://arxiv.org/abs/1411.4313).
- [642] J. Barea, J. Kotila, F. Iachello, $0\nu\beta\beta$ and $2\nu\beta\beta$ nuclear matrix elements in the interacting boson model with isospin restoration, Phys. Rev. C91 (2015) 034304. doi:[10.1103/PhysRevC.91.034304](https://doi.org/10.1103/PhysRevC.91.034304). arXiv:[1506.08530](https://arxiv.org/abs/1506.08530).
- [643] J. Hyvärinen, J. Suhonen, Nuclear matrix elements for $0\nu\beta\beta$ decays with light or heavy Majorana-neutrino exchange, Phys. Rev. C91 (2015) 024613. doi:[10.1103/PhysRevC.91.024613](https://doi.org/10.1103/PhysRevC.91.024613).
- [644] M. Horoi, A. Neacsu, Shell model predictions for ^{124}Sn double- β decay, Phys. Rev. C93 (2016) 024308. doi:[10.1103/PhysRevC.93.024308](https://doi.org/10.1103/PhysRevC.93.024308). arXiv:[1511.03711](https://arxiv.org/abs/1511.03711).
- [645] S. Weinberg, Baryon and Lepton Nonconserving Processes, Phys. Rev. Lett. 43 (1979) 1566–1570. doi:[10.1103/PhysRevLett.43.1566](https://doi.org/10.1103/PhysRevLett.43.1566).
- [646] B. Pontecorvo, Inverse beta processes and nonconservation of lepton charge, Sov. Phys. JETP 7 (1958) 172–173.
- [647] Z. Maki, M. Nakagawa, S. Sakata, Remarks on the unified model of elementary particles, Prog. Theor. Phys. 28 (1962) 870–880. doi:[10.1143/PTP.28.870](https://doi.org/10.1143/PTP.28.870).
- [648] J. Engel, J. Menéndez, Status and Future of Nuclear Matrix Elements for Neutrinoless Double-Beta Decay: A Review, Rept. Prog. Phys. 80 (2017) 046301. doi:[10.1088/1361-6633/aa5bc5](https://doi.org/10.1088/1361-6633/aa5bc5). arXiv:[1610.06548](https://arxiv.org/abs/1610.06548).
- [649] M. J. Dolinski, A. W. P. Poon, W. Rodejohann, Neutrinoless Double-Beta Decay: Status and Prospects, Annual Review of Nuclear and Particle Science 69 (2019). URL: <https://doi.org/10.1146/annurev-nucl-101918-023407>. doi:[10.1146/annurev-nucl-101918-023407](https://doi.org/10.1146/annurev-nucl-101918-023407). arXiv:[1902.04097](https://arxiv.org/abs/1902.04097).
- [650] J. M. Yao, B. Bally, J. Engel, R. Wirth, T. R. Rodríguez, H. Hergert, *Ab Initio* Treatment of Collective Correlations and the Neutrinoless Double Beta Decay of ^{48}Ca , Phys. Rev. Lett. 124 (2020) 232501. doi:[10.1103/PhysRevLett.124.232501](https://doi.org/10.1103/PhysRevLett.124.232501). arXiv:[1908.05424](https://arxiv.org/abs/1908.05424).
- [651] V. Cirigliano, W. Dekens, J. De Vries, M. L. Graesser, E. Mereghetti, S. Pastore, M. Piarulli, U. Van Kolck, R. B. Wiringa, Renormalized approach to neutrinoless double- β decay, Phys. Rev. C100 (2019) 055504. doi:[10.1103/PhysRevC.100.055504](https://doi.org/10.1103/PhysRevC.100.055504). arXiv:[1907.11254](https://arxiv.org/abs/1907.11254).
- [652] J. Menendez, D. Gazit, A. Schwenk, Chiral two-body currents in nuclei: Gamow-Teller transitions and neutrinoless double-beta decay, Phys. Rev. Lett. 107 (2011) 062501. doi:[10.1103/PhysRevLett.107.062501](https://doi.org/10.1103/PhysRevLett.107.062501). arXiv:[1103.3622](https://arxiv.org/abs/1103.3622).
- [653] L.-J. Wang, J. Engel, J. M. Yao, Quenching of nuclear matrix elements for $0\nu\beta\beta$ decay by chiral two-body currents, Phys. Rev. C98 (2018) 031301. doi:[10.1103/PhysRevC.98.031301](https://doi.org/10.1103/PhysRevC.98.031301). arXiv:[1805.10276](https://arxiv.org/abs/1805.10276).
- [654] X. Feng, L.-C. Jin, X.-Y. Tuo, S.-C. Xia, Light-Neutrino Exchange and Long-Distance Contributions to $0\nu2\beta$ Decays: An Exploratory Study on $\pi\pi \rightarrow ee$, Phys. Rev. Lett. 122 (2019) 022001. doi:[10.1103/PhysRevLett.122.022001](https://doi.org/10.1103/PhysRevLett.122.022001). arXiv:[1809.10511](https://arxiv.org/abs/1809.10511).
- [655] W. Detmold, D. Murphy, Nuclear Matrix Elements for Neutrinoless Double Beta Decay from Lattice QCD, PoS LATTICE2018 (2019) 262. doi:[10.22323/1.334.0262](https://doi.org/10.22323/1.334.0262). arXiv:[1811.05554](https://arxiv.org/abs/1811.05554).
- [656] X.-Y. Tuo, X. Feng, L.-C. Jin, Long-distance contributions to neutrinoless double beta decay $\pi^- \rightarrow \pi^+ ee$, Phys. Rev. D100 (2019) 094511. doi:[10.1103/PhysRevD.100.094511](https://doi.org/10.1103/PhysRevD.100.094511). arXiv:[1909.13525](https://arxiv.org/abs/1909.13525).
- [657] R. Machleidt, The High precision, charge dependent Bonn nucleon-nucleon potential (CD-Bonn), Phys. Rev. C63 (2001) 024001. doi:[10.1103/PhysRevC.63.024001](https://doi.org/10.1103/PhysRevC.63.024001). arXiv:[nucl-th/0006014](https://arxiv.org/abs/nucl-th/0006014).

- [658] R. N. Mohapatra, J. C. Pati, Left-Right Gauge Symmetry and an Isoconjugate Model of CP Violation, *Phys. Rev.* D11 (1975) 566–571. doi:[10.1103/PhysRevD.11.566](https://doi.org/10.1103/PhysRevD.11.566).
- [659] G. Senjanovic, R. N. Mohapatra, Exact Left-Right Symmetry and Spontaneous Violation of Parity, *Phys. Rev.* D12 (1975) 1502. doi:[10.1103/PhysRevD.12.1502](https://doi.org/10.1103/PhysRevD.12.1502).
- [660] R. N. Mohapatra, New Contributions to Neutrinoless Double beta Decay in Supersymmetric Theories, *Phys. Rev.* D34 (1986) 3457–3461. doi:[10.1103/PhysRevD.34.3457](https://doi.org/10.1103/PhysRevD.34.3457), [,778(1986)].
- [661] J. D. Vergados, Neutrinoless Double Beta Decay Without Majorana Neutrinos in Supersymmetric Theories, *Phys. Lett.* B184 (1987) 55–62. doi:[10.1016/0370-2693\(87\)90487-4](https://doi.org/10.1016/0370-2693(87)90487-4).
- [662] M. Hirsch, H. V. Klapdor-Kleingrothaus, S. G. Kovalenko, Supersymmetry and neutrinoless double beta decay, *Phys. Rev.* D53 (1996) 1329–1348. doi:[10.1103/PhysRevD.53.1329](https://doi.org/10.1103/PhysRevD.53.1329). arXiv:[hep-ph/9502385](https://arxiv.org/abs/hep-ph/9502385), [,787(1995)].
- [663] A. Kobach, Baryon Number, Lepton Number, and Operator Dimension in the Standard Model, *Phys. Lett.* B758 (2016) 455–457. doi:[10.1016/j.physletb.2016.05.050](https://doi.org/10.1016/j.physletb.2016.05.050). arXiv:[1604.05726](https://arxiv.org/abs/1604.05726).
- [664] K. S. Babu, C. N. Leung, Classification of effective neutrino mass operators, *Nucl. Phys.* B619 (2001) 667–689. doi:[10.1016/S0550-3213\(01\)00504-1](https://doi.org/10.1016/S0550-3213(01)00504-1). arXiv:[hep-ph/0106054](https://arxiv.org/abs/hep-ph/0106054).
- [665] A. de Gouvea, J. Jenkins, A Survey of Lepton Number Violation Via Effective Operators, *Phys. Rev.* D77 (2008) 013008. doi:[10.1103/PhysRevD.77.013008](https://doi.org/10.1103/PhysRevD.77.013008). arXiv:[0708.1344](https://arxiv.org/abs/0708.1344).
- [666] L. Lehman, Extending the Standard Model Effective Field Theory with the Complete Set of Dimension-7 Operators, *Phys. Rev.* D90 (2014) 125023. doi:[10.1103/PhysRevD.90.125023](https://doi.org/10.1103/PhysRevD.90.125023). arXiv:[1410.4193](https://arxiv.org/abs/1410.4193).
- [667] M. L. Graesser, An electroweak basis for neutrinoless double β decay, *JHEP* 08 (2017) 099. doi:[10.1007/JHEP08\(2017\)099](https://doi.org/10.1007/JHEP08(2017)099). arXiv:[1606.04549](https://arxiv.org/abs/1606.04549).
- [668] H. Pas, M. Hirsch, H. V. Klapdor-Kleingrothaus, S. G. Kovalenko, A Superformula for neutrinoless double beta decay. 2. The Short range part, *Phys. Lett.* B498 (2001) 35–39. doi:[10.1016/S0370-2693\(00\)01359-9](https://doi.org/10.1016/S0370-2693(00)01359-9). arXiv:[hep-ph/0008182](https://arxiv.org/abs/hep-ph/0008182).
- [669] L. Graf, F. F. Deppisch, F. Iachello, J. Kotila, Short-Range Neutrinoless Double Beta Decay Mechanisms, *Phys. Rev.* D98 (2018) 095023. doi:[10.1103/PhysRevD.98.095023](https://doi.org/10.1103/PhysRevD.98.095023). arXiv:[1806.06058](https://arxiv.org/abs/1806.06058).
- [670] B. P. Abbott, et al. (LIGO Scientific, Virgo), Observation of Gravitational Waves from a Binary Black Hole Merger, *Phys. Rev. Lett.* 116 (2016) 061102. doi:[10.1103/PhysRevLett.116.061102](https://doi.org/10.1103/PhysRevLett.116.061102). arXiv:[1602.03837](https://arxiv.org/abs/1602.03837).
- [671] B. P. Abbott, et al., Multi-messenger Observations of a Binary Neutron Star Merger, *Astrophys. J.* 848 (2017) L12. doi:[10.3847/2041-8213/aa91c9](https://doi.org/10.3847/2041-8213/aa91c9). arXiv:[1710.05833](https://arxiv.org/abs/1710.05833).
- [672] B. P. Abbott, et al. (LIGO Scientific, Virgo), GW170817: Observation of Gravitational Waves from a Binary Neutron Star Inspiral, *Phys. Rev. Lett.* 119 (2017) 161101. doi:[10.1103/PhysRevLett.119.161101](https://doi.org/10.1103/PhysRevLett.119.161101). arXiv:[1710.05832](https://arxiv.org/abs/1710.05832).
- [673] B. P. Abbott, et al. (LIGO Scientific, Virgo), GW170817: Measurements of neutron star radii and equation of state, *Phys. Rev. Lett.* 121 (2018) 161101. doi:[10.1103/PhysRevLett.121.161101](https://doi.org/10.1103/PhysRevLett.121.161101). arXiv:[1805.11581](https://arxiv.org/abs/1805.11581).
- [674] S. Gandolfi, J. Lippuner, A. W. Steiner, I. Tews, X. Du, M. Al-Mamun, From the microscopic to the macroscopic world: from nucleons to neutron stars, *J. Phys. G* 46 (2019) 103001. doi:[10.1088/1361-6471/ab29b3](https://doi.org/10.1088/1361-6471/ab29b3). arXiv:[1903.06730](https://arxiv.org/abs/1903.06730).
- [675] Z. Arzoumanian, K. C. Gendreau, C. L. Baker, T. Cazeau, P. Hestnes, J. W. Kellogg, S. J. Kenyon, R. P. Kozon, K.-C. Liu, S. S. Manthripragada, C. B. Markwardt, A. L. Mitchell, J. W. Mitchell, C. A. Monroe, T. Okajima, S. E. Pollard, D. F. Powers, B. J. Savadkin, L. B. Winteritz, P. T. Chen, M. R. Wright, R. Foster, G. Prigozhin, R. Remillard, J. Doty, The neutron star interior composition explorer (NICER): mission definition, in: T. Takahashi, J.-W. A. den Herder, M. Bautz (Eds.), *Space Telescopes and Instrumentation 2014: Ultraviolet to Gamma Ray*, volume 9144, International Society for Optics and Photonics, SPIE, 2014, pp. 579–587. URL: <https://doi.org/10.1117/12.2056811>. doi:[10.1117/12.2056811](https://doi.org/10.1117/12.2056811).
- [676] K. C. Gendreau, Z. Arzoumanian, P. W. Adkins, C. L. Albert, J. F. Anders, A. T. Aylward, C. L. Baker, E. R. Balsamo, W. A. Bamford, S. S. Benegalrao, et al., The Neutron star Interior Composition Explorer (NICER): design and development, in: J.-W. A. den Herder, T. Takahashi, M. Bautz (Eds.), *Space Telescopes and Instrumentation 2016: Ultraviolet to Gamma Ray*, volume 9905, International Society for Optics and Photonics, SPIE, 2016, pp. 420 – 435. URL: <https://doi.org/10.1117/12.2231304>. doi:[10.1117/12.2231304](https://doi.org/10.1117/12.2231304).
- [677] M. Feroci, et al. (LOFT), The Large Observatory for X-ray Timing (LOFT), *Exper. Astron.* 34 (2012) 415. doi:[10.1007/s10686-011-9237-2](https://doi.org/10.1007/s10686-011-9237-2). arXiv:[1107.0436](https://arxiv.org/abs/1107.0436).
- [678] S. Zane (LOFT Detector? Group), LOFT - Large Observatory for X-ray Timing, *JINST* 9 (2014) C12003. doi:[10.1088/1748-0221/9/12/C12003](https://doi.org/10.1088/1748-0221/9/12/C12003). arXiv:[1410.8681](https://arxiv.org/abs/1410.8681).
- [679] A. L. Watts, et al., Dense matter with eXTP, *Sci. China Phys. Mech. Astron.* 62 (2019) 29503. doi:[10.1007/s11433-017-9188-4](https://doi.org/10.1007/s11433-017-9188-4).

- [680] G. Baardsen, A. Ekström, G. Hagen, M. Hjorth-Jensen, Coupled-cluster studies of infinite nuclear matter, Phys. Rev. C88 (2013) 054312. doi:[10.1103/PhysRevC.88.054312](https://doi.org/10.1103/PhysRevC.88.054312). arXiv:[1306.5681](https://arxiv.org/abs/1306.5681).
- [681] G. Hagen, T. Papenbrock, A. Ekström, K. A. Wendt, G. Baardsen, S. Gandolfi, M. Hjorth-Jensen, C. J. Horowitz, Coupled-cluster calculations of nucleonic matter, Phys. Rev. C89 (2014) 014319. doi:[10.1103/PhysRevC.89.014319](https://doi.org/10.1103/PhysRevC.89.014319). arXiv:[1311.2925](https://arxiv.org/abs/1311.2925).
- [682] S. Gandolfi, J. Carlson, S. Reddy, The maximum mass and radius of neutron stars and the nuclear symmetry energy, Phys. Rev. C85 (2012) 032801. doi:[10.1103/PhysRevC.85.032801](https://doi.org/10.1103/PhysRevC.85.032801). arXiv:[1101.1921](https://arxiv.org/abs/1101.1921).
- [683] I. Tews, S. Gandolfi, A. Gezerlis, A. Schwenk, Quantum Monte Carlo calculations of neutron matter with chiral three-body forces, Phys. Rev. C93 (2016) 024305. doi:[10.1103/PhysRevC.93.024305](https://doi.org/10.1103/PhysRevC.93.024305). arXiv:[1507.05561](https://arxiv.org/abs/1507.05561).
- [684] A. Rios, A. Polls, I. Vidana, Hot neutron matter from a Self-Consistent Green's Functions approach, Phys. Rev. C79 (2009) 025802. doi:[10.1103/PhysRevC.79.025802](https://doi.org/10.1103/PhysRevC.79.025802). arXiv:[0809.1467](https://arxiv.org/abs/0809.1467).
- [685] A. Carbone, A. Cipollone, C. Barbieri, A. Rios, A. Polls, Self-consistent Green's functions formalism with three-body interactions, Phys. Rev. C88 (2013) 054326. doi:[10.1103/PhysRevC.88.054326](https://doi.org/10.1103/PhysRevC.88.054326). arXiv:[1310.3688](https://arxiv.org/abs/1310.3688).
- [686] A. Carbone, A. Rios, A. Polls, Symmetric nuclear matter with chiral three-nucleon forces in the self-consistent Green's functions approach, Phys. Rev. C88 (2013) 044302. doi:[10.1103/PhysRevC.88.044302](https://doi.org/10.1103/PhysRevC.88.044302). arXiv:[1307.1889](https://arxiv.org/abs/1307.1889).
- [687] C. Drischler, A. Carbone, K. Hebeler, A. Schwenk, Neutron matter from chiral two- and three-nucleon calculations up to N^3LO , Phys. Rev. C94 (2016) 054307. doi:[10.1103/PhysRevC.94.054307](https://doi.org/10.1103/PhysRevC.94.054307). arXiv:[1608.05615](https://arxiv.org/abs/1608.05615).
- [688] J. Xu, A. Carbone, Z. Zhang, C. M. Ko, Nuclear matter properties at finite temperatures from effective interactions, Phys. Rev. C100 (2019) 024618. doi:[10.1103/PhysRevC.100.024618](https://doi.org/10.1103/PhysRevC.100.024618). arXiv:[1904.09669](https://arxiv.org/abs/1904.09669).
- [689] A. Carbone, A. Schwenk, Ab initio constraints on thermal effects of the nuclear equation of state, Phys. Rev. C100 (2019) 025805. doi:[10.1103/PhysRevC.100.025805](https://doi.org/10.1103/PhysRevC.100.025805). arXiv:[1904.00924](https://arxiv.org/abs/1904.00924).
- [690] A. Carbone, A. Polls, A. Rios, Microscopic Predictions of the Nuclear Matter Liquid-Gas Phase Transition, Phys. Rev. C98 (2018) 025804. doi:[10.1103/PhysRevC.98.025804](https://doi.org/10.1103/PhysRevC.98.025804). arXiv:[1807.00596](https://arxiv.org/abs/1807.00596).
- [691] I. Tews, T. Krüger, K. Hebeler, A. Schwenk, Neutron matter at next-to-next-to-next-to-leading order in chiral effective field theory, Phys. Rev. Lett. 110 (2013) 032504. doi:[10.1103/PhysRevLett.110.032504](https://doi.org/10.1103/PhysRevLett.110.032504). arXiv:[1206.0025](https://arxiv.org/abs/1206.0025).
- [692] T. Krüger, I. Tews, K. Hebeler, A. Schwenk, Neutron matter from chiral effective field theory interactions, Phys. Rev. C88 (2013) 025802. doi:[10.1103/PhysRevC.88.025802](https://doi.org/10.1103/PhysRevC.88.025802). arXiv:[1304.2212](https://arxiv.org/abs/1304.2212).
- [693] J. W. Holt, N. Kaiser, W. Weise, Nuclear chiral dynamics and thermodynamics, Prog. Part. Nucl. Phys. 73 (2013) 35–83. doi:[10.1016/j.ppnp.2013.08.001](https://doi.org/10.1016/j.ppnp.2013.08.001). arXiv:[1304.6350](https://arxiv.org/abs/1304.6350).
- [694] L. Coraggio, J. W. Holt, N. Itaco, R. Machleidt, L. E. Marcucci, F. Sammarruca, Nuclear-matter equation of state with consistent two- and three-body perturbative chiral interactions, Phys. Rev. C89 (2014) 044321. doi:[10.1103/PhysRevC.89.044321](https://doi.org/10.1103/PhysRevC.89.044321). arXiv:[1402.0965](https://arxiv.org/abs/1402.0965).
- [695] C. Wellenhofer, J. W. Holt, N. Kaiser, W. Weise, Nuclear thermodynamics from chiral low-momentum interactions, Phys. Rev. C89 (2014) 064009. doi:[10.1103/PhysRevC.89.064009](https://doi.org/10.1103/PhysRevC.89.064009). arXiv:[1404.2136](https://arxiv.org/abs/1404.2136).
- [696] C. Drischler, K. Hebeler, A. Schwenk, Asymmetric nuclear matter based on chiral two- and three-nucleon interactions, Phys. Rev. C93 (2016) 054314. doi:[10.1103/PhysRevC.93.054314](https://doi.org/10.1103/PhysRevC.93.054314). arXiv:[1510.06728](https://arxiv.org/abs/1510.06728).
- [697] J. W. Holt, N. Kaiser, Equation of state of nuclear and neutron matter at third-order in perturbation theory from chiral effective field theory, Phys. Rev. C95 (2017) 034326. doi:[10.1103/PhysRevC.95.034326](https://doi.org/10.1103/PhysRevC.95.034326). arXiv:[1612.04309](https://arxiv.org/abs/1612.04309).
- [698] C. Wellenhofer, J. W. Holt, N. Kaiser, Divergence of the isospin-asymmetry expansion of the nuclear equation of state in many-body perturbation theory, Phys. Rev. C93 (2016) 055802. doi:[10.1103/PhysRevC.93.055802](https://doi.org/10.1103/PhysRevC.93.055802). arXiv:[1603.02935](https://arxiv.org/abs/1603.02935).
- [699] C. Drischler, V. Soma, A. Schwenk, Microscopic calculations and energy expansions for neutron-rich matter, Phys. Rev. C89 (2014) 025806. doi:[10.1103/PhysRevC.89.025806](https://doi.org/10.1103/PhysRevC.89.025806). arXiv:[1310.5627](https://arxiv.org/abs/1310.5627).
- [700] K. Hebeler, A. Schwenk, Chiral three-nucleon forces and neutron matter, Phys. Rev. C82 (2010) 014314. doi:[10.1103/PhysRevC.82.014314](https://doi.org/10.1103/PhysRevC.82.014314). arXiv:[0911.0483](https://arxiv.org/abs/0911.0483).
- [701] K. Hebeler, J. M. Lattimer, C. J. Pethick, A. Schwenk, Equation of state and neutron star properties constrained by nuclear physics and observation, Astrophys. J. 773 (2013) 11. doi:[10.1088/0004-637X/773/1/11](https://doi.org/10.1088/0004-637X/773/1/11). arXiv:[1303.4662](https://arxiv.org/abs/1303.4662).
- [702] C. Gonzalez-Boquera, M. Centelles, X. Viñas, A. Rios, Higher-order symmetry energy and neutron star core-crust transition with Gogny forces, Phys. Rev. C96 (2017) 065806. doi:[10.1103/PhysRevC.96.065806](https://doi.org/10.1103/PhysRevC.96.065806). arXiv:[1706.02736](https://arxiv.org/abs/1706.02736).
- [703] N. Kaiser, Quartic isospin asymmetry energy of nuclear matter from chiral pion-nucleon dynamics, Phys. Rev. C91 (2015) 065201. doi:[10.1103/PhysRevC.91.065201](https://doi.org/10.1103/PhysRevC.91.065201). arXiv:[1504.00604](https://arxiv.org/abs/1504.00604).

- [704] H. Heiselberg, V. Pandharipande, Recent progress in neutron star theory, *Ann. Rev. Nucl. Part. Sci.* 50 (2000) 481–524. doi:[10.1146/annurev.nucl.50.1.481](https://doi.org/10.1146/annurev.nucl.50.1.481). arXiv:[astro-ph/0003276](https://arxiv.org/abs/astro-ph/0003276).
- [705] X. Roca-Maza, M. Centelles, X. Viñas, M. Brenna, G. Colò, B. K. Agrawal, N. Paar, J. Piekarewicz, D. Vretenar, Electric dipole polarizability in ^{208}Pb : Insights from the droplet model, *Phys. Rev. C* 88 (2013) 024316. doi:[10.1103/PhysRevC.88.024316](https://doi.org/10.1103/PhysRevC.88.024316). arXiv:[1307.4806](https://arxiv.org/abs/1307.4806).
- [706] J. M. Lattimer, A. W. Steiner, Constraints on the symmetry energy using the mass-radius relation of neutron stars, *Eur. Phys. J. A* 50 (2014) 40. doi:[10.1140/epja/i2014-14040-y](https://doi.org/10.1140/epja/i2014-14040-y). arXiv:[1403.1186](https://arxiv.org/abs/1403.1186).
- [707] X. Roca-Maza, N. Paar, Nuclear Equation of State from ground and collective excited state properties of nuclei, *Prog. Part. Nucl. Phys.* 101 (2018) 96–176. doi:[10.1016/j.ppnp.2018.04.001](https://doi.org/10.1016/j.ppnp.2018.04.001). arXiv:[1804.06256](https://arxiv.org/abs/1804.06256).
- [708] S. Abrahanyan, et al., Measurement of the Neutron Radius of ^{208}Pb Through Parity-Violation in Electron Scattering, *Phys. Rev. Lett.* 108 (2012) 112502. doi:[10.1103/PhysRevLett.108.112502](https://doi.org/10.1103/PhysRevLett.108.112502). arXiv:[1201.2568](https://arxiv.org/abs/1201.2568).
- [709] F. J. Fattoyev, J. Piekarewicz, C. J. Horowitz, Neutron Skins and Neutron Stars in the Multimessenger Era, *Phys. Rev. Lett.* 120 (2018) 172702. doi:[10.1103/PhysRevLett.120.172702](https://doi.org/10.1103/PhysRevLett.120.172702). arXiv:[1711.06615](https://arxiv.org/abs/1711.06615).
- [710] K. Hebeler, J. M. Lattimer, C. J. Pethick, A. Schwenk, Constraints on neutron star radii based on chiral effective field theory interactions, *Phys. Rev. Lett.* 105 (2010) 161102. doi:[10.1103/PhysRevLett.105.161102](https://doi.org/10.1103/PhysRevLett.105.161102). arXiv:[1007.1746](https://arxiv.org/abs/1007.1746).
- [711] C. J. Horowitz, E. F. Brown, Y. Kim, W. G. Lynch, R. Michaels, A. Ono, J. Piekarewicz, M. B. Tsang, H. H. Wolter, A way forward in the study of the symmetry energy: experiment, theory, and observation, *J. Phys. G* 41 (2014) 093001. doi:[10.1088/0954-3899/41/9/093001](https://doi.org/10.1088/0954-3899/41/9/093001). arXiv:[1401.5839](https://arxiv.org/abs/1401.5839).
- [712] J. Birkhan, et al., Electric dipole polarizability of ^{48}Ca and implications for the neutron skin, *Phys. Rev. Lett.* 118 (2017) 252501. doi:[10.1103/PhysRevLett.118.252501](https://doi.org/10.1103/PhysRevLett.118.252501). arXiv:[1611.07072](https://arxiv.org/abs/1611.07072).
- [713] J. Simonis, S. Bacca, G. Hagen, First principles electromagnetic responses in medium-mass nuclei, *Eur. Phys. J. A* 55 (2019) 241. doi:[10.1140/epja/i2019-12825-0](https://doi.org/10.1140/epja/i2019-12825-0). arXiv:[1905.02055](https://arxiv.org/abs/1905.02055).
- [714] C. J. Horowitz, K. S. Kumar, R. Michaels, Electroweak Measurements of Neutron Densities in CREX and PREX at JLab, USA, *Eur. Phys. J. A* 50 (2014) 48. doi:[10.1140/epja/i2014-14048-3](https://doi.org/10.1140/epja/i2014-14048-3). arXiv:[1307.3572](https://arxiv.org/abs/1307.3572).
- [715] J. Hoppe, C. Drischler, K. Hebeler, A. Schwenk, J. Simonis, Probing chiral interactions up to next-to-next-to-next-to-leading order in medium-mass nuclei, *Phys. Rev. C* 100 (2019) 024318. doi:[10.1103/PhysRevC.100.024318](https://doi.org/10.1103/PhysRevC.100.024318). arXiv:[1904.12611](https://arxiv.org/abs/1904.12611).
- [716] G. Hagen, T. Papenbrock, D. J. Dean, A. Schwenk, A. Nogga, M. Wloch, P. Piecuch, Coupled-cluster theory for three-body Hamiltonians, *Phys. Rev. C* 76 (2007) 034302. doi:[10.1103/PhysRevC.76.034302](https://doi.org/10.1103/PhysRevC.76.034302). arXiv:[0704.2854](https://arxiv.org/abs/0704.2854).
- [717] R. Roth, S. Binder, K. Vobig, A. Calci, J. Langhammer, P. Navratil, Ab Initio Calculations of Medium-Mass Nuclei with Normal-Ordered Chiral NN+3N Interactions, *Phys. Rev. Lett.* 109 (2012) 052501. doi:[10.1103/PhysRevLett.109.052501](https://doi.org/10.1103/PhysRevLett.109.052501). arXiv:[1112.0287](https://arxiv.org/abs/1112.0287).
- [718] A. Carbone, A. Rios, A. Polls, Correlated density-dependent chiral forces for infinite matter calculations within the Green's function approach, *Phys. Rev. C* 90 (2014) 054322. doi:[10.1103/PhysRevC.90.054322](https://doi.org/10.1103/PhysRevC.90.054322). arXiv:[1408.0717](https://arxiv.org/abs/1408.0717).
- [719] J. W. Holt, N. Kaiser, W. Weise, Density-dependent effective nucleon-nucleon interaction from chiral three-nucleon forces, *Phys. Rev. C* 81 (2010) 024002. doi:[10.1103/PhysRevC.81.024002](https://doi.org/10.1103/PhysRevC.81.024002). arXiv:[0910.1249](https://arxiv.org/abs/0910.1249).
- [720] N. Kaiser, V. Niessner, Density-dependent NN-interaction from subleading chiral 3N-forces: short-range terms and relativistic corrections, *Phys. Rev. C* 98 (2018) 054002. doi:[10.1103/PhysRevC.98.054002](https://doi.org/10.1103/PhysRevC.98.054002). arXiv:[1810.09412](https://arxiv.org/abs/1810.09412).
- [721] N. Kaiser, B. Singh, Density-dependent NN interaction from subleading chiral three-nucleon forces: Long-range terms, *Phys. Rev. C* 100 (2019) 014002. doi:[10.1103/PhysRevC.100.014002](https://doi.org/10.1103/PhysRevC.100.014002). arXiv:[1903.03183](https://arxiv.org/abs/1903.03183).
- [722] N. Kaiser, Density-dependent NN interaction from subsubleading chiral 3N forces: Intermediate-range contributions, *Phys. Rev. C* 101 (2020) 014001. doi:[10.1103/PhysRevC.101.014001](https://doi.org/10.1103/PhysRevC.101.014001). arXiv:[1910.03082](https://arxiv.org/abs/1910.03082).
- [723] K. Hebeler, H. Krebs, E. Epelbaum, J. Golak, R. Skibinski, Efficient calculation of chiral three-nucleon forces up to N3LO for ab initio studies, *Phys. Rev. C* 91 (2015) 044001. doi:[10.1103/PhysRevC.91.044001](https://doi.org/10.1103/PhysRevC.91.044001). arXiv:[1502.02977](https://arxiv.org/abs/1502.02977).
- [724] K. Hebeler, R. J. Furnstahl, Neutron matter based on consistently evolved chiral three-nucleon interactions, *Phys. Rev. C* 87 (2013) 031302. doi:[10.1103/PhysRevC.87.031302](https://doi.org/10.1103/PhysRevC.87.031302). arXiv:[1301.7467](https://arxiv.org/abs/1301.7467).
- [725] N. Kaiser, Third-order particle-hole ring diagrams with contact-interactions and one-pion exchange, *Eur. Phys. J. A* 53 (2017) 104. doi:[10.1140/epja/i2017-12290-9](https://doi.org/10.1140/epja/i2017-12290-9). arXiv:[1703.07745](https://arxiv.org/abs/1703.07745).
- [726] C. Wellenhofer, J. W. Holt, N. Kaiser, Thermodynamics of isospin-asymmetric nuclear matter from chiral effective field theory, *Phys. Rev. C* 92 (2015) 015801. doi:[10.1103/PhysRevC.92.015801](https://doi.org/10.1103/PhysRevC.92.015801). arXiv:[1504.00177](https://arxiv.org/abs/1504.00177).

- [727] P. D. Stevenson, Automatic generation of vacuum amplitude many-body perturbation series, *Int. J. Mod. Phys. C* 14 (2003) 1135. URL: <http://www.worldscientific.com/doi/abs/10.1142/S0129183103005236>. doi:[10.1142/S0129183103005236](https://doi.org/10.1142/S0129183103005236). arXiv:<http://www.worldscientific.com/doi/pdf/10.1142/S0129183103005236>.
- [728] P. Arthuis, T. Duguet, A. Tichai, R. D. Lasseri, J. P. Ebran, ADG: Automated generation and evaluation of many-body diagrams I. Bogoliubov many-body perturbation theory, *Comput. Phys. Commun.* 240 (2019) 202–227. doi:[10.1016/j.cpc.2018.11.023](https://doi.org/10.1016/j.cpc.2018.11.023). arXiv:[1809.01187](https://arxiv.org/abs/1809.01187).
- [729] G. P. Lepage, A New Algorithm for Adaptive Multidimensional Integration, *J. Comput. Phys.* 27 (1978) 192. doi:[10.1016/0021-9991\(78\)90004-9](https://doi.org/10.1016/0021-9991(78)90004-9).
- [730] N. Kaiser, Exact calculation of three-body contact interaction to second order, *Eur. Phys. J. A* 48 (2012) 58. doi:[10.1140/epja/i2012-12058-9](https://doi.org/10.1140/epja/i2012-12058-9). arXiv:[1203.6283](https://arxiv.org/abs/1203.6283).
- [731] C. Wellenhofer, C. Drischler, A. Schwenk, Dilute Fermi gas at fourth order in effective field theory, *Phys. Lett. B* 802 (2020) 135247. doi:[10.1016/j.physletb.2020.135247](https://doi.org/10.1016/j.physletb.2020.135247). arXiv:[1812.08444](https://arxiv.org/abs/1812.08444).
- [732] M. J. H. Ku, A. T. Sommer, L. W. Cheuk, M. W. Zwierlein, Revealing the Superfluid Lambda Transition in the Universal Thermodynamics of a Unitary Fermi Gas, *Science* 335 (2012) 563. URL: <https://ui.adsabs.harvard.edu/abs/2012Sci...335..563K>. doi:[10.1126/science.1214987](https://doi.org/10.1126/science.1214987). arXiv:[1110.3309](https://arxiv.org/abs/1110.3309).
- [733] C. Drischler, R. J. Furnstahl, J. A. Melendez, D. R. Phillips, How Well Do We Know the Neutron-Matter Equation of State at the Densities Inside Neutron Stars? A Bayesian Approach with Correlated Uncertainties, *Phys. Rev. Lett.* 125 (2020) 202702. doi:[10.1103/PhysRevLett.125.202702](https://doi.org/10.1103/PhysRevLett.125.202702). arXiv:[2004.07232](https://arxiv.org/abs/2004.07232).
- [734] C. Drischler, J. A. Melendez, R. J. Furnstahl, D. R. Phillips, Quantifying uncertainties and correlations in the nuclear-matter equation of state, *Phys. Rev. C* 102 (2020) 054315. doi:[10.1103/PhysRevC.102.054315](https://doi.org/10.1103/PhysRevC.102.054315). arXiv:[2004.07805](https://arxiv.org/abs/2004.07805).
- [735] J. Hu, P. Wei, Y. Zhang, Bayesian truncation errors in equations of state of nuclear matter with chiral nucleon-nucleon potentials, *Phys. Lett. B* 798 (2019) 134982. doi:[10.1016/j.physletb.2019.134982](https://doi.org/10.1016/j.physletb.2019.134982). arXiv:[1909.11826](https://arxiv.org/abs/1909.11826).
- [736] S. Binder, J. Langhammer, A. Calci, R. Roth, Ab Initio Path to Heavy Nuclei, *Phys. Lett. B* 736 (2014) 119–123. doi:[10.1016/j.physletb.2014.07.010](https://doi.org/10.1016/j.physletb.2014.07.010). arXiv:[1312.5685](https://arxiv.org/abs/1312.5685).
- [737] A. Tichai, J. Langhammer, S. Binder, R. Roth, Hartree-Fock many-body perturbation theory for nuclear ground-states, *Phys. Lett. B* 756 (2016) 283–288. doi:[10.1016/j.physletb.2016.03.029](https://doi.org/10.1016/j.physletb.2016.03.029). arXiv:[1601.03703](https://arxiv.org/abs/1601.03703).
- [738] J. Simonis, K. Hebeler, J. D. Holt, J. Menendez, A. Schwenk, Exploring sd-shell nuclei from two- and three-nucleon interactions with realistic saturation properties, *Phys. Rev. C* 93 (2016) 011302. doi:[10.1103/PhysRevC.93.011302](https://doi.org/10.1103/PhysRevC.93.011302). arXiv:[1508.05040](https://arxiv.org/abs/1508.05040).
- [739] J. Simonis, S. R. Stroberg, K. Hebeler, J. D. Holt, A. Schwenk, Saturation with chiral interactions and consequences for finite nuclei, *Phys. Rev. C* 96 (2017) 014303. doi:[10.1103/PhysRevC.96.014303](https://doi.org/10.1103/PhysRevC.96.014303). arXiv:[1704.02915](https://arxiv.org/abs/1704.02915).
- [740] R. F. Garcia Ruiz, et al., Unexpectedly large charge radii of neutron-rich calcium isotopes, *Nature Phys.* 12 (2016) 594. doi:[10.1038/nphys3645](https://doi.org/10.1038/nphys3645). arXiv:[1602.07906](https://arxiv.org/abs/1602.07906).
- [741] G. Hagen, G. R. Jansen, T. Papenbrock, Structure of ^{78}Ni from first principles computations, *Phys. Rev. Lett.* 117 (2016) 172501. doi:[10.1103/PhysRevLett.117.172501](https://doi.org/10.1103/PhysRevLett.117.172501). arXiv:[1605.01477](https://arxiv.org/abs/1605.01477).
- [742] T. D. Morris, J. Simonis, S. R. Stroberg, C. Stumpf, G. Hagen, J. D. Holt, G. R. Jansen, T. Papenbrock, R. Roth, A. Schwenk, Structure of the lightest tin isotopes, *Phys. Rev. Lett.* 120 (2018) 152503. doi:[10.1103/PhysRevLett.120.152503](https://doi.org/10.1103/PhysRevLett.120.152503). arXiv:[1709.02786](https://arxiv.org/abs/1709.02786).
- [743] H. Hergert, In-Medium Similarity Renormalization Group for Closed and Open-Shell Nuclei, *Phys. Scripta* 92 (2017) 023002. doi:[10.1088/1402-4896/92/2/023002](https://doi.org/10.1088/1402-4896/92/2/023002). arXiv:[1607.06882](https://arxiv.org/abs/1607.06882).
- [744] J. S. Read, B. D. Lackey, B. J. Owen, J. L. Friedman, Constraints on a phenomenologically parameterized neutron-star equation of state, *Phys. Rev. D* 79 (2009) 124032. doi:[10.1103/PhysRevD.79.124032](https://doi.org/10.1103/PhysRevD.79.124032). arXiv:[0812.2163](https://arxiv.org/abs/0812.2163).
- [745] I. Tews, J. Carlson, S. Gandolfi, S. Reddy, Constraining the speed of sound inside neutron stars with chiral effective field theory interactions and observations, *Astrophys. J.* 860 (2018) 149. doi:[10.3847/1538-4357/aac267](https://doi.org/10.3847/1538-4357/aac267). arXiv:[1801.01923](https://arxiv.org/abs/1801.01923).
- [746] I. Tews, J. Margueron, S. Reddy, Critical examination of constraints on the equation of state of dense matter obtained from GW170817, *Phys. Rev. C* 98 (2018) 045804. doi:[10.1103/PhysRevC.98.045804](https://doi.org/10.1103/PhysRevC.98.045804). arXiv:[1804.02783](https://arxiv.org/abs/1804.02783).
- [747] E. R. Most, L. R. Weih, L. Rezzolla, J. Schaffner-Bielich, New constraints on radii and tidal deformabilities of neutron stars from GW170817, *Phys. Rev. Lett.* 120 (2018) 261103. doi:[10.1103/PhysRevLett.120.261103](https://doi.org/10.1103/PhysRevLett.120.261103). arXiv:[1803.00549](https://arxiv.org/abs/1803.00549).
- [748] Y. Lim, J. W. Holt, Neutron star tidal deformabilities constrained by nuclear theory and experiment, *Phys. Rev. Lett.* 121 (2018) 062701. doi:[10.1103/PhysRevLett.121.062701](https://doi.org/10.1103/PhysRevLett.121.062701). arXiv:[1803.02803](https://arxiv.org/abs/1803.02803).

- [749] Z. Carson, A. W. Steiner, K. Yagi, Constraining nuclear matter parameters with GW170817, Phys. Rev. D99 (2019) 043010. doi:[10.1103/PhysRevD.99.043010](https://doi.org/10.1103/PhysRevD.99.043010). [arXiv:1812.08910](https://arxiv.org/abs/1812.08910).
- [750] Z. Carson, A. W. Steiner, K. Yagi, Future Prospects for Constraining Nuclear Matter Parameters with Gravitational Waves, Phys. Rev. D100 (2019) 023012. doi:[10.1103/PhysRevD.100.023012](https://doi.org/10.1103/PhysRevD.100.023012). [arXiv:1906.05978](https://arxiv.org/abs/1906.05978).
- [751] C. D. Capano, I. Tews, S. M. Brown, B. Margalit, S. De, S. Kumar, D. A. Brown, B. Krishnan, S. Reddy, Stringent constraints on neutron-star radii from multimessenger observations and nuclear theory, Nature Astron. 4 (2020) 625–632. doi:[10.1038/s41550-020-1014-6](https://doi.org/10.1038/s41550-020-1014-6). [arXiv:1908.10352](https://arxiv.org/abs/1908.10352).
- [752] R. C. Tolman, Static solutions of Einstein’s field equations for spheres of fluid, Phys. Rev. 55 (1939) 364–373. doi:[10.1103/PhysRev.55.364](https://doi.org/10.1103/PhysRev.55.364).
- [753] J. R. Oppenheimer, G. M. Volkoff, On Massive neutron cores, Phys. Rev. 55 (1939) 374–381. doi:[10.1103/PhysRev.55.374](https://doi.org/10.1103/PhysRev.55.374).
- [754] A. W. Steiner, J. M. Lattimer, E. F. Brown, The Neutron Star Mass-Radius Relation and the Equation of State of Dense Matter, Astrophys. J. 765 (2013) L5. doi:[10.1088/2041-8205/765/1/L5](https://doi.org/10.1088/2041-8205/765/1/L5). [arXiv:1205.6871](https://arxiv.org/abs/1205.6871).
- [755] S. Bogdanov, F. K. Lamb, S. Mahmoodifar, M. C. Miller, S. M. Morsink, T. E. Riley, T. E. Strohmayer, A. K. Tung, A. L. Watts, A. J. Dittmann, D. Chakrabarty, S. Guillot, Z. Arzoumanian, K. C. Gendreau, Constraining the Neutron Star Mass-Radius Relation and Dense Matter Equation of State with *NICER*. II. Emission from Hot Spots on a Rapidly Rotating Neutron Star, Astrophys. J. 887 (2019) L26. doi:[10.3847/2041-8213/ab5968](https://doi.org/10.3847/2041-8213/ab5968). [arXiv:1912.05707](https://arxiv.org/abs/1912.05707).
- [756] T. E. Riley, A. L. Watts, S. Bogdanov, P. S. Ray, R. M. Ludlam, S. Guillot, Z. Arzoumanian, C. L. Baker, A. V. Bilous, D. Chakrabarty, K. C. Gendreau, A. K. Harding, W. C. G. Ho, J. M. Lattimer, S. M. Morsink, T. E. Strohmayer, A *NICER* View of PSR J0030+0451: Millisecond Pulsar Parameter Estimation, Astrophys. J. 887 (2019) L21. doi:[10.3847/2041-8213/ab481c](https://doi.org/10.3847/2041-8213/ab481c). [arXiv:1912.05702](https://arxiv.org/abs/1912.05702).
- [757] M. C. Miller, F. K. Lamb, A. J. Dittmann, S. Bogdanov, Z. Arzoumanian, K. C. Gendreau, S. Guillot, A. K. Harding, W. C. G. Ho, J. M. Lattimer, R. M. Ludlam, S. Mahmoodifar, S. M. Morsink, P. S. Ray, T. E. Strohmayer, K. S. Wood, T. Enoto, R. Foster, T. Okajima, G. Prigozhin, Y. Soong, PSR J0030+0451 Mass and Radius from *NICER* Data and Implications for the Properties of Neutron Star Matter, Astrophys. J. 887 (2019) L24. doi:[10.3847/2041-8213/ab50c5](https://doi.org/10.3847/2041-8213/ab50c5). [arXiv:1912.05705](https://arxiv.org/abs/1912.05705).
- [758] G. Raaijmakers, T. E. Riley, A. L. Watts, S. K. Greif, S. M. Morsink, K. Hebeler, A. Schwenk, T. Hinderer, S. Nissanke, S. Guillot, Z. Arzoumanian, S. Bogdanov, D. Chakrabarty, K. C. Gendreau, W. C. G. Ho, J. M. Lattimer, R. M. Ludlam, M. T. Wolff, A *NICER* view of PSR J0030+0451: Implications for the dense matter equation of state, Astrophys. J. 887 (2019) L22. doi:[10.3847/2041-8213/ab451a](https://doi.org/10.3847/2041-8213/ab451a). [arXiv:1912.05703](https://arxiv.org/abs/1912.05703).
- [759] E. Berkowitz, M. Clark, A. Gambhir, K. McElvain, A. Nicholson, E. Rinaldi, P. Vranas, A. Walker-Loud, C. C. Chang, B. Joó, T. Kurth, K. Orginos, Simulating the weak death of the neutron in a femtoscale universe with near-Exascale computing, 2018. [arXiv:1810.01609](https://arxiv.org/abs/1810.01609).